The isotope tracing methods for industrial contamination of the atmosphere

PhD Thesis

Thesis supervisor: Prof. Vladislav Chrastný

Thesis reviewers: Dr. Luke Beesley
(The James Hutton Institute, Aberdeen)

Assoc. Prof., Dr. Tomáš Navrátil
(Institute of Geology of the Czech Academy of Sciences, Prague)

Dr. Jakub Kierczak
(University of Wrocław, Wrocław)

Czech University of Life Sciences Prague

Faculty of Environmental Sciences

Department of Environmental Geosciences

Prague, 2020

The isotope tracing methods for industrial contamination of the atmosphere

Anna Francová

Thesis

This thesis is submitted in fulfillment of the requirements for the PhD degree at the Czech University of Life Sciences Prague, Faculty of Environmental Sciences.

The isotope tracing methods for industrial contamination of the atmosphere.

Anna Francová

Czech University of Life Sciences Prague (2020)

Acknowledgement

I would like to thank my supervisor Prof. Chrastný for giving me an opportunity and trust to join him in his research. His guidance and vast knowledge were irreplaceable during my studies and preparation of this PhD thesis. I would also like to thank prof. Komárek for his valuable advices and leadership, all my colleagues for the good time we had together, and last but not least, my family and friends for their support and love.

Abstract

The main objective of the thesis was evaluation of the selected environmental samples as a potential matrix for tracking trace metal pollution sources industrial areas. A comprehensive view of non-traditional use of environmental samples as a substitute for commonly used methods for monitoring pollution sources including stable isotope "fingerprint" method was carried out. The suitability of sample types for different conditions of pollution monitoring (long-term vs. short-term pollution, local vs. remote pollution sources) was also evaluated. Conservative, Pb isotope system and less conservative- nickel (Ni) and copper (Cu) and their use for fingerprinting of pollution were investigated. Six types of specimens were observed: epiphytic lichen *Physcia tenella* (Scop.) DC, bryophyte *Hypnum cupressiforme* (Hedw.), particulate matter (PM$_{10}$) collected at 24-hour intervals, snow (collected without upper frozen layer), different soil horizons, tree rings extracted from coniferous trees *Larix decidua* (Mill.), *Picea abies* (L.) H. Karst. and *Pinus sylvestris* (L.). The research was conducted on two localities, which are long-term and historically affected by industrial activities - Ostrava region in the Czech Republic and North-Eastern (N/E) Norway, near the Norwegian-Russian border.

When considering the use of environmental samples as fingerprint for industrial pollution, the nature of the sample must be taken into account. Lichens, mosses and upper organic soil horizons are suitable for tracking long-term pollution and more remote sources. On the other hand, PM$_{10}$ samples have proven to be highly dependent on season and wind direction as local recent contamination tracers. Overall, it has been found that it is ideal to use PM$_{10}$ samples in combination with snow samples, as they most accurately reflect the short-term air pollution situation. Using snow samples, it was possible to accurately identify the major local industrial sources using the Pb isotopes. Tree rings samples can be used to study historical pollution in areas where commonly used samples (peat, lake sediments, etc.) are not available.

Stable isotopes of Cu and Ni, as opposed to Pb, are not considered traditional pollution tracers. Their isotopic composition does not change during industrial processes, but unlike Pb, fractionations tend to occur in contact with the environment and so their use is limited by the analysis of given fractionation processes. The main sources of pollution in the monitored areas are the combustion of coal in industry, the use of low-

quality coal in households, metallurgical activities and, in some areas, the current and historical impact of traffic and used gasoline.

Abstrakt

Hlavním cílem předkládané disertační práce bylo sledování zdrojů znečištění životního prostředí ve dvou průmyslových oblastech pomocí vybraných environmentálních vzorků jako matrice pro stopování znečištění stopovými kovy. Hlavním cílem práce bylo poskytnout komplexní pohled na netradiční použití environmentálních vzorků jako náhrady běžně užívaných metod pro sledování zdrojů znečištění, využité jako matrice pro koncentrační a izotopové analýzy. V práci byla testována metoda izotopového stopování pomocí stabilních izotopů kovů; konzervativní systém – Pb a netradiční – Ni a Cu. Hodnocena byla také vhodnost jednotlivých typů vzorků pro různé podmínky sledování znečišťování (dlouhodobé vs krátkodobé znečišťování, místní vs vzdálené zdroje znečištění). Výzkum byl zaměřen na dvě lokality, které jsou dlouhodobě a historicky spjaty s průmyslem – Ostravsko v České republice a severo-východní část Norska v okolí města Kirkenes. Bylo sledováno 6 typů vzorků: epifytický lišejník terčovník tenounký (*Physcia tenella*), mech rokyt cypřišovitý (*Hypnum cupressiforme*), PM_{10} sbírané v intervalu 24 hodin, sníh (sbírán bez horní zmrzlé vrstvy), půda, letokruhy stromů modřín opadavý (*Larix decidua*), smrk ztepilý (*Picea abies*) a borovice lesní (*Pinus sylvestris*).

Výzkum prokázal, že použití environmentálních vzorků jako stopovačů průmyslového znečištění je možné s přihlédnutím k povaze vzorku. Bylo zjištěno, že lišejníky, mechy a svrchní organické horizonty půdy jsou vhodné pro stopování dlouhodobého znečištění a zároveň i pro sledování zdrojů značně vzdálených. Nicméně je nutné přihlédnout ke skutečnosti, že dané vzorky kumulují všechny prvky, které vstřebají, proto je koncentrace kovů a i signál stabilních izotopů olova homogenizován. Vzorky PM_{10} se jako stopovače místního bodového znečištění ukázaly být značně závislé na roční době a směru větru. Celkově bylo zjištěno, že PM_{10} je ideální používat v kombinaci s analýzami vzorků sněhů, které nejpřesněji odrážejí krátkodobou situaci ve znečišťování ovzduší. Použitím vzorků čerstvého sněhu bylo možné přesně identifikovat hlavní lokální znečišťovatele pomocí signálu izotopů olova. Vzorky letokruhů stromů mohou sloužit pro studium historického znečištění v oblastech, kde běžně používané vzorky (rašelina, jezerní sedimenty atd.) nejsou dostupné.

Stabilní izotopy Cu a Ni, na rozdíl od Pb, nejsou považovány za tradiční stopovače znečištění. Jejich izotopové složení se během průmyslových procesů nemění a patrně dochází k frakcionacím při styku s životním prostředím. Jejich využití je tak limitováno

analýzou daných frakcionačních procesů. Hlavními identifikovanými zdroji znečištění ve sledovaných oblastech je spalování uhlí v průmyslu, používání nekvalitního uhlí v domácnostech, hutní výroba a v některých oblastech i současný a historický vliv dopravy a používaných benzínů.

Table of contents

Chapter I

General introduction

Content

Problem outline

Intensive industrial activities, particularly mining and smelting, often lead to widespread contamination of the environment with metals and metalloids. Increased concentrations of these substances may be risk for humans and animals due to their ability to accumulate in the food chain. As most of the monitoring procedures only focuses on concentration data, it is not always possible to identify source and extent of pollution. This PhD thesis is part of the project whose goal is to create an effective methodology based on isotope tracing using samples from the environment. The project focuses on two contaminated sites in Norway and the Czech Republic; namely Norway-Finland-Russia border, intensive metallurgical industry takes place, and the Ostrava region, which is mainly contaminated by heavy industry and traffic. The extent of contamination will be assessed by analyzing "non-traditional" (Ni, Cd, Cu) and "traditional" (Pb) isotopic systems. The holistic approach of thesis works to identify and quantify the various sources of metals in combination with concentration and mineralogical analysis will be powerful tool for analyses of environment, risk assessment and the subsequent legislative measures.

Atmospheric pollution

Air pollution and particularly atmospheric deposition of trace metals into natural environments has been an object of an increasing interest in past decade. As a result of anthropogenic activities in recent years content of metals in the environment has dramatically increased (Waterlot et al., 2012). Atmospheric deposition is the most extensive form of contamination because long-range transport can result in particles being carried very long distances, although much contamination from this source tends to be more localized (Alloway, 2013). There is a deposition of trace metals due to long range transport, even to formerly pristine forests and soils, especially in industrialized areas (Hernandez et al., 2003). Atmospheric input of pollutants into ecosystems is subsumed of wet and dry deposition. The main forms of wet deposition are vertical deposition (rain and snow) and horizontal deposition (fog and ice accretions; Voldrichova et al., 2014).

Changes in the composition of the atmosphere were reported as a result of the combustion of fossil fuels. Atmosphere started to be discharged, various compounds that are persistent in the environment, able to be transported in long or short distances and can affect human health, started to be emitted into the air. Those compounds can be grouped to four categories:

• gaseous pollutants (e.g. SO_2, NOx, CO, ozone, Volatile Organic Compounds),
• persistent organic pollutants (e.g. dioxins),
• trace metals (e.g. Pb, Hg)
• particulate matter (Kampa and Castanas, 2008).

The impacts of atmospheric deposition of substances emitted into the environment have been studied for over a hundred years. A pioneer in this field was W. Nylander (1886) (as cited in Wolterbeek, 2002), who first described the decline of epiphytic lichens number of due to high levels of atmospheric pollution, which was the foundation for the use of lichens as air quality monitors. Degradation in the health of forests due to atmospheric pollution is also known for a long time and the associated loss of forests in Europe as well (Bussotti and Ferretti, 1998).

An extreme case of industrial air pollution on forest ecosystems can be found on the Kola Peninsula in northwest Russia (Gregurek et al., 1998a). There are three industrial centres: Nickel, Zapolarnyj and Monchegorsk. Non-ferrous ores are processed

primarily in Nickel facility. Large amounts of trace metals are released especially from Monchegorsk smelter. Nickel, Zapolarnyj and Monchegorsk rank among the largest emitters of sulphur in Europe (Khokhar et al., 2008).

There has been relatively sharp gradient of pollution in the Czech Republic. Areas on northeast and northwest are primarily polluted by emissions from heavy industry. The opposite of those areas is almost uncontaminated rural south (Novak et al., 2008). The pollution in industrial areas reached peak in 1980s and gradual decrease in the amount of emissions of polluting substances followed ever since. Recently, a 300-km shift in the highest industrial pollution has been reported from the northwest to the northeast, from the North Bohemian soft-coal basin to the Lower Silesia stone-coal basin (Bohdalkova et al., 2012).

Metal(loid)s as polluters of the atmosphere

Pollutants are defined as substances that may bring harm to humans, animals, vegetation or materials. All chemicals that are released into the environment and cause damage to living organisms are considered as environmental contaminants (European Environment Agency, 2015).

Some natural processes, such as volcanoes or forest fires, can release different pollutants into the environment. Anthropogenic processes, however, are a major source of air pollution. Deposition of trace metals and atmospheric precipitation is considered as a major environmental problem as metals are known to have a significant impact on ecosystems (Agnan et al., 2013) and human health (Pacyna et al., 2009). Metals are, in comparison to other types of environmental pollutants, particularly dangerous due to their toxicity and persistence (Luo et al., 2015).

Trace metals are essential elements of the Earth's crust (Kampa and Castanas, 2008) and occur in natural areas in a certain amount as the "background". The amount of metals in the background varies according to the sources of elements (Telmer et al., 2004). Trace metals cannot be degraded or destroyed but can be transported by air and can easily enter the water sources, thus get into the human food chain (Kampa and Castanas, 2008). They are not biodegradable which leads to their accumulation in tissues (Wong et al., 2006). Nevertheless, trace elements are at higher concentrations (although still relatively low) toxic to living organisms. Therefore anthropogenic changes of natural fluxes of trace metals in the biosphere became a serious concern (Bourennane et al., 2010).

In addition to metal contributions from geological background, metals come into the environment mainly from anthropogenic activities, such as use of fossil fuels or wastewater discharge (Kampa and Castanas, 2008). In the last century the input of metals into the environment caused by humans far exceeded the natural input due to paedogenesis, both at the regional and global scale (Facchinelli et al., 2001). An increase in emissions of metals and their deposition lead to enrichment of environment by metals (Pacyna et al., 2009).

There are four major groups of parameters affecting the emissions of trace metals to the atmosphere:

- sum of the trace metals in raw materials,
- physico-chemical properties of trace metals affecting its behaviour during the industrial processes,
- the technology of industrial processes and
- the type and efficiency of control equipment (Pacyna et al., 2009).

There is a continuous reduction of trace metal emissions in Europe over the last decade. The combustion of fuels, especially coal, is still the most important source of anthropogenic emissions of metals. The amount of emissions exhaling from power plants and large plans are effectively controlled and thus can be reduced, unlike the small sources (mainly households). The problem with small sources, particularly local heating, is that the emissions of pollutants are not controlled in any way. Small sources are a problem mainly because the various types of waste are being incinerated also as the cheapest types of fuels (Pacyna et al., 2007).

Lead (Pb) is one of the most extensively investigated trace metals. One major dispersion pathway for Pb is atmospheric transport, as Pb bearing aerosols are emitted from industrial activities, combustion of coal and leaded gasoline (Le Roux et al., 2005). The isotopic composition of lead is variable in nature as only one (^{204}Pb) of the four stable isotopes (^{204}Pb, ^{206}Pb, ^{207}Pb and ^{208}Pb) is not the end product of the decay of Th and U isotopes (Bacon and Dinev, 2005). Because the isotopic composition of Pb is not affected by physical or chemical fractionation processes, Pb and its isotopes provide an ideal tool for characterizing sources and pathways of atmospheric pollution. The isotopic "fingerprint" of Pb can be used to investigate long range transport and to back-calculate atmospheric mixing processes (Mukai et al., 2001). Each Pb source has its own specific isotopic composition. Isotopic composition of ^{206}Pb/^{207}Pb is most commonly used for environmental pollution assessment (Komárek et al., 2008).

Copper, which (Cu) has two stable isotopes (^{63}Cu and ^{65}Cu), is emitted into the atmosphere mainly from Cu processing plants (Pacyna et al, 2007). Environment around these smelters often tends to be heavily contaminated with Cu in gaseous or solid form, which is deposited to the surfaces, thus contaminates soil and consequently the groundwater (Adamo et al., 1996). As Cu does not fractionate during the smelting process, probably because of its high boiling temperature, smelting products can effectively reflect the mineralogical differences of the used ores (Mattielli et al., 2006). Cu ores and minerals show a wide range of isotope ratios (Mathur et al., 2009), which is far larger than the isotope fractionation in natural soils, it is however possible that Cu stable isotope ratios of anthropogenic emissions are different from those of natural soils (Bigalke et al., 2010).

Naturally occurring nickel (Ni) is composed of five stable isotopes; ^{58}Ni, ^{60}Ni, ^{61}Ni, ^{62}Ni and ^{64}Ni with. Ni is commonly present in two main types of ore: sulphide and laterite. Sulphide ores are derived from volcanic or hydrothermal processes and apart from Ni also include Cu and/or Co, and often precious metals (Hoatson et al., 2006). Laterites occur abundantly mainly in tropical climates around the equator, arid regions of central Western Australia or humid areas of Eastern Europe (Moskalyk and Alfantazi, 2002). Ni isotopes are significantly fractionated by Earth surface processes, and thus have some potential in attempts to understand modern and ancient biogeochemical processes (Gall et al., 2013).

Identification of pollution sources

Trace metal pollution is covert, persistent and irreversible (Wang et al., 2001). Industrialisation has caused perturbation of trace metals, including Pb, Cu, Ni, Cd, Cr, Zn, Ag and Mo, in the earth's atmosphere, surface sediments and water bodies. These pollutants not only affect the sites where they are produced, but are transported through the atmosphere thereby influencing the wider environment (Marx et al., 2009).

Leaded gasoline

The former use of leaded gasoline had represented one of the main sources of global Pb pollution in the period between the 1940s and the 1980s (Novák et al., 2010). The knowledge about the origin of gasoline, i.e. about the origin and age of Pb ore used for alkyl-Pb antiknock additives (tetraethyllead Pb(C$_2$H$_5$)$_4$, tetra- methyllead Pb(CH$_3$)$_4$) is vital for a precise identification of Pb originating from leaded gasoline combustion (Monna et al., 1997). The isotopic composition of Pb ores used thus reflects the

Table 1.1 Examples of selected metal(loid) contaminants associated with different industries (adapted from Alloway, 2013)

Industrial source	Metal(loid)s
Chlor-alkali (Cl2 and NaOH) industry	Cd, Cu, Pb, As
Sulphuric acid works	Cu, Pb, Ni, As
Nitric acid works	Cu, Ni, As
Phosphoric acid works	Cd, Cu, Pb, As
Electrical components	Cu, Pb
Steel works	Cu, Pb, Ni, As
Pesticide works	Cu, Pb, As
Non-ferrous metal smelting	Cd, Cu, As
Waste disposal (incineration etc.)	Cd, Cu, Ni, Pb, As

composition of leaded gasoline. The $^{206}Pb/^{204}Pb$ $^{206}Pb/^{204}Pb$ and $^{206}Pb/^{207}Pb$ ratios commonly found in Pb ores throughout the world range between 16.0 – 18.5 and 1.19 – 1.25, respectively (Hansmann and Köppel, 2000). Exception to this rule is the commonly used Pb ore from the Broken Hill deposit, Australia, which is characterised by extremely low $^{206}Pb/^{207}Pb$ ratios (1.03 – 1.10). On the other hand, Pb originating from the Mississippi Valley ore deposit, USA, exhibits significantly more radiogenic Pb isotopic composition ($^{206}Pb/^{204}Pb$ = 20.0; $^{206}Pb/^{207}Pb$ = 1.31–1.35) (Novák et al., 2003, Novák et al., 2010). According to data obtained from peat deposits by Weiss et al., 1999, the introduction of the European leaded gasoline around 1945 resulted in a steep decrease of the $^{206}Pb/^{207}Pb$ ratio of atmospheric Pb.

The Pb emissions in Europe culminated in the mid-1970s and they were then more than one order of magnitude higher than the 2005 emissions of this element. These changes are quite directly related to the changes of regulation in the use of lead additives to gasoline. Alkyl-Pb was used as an anti-knock additive to petrol in significant amounts after 1950. According to Novák et al. (2003), the leaded gasoline used in the Czech Republic contained Pb with a low $^{206}Pb/^{207}Pb$ ratio from the Broken Hill deposit, with additives originating from East Germany or Russia (1.110 – 1.130). In the 1970s, the German government was the first in Europe to regulate lead additives in gasoline (Pacyna et al., 2009). Lead emissions from traffic in Czech Republic peaked in 1985, and alkyl-Pb was completely phased out by law in 2000 (Novák et al., 2010).

Coal combustion

Coal combustion has been another important anthropogenic source influencing the isotopic composition of Pb for many decades. Lead released during coal combustion can be distinguished from other sources using Pb isotopes because of its different isotopic composition. The $^{206}Pb/^{207}Pb$ ratio in European coals is not age dependent and ranges between 1.16 and 1.21 (Hansmann and Köppel, 2000; Novák et al., 2003). Lead isotopic studies in peat deposits proved that coal combustion was the predominant source of Pb in the atmosphere before the introduction of leaded gasoline and air pollution control (APC) policies in thermal plants (Novák et al., 2003). Coal burning in Central Europe is often difficult to discern from the background source ($^{206}Pb/^{207}Pb \sim 1.19$), but contributes to the isotopic composition of an "industrial" Pb mixture, which can be detected in recent atmospheric aerosols and yields $^{206}Pb/^{207}Pb$ values of ~ 1.15 (Weiss et al., 1999; Novák et al., 2003).

Metallurgical activities

The isotopic composition of Pb emitted to the atmosphere during pyrometallurgical processes reflects closely the isotopic composition of the material processed, such as Pb ore or secondary processed materials containing Pb (e.g., Pb batteries) (Ettler et al., 2004). The predominant influence of Pb smelters on local contaminations of the atmosphere, soils and sediments has been proved by several Pb isotopic studies (e.g. Ettler et al., 2006; Komárek et al., 2007).

The Czech Republic is one of very few countries in the world where historical rates of Pb emissions have been published, based on careful compilation of data archived since the Middle Ages (Novák et al., 2003; Novak et al., 2008). Bohemian Kingdom, the predecessor of today's Czech Republic, was the third largest silver producer in Europe. Both Ag smelting, a procedure using Pb, and Pb smelting, peaked in 1890. Lead emissions from ore smelting rapidly decreased to zero after 1950. During the Communist years (1948–1989), the country was the third largest soft coal producer, while neighbouring East Germany was the largest soft coal producer in the world (Novák et al., 2010).

Concentration pollution data do not provide complete information about sources of pollution, e.g., what is the exact contamination range or how far does the metals migrate from their source (Äyräs et al., 1997) or what is the exact contribution of the background (Komárek et al., 2008).

Table 1.2 Examples of Pb isotopic compositions (^{206}Pb/^{207}Pb) of different anthropogenic Pb sources in the environment (Czech Republic)

Material	Locality	^{206}Pb/^{207}Pb	Reference
Coal	Ostrava – Hlubina	1.180 - 1.234	Mihaljevič et al., 2009
	Ostrava – Petr Bezruč	1.190	Mihaljevič et al., 2009
	Orlová – Lazy	1.167 – 1.173	Mihaljevič et al., 2009
	Radvanice – Kateřina	1.312	Mihaljevič et al., 2009
	Petřvald – J. Fučík	1.172 – 1.195	Mihaljevič et al., 2009
	Frýdek - Místek – Staříč	1.195	Mihaljevič et al., 2009
	Příbram	1.165	Ettler et al., 2004
Coal from energy industry	Ostrava	1.159 – 1.205	EU project Nr. CZ.1.02/2.1.00/11.13405
Primary ore from steel metallurgy	Ostrava	1.232	
Slag from lead metallurgy	Příbram	1.165	Ettler et al., 2004
Galena	Příbram	1.164	Ettler et al., 2004
Fly-ash from petrol combustion	Prague	1.135	Ettler et al., 2004
Leaded gasoline	Prague	1.111	Novák et al., 2003

Recent investigations of environmental pollution are mostly based on chemical analyses of different samples from environment (e.g. water, soil, precipitation). Different industrial processes emit different mineralogical phases, which allows the pollution source identification, even if the overall chemistry of the different emissions is similar. Thus, it is possible to obtain a clear "fingerprint" of mineral phases related to various industrial process and to assign an observed contamination directly to its source(s). The isotope composition of metals in the environment reflects their mixing from different sources, and source apportionment can be quantified in cases where all potential sources are characterized and have specific ratios (Komárek et al., 2008).

This approach has been widely used in the past for tracing Pb pollution and its sources, especially thanks to the wide availability of analytical techniques necessary for such studies (mainly quadrupole ICP-MS). Other isotope systems have recently been suggested as tracers of environmental pollution in pioneer studies, such as Cd, Cu, Cr and Zn (e.g., in Shiel et al., 2013 etc.).

Thanks to the recent development of high-resolution mass spectrometry, which allows high precision analysis and resolution of small isotopic variations, other isotopes may now also be studied (Pichat et al., 2003). These isotopes have been used to research anthropogenic pollution in airborne particles (Mattielli et al., 2009), metal industry processes (Shiel et al., 2010), and soils surrounding heavily contaminated sites (Bigalke et al., 2010).

Effects of atmospheric pollution on human health

Regarding human health, dangerous pollutant can be any substance that may possibly cause serious illness, contribute to increased mortality and/or possess a potential risk to humans. The hazards of substances to human health are based on clinical and epidemiological studies that examine the impact on human health. In the context of human health, "risk" is the probability that a noxious health effects may occur (Kampa and Castanas, 2008). Main concern is focused on the exposure of metals to humans and other organisms, especially due their ability to accumulate in the tissues (Kunzli et al., 2000). Children represent the most sensitive group, as the exposure of children to trace metals can increase greatly through the ingestion of metal-laden soil particles and dust via frequent hand-to-mouth activities (Wong et al., 2006).

The direct health impacts of trace metal contamination of the urban environment are usually difficult to assess due to the complexity of the medical factors involved (Shen et al., 1996). There are always multiple variations of substances of different composition in the atmosphere. Combination with various dosages and time of exposure can lead to diverse impacts on human health (Nriagu, 1988).

Bioavailability and bioaccessibility of metal(loid)s

Adriano (2001) defines bioavailability as a potential for living organisms to take up chemicals from food or from the abiotic environment to the extent that the chemicals may become involved in the metabolism of an organism.

Bioavailability/bioaccessibility of targeted compound can be influenced both by the nature of accepting organism and the chemical itself (physical-chemical properties, concentration etc.), and by the environmental factors (in soil e.g., pH, cation exchange capacity, type and the concentration of organic matter, redox potential, amount of Fe, Mn oxides and clay minerals etc.) (Adriano, 2001).

Human intake of trace elements occurs mainly via food ingestion as a consequence of bio-accumulation and biotransformation processes in biota. In the context of human health-risk assessment, bioavailability refers to the fraction of substance that reaches the blood from the gastrointestinal tract (bioavailable fraction) and that is available to promote its action in the exposed organism (Ruby et al., 1996). The determination of trace elements in food products and bioaccessibility and bioavailability studies of these minerals is of special concern because some of them are essential elements for humans but also because some are highly toxic. Toxic elements tend to accumulate in animals and humans and, as commented above, some species (Moreda-Piñeiro et al., 2011).

After air inhalation during breathing, suspended atmospheric particulate matter is deposited in the lung throughout several mechanisms, which are depending on the particles sizes. Following deposition, clearance of particles deposited in the respiratory system may occur via absorption of the dissolved fraction via blood, transport to lymph nodes or transport to the gastrointestinal tract (Kastury et al., 2017). PM can also enter the digestive system via swallowing of saliva and mucus (Chatelin et al., 2017; Mutlu et al., 2018). This fraction of atmospheric PM can be digested and the PM-bound trace metal then become soluble and bioaccessible fraction, which can be absorbed by the intestinal tract via passive transfer, facilitated diffusion, active transport, and micropinocytosis (Kastury et al., 2017; Gao et al., 2018).

According to Wragg et al., 2003, inhalation bioaccessibility may be defined as the fraction of toxicants dissolved in simulated lung fluids (SLFs) lining the respiratory system that is potentially available to cross the air-blood barrier of the respiratory system to reach blood circulation. Most particles in PM_{10} fraction will be deposited in the upper airways, where mucociliary mechanisms of clearance dominate to effectively remove particles via the gastrointestinal route (Kastury et al., 2017). Only particles with a smaller diameter (i.e., <5 mm) will reach the pulmonary region of the respiratory tract where they are more likely to dissolve in lung fluids or be phagocytized by resident macrophages (Wiseman, 2015). According to many researchers, the smaller the particle size, the deeper it travels into the lungs (Kastury et al., 2017).

The trend in exposure assessment methods is currently shifting away from total metal(loid) content analysis and towards assessing the fraction of metal(loid)s that are released from particles. The description of interstitial lung fluid composition in initiated the formulation of several SLFs and prompted the development of multiple in-vitro inhalation bioaccessibility models (Gamble, 1967 as cited in Kastury et al., 2017). Commonly known as the 'Gamble solution', this SLF originated from the extracellular fluid composition in the skeletal muscle described by Gamble in 1967. Extracellular fluid has a near neutral pH (7.4) and consists of a balance of cations (sodium,

potassium, calcium, magnesium) and anions (bicarbonate, chloride, monohydrogen phosphate, sulfate, organic acids, proteins) with presence of low concentrations of carbonic acid and non-electrolytes (nutrients, such as glucose and amino acid; waste products of protein metabolism) (Gamble, 1967 as cited in Kastury et al., 2017).

Environmental samples as contamination accumulators

Bioaccumulation

Bioaccumulation is a phenomenon, when an increase in the concentration of a chemical in a biological organism over time occurs, compared to the chemical's concentration in the environment (Kampa and Castanas, 2008).

Generally speaking, proper bioaccumulator must:

- accumulate the pollutant without being killed by the levels with which it comes into contact,
- have a wide geographical distribution,
- be abundant and representative of the collection area,
- allow the collection of sufficient tissues for analysis,
- be easy to collect and resistant to laboratory conditions,
- have a high concentration factor for the contaminant under study, and thus allow direct analysis with no prior increase in concentration and
- have a simple correlation between the quantity of contaminant contained in the organism and the average contaminant concentration in the surrounding environment (Szczepaniak and Biziuk, 2003).

Methods of bioaccumulation monitoring can be divided into two categories: active and passive. Active monitoring includes monitoring of certain species exposed to pollutants under controlled conditions. These include transplanting of tested organisms on observation site and methods in the test chamber. Passive methods include observation of appropriate bioaccumulators species directly at the place of their occurrence, i.e. the place of pollutants deposition (Godinho et al., 2009). Passive methods have a major

drawback, as in the environment all processes act at once and uncontrollably, and it is difficult to separate the individual processes and find the particular one (Ceburnis and Valiulis, 1999). Bioaccumulators may also exhibit a different behaviour due to different micro- and macroclimate conditions, such as temperature, humidity, light, acidity and altitude (Gerdol et al., 2014).

Evaluating of the pollution level by metals using living organisms was found particularly useful. Despite various constraints that this method brings, is still reliable way of evaluating the content of the pollutants in the environment (Szczepaniak and Biziuk, 2003).

Biomonitoring

Biomonitoring can be defined as a method of using biological materials/organisms to obtain information about the state of the biosphere. Information can be obtained either by observing changes in the behaviour of the monitored organism (change in species composition, richness, physiological or ecological performance, morphology), or by analysing the concentration of substances in tissues of biomonitor (Szczepaniak and Biziuk, 2003). Biomonitors are organisms that can be used for the quantitative determination of contaminants. Sensitive biomonitors may be of the optical type and are used as integrators of the stress caused by contaminants, and as preventive alarm systems (Conti and Cecchetii, 2001). Main advantages of biomonitoring are the simplicity and low financial demands of sampling, and continuous and regular presence of the organism, if proper organism is selected (Rai, 2016).

Biomonitoring can serve to determine the concentrations of trace elements in aerosols and their deposition. Properly selected monitor should concentrate elements of interest and quantitatively reflect environmental conditions. Organisms suitable for monitoring of state of the environment are lichens, mosses, ferns, grass, tree bark, tree rings, and pine needles (Wolterbeek, 2002). The use of cosmopolite organisms to assess pollution has developed notably during the last decades. Such organisms may be used as indicators of the bioavailability of the given contaminant over time, allowing comparison between contamination levels in geographically different areas (Conti and Cecchetii, 2001).

Characterization of pollution tracers

As scientific understanding of the environmental and health impacts of air pollution improves, there is an increasing demand for air quality monitoring techniques that can be easily applied in different situations. Although mosses and lichens are widely used in biomonitoring research, the application of other materials, such as grass, tree bark, tree rings, and pine needles are being commonly used pollution studies (Suchara et al., 2011; Stille et al., 2012; Cocozza et al., 2016; Kalinovic et al., 2016). Although for some biomonitors used, the mechanisms of trace element uptake and retention are still not sufficiently known (Szczepaniak and Biziuk, 2003; Salo et al., 2012)

Lichens

Lichens are considered to be the result of a symbiotic association of a fungus and an alga. More precisely the term "alga" indicates either a *Cyanobacteriae* or a *Chlorophyceae*; the fungus is usually an *Ascomycetes*. In this association, the alga is the part that contains chlorophyll and provides nutrients for water and minerals supplying fungus (Conti and Cecchetii, 2001). These organisms are perennial (i.e. live two and more years) and their morphology does not change over time. They grow slowly, have a large-scale dependence upon the environment for their nutrition and do not shed parts during growth. Lichens lack cuticle protecting them from atmospheric effects, means that the different contaminants are absorbed over the entire surface of the organism. Contaminants thus may accumulate in lichen tissues in concentrations that are significantly higher than their physiological requirements (Wolterbeek, 2002; Garty and Garty-Spitz, 2011).

Epiphytic lichens gain moisture and nutrients exclusively from wet precipitation, they are therefore very suitable organisms for monitoring of the atmospheric metals deposition. Lichens intercept allogeneic substances dissolved in wet precipitation, dry depositions, and gaseous emissions and can accumulate substances throughout the whole year (Aznar et al., 2008). Therefore concentrations of the trace elements in the lichen tissues largely reflect the environmental levels of these elements. The sensitivity of individual species of lichens to atmospheric deposition varies and depends on the type of growth form. Foliose-types of lichens are far more sensitive to contamination than microfoliose- and crustose-types (Seaward, 1993).

Great longevity of the most lichens species and also their occurrence on many polluted sites has led to the introduction of their use as long-term monitors of atmospheric

depositions. In addition, lichens as biomonitors have several advantages over conventional air sampling techniques (Szczepaniak and Biziuk, 2003).

Lichens may be used as bioaccumulators and biomonitors in different ways:

- by mapping all species present in a specific area,

- by the sampling of chosen lichen species and measurement of the pollutants that accumulate in the thallus or

- by transplanting suitable species of lichens from an uncontaminated area to a contaminated one, then measuring the morphological changes in the lichen thallus and/or evaluating the physiological parameters and/or evaluating the bioaccumulation of the pollutants (Seaward, 1993).

Since 1960s, lichens have been widely used as biomonitors of atmospheric pollution, demonstrating an exceptional capability to accumulate trace metals (Garty and Garty-Spitz, 2011; Doğrul Demiray et al., 2012). Lichen thalli analysis is one of the most commonly used lichen biomonitoring methods. (Doğrul Demiray et al., 2012). Analysis is based on the physical, chemical and biological properties of lichens which enable them to be used as monitors of metal deposition from the atmosphere (Jeran et al., 2002). It is a sensitive tool for detection of variety of atmospheric pollutants, such as trace metals, chlorinated hydrocarbons or radioactive fallout. They are also suitable for monitoring of air pollution using isotopes. Using lichens as biomonitors proved its worth as a suitable alternative to traditional methods of air sampling. Use of lichens is simple, cost effective, and provides the ability to monitor large areas at any time of year. This allows spatial and temporal evaluation of the accumulation of pollutants in the environment (Doğrul Demiray et al., 2012).

Mosses

Mosses are bryophytes that have no roots and cuticle layer. Mosses get most of their nutrients directly from atmospheric deposition. Nutrients are distributed throughout the whole body of moss due to lack of true vascular system (Rühling and Tyler, 2004), while metals are received primarily from atmospheric deposition rather than from the mineral components of the soil (Lee et al., 2005).

Mosses was been widely used as biomonitors of air pollution by metals in different countries (Cao et al., 2008). Moss biomonitoring seems to be more popular than lichens based methods (Berg and Steinnes, 1997; Sucharová and Suchara, 1998; Grodzińska et

al., 1999; Figueira et al., 2002) because it causes fewer technical and analytical problems than lichens and tree bark. Furthermore, mosses species are more tolerant to atmospheric pollutants than foliose lichens (Bargagli et al., 2002).

Mosses as indicators have the following advantages:

- many species grow under different environmental conditions, even in industrial and urban areas,

- they do not have epidermis and cuticle, so metal ions easily enter cells,

- they do not have a root system, thus there is no uptake of mineral substrates from other sources than the atmosphere,

- transport of minerals between segments is limited because of lack of vascular tissue and

- mosses accumulate metals in a passive way, acting like ion exchangers (Berg and Steinnes, 1997).

Monitoring methods related to mosses also have their drawbacks and limitations. Lack of suitable species of mosses in the monitored area may be one of the main restrictions. These areas are mostly anthropogenically polluted or heavily urbanized. In such cases, moss bag method is commonly used. Piece of moss from the relatively unpolluted natural area is removed and placed in nylon net and relocated to the area of interest. Moss is then analysed same like natural moss. Concentrations of pollutants from displaced mosses correlate with concentrations of metals from natural moss (Szczepaniak and Biziuk, 2003).

The use of mosses as monitors of air pollution has been shown as a good way, although to achieve the best results it is recommended their combined use of lichens to complement the information on the uptake and upkeep of metals. Biomonitoring of mosses represents simple and inexpensive method of air quality control (Szczepaniak and Biziuk, 2003).

Snow

In the last few decades, complex processes of atmospheric compounds, including transport and deposition pathways, impact on climate change, aquatic/soil systems and human health became better understood with use of snow chemistry (Steffen et al., 2002). Snow is considered to be an ideal medium to observe deposition of pollutants

from the atmosphere. Snowflakes can accumulate more organic and inorganic pollutants from the atmosphere than raindrops because of their larger surface area and slower fall velocity (Cereceda-Balic et al., 2012). Concentrations of dissolved elements in melted and filtered snow may be used to estimate deposition during winter (Walker et al., 2003b). Snow sampling allows geochemical scanning of large areas and provides information about current air pollution, while the re-suspension of earlier pollution load has no effect due to snow coverage deposited on all surfaces (Gregurek et al., 1998b). Atmospheric deposition events can be easily and cheaply sampled (Cereceda-Balic et al., 2012) in comparison with direct deposition monitoring. The analysis of the chemical composition of snow provides useful information about long-range distribution patterns of anthropogenic substances emitted into the atmosphere (Kuoppamäki et al., 2014).

It is possible to obtain fingerprints for each industrial emission source by observing element ratios of snow meltwater to meltwater + filter residue, as was introduced in Reimann et al. (1996) and detailed in De Caritat et al. (1998). The most important feature of these ratios is the consistency with which they change with distance from the smelters. When the snow sample is melted and filtered, it is possible to differentiate between water soluble (filtrate) and particulate dry deposition (filter residue) (Reimann et al., 1996). The obtained filter residue is further useful for mineralogical analyses (e.g., SEM), a supplementary tool for source identification (Gregurek et al., 1999). Now there is reasonable consensus on modern and preindustrial concentrations of Pb and other metals in snow in both Antarctica and Greenland and there is agreement that modern concentrations correlate with emissions from vehicles and metal production processes (Candelone et al., 1994).

Soil

Soil serve as the most important sink for trace metal contaminants in the terrestrial ecosystem. Their presence in the terrestrial environment represents a stationary source of trace metals, which may have a long half-life of perhaps several hundred years (e.g., Pb). Soils naturally contain a certain amount of metals called background. The amount of metal in the background depends primarily on the parent rock from which the soil originated. Urban soils are therefore an important indicator of human exposure to trace metals in the urban terrestrial environment (Nriagu, 1988; Mielke et al., 1999).

Accumulation of anthropogenic trace metals in soil depends on wet and dry depositions that transmit particles from air to soil (Dudka et al., 1996). Determination of total metals and their chemical speciation may provide useful information on metal bioavailability and toxicity (Knight et al., 1998).T he origin of natural and undisturbed soils can usually

be traced back to the natural and geological processes of their parent materials, whether their formation is associated with geological weathering, volcanic activities, and/or sedimentation. Therefore, the geological composition of bedrock enables an approximate estimation of background levels of trace metals in soils and often leads to the postulation of anthropogenic inputs when excessive trace metals are detected (Banat et al., 2005). Although this approach has been widely accepted in the evaluation of trace metal contamination of soils, its applicability can be severely limited in an urban setting where it is highly questionable that the soils originate from a single source (Wong et al., 2006).

Anthropogenic contamination of soils with metals represents a very serious environmental problem especially in industrial and urban areas (e.g., Komárek et al., 2007; Mihaljevič et al., 2006). While the vast majority of trace metals in soils are derived from anthropogenic sources, Pb isotopic studies proved that increased Pb concentrations can originate from natural processes as well (Hansmann and Köppel, 2000).

On a global scale all negative impacts negatively affect soil quality as well as the valuable ecosystem services provided by soil. Soil contamination can lead to intoxication of soil microbes, animals, plants and humans indirectly by ingestion of contaminated food plants (Bourennane et al., 2010). Long-term and extensive pollution may cause severe damage to vegetation and soil, including extended land degradation and creation of industrial barrens (Komárek et al., 2008). Assessing the spatial extent of diffuse soil contamination is a useful tool in understanding and monitoring the adverse effects of this large scale phenomenon (Reimann et al., 2000).

Tree rings

It is known that soils do not serve as ideal natural historical archives of pollution because metals are distributed between anthropogenic and geogenic sources and newer anthropogenic deposition cannot be precisely distinguished from older depositions (Battipaglia et al., 2010). Therefore, especially tree rings, peat deposits and lake/marine sediments are more suitable archives of pollution history often going thousands of years back (e.g., Le Roux et al., 2004; Renberg et al., 2002). Trees growing in areas with temperate climate have visually distinguishable tree rings and those can be precisely dated (Nabais et al., 1999). Annual growth rings of hardwoods, which are much more wide-spread across terrestrial environments and climatic zones than other established archives, may represent a useful alternative for historical pollution tracking (Savard, 2010). Although the time evolution of Pb isotopic composition is usually similar in

sediments and tree rings, the mode of metal accumulation is different (Novák et al., 2010).

Retrospective analyses of separate tree rings or bark encapsulated in the xylem are called dendroanalyses or dendrochemistry. Dendroanalyses assume that during growth separate tree rings reflect the composition of the environment and reflect the variations in the atmospheric deposition of elements and changes of the chemical composition of the soils and sediments (Watmough, 1999). Tree rings provide information about chemical changes in the concentration of pollutants over time, as well as about how variations in atmospheric deposition affect some key physiological processes and how trees adapt under changing ecological conditions (Leonelli et al., 2012).

Lead is a suitable element for isotopic dendroanalyses due to its minimal lateral mobility within the xylem (Watmough, 1999). Dendroanalysis is thus often applied in Pb isotopic studies for identifying Pb sources (Watmough, 1999; Bellis et al., 2002; Bindler et al., 2004; Patrick and Farmer, 2006).

Particulate matter (PM$_{10}$)

Particulate air pollution is a mixture of solid, liquid, or solid and liquid particles suspended in the air. The size of suspended particles varies, from a few nm to tens of µm. The largest particles (coarse fraction) are mechanically produced by attrition of larger particles. Small particles (<1 µm) are largely formed from gases, the smallest (<0·1 µm, ultrafine) of which are formed by nucleation resulting from condensation or chemical reactions that form new particles (Brunekreef and Holgate, 2002).

The potential risk of inhaled particles depends on the amount, the deposition site in the respiratory tract and the residence time before being removed (Sturm, 2010). The degree of penetration and deposition of PM in the human respiratory tract is related to its size, whereas the clearance process is determined by its solubility and chemical composition (Aleksandropoulou and Lazaridis, 2013). The atmospheric aerosols can be divided into fractions according to their particle size. A distinction is made between PM$_{10}$ ("thoracic" particles smaller than 10 µm in diameter that can penetrate into the lower respiratory system), PM$_{2.5}$ ("respirable" particles smaller than 2.5 µm that can penetrate into the gas-exchange region of the lung) (Brunekreef and Holgate, 2002). Fine particles with aerodynamic diameters of less than 1–2µ m can easily reach the alveolar region, and the carried trace elements can be adsorbed with an extent of up to 60– 80% (Dean et al., 2017).

Atmospheric particulate matter has various sources, both natural (crustal weathering, seawater drops evaporation, volcanism and natural forest fires) and anthropogenic (fossil fuel combustion, traffic, industrial activities, incineration and biomass burning). Particles generated by these processes are important carriers of various trace metals and carbon compounds (Muránszky et al., 2011).

Chapter II

Evaluating the suitability of different environmental samples for tracing atmospheric pollution in industrial areas

A. Francová, V. Chrastný, H Šillerová, M. Vítková, J. Kocourková, M. Komárek

Content

Abstract

Samples of lichens, snow and particulate matter (PM_{10}, 24 h) are used for the source identification of air pollution in the heavily industrialized region of Ostrava, Upper Silesia, Czech Republic. An integrated approach that uses different environmental samples for metal concentration and Pb isotope analyses was applied. The broad range of isotope ratios in the samples indicates a combination of different pollution sources, the strongest among them being the metallurgical industry, bituminous coal combustion and traffic. Snow samples are proven as the most relevant indicator for tracing metal(loid)s and recent local contamination in the atmosphere. Lichens can be successfully used as tracers of the long-term activity of local and remote sources of contamination. The combination of PM_{10} with snow can provide very useful information for evaluation of current pollution sources.

Introduction

Air pollution and the atmospheric deposition of metals onto natural environments has attracted increasing interest in the past decades (Aubert et al., 2006; Hernandez et al., 2003; Walker et al., 2003a; Zhang and Liu, 2004). The deposition of metals is considered a major environmental problem because metals are known to have a significant effect on ecosystems (Bargagli et al., 2002; Agnan et al., 2013) and human health (Pacyna et al., 2009). Compared to other types of environmental pollutants, metals are particularly dangerous because of their ubiquity and persistence (Luo et al., 2015).

One of the most important pollutant carriers in the atmosphere is particulate matter (PM). Particulate matter comes primarily from anthropogenic sources, such as coal-based power generation and industrial activities (e.g., heat generation, iron industry, coal coking, smelting), traffic and re-suspension processes from urban surfaces (Konieczyński et al., 2012). Three types of PM sources can be defined: i) long-distance sources (e.g., particles transported by wind); ii) short-distance sources (e.g., re-suspension of road- deposited sediments); and iii) traffic related sources and other general sources with low influence (Tippayawong et al., 2006). Although efforts have been made to lower industrial emissions, this problem persists with small combustion utilities, e.g., domestic sources. These sources are important, especially during winter, because different fuels are used and are hard to control (Konieczynski et al. 2012). Particulate matter has become an important subject of studies with the urban air quality being of special interest. Some studies (Wróbel et al., 2000; Grynkiewicz Bylina et al., 2005) indicated elevated concentrations of PM_{10} and $PM_{2.5}$ because of the growing amount of traffic, which has had a significant effect on the emission of particulate matter since the 1990s (Zajusz-Zubek et al., 2015).

The main forms of wet atmospheric deposition are vertical deposition (rain and snow) and horizontal deposition (fog and ice accretions) (Voldrichova et al., 2014). Snow is considered to be an ideal medium to monitor the deposition of pollutants from the atmosphere (Cereceda-Balic et al., 2012). Snow sampling allows the geochemical scanning of large areas and provides information regarding current air pollution, while the re-suspension of earlier pollution load has no effect because of snow coverage on

all surfaces (Gregurek et al. 1998b). A relatively high accumulation rate for snow favours investigations of pollutant sources during winter with snow episodes (Rosman et al., 2000). Atmospheric deposition events can be easily sampled (Cereceda-Balic et al., 2012) compared to direct deposition monitoring (Gregurek et al. 1998b). The deposition time can be defined from meteorological data (Kuoppamäki et al., 2014). Generally, snowflakes accumulate more inorganic pollutants from the atmosphere than raindrops because of their larger surface area and slower deposition (Cereceda-Balic et al., 2012).

Epiphytic lichens present another suitable sampling strategy for monitoring the atmospheric deposition of metals because they have no roots or well-developed cuticles, which allows them to absorb moisture and nutrients exclusively from the atmosphere (Simonetti et al., 2003). Lichens accumulate soluble elements and insoluble metal-rich particulates largely through (Wolterbeek, 2002) intercellular accumulation and the entrapment of metal particles (Szczepaniak and Biziuk 2003). Since the 1960s, lichens have been widely used as biomonitors of atmospheric pollution (Conti and Cecchetti, 2001 and references therein) because of their simplicity, cost efficiency, and ability to monitor large areas at any time of the year, which allows spatial and temporal evaluation of the accumulation of pollutants in the environment (Doğrul Demiray et al., 2012). For example, Simonetti et al. (2003) studied the isotope compositions of Pb in epiphytic lichens (*Usnea* and *Bryoria* spp.) in North America and proved that lichens can be effectively used as tracers of atmospheric pollution even at a regional scale. Similar studies were also performed in the Czech Republic. Sucharová et al. (2014) measured the Pb concentrations and Pb isotope compositions in moss samples from sites all across the Czech Republic. The authors demonstrated that the concentration of Pb in moss over the past fifteen years has been decreasing. Nevertheless, 90% of the Czech Republic is still affected by 435 µg m^{-2} year $^{-1}$ of atmospheric deposition of airborne Pb. Sucharová et al. (2014) also examined the surroundings of Ostrava, one of the most polluted areas in the EU. Many studies addressed the advantages of lichens and/or mosses for biomonitoring. Bargagli et al. (2002) found mosses to accumulate higher concentrations of lithophile elements (Al, Cr, Fe, Mn, Ni, and Ti) and atmophile elements (Hg, Cd, Pb, Cu, V, and Zn) in lichen. According to Reimann et al. (1999), lichens reflect the precipitation chemistry only to a limited degree for Ag, Al, As, Bi, Co, Cr, Cu, Fe, (Hg), Mg, Mo, Ni, Pb, (S), V, and Zn. However, inputs either via rain or snow for many elements seems to play an important role in determining the composition of lichen. Mosses reflect the precipitation chemistry for Ag, Al, As, B, Bi, Cd, Co, Cr, Cu, Fe, Mg, Mo, Ni, Pb, Rb, (S), Sr, and V. In general, moss reflects rain chemistry rather than snow.

Stable Pb isotopes are a powerful fingerprinting tool for tracing pollution sources in the environment. This method is based on the fact that natural sources (background Pb derived from weathering bedrocks) and anthropogenic sources have different Pb isotope compositions. Each Pb source has its own distinct isotope composition, so distinguishing individual sources of Pb in an environmental sample is possible (Gregurek et al., 1998b; Komárek et al., 2008). The main drawbacks of using Pb isotopes for tracing arise when the sources isotopically overlap or are not well defined. In this case, using only one type of environmental sample to trace anthropogenic inputs may be challenging and inefficient, and different samples are often necessary for source apportionment studies (Sen et al., 2016). Lichens, snow and PM_{10} are subjected to the same sources of anthropogenic pollution and thus should display similar Pb isotope signatures. Because the combination of these samples provides information on airborne pollution in general, investigating the content of metal(loid)s and Pb isotope composition provides a more holistic view on urban pollution (LeGalley et al., 2013). While many authors have focused on analyses of one type of sample (*lichens*: Riga-Karandinos and Karandinos, 1998; Jeran et al., 2002; Simonetti et al., 2003; *snow:* Gregurek et al., 1998b; Kuoppamäki et al., 2014; Wang et al., 2015; *PM:* Sharma et al., 2014; Zajusz-Zubek et al., 2015; Padoan et al., 2016) or different types of samples (e.g., Bargagli et al., 2002; Walker et al., 2003a; Le Roux et al., 2005; Cloquet et al., 2006; Aubert et al., 2012; Salo et al., 2012; LeGalley et al., 2013), only a few studies have investigated the suitability of different environmental samples for analyses of atmospheric pollution and identified the associated downsides (e.g., Bergamaschi et al., 2002; Dmuchowski et al., 2011).

Materials and methods

Study area

The study area is located in the Moravia–Silesian Region in the Northeast Czech Republic. The landscape forms a valley that is known as the Moravian Gate, which leads from the southwest to the northeast and into the Silesian region of Poland (**Fig**. **2.1**). Air typically flows through the valley, predominantly from the southwest. This area is considered to be one of the regions with the worst air quality in the EU

(Horalek et al., 2007). Anthropogenic pollution in this area mainly results from the heavy steel and coal industries but also from the dense transport infrastructure in the region (Mikuška et al., 2015). During winter, the air quality is highly influenced by emissions from local combustion sources (heating). The city of Ostrava is known for its long mining and smelting history. Black coal mines in the area originate from the 19th century, and three areas currently have a total of 8 active mines and 63 closed mines. The maximum coal production occurred in the 1980s, with a production of approximately 25×10^6 tons of coal (Novák et al., 2003). Additionally, several stationary industrial sources of pollutants (e.g., metals, particulate matter, nitrogen oxides, sulphur dioxide, and benzo(a)pyrene) exist directly in the city or in the close vicinity. The mixing of emissions from multiple sources and the complex atmospheric chemistry and transport patterns means that tracing and quantifying the emissions from different sources by studying the deposition of metal(loid)s in the environment highly challenging.

Sampling and sample preparation

Sampling sites can be divided into three different transects both in the city of Ostrava and its surroundings. The sites were chosen according to the predominant wind direction and positioned with respect to the main industries in the region. (**Fig. 2.1**). Sampling on each site was performed during two sampling campaigns. The first occurred in February 2015, when snowpacks, lichens and PM_{10} filters were collected. Snow samples were collected in duplicates from intact snow into 2-L acid-cleaned PET containers avoiding the upper layer which may be affected by dry deposition.

The total depth of the snow was between 20 and 40 cm, and the distance between samples at each site was 30-50 m. The duplicates were mixed after melting and acidified by concentrated HNO_3 (analytical grade). The four most abundant epiphytic lichens species, namely, *Physcia tenella* (Scop.) DC, *Hypogymnia physodes* (L.) Nyl.,*Xanthoria parietina* (L.) Th.Fr. and *Parmelia sulcata* Taylor, were collected from trees on every sampling site. Lichens were sampled from bark by using a ceramic knife to avoid possible contamination and placed in a plastic bag. The foliose lichen *Physcia tenella* was chosen for analyses because of its occurrence at all the sampling sites. Particulate matter sampling was performed by the Public Health Institute in Ostrava.
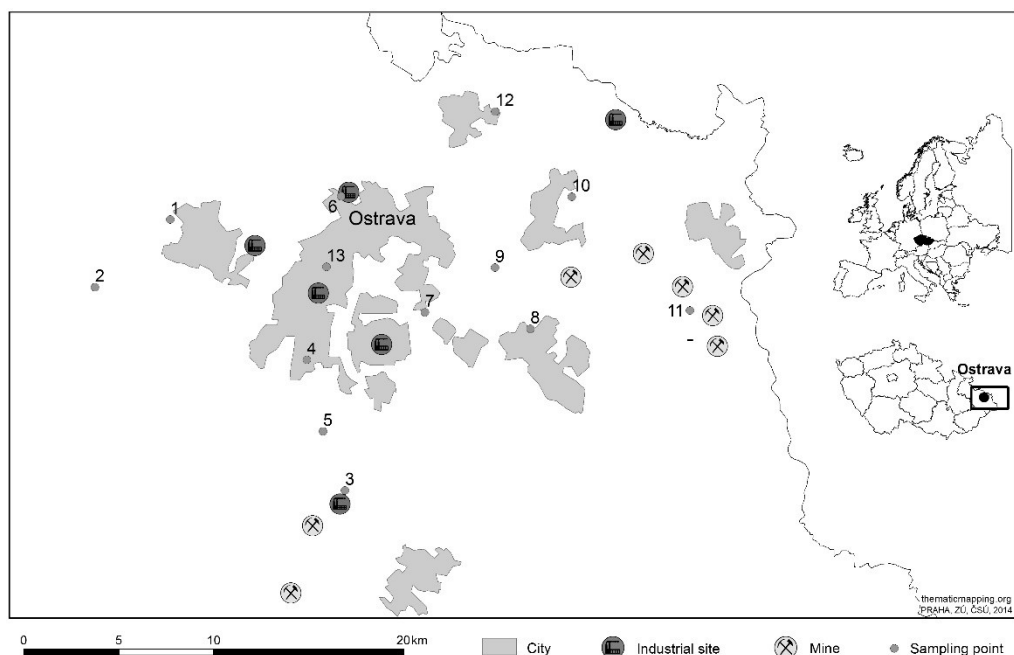
Figure 2.1

Study area – selected sampling points and industrial sources of contamination.

Airborne particulate matter samples were collected on nitrocellulose filters by using one mobile air sampler (High Volume Sampler DH-80, Digitel, Germany). The total sampling time was 24 h to obtain a sufficient air volume to determine the trace metal concentration. The average air volume that was collected every 24 h was approximately 500 m^3. Wind direction and velocity was measured every sampling day by the Public Health Institute, Ostrava, Czech Republic.

Ultrapure chemicals (Rotipuran Ultra, Carl Roth, Germany) and ultrapure H$_2$O (Milli-Q System, $<1\times10^{-18}$ Ohm cm^{-1}) were used for sample treatment and mineralization. The volume of the melted snow samples (bulk samples) was reduced by evaporation on a hot plate (100°C) to 50 mL. The solids in the snow samples are often filtered out (e.g. in Gregurek et al. 1998b; Wang et al. 2015) and subsequently mineralised for further analysis (Kashulina et al., 2014). Shotyk et al. (2005) state that particles originating from industrial sources have an average size of 0.5 μm in diameter, which is smaller than lithogenic particles containing Pb from natural sources. We did not filtrate the snow in this study to avoid risk of analyte loss and/or its contamination. The unfiltered snow samples were mineralised, which provided information on the metal

concentrations and Pb isotopes in the bulk sample. Mineralisation was performed in closed Savillex digestion vessels in a mixture of 6 mL HNO_3, 3 mL HCl and 1 mL HF and kept at 150°C for 24 h. After 24 h, the samples were evaporated to near dryness, and 2 mL of H_2O_2 and 2 mL of HNO_3 were added and heated again for four hours. The samples were then diluted with 25 mL of 2% HNO_3.

Lichens were dried overnight (60 °C), cleaned from bark and other residues, and ground and homogenised in a ceramic mortar. A mass of 0.25 g was mineralised in a mixture of 6 mL HNO_3 and 2 mL HF and heated in a sealed 60 mL Savillex digestion vessel on a hot plate at 150°C for 24 h. After 24 h, the samples were evaporated, supplemented by 2 mL of H_2O_2 and 2 mL of HNO_3 and heated again for four hours, then diluted to 25 mL by 2% HNO_3. The samples were analysed in duplicates.

PM_{10} nitrocellulose filter bases were dissolved by using 10 mL of HCl in Savillex digestion vessels (according to USEPA protocol 3050B) (USEPA, 1996a). A volume of 6 mL of HNO_3 and 2 mL of HF were added to the vessels after the dissolution of the nitrocellulose and heated for 24 hours on a hot plate at 150°C while sealed. The samples were then evaporated, supplemented with 2 mL of H_2O_2, and evaporated again. Then, 2% HNO_3 was added to a final volume of 25 mL.

The mineral horizon of deep soil (50-55 cm) was sampled in order to obtain background values of isotope composition in the area. A mass of 0.25 g was mineralised in 6 mL HNO_3 and 2 mL HF and heated in a sealed 60 mL Savillex digestion vessel on a hot plate at 150°C for 24 h. Samples were then evaporated, supplemented by 2 mL of H_2O_2 and 2 mL of HNO_3, heated again for four hours and then diluted to 25 mL by 2% HNO_3.

Concentration and isotope analyses

The concentrations of selected metal(loid)s (Cd, Cr, Cu, Ni, Pb, Zn, and As) were determined by using an inductively coupled plasma mass spectrometry (ICP-MS iCAP Q, Thermo Fisher Scientific, Germany). The certified reference materials BCR-482 Lichen (IRMM, Belgium) (for lichen analysis) and SRM 1640a Natural Water (NIST, USA) (for snow analysis) were used for QA/QC.The recovery rates for SRM 1640a were: 99 % (Al), 97 % (As), 104 % (Cd), 104 % (Cr), 102 % (Cu), 101 % (Ni), 93 % (Pb) and 97 % (Zn). The recovery rates for BCR-482 Lichen were: 98% (Al), 107% (As), 97% (Cd), 94% (Cr), 92% (Cu), 93% (Ni), 100% (Pb) and 98% (Zn). All the Pb isotope measurements (^{206}Pb, ^{207}Pb and ^{208}Pb) were determined by

using the ICP-MS. Correction for mass bias was performed by using analyses of SRM 981 (Common lead NIST, USA) after every two samples. We used the following certified values as references: 1.093 and 2.168 for $^{206}Pb/^{207}Pb$ and $^{206}Pb/^{208}Pb$ respectively. The samples were diluted to a concentration of 10-30 µg L^{-1} Pb to ensure that the detection always remained within the range of the 'pulse' mode. The standard errors for the measurements of the $^{206}Pb/^{207}Pb$ and $^{208}Pb/^{206}Pb$ ratios in SRM 981 were <0.3% RSD and <0.3% RSD, respectively. The standard errors for the measurements of the ratios in the environmental samples were as follows: <0.4 % RSD for $^{206}Pb/^{207}Pb$ and <0.3% RSD for $^{208}Pb/^{206}Pb$ in PM$_{10}$, <0.4 % RSD for $^{206}Pb/^{207}Pb$ and <0.4% RSD for $^{208}Pb/^{206}Pb$ in snow, and <0.3 % RSD for $^{206}Pb/^{207}Pb$ and <0.3% RSD for $^{208}Pb/^{206}Pb$ in lichens

Scanning electron microscopy analysis

Filters from the most exposed areas were subjected to investigations by scanning electron microscopy (SEM). First, a circle that was approximately 1 cm in diameter was cut from selected filters and placed on a conductive tape. All the samples were carbon-coated before analysis. A TESCAN VEGA3XMU scanning electron microscope (TESCAN Ltd., Czech Republic) that was equipped with a Bruker QUANTAX200 energy dispersive X-ray spectrometer (EDS) was used for imaging and semi-quantitative chemical analyses of the particles.

Results and discussion

Concentration of selected metal(loid)s

The concentrations of As, Cd, Cr, Cu, Ni, Pb and Zn in lichens, snowpacks and airborne particulate matter PM$_{10}$ are presented in **Table S 2.1-S 2.4**. The median concentrations followed this order: lichens: Zn > Pb > Cr > As > Cu > Ni > Cd; snowpacks: Zn > As > Cr > Pb > Cu > Ni > Cd; winter PM$_{10}$: Zn > Pb > Cu > As > Cr > Ni > Cd; and summer PM$_{10}$: Zn > Pb > Cr > As > Cu > Ni > Cd.

Significant differences in the concentration of the selected metal(loid)s existed across the 13 sampling sites. However, the concentration in lichen and snowpacks showed a similar trend: site 2 to the west of Ostrava was the least affected (**Fig. 2.2** and **Fig. 2.3**), and site 13 in the city centre was the most polluted (**Fig. 2.2** and **Fig. 2.3**; **Table S 2.1-2.4**). In other words, the remote forested area to the west (site 2) exhibited "background" concentrations of metal(loid)s, while samples that were collected in the city centre may reflect contamination from several sources. The sampling sites in the city centre (site 13) and near the smelter (site 7) were the most polluted by the selected metal(loid)s (**Fig. 2.2** and **Fig. 2.3**). High concentrations of the selected elements in the snow samples are clear evidence of recent contamination in Ostrava and its surroundings. Snow reflects the current conditions because no re-suspension of earlier pollution loads occurs (Gregurek et al. 1998b).

The PM_{10} fraction from the winter season exhibited different concentrations than the other samples (**Fig. 2.4**; **Table S 2.3 and S 2.4**). The lowest concentrations of metal(loid)s were observed at sampling site 4, which is a suburban settlement near the city of Ostrava. The highest concentration of metal(loid)s in PM_{10} was recorded at sampling site 7 near the smelter. The concentration was 2-15 times higher than at any other sampling site. Problems with poor air quality occur frequently in Ostrava, especially during winter, because of temperature inversion episodes and smog formation, which is characterized by increased total PM concentrations (Mikuška et al., 2015). The PM_{10} fraction that was collected during summer exhibited higher total concentrations of metal(loid)s at sites 10 and 12 near the border with Poland, which may indicate contributions of metal(loid)s from Poland (e.g., industrial area of Olkusz) (Chrastný et al., 2015) that are brought by north-western winds.

Pb concentrations

Lead was the second most abundant of the seven metal(loid)s in the samples (up to 43.6 mg kg^{-1} in lichens, up to 24.3 µg L^{-1} in snow, up to 1326 ng m^{-3} in winter PM_{10} and 339 ng m^{-3} in summer PM_{10}). The median values of the Pb concentrations in the studied lichens, snow and PM_{10} samples were higher than most values that have been reported in other studies (**Table 2.2**). The Pb concentrations varied the most in the PM_{10} fraction. For example, Pb exhibited low concentrations at sites 1, 2 and 4 during winter (see **Table 2.1**), which are on the edge of the city and thus far enough from industrial sources. The distance from a polluter is an important parameter that

influences Pb concentrations. The importance of the distance of a sampled site from the source was
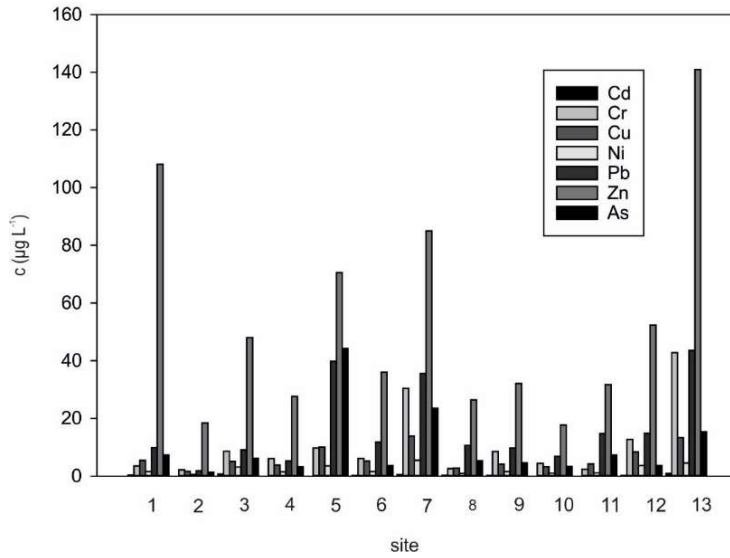
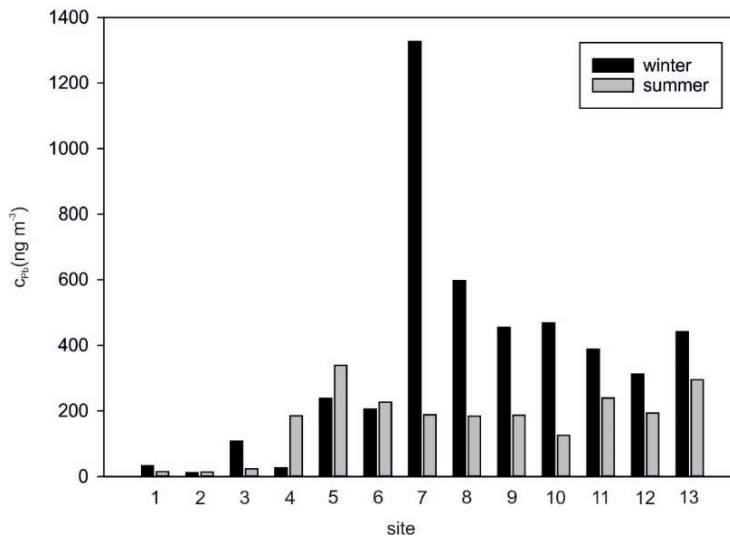**Figure 2.2** Concentration of metal(loid)s in samples of lichen (*Physcia tenella*).

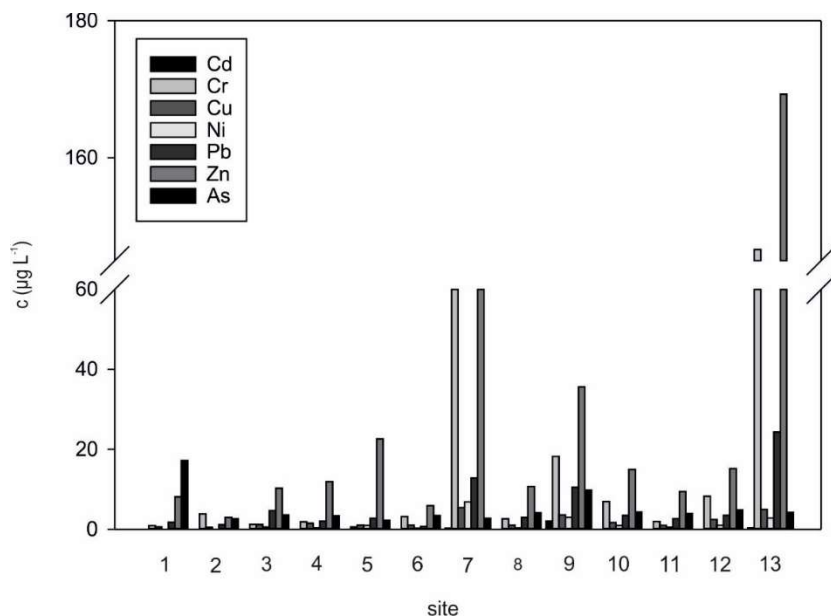**Figure 2.3** Concentration of metal(loid)s in samples of snow.

Figure 2.4 Comparison of Pb concentration in winter and summer PM$_{10}$ samples.

already highlighted by Bollhöfer et al. (1999). The same trend was observed by Aznar et al. (2008), who stated that sites that are located downwind of point sources receive more atmospheric pollutants. This effect, however, decreased with increasing distance from the smelter. Another possible explanation for the major differences in the PM$_{10}$ samples may be the contribution of the current wind direction.

The highest concentrations of Pb were observed at site 13 in lichens and snow, at site 7 in winter PM$_{10}$ and at site 5 in summer PM$_{10}$. The major portion of Pb that was emitted into the atmosphere originated from steel smelting or smelting furnace burning coal industries (Qi et al., 2016). Additionally, re-suspended soil dust that is enriched with Pb from the former use of leaded gasoline can be a major source of Pb along urban roadsides (Maher et al., 2008).

Differences between sampling locations and between sampling periods were also observed by SEM analyses. Representative textures and point chemical analyses (SEM/EDS) of selected PM$_{10}$ are given in **Figure 2.5**. Particulate matter may contain crystalline phases (typically coarser particles of quartz or aluminosilicates of natural origin), non-crystalline fly ash droplets (complex chemical compositions including Si-, Al-, Ca-, and Fe-rich particles of spherical shape, which indicates a high-temperature anthropogenic process), soot and biological materials (Song et al., 2014

Table 2.1 Lead concentration in samples of *Physcia tenella*, snow, winter and summer PM_{10}.

Sampling site	Lichen (mg kg^{-1})	Snow (µg L^{-1})	PM_{10} winter (ng m^{-3})	PM_{10} summer (ng m-3)
1	9.92	1.75	32.8	14.9
2	1.83	1.11	12.1	13.8
3	9.08	4.70	108	23.3
4	5.26	2.00	26.1	185.1
5	39.8	2.70	238	339
6	11.8	0.72	205	227
7	35.5	12.8	1326	188
8	10.7	2.97	597	184
9	9.73	10.5	454	186
10	6.86	3.42	468	125
11	14.7	2.64	388	239
12	14.8	3.45	313	193
13	43.6	24.3	442	295
Median	10.7	2.97	313	186

and references therein). Generally, silicate and Fe oxide particles were identified in all the sample matrices. Globules that were rich in Si or Fe were often observed, which agrees with the spheroidal particles that were reported by Campos-Ramos et al. (2009). Moreover, traces of Cl in the samples point to combustion processes (Campos-Ramos et al., 2009). Calcium sulphates that probably correspond to gypsum ($CaSO_4 \cdot 2H_2O$) were also identified (Song et al., 2014). Tiny droplets that contained metals were detected within most of the studied samples, which indicates that metal-bearing particles that were smaller than 1 µm were preferably trapped by the used filters. Metal-bearing particles occurred mostly as spherules, which suggest coal fly ash and exhaust from smelters as their source (Magiera et al. 2008; Sapkota and Cioppa 2012). In particular, up to 16 wt.% of Zn was recognized in such particles. However, Pb was detected in only one sample (0.20 wt.%, **Fig.2.5c**), which could be explained by the presence of nanoscale metal particles that are not detectable by the SEM technique that we used. In contrast, spheroidal lead sulphates that were > 2 µm in size were detected in rural areas in Mexico (Campos-Ramos et al., 2009). Significant variations were observed between the winter and summer PM_{10} filters that were collected from site 13.

Table 2.2 Comparison of median concentration in samples of lichens, snow and PM_{10} filters from this and other studies.

Sample	Pb	Reference
Lichen (mg kg^{-1})		
Czech Rep. (Ostrava)	10.7	this study
Greece (Megalopolis)	8.60	Riga-Karandinos and Karandinos, 1998
Italy (Pisa)	3.44	Scerbo et al., 2002
Nepal (Khumbu valley)	16.3	Bergamaschi et al., 2002
Canada (Yukon)	2.35	Simonetti et al, 2003
Finland (Turku, Harjavalta)	1.40	Salo et al., 2012
Snow (μg L^{-1})		
Czech Rep. (Ostrava)	2.97	this study
Russia (Kola Peninsula)	0.28	Gregurek et al, 1998
Tibet (Mt. Nayinqentanglha)	2.14	Huang et al., 2013
Finland (Lahti)	0.14	Kuoppamäki et al., 2014
China (all over the country)	2.50	Wang et al., 2015
PM_{10} (ng m^{-3})		
- winter	313	this study
- summer	186	
Iran (Tehran, summer)	121	Hassanvand et al., 2015
India (Kolkata, winter)	394	Das et al., 2015
Spain (Cantabria region, unknown)	8.15	Fernandez-Olmo et al., 2016
Italy (Turin, all year)	16.3	Padoan et al., 2016

Many spherical droplets and carbon-rich shapes were found in the winter-season sample (**Fig. 2.5c**), while no globs were observed within the sample from a summer season (**Fig. 2.5d**). The most contaminated site was site 10, which could also be attributed to the transfer of pollutants from Poland. However, no metal-bearing particles were detected by SEM in this sample. The effect of the steel industry on site 7 was almost eliminated because of the northern direction of the wind during the sampling day. This phenomenon may be related to a different wind direction during the sampling period. The contamination at all the sites was also higher because of the re-suspension of particles from adjacent surfaces.

Pb isotope composition

The Pb isotope compositions ($^{206}Pb/^{207}Pb$ and $^{208}Pb/^{206}Pb$) in the studied samples are presented in **Table 2.3**. The lead concentrations in most samples were high with a relatively wide $^{206}Pb/^{207}Pb$ isotope ratio pattern, which indicates that several sources contributed to the final Pb isotope compositions (Novák et al., 2003; Ettler et al., 2004; Komárek et al., 2008; Mihaljevič et al., 2009; Morton-Bermea et al., 2011; Del Rio-Salas et al., 2012; Chen et al., 2016). A number of different sources (coal burning in industrial facilities and in household, ironworks, Olkusz smelter) and their mixing resulted in a final isotope composition that can be further quantified. The burning of Czech lignite produces 5% of fly ash, which contains as much as 3000 ppm Pb (Novák et al., 2003). The coal from the studied region exhibited highly variable Pb isotope compositions ($^{206}Pb/^{207}Pb$ ratios between 1.167 and 1.312).

Lichen samples

We could identify the predominant contribution of locally used coal, either from industry or in local heating, which overlapped other less significant sources. The input of less radiogenic isotopes at site 13 ($^{206}Pb/^{207}Pb = 1.167$) may have originated from re-suspended particles that contained Pb from the former use of leaded gasoline as the site in the city centre with heavy traffic. Lichens that were sampled near roads by Cloquet et al. (2006) were suggested to have incorporated Pb from leaded gasoline that had fixed to soil particles ($^{206}Pb/^{207}Pb$ ratios approximately 1.13). The background value of the Ostrava region (from 1.167 to 1.208 for $^{206}Pb/^{207}Pb$) was wider than the ratios that were observed in other studies. Lichens that were sampled near Johannesburg by Monna et al. (2006) yielded a very wide range of $^{206}Pb/^{207}Pb$ ratios (1.082 – 1.257), where the highest $^{206}Pb/^{207}Pb$ ratios were found in lichens that were sampled near mine dumps. Particles from tailing dumps are likely to be re-suspended by winds and incorporated into lichens that grow nearby (Monna et al., 2006). The isotope compositions of Pb in the lichens exhibited lower variations in comparison to snow samples (**Fig. 2.8**), possibly because the data represented an integration of Pb from several years (Wolterbeek, 2002). Wu et al. (2016) suggested to use only 20 mm of the lichen outer parts to obtain pollution information from last 5 years of lichen growth. This method, however, is usable only in areas where lichens with sufficient thali size can be found. For this reason, we could not follow this method and obtain more specific and recent pollution data.
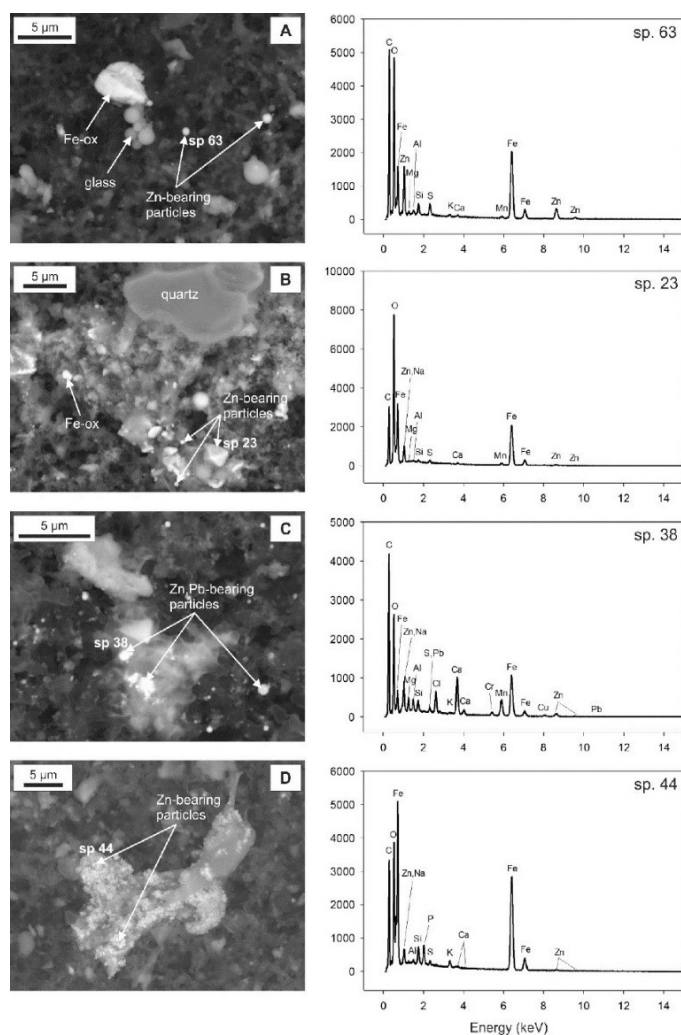
Figure 2.5 Images of PM_{10} in backscattered electrons (SEM) with corresponding EDS spectra of selected metal-bearing particles. (A) Site 12 summer sample, 5-mm iron oxide particle next to aluminium-silicate glassy globules and iron oxide-based droplets (<1 mm), containing up to 14 wt% Zn; (B) site 7 winter sample, Fe oxide droplets of various shapes and sizes, and Zn-bearing phases (up to 3 wt% Zn) that are associated with silicates; (C) site 13 winter sample, Fe oxide droplets and tiny metal-bearing spheres that are spread within a silicate/carbon-rich matrix; (D) site 13 summer sample, Zn-bearing Fe oxide-based clusters that are embedded in a silicate matrix.

Snow samples

The snow samples showed a wide variability of isotope compositions (**Fig. 2.6** and **Fig.2.8**), as it represent complex spectre of heavy particles currently occurring in the atmosphere. The following three sites (**Fig. 2.6b**) indicates three distinct strong sources of Pb: i) site 7, $^{206}Pb/^{207}Pb$ = 1.232 from metallurgy and the smelting of steel (Komárek et al., 2008) and/or coal that was mined from two mines in Ostrava (1.224 - 1.234; Mihaljevič et al. 2009); ii) site 9, $^{206}Pb/^{207}Pb$ = 1.214 from the smelting

of steel and metallurgy (Deboudt et al., 1999); and iii) site 13, $^{206}Pb/^{207}Pb = 1.167$ from the use of local coal that was mined in Karviná in ironworks ($^{206}Pb/^{207}Pb = 1.167$, Mihaljevič et al., 2009). The samples that were collected from site 6 and site 2 represent roughly background values ($^{206}Pb/^{207}Pb = 1.174 - 1.179$). The rest of the samples represent the mixing of emissions from strong sources with the background or a number of smaller local sources, e.g., the burning of local coal during household combustion. Clearly, the sampling sites 7, 9 and 10 were the most affected by the steel smelting plant and by the combustion of local coal. Similar results were suggested by Yu et al. (2013) in snow samples that were collected in China, where the $^{206}Pb/^{207}Pb$ ratios ranged between 1.160 and 1.200. During snowfall (or precipitation in general), larger particles tend to be deposited closer to the pollution source than finer particles. Snow thus reflexes the actual amount of pollutants emitted from the source and contribution of particular source can be easily estimated. It is also very convenient to combine snow analyses with PM_{10} as PM_{10} represents the lighter part of atmospheric aerosols sedimenting further from the source.

PM_{10} samples

The Pb isotope ratio ($^{206}Pb/^{207}Pb$) in the PM_{10} fraction lay within a narrow range of values (**Fig. 2.6** and **Fig. 2.8**). Both the winter and summer samples showed smaller ranges than the snow and lichen samples, varying from 1.165 to 1.188 in winter and from 1.166 to 1.175 in summer, probably because of the influence of local combustion systems during winter. Bollhöfer and Rosman (2001) sampled the inner city PM in Prague, Czech Republic, with a median value of $^{206}Pb/^{207}Pb = 1.127$ (the median isotope ratio of the PM that was sampled in this study was 1.169 during winter and 1.167 during summer). Data that were obtained from PM_{10} samples from the winter sampling campaign exhibited influence from strong local sources of Pb (**Table 2.3**). The Pb isotope composition in the samples could be attributed to different sources, including household combustion and the use of coal of miscellaneous origin. The samples of the summer PM_{10} filters showed contrasting results and were less isotopically variable than the samples from the winter campaign. Large variations between the obtained winter and summer samples could be observed, which indicates that PM that is sampled throughout the year exhibits a typical seasonal trend (Padoan et al., 2016).

Table 2.3 Pb isotope composition in lichen (*Physcia tenella*), snow and PM_{10} filter samples.

| Sampling site	Snow		Lichen		PM_{10} winter		PM_{10} summer	
	$^{206}Pb/^{207}Pb$	$^{208}Pb/^{206}Pb$	$^{206}Pb/^{207}Pb$	$^{208}Pb/^{206}Pb$	$^{206}Pb/^{207}Pb$	$^{208}Pb/^{206}Pb$	$^{206}Pb/^{207}Pb$	$^{208}Pb/^{206}Pb$
1	1.176	2.089	1.171	2.097	1.166	2.099	1.175	2.094
2	1.179	2.080	1.175	2.090	1.165	2.102	1.171	2.093
3	1.173	2.087	1.178	2.080	1.165	2.111	1.166	2.097
4	1.167	2.094	1.187	2.067	1.167	2.100	1.167	2.092
5	1.197	2.060	1.172	2.085	1.167	2.094	1.166	2.070
6	1.174	2.087	1.182	2.068	1.169	2.094	1.167	2.102
7	1.232	1.977	1.185	2.061	1.188	2.031	1.166	2.107
8	1.190	2.057	1.181	2.076	1.183	2.060	1.167	2.094
9	1.214	2.011	1.184	2.064	1.179	2.074	1.166	2.096
10	1.204	2.030	1.172	2.086	1.177	2.086	1.167	2.095
11	1.189	2.060	1.173	2.088	1.171	2.080	1.166	2.096
12	1.177	2.083	1.175	2.085	1.178	2.066	1.167	2.095
13	1.167	2.098	1.167	2.095	1.166	2.098	1.166	2.097
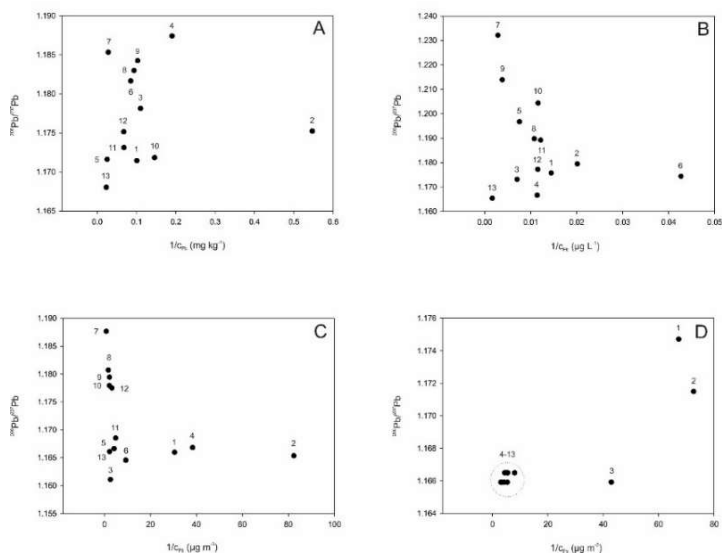
Figure 2.6 $^{206}Pb/^{207}Pb$ ratio vs. Pb concentration in lichens (A), snow (B) and PM_{10} filters that were sampled during winter (C) and summer (D).

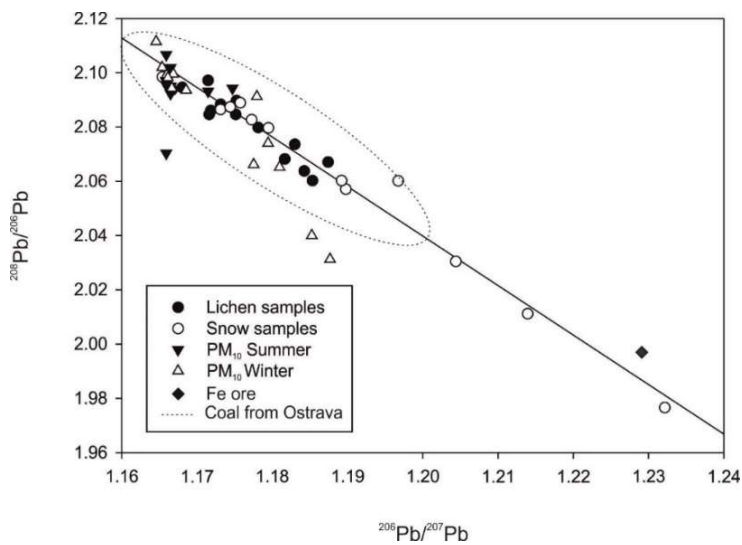**Figure 2.7** Three-isotope plot ($^{206}Pb/^{207}Pb$ versus $^{208}Pb/^{206}Pb$) showing the distribution of Pb isotope compositions in lichen, snow and PM_{10}.
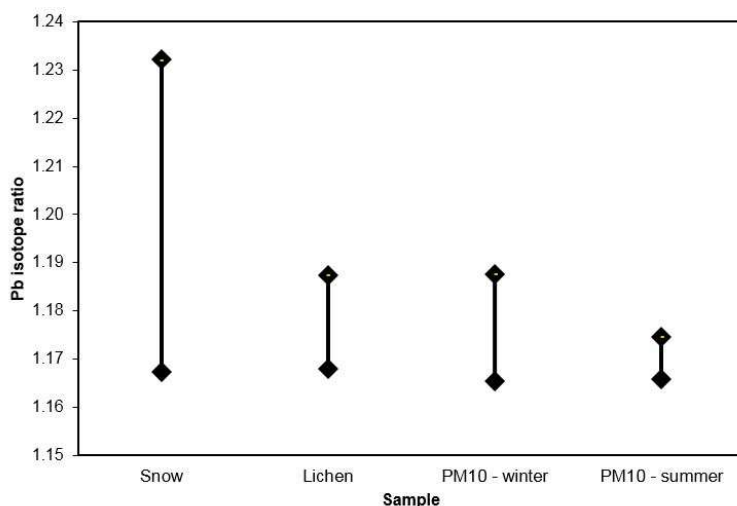
Figure 2.8 Ranges of $^{206}Pb/^{207}Pb$ ratios in samples of snow, lichen and PM_{10}.

Winter samples include metals from the combustion of local coal, while summer samples does not contain particles from those sources; thus, only current sources of particles should be detectable. Additionally, samples with low concentrations of Pb showed lower $^{206}Pb/^{207}Pb$ ratios (site 1 and site 2). The influence of the steel industry, as recognised in other samples, was not apparent. The reason for this phenomenon could have been the unstable wind direction during the sampling period, which mixed sources from different directions. Strong effects from the meteorological conditions during sampling were also observed by Erel et al. (1997) and Gioia et al. (2010). In these studies, variations between Pb isotope signatures and the actual wind direction/speed were identified; for example, Gioia et al. (2010) found strong vehicular sources of PM_{10} in N winds, and S winds brought more radiogenic Pb from industrial areas. In our study, considerable differences were observed on sites in wind tailing of the strong source (site 7, 8 and 9; **Fig. 2.4**). Furthermore, the homogeneity in summer PM_{10} might be caused by different weather conditions in summer. Better dispersion conditions in summer allows pollution to quickly leave the area. There are also no temperature inversion episodes, which may hold the pollution in the area. Atmospheric aerosols can thus be easily homogenised.

Identification of contamination sources with different sampling strategies

Three likely anthropogenic sources of Pb can be identified based on our Pb isotope composition analyses: i) metallurgical activities, ii) the combustion of local bituminous coal, and iii) the re-suspension of particles that contain Pb from the former use of leaded petrol. According to the relatively high Pb concentrations in the studied samples, we can assume that natural Pb did not contribute significantly to the overall Pb in the samples (Cloquet et al., 2015). The deep soils (50 - 55 cm) in the study area had an isotope composition of $^{206}Pb/^{207}Pb = 1.215$. Comparably high isotope ratios were only found in snow samples at sites near the smelter and in tailing dumps. These findings prove insignificant contributions from geogenic sources, so industrial sources largely contributed to the environment (Ettler et al., 2004; Komárek et al., 2007; Chen et al., 2016). The isotope composition of Pb that is emitted into the atmosphere during metallurgical processes closely reflects the isotope composition of the processed material, such as Pb ore or secondary processed materials that contain Pb (Ettler et al., 2004; Komárek et al., 2007). During the EU project Nr. CZ.1.02/2.1.00/11.13405, we measured a primary ore from a steel metallurgy in the city of Ostrava. The value of $^{206}Pb/^{207}Pb$ for the ore was 1.23, which is very close to the isotope ratios that were found in the snow samples (mainly at sites near the smelter) and corresponds to the $^{206}Pb/^{207}Pb$ ratios that were measured in aerosols near a steel metallurgy plant in France ($^{206}Pb/^{207}Pb$ = 1.22; Deboudt et al. 1999). Lead in coals tends to be more radiogenic because it contains U and Th as trace constituents (Witt et al., 2010). Coal that is mined in the Ostrava region covers a very wide range of isotope ratios (1.167 - 1.312, Mihaljevič et al. 2009), and the measured ratios in almost all our samples fell within this range. Moreover, the $^{206}Pb/^{207}Pb$ values varied from 1.159 to 1.205 for coal that was used in the energy industry in Ostrava (from EU project Nr. CZ.1.02/2.1.00/11.13405). In the region of Central Europe, distinguishing Pb that originates from coal burning from the background source ($^{206}Pb/^{207}Pb$~1.19) is difficult, but this source surely contributes to the isotope composition of the "industrial" Pb mixture in the studied area (Novák et al., 2003; Komárek et al., 2008). The influence of mining processes on the environment can be recorded years after mine closure (Saunier et al., 2013). Coal burning and other industrial activities became more important sources of Pb emissions after phasing out of the leaded gasoline (Veron et al., 1999). The re-suspension of particles that contain Pb from leaded gasoline is a possible source of less radiogenic isotopes in areas, where Pb with low $^{206}Pb/^{207}Pb$ ratio was added to gasoline. Even despite the fact that leaded gasoline was phased out almost twenty years ago. Del Rio-Salas et al. (2012) discovered traces of leaded gasoline in samples of dust in Mexico (leaded gasoline was phased out in 1997 in Mexico and in 2000 in the Czech Republic), which indicates the influence of Pb-gasoline on soils and soil-derived particles that are influenced by re-

suspension. Kelepertzis et al. (2016) also observed low $^{206}Pb/^{207}Pb$ ratios from the re-suspension of particulates that were deposited from past vehicular exhaust emissions of leaded gasoline (samples of urban soils from Athens). According to Novák et al. (2003), the gasoline that was used in the Czech Republic contained Pb with a low $^{206}Pb/^{207}Pb$ ratio from the Broken Hill deposit, Australia (1.030 – 1.100), with additives originating from East Germany or Russia (1.110 – 1.130). After phasing out, the influence of this source became less important and the contribution from local industrial Pb became more apparent (Cloquet et al., 2015). The variability of isotope compositions in relation to seasonal variations in emissions is also important, i.e., increases in coal burning during winter and decreases in industrial and automobile emissions during summer holidays (Deboudt et al., 1999).

Relevance of the studied indicators for source identification

Lichens can accumulate and integrate pollution from many different sources, including local and even distant sources, and accumulate contaminants for several years or even over their entire lifetime (Conti and Cecchetii 2001). For this reason, the concentration of atmospheric Pb and Pb isotope ratios tend to be homogenised through time (Cloquet et al., 2015). Saunier et al. (2013) found lichens to be contaminated mainly through the dust fixation of particles that are transported by wind rather than selective bioaccumulation. Lichens can also accumulate pollutants by re-suspension of dust particles. In this study, we found lower isotope variations in lichens compared to snowpacks and similar isotope compositions as in the winter PM_{10} fraction. We suggest lichens to be used as tracers of the long-term activity of local and remote sources of contamination. However, a number of studies proved lichens suitability as biomonitors of metal(loid)s (e.g., Jeran et al. 2002; Aubert et al. 2006).

In this work, we propose fresh snow as the most reliable and useful environmental sample for tracing recent industrial sources of metal contamination in complex industrial areas (Gregurek et al. 1998b; Rosman et al. 2000; Walker et al. 2003a) because continuous snow cover stops the re-suspension of particles that are deposited on surfaces covered by permanent snow cover. There is an apparent similar trend when comparing snow and PM_{10} data. However, the interpretation of these results relies heavily on the knowledge of the isotope composition of Pb in atmospheric aerosols, which is sometimes poorly known (Rosman et al., 2000). Relatively heavier atmospheric particles are deposited near local sources, while lighter PM_{10} is transported according to the wind direction and can be attributed to both local and remote sources

(Shotyk et al., 2015). The mixing between local and remote sources is suggested because PM_{10} remains in the atmosphere for a much longer time than heavier particles. Thus, much lower Pb isotope variability within the PM_{10} fraction compared to the snow samples was found.

The composition of PM_{10} samples depends on the current wind direction and air mass flow (Erel et al., 2006). The PM_{10} fraction consists of particles with a mean aerodynamic diameter of 10 μm or less, which can travel long distances, assuming that PM_{10} filters can reflect remote sources because of the mixing of air (Erel et al., 2006). Any differences in Pb concentrations and isotope compositions between winter and summer samples are also important because these samples reflect changes in atmosphere during seasons (Padoan et al., 2016). Samples may also be affected by the re-suspension of road particles (Del Rio-Salas et al., 2012; Kelepertzis et al., 2016). Our results thus suggest that PM_{10} samples are not useful for tracing long-term activities of local sources of contamination because they reflect sources in relation to the actual wind direction. On the other hand, the combination of PM_{10} and snow can becomes a powerful tool for evaluation of current pollution sources as PM_{10} provides information on pollution for a particular single day. Short term sampling reflects the influence of local point sources.

Conclusions

Because there is no fractionation of Pb isotopes during industrial processes, sources of atmospheric pollution in industrial areas can be relatively well defined. As expected, the highest concentrations of Pb were observed in the city centre and near the smelter. The isotope ratios of $^{206}Pb/^{207}Pb$ in snow samples varied greatly, with the highest values obtained from sites near the smelter. The Pb isotope ratio ranges in lichens and PM_{10} (especially those that were sampled during summer) were narrower. According to these findings, the main sources of Pb were i) metallurgical activities, ii) the combustion of local bituminous coal, and iii) traffic as possible historic source of less radiogenic Pb from the re-suspension of particles. We have confirmed that every sample is suitable for a different sampling scenario. Lichens can be used to trace the long-term activities of local and remote sources; however, the Pb concentrations and signals from pollution tend to be homogenised because of the long exposition time. Additionally, this method

is not useful in highly polluted areas with low abundance of lichen species. Snow samples proved to be the best indicators for tracing local recent pollution because they accurately capture time and space variability during the winter. Furthermore, we propose the use of PM_{10} with snow samples to obtain a broader and general idea. The PM_{10} filters that were obtained from the winter and summer sampling campaigns differed greatly; large variations between the summer and winter samples were observed. Winter samples may be used as records of wintertime local coal combustion, while summer samples can mainly detect industrial sources of pollution. Daily or short-term sampling of PM_{10} represents a very useful tool to obtain information on the actual pollution situation. Nevertheless, PM_{10} samples should be used in relation to the actual wind direction.

Supplementary material

Table S 2.1 Concentrations of selected metal(loid)s (mg kg^{-1}) in *Physcia tenella*

Sampling site	Cd	Cr	Cu	Ni	Pb	Zn	As
1	0.36	3.52	5.43	1.58	9.92	108	7.35
2	0.05	2.16	1.65	0.52	1.83	18.4	1.33
3	0.74	8.63	5.08	3.13	9.08	47.9	6.16
4	0.11	6.03	3.80	1.47	5.26	27.6	3.24
5	0.20	9.73	10.1	3.56	39.8	70.5	44.2
6	0.24	6.09	5.23	1.60	11.8	36.0	3.68
7	0.48	30.4	13.8	5.49	35.5	84.9	23.5
8	0.29	2.58	2.78	0.93	10.7	26.4	5.32
9	0.27	8.50	4.11	1.61	9.73	32.1	4.59
10	0.15	4.39	3.27	1.01	6.86	17.7	3.30
11	0.22	2.37	4.21	1.16	14.7	31.7	7.27
12	0.24	12.7	8.38	3.68	14.8	52.3	3.74
13	0.93	42.8	13.3	4.55	43.6	141	15.4
Median	0.24	6.09	5.08	1.60	10.7	36.0	5.32

Table S 2.2 Concentrations of selected metal(loid)s ($\mu g\ L^{-1}$) in snow samples

Sampling site	Cd	Cr	Cu	Ni	Pb	Zn	As
1	0.06	0.89	0.58	0.18	1.75	8.09	17.2
2	0.09	3.83	0.45	0.16	1.11	2.96	2.61
3	0.13	1.19	1.18	0.52	4.70	10.2	3.58
4	0.09	1.86	1.49	0.33	2.00	11.9	3.37
5	<0.02[*]	0.57	1.04	0.96	2.70	22.60	2.19
6	0.05	3.14	1.01	0.28	0.72	5.89	3.38
7	0.29	61.9	5.42	6.83	12.8	61.8	2.70
8	0.09	2.61	1.01	0.32	2.97	10.7	4.12
9	2.03	18.2	3.57	3.01	10.5	35.6	9.80
10	0.17	6.96	1.63	0.91	3.42	15.0	4.34
11	0.10	1.93	0.98	0.49	2.64	9.44	3.92
12	0.17	8.22	2.41	0.99	3.45	15.1	4.82
13	0.38	147	4.92	2.79	24.3	169	4.19
Median	0.10	3.14	1.18	0.52	2.97	11.9	3.92

* under limit the of quantification

Table S 2.3 Concentrations of selected metal(loid)s ($ng\ m^{-3}$) in PM_{10} filter samples collected during the winter period

Sampling site	Cd	Cr	Cu	Ni	Pb	Zn	As
1	2.73	46.9	36.3	32.6	32.8	236	40.8
2	< 0.01[*]	172	21.5	117	12.1	175	50.2
3	< 0.03[*]	115	40.0	70.0	108	1082	50.8
4	1.77	34.9	31.5	29.5	26.1	231	26.6
5	5.26	53.7	206	177	238	1033	155
6	5.24	85.7	196	40.0	205	1881	191
7	56.8	185	300	51.7	1326	13572	57.0
8	14.0	53.3	94.3	53.0	597	1996	119
9	12.1	62.5	315	34.0	454	1804	90.4
10	12.4	33.4	70.1	28.8	468	2248	70.4
11	11.9	26.1	368	249	388	1057	73.3
12	6.86	41.5	2454	2239	313	1965	134
13	12.8	134	76.1	109	442	3192	115
Median	6.85	53.7	94.3	53.0	313	1804	73.3

*: under limit the of quantification

Table S 2.4 Concentrations of selected metal(loid)s (ng m^{-3}) in PM$_{10}$ filter samples collected during the summer period

Sampling site	Cd	Cr	Cu	Ni	Pb	Zn	As
1	0.36	35.3	40.8	21.0	14.9	191	11.3
2	1.36	25.7	22.0	15.6	13.8	549	47.4
3	0.86	224	41.2	105	23.3	472	20.2
4	8.10	116	89.3	58.3	185.1	910	47.4
5	8.71	84.9	83.4	29.9	339	1462	51.6
6	5.86	5033	85.3	3963	227	598	115
7	4.78	31.8	42.8	19.6	188	652	14.3
8	4.05	85.0	69.2	26.8	184	737	110
9	4.40	55.4	449	93.3	186	778	100
10	2.40	13582	283	11232	125	239	128
11	4.37	59.4	62.7	354.9	239	844	101
12	7.17	11166	181	8770	193	1319	102
13	7.19	57.81	74.0	34.3	295	708	75.9
Median	4.40	84.9	74.0	58.3	186	708	75.9

Chapter III

Suitability of selected bioindicators of atmospheric pollution in the industrialised region of Ostrava, Upper Silesia, Czech Republic

A. Francová, V. Chrastný, H. Šillerová, J. Kocourková, M. Komárek

Content

Abstract

This study is a continuation of our preceding research identifying suitable environmental samples for the tracing of atmospheric pollution in industrial areas. Three additional types of environmental samples were used to characterize contamination sources in the industrial area of Ostrava city, Czech Republic. The region is known for its extensive metallurgical and mining activities. Fingerprinting of stable Pb isotopes was applied to distinguish individual sources of anthropogenic Pb. A wide range of $^{206}Pb/^{207}Pb$ ratios was observed in the investigated samples: $^{206}Pb/^{207}Pb = 1.168 - 1.198$ in mosses; $^{206}Pb/^{207}Pb = 1.167 - 1.215$ in soils and $^{206}Pb/^{207}Pb = 1.158 - 1.184$ in tree cores. Black and brown coal combustion, as well as metallurgical activities, are the two main sources of pollution in the area. Fossil fuel burning in industry and households seems to be a stronger source of Pb emissions than from the metallurgical industry. Concentration analyses of tree rings showed that a significant increase in As concentrations occurred between 1999 and 2016 (from 0.38 mg kg^{-1} to 13.8 mg kg^{-1}). This shift corresponds to the use of brown coal from Bílina, Czech Republic with an increased As concentration. The burning of low quality fuels in households remains a problem in the area, as small ground sources have a greater influence on the air quality than do industrial sources.

Introduction

The monitoring of air pollution through the use of living organisms provides low-cost information on the nature and quantity of pollutants (Loppi and Bonini 2000). Biomonitoring represents a suitable approach for the screening of air quality at higher spatial resolutions (Vuković et al., 2015). The use of stable Pb isotopes has been proven as a valid tool for tracing ("fingerprinting") environmental pollution. This method is based on comparisons of the Pb isotopic composition (e.g., ^{206}Pb/^{207}Pb) in environmental samples and different Pb sources in the area. Each Pb source has its own specific isotopic composition, thus it is possible to distinguish the individual sources of Pb in the environment (Komárek et al., 2008).

Mosses are bryophytes that have no roots or cuticle layer and thus obtain most of their nutrients (and metals) directly from atmospheric deposition than from the mineral components of the soil (Lee et al., 2005). Terrestrial moss accumulates nutrients and heavy metals from atmospheric deposition almost entirely through the surfaces of their above-ground parts. Metals are effectively adsorbed on pectins and on the cell structures of the body segments of 1 – 3-year-old mosses. For this reason, the concentrations of metals in mosses correlate closely with their atmospheric deposition loads over a given period of time (Sakalys et al., 2009) and it is usually assumed that the elements acquired by mosses represent some fraction of the elements present in their immediate environment (Loppi and Bonini 2000). Nutrients are distributed throughout the entire body of the moss due to the lack of a true vascular system (Grodzińska and Szarek-Łukaszewska 2001). Terrestrial mosses are therefore used as bioindicators of current deposition load levels (Sucharová et al., 2014). Moss biomonitoring seems to be more popular than lichens based methods (Berg and Steinnes 1997; Sucharová et al. 2014; Figueira et al. 2002; Sucharová and Suchara 1998), because it causes fewer technical and analytical problems than lichens, as moss species are more tolerant than foliose lichens to atmospheric pollutants (Bargagli et al., 2002).

Lichens and mosses are suitable biochemical tracers of environmental pollution, although unlike tree rings, they cannot be used as archives of pollution (Tommasini et al., 2000). The majority of Pb in wood is derived from atmospheric pollution. Pb can be transported into the tree either directly through aerial interception, or indirectly, through the uptake of Pb accumulated in the soil (Bindler et al., 2004). A number of studies have assessed dendrochemical records using Pb isotope analyses and some of

them proved to be faithful records of historical changes in heavy metal deposition (Mihaljevič et al., 2008; Novák et al., 2010; Zuna et al., 2011). However, there is still much uncertainty over their reliability as historical archives (Bindler et al., 2004).

The accumulation of anthropogenic trace metals in soil depends on wet and dry deposition that transmits particles from air to soil. Trace metals are common pollutants in urban industrial soils (Dudka et al., 1996). In recent years, the most significant entry of metals into the soil has been through anthropogenic processes, such as smelting, mining and agricultural activities (Epelde et al., 2012). Leaded gasoline is often blamed for the unusually low $^{206}Pb/^{207}Pb$ isotope ratios (1.15 – 1.16) found in the atmosphere, in plant materials, and in soils' O-horizons throughout Europe (Sucharová et al., 2014). According to Reimann et al (2012), the median $^{206}Pb/^{207}Pb$ isotope ratio for European agricultural soils is 1.258 for northern Europe and 1.195 for central and southern Europe.

The main aims of this study are to i) evaluate the suitability of different environmental samples (moss, soil, tree cores), with different durations and methods of contaminant accumulation, for source fingerprinting using Pb isotope analysis in highly industrialised areas; ii) determine main sources of Pb pollution in the area and iii) create a database of suitable environmental samples for the overall assessment of pollution in the area. We searched for Pb of anthropogenic origin in samples collected in industrial city. We demonstrate that it is important to choose suitable type of sample for the isotope fingerprinting, as there are different entrapment mechanisms for each sample type.

Materials and methods

Study area

The study area is located in the Moravia–Silesian Region in northeastern Czech Republic. The landscape forms a valley known as the Moravian Gate, which runs from the southwest to the northeast and into the Silesian region of Poland (**Fig. 3.1**). Air predominantly flows through the valley from the southwest. The Moravian-Silesian Region is one of the most urbanised and industrial areas in Central Europe and for a

long time there has been a problem of high levels of air pollution particles of anthropogenic origin, which are among the highest in Europe. The sources of the particles are i) high concentrations of industrial production; ii) large densities of local heating using solid fuels and iii) concentrated transport infrastructure (Blažek et al., 2013). The specific levels of pollutant concentrations in the air depend on the characteristics of the resources, the amount of pollutants discharged by them and the physical geographic conditions of the country. The intensity and pattern of the pollutants' dispersion is dominantly determined by weather conditions. To further understand the dynamics of the air pollution changes, it is necessary not only to consider changes in emissions, but in particular, the relationship between concentrations of pollutants and meteorological conditions (see Francová et al. 2017). The city of Ostrava is known for its long mining and smelting traditions. Considerable changes brought a restructuring of the economy as a result of systemic transformations in the late 80's and 90's of the last century. Technological changes, the closing of unprofitable and environmentally harmful industrial companies, and increased public awareness of environmental protection has led to systematic improvements of air quality since the mid-90s (Blažek et al., 2013). Due to the mixing of emissions from multiple sources and complex atmospheric chemistry and transport patterns, it is highly challenging to trace and quantify the emissions from different sources by studying the deposition of metal(loid)s in the environment.

Sampling and sample preparation

Sampling sites were divided into three different transects, both in the city of Ostrava and in its surroundings. The sites were chosen according to the predominant wind direction and the position with respect to the main industries in the region. (**Fig. 3.1**). Sampling on each site was conducted during June 2015 and October 2016. All types of samples were obtained on every sampling location.

Three types of samples were chosen: moss, soil and tree cores. Usage of moss and soil samples is very common in studies addressing contaminated sites (Sucharová et al., 2014; Ares et al., 2015; Doležalová Weissmannová et al., 2015; Reimann et al., 2016). While soil serves as a sink of all emitted metal(loid)s for a long period of time, lifetime of moss is relatively short (5-10 years) and the accumulation time of the contaminants is shorter. We also assume homogenization of the $^{206}Pb/^{207}Pb$ signal, which may make identification of actual pollution sources difficult. Tree cores were used in addition sample types described above. Tree cores serve as archive of historical metal(loid)s
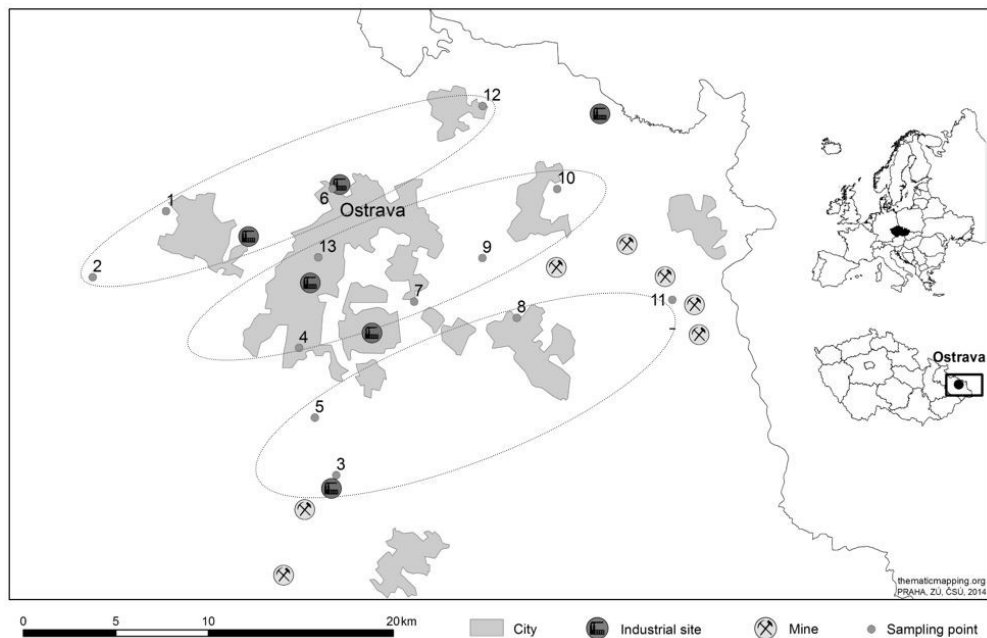
Figure 3.1 Simplified map of 13 sampling points with industrial sites, mines and city outlines characterised. Dotted lines define sampling transects.

deposit and are easily found and sampled (in comparison with e.g. peat or lake sediments).

Samples of terrestrial mosses were collected from the ground at each sampling site. Mosses were trimmed from the surface using a ceramic knife, cleaned of large solid particulates or bits of other plants, and placed in a plastic bag. *Hypnum cupressiforme* (Hedw.) was the most abundant and was present at every sampling location and thus was chosen for analysis. Two additional moss species were collected, *Brachythecium rutabulum* (Hedw.) and *Polytrichumformosum* (Hedw.). Duplicate soil samples were collected using a stainless-steel sampler. Each sample was divided according to the soil horizon. Only the upper horizon (approximately $0 – 10$ cm) and the lower mineral horizon (35 - 50 cm) were used for further analysis. The soil samples were then air-dried at 60°C, ground in a ceramic mortar and passed through a 2 mm sieve. Ultrapure chemicals (Rotipuran Ultra, Carl Roth, Germany) and ultrapure H_2O (Milli-Q System, $<1 \times 10^{-18} \, \Omega \, cm^{-1}$) were used for sample treatment and mineralisation. All moss and soil samples were analysed in duplicate. Mosses were washed in deionised water in order to remove soil and other particles. Samples were dried at 60°C to constant weight.

Dried mosses were manually cleaned of remaining particles and parts of plants, then ground and homogenised in a ceramic mortar. Only the green tips of mosses were used. The feed of 0.250 g was supplemented with a mixture of 6 mL HNO_3, 2 mL HF and heated in a sealed 60 mL Savillex digestion vessel on a hot plate at 150°C for 24 hours.

Soil pH was determined in duplicate using a 0.2 M KCl solution (pH 5.7). 5 g of soil was transported to 100 mL PE centrifugation bottles and diluted with 12.5 mL of 0.2 M KCl, shaken for 30 minutes and then left to settle for 2 hours. The pH value was then measured using a calibrated pH metre. Total dissolution of soil samples was carried out using a microwave unit (Anton-Paar, Austria). The dissolution method used was EPA 3051A (USEPA, 2007): 9 mL of HNO_3, 3 mL of HCl and 1 mL of HF were added to a 0.250 g soil sample. Dissolved samples were then transferred to a Savillex digestion vessel, completely evaporated and then diluted with demineralised water to 25 mL.

Tree cores (3 mm diameter) were extracted from coniferous trees *Larix decidua* (Mill.), *Picea abies* (L.) H. Karst. and *Pinus sylvestris* (L.) at a height of 1.5 m using a stainless steel corer. Coniferous trees are considered to have the greatest potential for the reconstruction of heavy metal pollution history because of the primitive nature of their wood (Watmough, 1999). Samples were collected from sites in steelworks tailings, in the city centre and in the forest. Cores were extracted from the side of the tree that is exposed to the pollution source. Each sample's outer wood section and bark were acid-washed in 10% HNO_3 to remove surface contamination and weakly bound metals (Watmough and Hutchinson 2003). The individual cores were cut into 10-year segments using a ceramic knife and then dried at 60°C overnight. After drying, they were transferred into porcelain crucibles for ashing at 400°C for 6 hours. The digestion of individual segments (weights in the range of 0.1–0.2 g) was carried out using the EPA 3052 (USEPA, 1996b) method with a microwave unit (Anton Paar, Austria). The dissolved samples were then transferred to a Savillex digestion vessels and evaporated to incipient dryness and then diluted with demineralised water to 25 mL.

Concentration and isotope analyses

The concentrations of the selected metal(loid)s (Cd, Cr, Cu, Ni, Pb, Zn, As, Fe) were determined using the ICP-MS (iCAP Q, Thermo Fisher Scientific, Germany). The certified reference materials BCR-482 Lichen (IRMM, Belgium) (for moss analysis) and Montana Soil 2711a (NIST, USA) (for soil analysis) were used for QA/QC. The recovery rates for SRM 1640a were 107% (As), 108% (Cd), 107% (Cr), 103% (Cu), 105% (Ni), 105% (Pb) and 101% (Zn). The recovery rates for BCR-482 Lichen were 100% (As), 90% (Cd), 92% (Cr), 98% (Cu), 92% (Ni), 94% (Pb) and 90%

(Zn), the recovery rates for MONTANA SOIL 2710a were 102% (As), 110% (Cd), 90% (Cr), 90% (Cu), 96% (Ni), 97% (Pb) and 101% (Zn). All the Pb isotope measurements ([206]Pb, [207]Pb and [208]Pb) were determined using the ICP-MS. Correction for mass bias was performed by using analyses of the SRM 981 (Common lead NIST, USA) after every two samples. We used the following certified values as references: 1.093 and 2.168 for [206]Pb/[207]Pb and [206]Pb/[208]Pb, respectively. The samples were diluted to a concentration of 10-30 µg L^{-1} Pb to ensure that detection always remained within the range of the 'pulse' mode. The standard errors for the measurements of the [206]Pb/[207]Pb and [208]Pb/[206]Pb ratios in SRM 981 were 0.1% RSD and 0.1% RSD, respectively. The standard errors for the measurements of the ratios in the environmental samples were as follows: 0.7% RSD for [206]Pb/[207]Pb and 0.8% RSD for [208]Pb/[206]Pb in moss, 0.8% RSD for [206]Pb/[207]Pb and 0.7% RSD for [208]Pb/[206]Pb in soil, and 0.7% RSD for [206]Pb/[207]Pb and 0.4% RSD for [208]Pb/[206]Pb in tree cores.

Results and discussion

Concentration of selected metal(loid)s

Table 3.1 summarises the analytical results for the concentration of metal(loid)s in the samples. In the city of Ostrava, metals can enter samples from various sources such as traffic, emissions from industrial establishments, combustion of coal and municipal wastes (Doležalová Weissmannová et al., 2015). On average, sampling sites 6 and 13 were the most polluted by metal(loid)s. Both sites are influenced by nearby large industrial sites (coking plant and steelworks). Concentrations of metal(loid)s in moss *Hypnum cupressiforme* were lowest at the forest sampling site (site 2), and highest in the city centre (site 13). As the *H. cupressiforme* carpets are very dense, this species tends to absorb elements from atmospheric deposition more effectively than other moss species that form less dense carpets (Sucharová and Suchara 1998). Significantly higher total concentrations of metal(loid)s were found in soil samples. As expected, the A horizon is more polluted by metal(loid)s than the C horizon. Horizon A was most polluted at site 6, which is situated near ironworks and a coke plant. Steel production processes can lead to extensive emission of dusts and solid wastes containing heavy metals, which are significant sources of contamination for surrounding soils (Qing et

al., 2015). Tree core samples exhibit low concentrations of metal(loid)s in general. The lowest concentrations of metal(loid)s were recorded from samples obtained from *Pinus sylvestris* at site 13. There are several unexpected shifts in the metal(loid)s concentrations at the site near steelworks (site 7). We observed a decrease in Pb concentrations in years 2006 – 2016, which would correspond with the phasing out of leaded gasoline, which occurred in 2000. There are also significant increases in As and Fe concentrations, which is contrary to a decrease in the economy's output and to overall improvement in emission production (for example, steelworks near site 7 have used cloth filters to reduce the amount of dust since 2011).

Concentration of Pb

Concentrations of Pb in the studied samples are presented in **Table 3.2** and **Table 3.3**. The results indicate that Pb is strongly enriched in topsoil (A-horizon) compared to the values observed in mineral soils (C-horizon). Sampling sites 6 and 13, which are both in close vicinity of steelworks and a coke plant, are the most polluted by Pb. Elevated values of Pb were also observed at forest site 2 in the humus layer. The enrichment of

Table 3.1 Statistical summary of metal(loid) total concentrations (mg kg^{-1}) in samples

Sample	Cd	Cr	Cu	Ni	Pb	Zn	As
Moss							
Median	0.8	22	9.4	4.8	13	70	12
Min	0.4	6.6	5.0	1.8	5.2	38	8.0
Max	1.5	73	37	14	55	200	17
Soil (A-horizon)							
Median	0.8	81	23	28	57	100	23
Min	0.2	63	12	22	8.4	52	16
Max	1.5	130	110	44	170	620	33
Soil (C-horizon)							
Median	0.3	82	17	27	15	69	19
Min	<0.1	39	13	20	6.6	36	6.9
Max	1.4	99	140	53	120	550	24
Tree rings							
Median	1.5	5.8	5.3	1.6	0.4	48	0.6
Min	<0.1	1.0	0.9	0.3	<0.1	14	<0.1
Max	11	44	34	11	3.4	420	110

Pb and other metal contaminants in organic-rich surface soils in comparison with the underlying mineral matrix is a common pattern in soil studies (Klaminder et al., 2011). The least contaminated samples were obtained at site 8, which is a backfill in a housing estate. Samples of the soil's horizon A seem to be the most polluted of all the examined samples. Mosses are the most affected at site 5, which is situated on the outskirts of Ostrava city, with no apparent reason for such high levels of Pb. High Pb values were also found at site 6, which corresponds to findings in the soil samples. In comparison to the soil Pb content, tree cores have low Pb concentrations. Lowered Pb concentrations in the younger parts of tree rings can be observed (**Table 3.3**). Lead is absorbed by foliage and tree bark and deposited in the most recent tree rings after translocation via the phloem. For Pb, direct above-ground uptake by trees may be more important than for other trace metals (Novák et al., 2010). Tree cores from all the examined trees exhibit highest Pb concentrations in the 1980's. These high values correspond to Pb emissions from coal combustion and industry (Zuna et al., 2011). The most expressive reduction of Pb is visible at site 7, where the Pb content dropped from 3.39 mg kg^{-1} in 1986 - 1996 to 0.12 mg kg^{-1} in recent years.

Table 3.2 Concentration of Pb (mg kg^{-1}) in studied samples

Sampling site	Moss	A-horizon	C-horizon
1	11	44	40
2	13	120	12
3	11	24	15
4	11	18	17
5	55	57	13
6	46	170	98
7	27	76	11
8	5.2	8.4	6.6
9	21	240	80
10	14	49	24
11	7.2	37	10
12	12	64	11
13	51	140	120

Table 3.3 Concentration of Pb (mg kg^{-1}) in samples of tree rings in years 1966 – 2016

Sampling site	Tree species	2016-2006	2006-1996	1996-1986	1986-1976	1976-1966
2	*Larix decidua*	0.3	0.1	0.1	0.9	0.9
7	*Picea abies*	0.1	3.3	3.4	-	-
9	*Pinus sylvestris*	0.3	0.5	1.6	-	-
10	*Pinus sylvestris*	0.4	0.7	-	-	-
13	*Pinus sylvestris*	0.2	0.4	0.3	0.3	-

Lead isotope composition

Ideally, the source emissions should have a well-defined Pb-isotope ratio that deviates from the local background (e.g., Ettler et al., 2006; Klaminder et al., 2003; Reimann et al., 2012). The Pb isotope compositions (^{206}Pb/^{207}Pb and ^{208}Pb/^{206}Pb) in the studied samples are presented in **Tables 3.4** and **3.5**. The range in most samples is very wide (1.158 - 1.215), which indicates contributions from several pollution sources. Contributions from lithogenic Pb can be identified in horizon C of the soil samples (1.174 - 1.215). Samples of tree cores exhibit lower isotope ranges than samples of soil and moss (^{206}Pb/^{207}Pb = 1.158 – 1.184).

Moss samples

Moss samples exhibit narrower ^{206}Pb/^{207}Pb isotope ratios (1.168 - 1.198; **Fig. 3.2**) than found in the soil samples. The flux of Pb in moss was possibly from two strong sources: i) ^{206}Pb/^{207}Pb = 1.198 derived from metallurgical activities at site 7; and ii) Pb derived from the use of local coal in industrial facilities at site 6 and site 13 (^{206}Pb/^{207}Pb = 1.171 and 1.167, respectively). The sample obtained at site 7, which is in close vicinity to the smelter, shows a higher isotope ratio than other samples (the isotope ratio of the primary ore used in smelter is 1.23). High Pb isotope ratios were also found at sampling sites 9 and 10, which are downwind of the smelter and therefore deposition of the emissions occurred. It is clear that the smelter is a local source of Pb with a high ^{206}Pb/^{207}Pb ratio. According to Sucharová et al. (2014) the Ostrava region represents the spatially largest Pb anomaly in the Czech Republic. Sucharová et al. (2014) found ^{206}Pb/^{207}Pb = 1.171 – 1.186 ratios in the Ostrava moss samples and postulate the origin to be the use of coal in energy production. An industrial source emitting Pb with a ^{206}Pb/^{207}Pb = 1.167 signature is recognisable in moss, lichen and snow samples from the city centre (site 13, see Francová et al. 2017 for further information) and in the

sample of horizon A soil at site 6. We can assume that this is the main source of Pb pollution in the city centre, probably of the industrial origin.

Soil samples

Pb isotope ratios in soil samples fall within a wide range of values ($^{206}Pb/^{207}Pb = 1.167$ - 1.201 in the A-horizon and $^{206}Pb/^{207}Pb = 1.174 - 1.215$ in the C-horizon; **Fig. 3.3** and **Fig. 3.4**). Three strong sources of Pb with low $^{206}Pb/^{207}Pb$ values were identified in the A-horizon: i) $^{206}Pb/^{207}Pb = 1.167$ at site 6; ii) $^{206}Pb/^{207}Pb = 1.173$ at site 9; and iii) $^{206}Pb/^{207}Pb = 1.172$ at site 13, all from the use of local coal (Mihaljevič et al., 2009) either in the steel industry, the energy industry or from household combustion. According to Novák et al. (2010) and Zuna et al. (2011), Pb in the soil surface layer (0 - 10 cm) is bound in exchangeable and surface-bound positions and this Pb has a ratio of $^{206}Pb/^{207}Pb = 1.16$-1.19. Pb in the deeper parts of the profile is bonded primarily to silicates and mostly has the isotope composition of lithogenic Pb ($^{206}Pb/^{207}Pb > 1.2$). Major natural atmospheric Pb sources generally have $^{206}Pb/^{207}Pb$ ratios of 1.20 – 1.22 and it is often assumed that an input of Pb with a $^{206}Pb/^{207}Pb$ ratio less than 1.19 is from an anthropogenic source. For example, the Equatorial Atlantic (Abouchami and Zabel 2003) or European loess soils (Klaminder et al., 2003; Sterckeman et al., 2006) which can be considered as some of the major soil dust emitting areas on a global scale, have
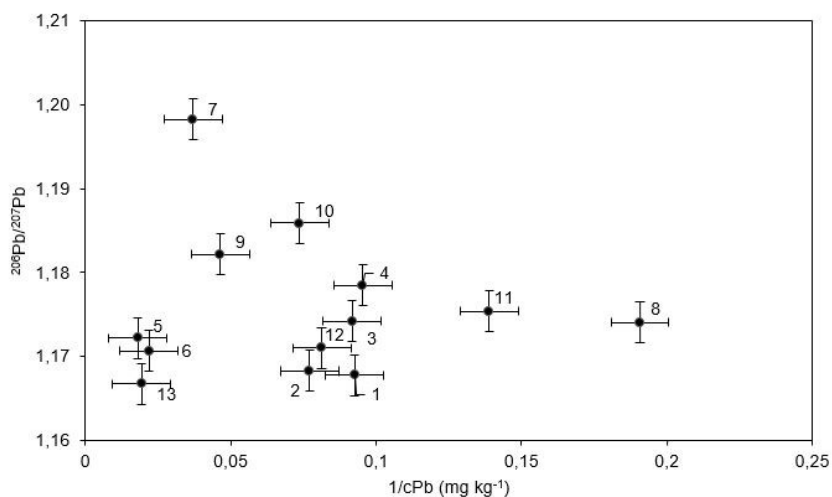

Figure 3.2 $^{206}Pb/^{207}Pb$ ratio vs. Pb concentration in samples of *Hypnum cupressiforme*.

[206]Pb/[207]Pb ratios ranging between 1.19 and 1.25. Soils reflect the accumulated Pb contamination of tens of years. They integrate the metal input from various sources and, thus, level out isotope differences of individual sources that might have existed at the time of Pb deposition. A leaded gasoline signal should still be present in the Czech Republic, as it was an important source of Pb to the European environment from the 1940's to the 1980's and was only banned 16 years ago (Sucharová et al., 2011). However, a signal of Broken Hill Pb was not visible in the analysed samples of the A or C soil horizons.

Tree rings

The range of isotope ratios in tree cores is narrower than in the other samples (1.158 – 1.184; **Fig. 3.6**). From the 1990's to present, a shift from low to higher ratios is apparent in the tree rings. This trend is most visible in samples of *Picea abies* from site 7, where the [206]Pb/[207]Pb isotope ratio went from 1.168 during 1986 - 1996 to 1.184 for 2006 – 2016 (**Fig. 3.5**). This corresponds to the likelihood that a source with a lower [206]Pb/[207]Pb ratio affected the tree rings during the 1990s. A similar change in [206]Pb/[207]Pb ratios can be observed at site 9 and 13, and the same shift of isotope ratios was also observed by Zuna et al. (2011) in peat samples from the Czech Republic. The samples indicate a recent reduction of the concentration of airborne Pb and an increase in the [206]Pb/[207]Pb ratio values. This observation is in agreement with the introduction of Pb-free gasoline and further reductions in industrial emissions. According to Novák et al. (2003), the leaded gasoline that was used in the Czech Republic contained Pb with a low [206]Pb/[207]Pb ratio from the Broken Hill deposit, Australia (1.030 – 1.100), with additives originating from East Germany or Russia (1.110 – 1.130). After being phased out in 2000, coal burning and industrial activities became more significant sources of Pb and contained higher [206]Pb/[207]Pb ratios (Veron et al., 1999). The smallest ratio range was observed in tree cores from *Larix decidua* at site 2 (ratios varied between 1.176 and 1.179). In combination with the low concentrations of Pb in all investigated years, we can assume that site 2 represents background Pb values for the area. We can further assume that the vast majority of Pb observed in the sampled trees was derived from the atmosphere. Isotope ratios in tree rings more closely resemble the isotope ratios in mosses, in which Pb is deposited exclusively from the atmosphere, than the ratios present in the soil samples.
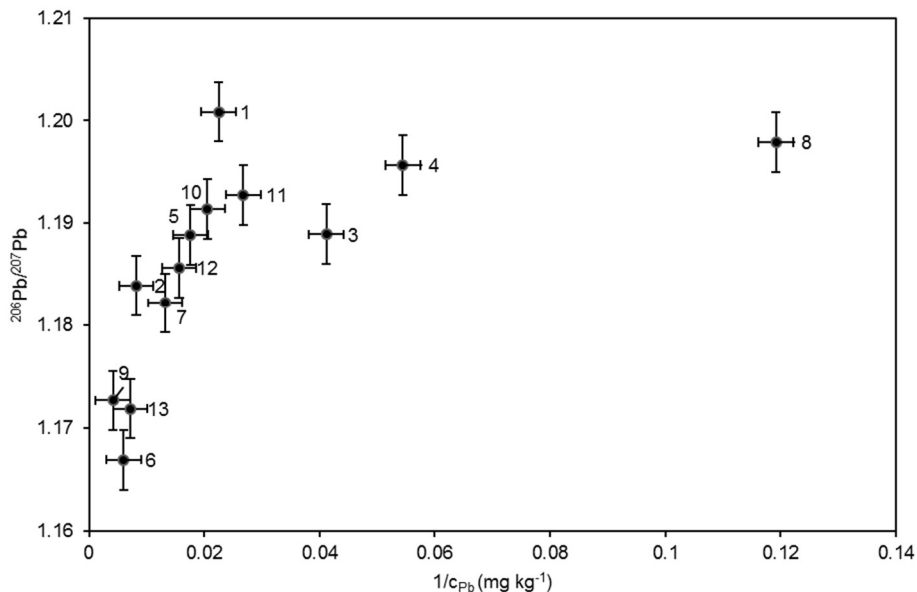
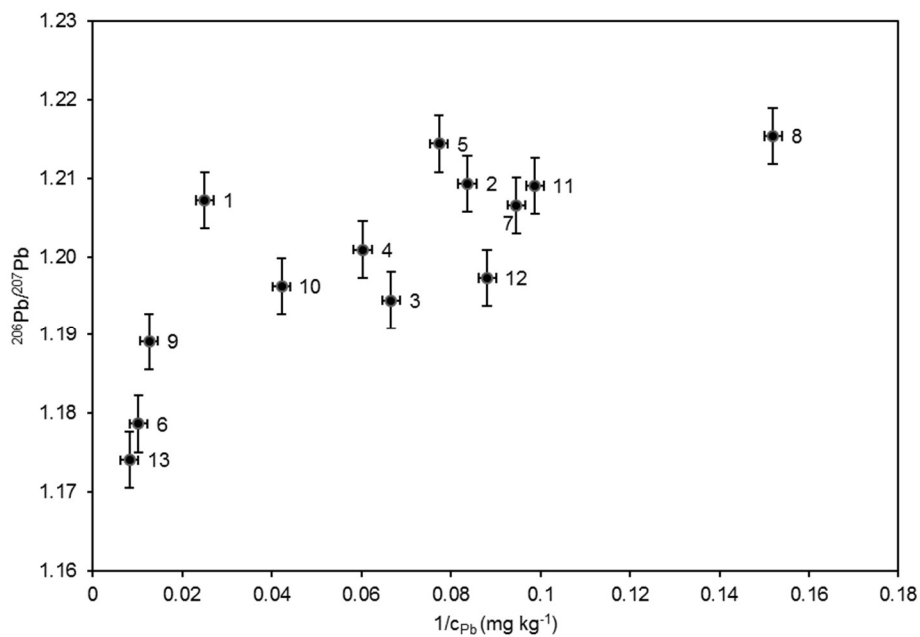**Figure 3.3** $^{206}Pb/^{207}Pb$ ratio vs. Pb concentration in samples of soil horizon A.

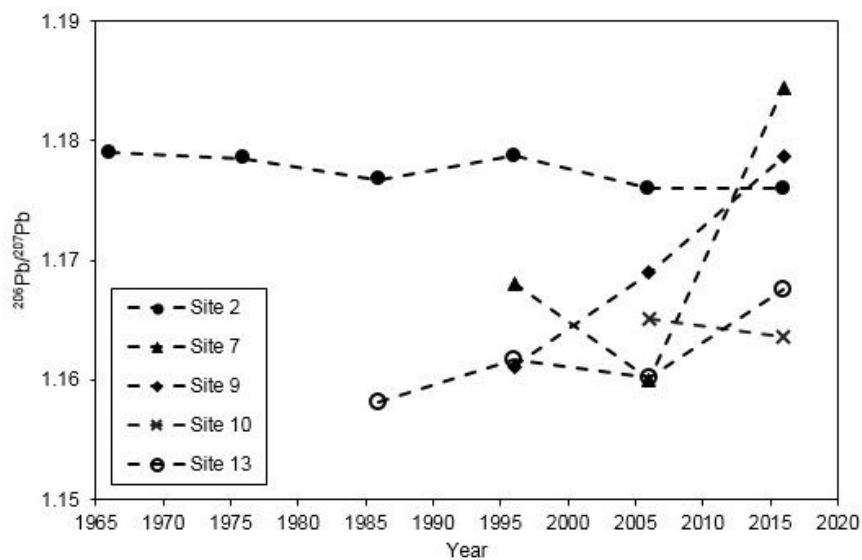**Figure 3.4** $^{206}Pb/^{207}Pb$ ratio vs. Pb concentration in samples of soil horizon C.

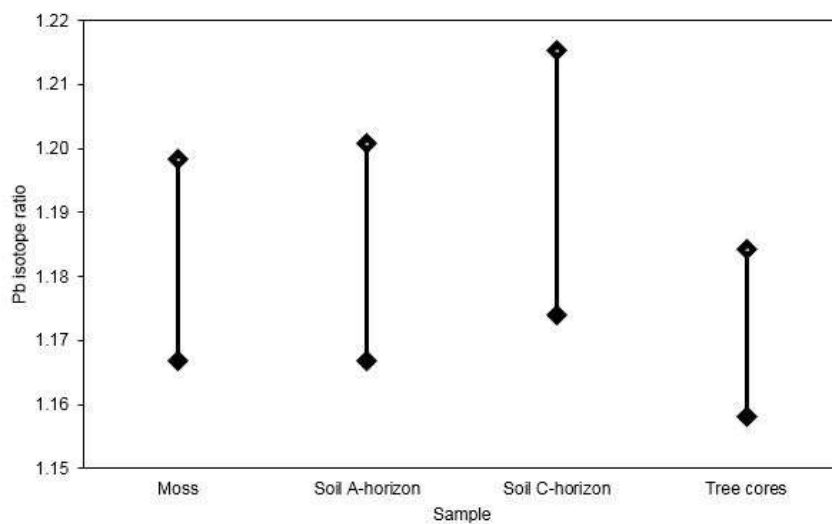**Figure 3.5** ^{206}Pb/^{207}Pb ratios in tree rings formed in years 1966–2016.

Figure 3.6 Ranges of ^{206}Pb/^{207}Pb ratios in samples of moss, soil and tree cores.

Identification of contamination sources

According to the Pb isotope compositions of the analysed samples, two main sources of Pb were identified: i) Pb derived from the burning of coal in industries and households and ii) metallurgy as a source of Pb with high $^{206}Pb/^{207}Pb$ ratios. The most important milestones in Pb pollution levels in the territory of the Czech Republic include a maxima in coal mining at the turn of the 19th - 20th centuries and another in the 1970's when most of the coal burning power plants were built (Novák et al., 2010). Coal mined in the Ostrava region covers a very wide range of Pb isotope ratios (1.167 - 1.312, Mihaljevič et al. 2009), and the measured ratios in almost all of our samples fell within this range (**Fig. 3.7**). Moreover, the $^{206}Pb/^{207}Pb$ values vary from 1.159 to 1.205 for the black coal that is used in the energy industry in Ostrava (Francová et al., 2017b). According to tree rings analyses, concentrations of As, Cr and Fe raised noticeably between 1999 and 2016. Explanation of this shift may lie in use of coal in Ostrava region and its transformation after end of the communism era in the Czech Republic. The upper Silesian basin is presently the only region where black coal is mined in Czech Republic, but 14 mines were closed during 1990 – 2001, and only three mining areas remain in operation. This resulted in a shortage of high-quality black coal and other sources of coal had to be found. While most industrial and power plants use black coal from Ostrava, Poland (polish side of Upper Silesian basin) and Russia, household combustion relies largely on cheaper, poor quality brown coal mined in Bílina, Czech Republic ($^{206}Pb/^{207}Pb$ = 1.192 – 1.209; Mihaljevič et al., 2009), which has a high As and Fe content (Mihaljevič et al. 2009; Pešek and Sivek 2012). Substitution of black coal with brown coal corresponds to concentration changes in the youngest tree rings. Furthermore, the metallurgical industry operating in Ostrava city mostly uses coke as fuel for steel production, for which the As content is approximately 30%–40% lower than that found in coal (Kunstmann and Bodenstein, 1961). Although efforts have been made to lower the impacts of industrial coal use, problems still persist with small combustion utilities, e.g., domestic sources. These sources are important, especially during winter, because different fuels are used that are hard to control (Konieczyński et al., 2012). Ground sources with low-lying chimneys have a much greater impact on air quality than sources with emissions through high chimneys. The value of $^{206}Pb/^{207}Pb$ for the primary ore from a steel metallurgy in the city of Ostrava is 1.23 (Francová et al., 2017b). This exact value was not found in any of the analysed samples because of the potencional signal homogenisation in samples. Nevertheless, high isotope ratios observed in samples obtained at site 7 clearly show the influence of ore derived Pb.
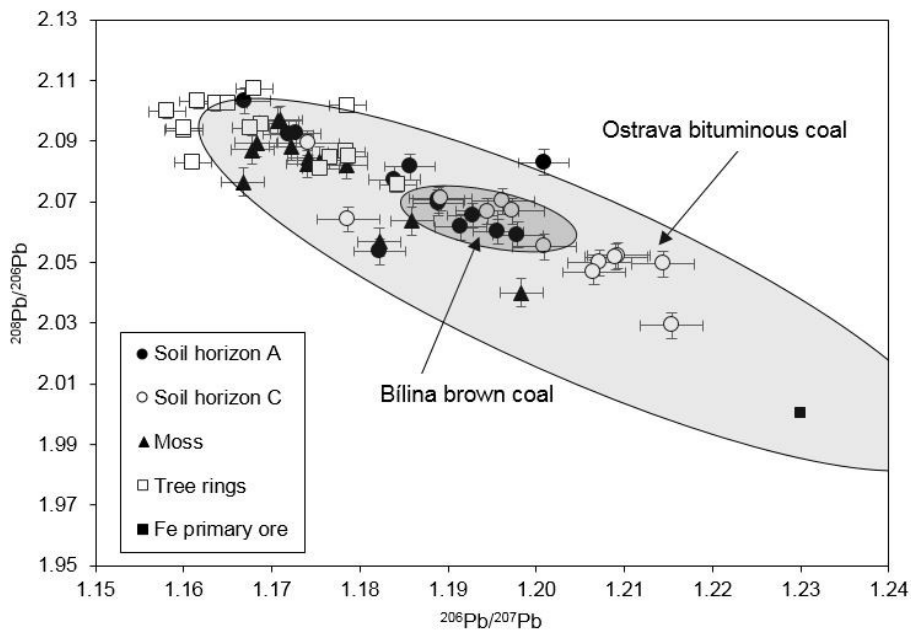
Figure 3.7

Three-isotope plot ($^{206}Pb/^{207}Pb$ versus $^{208}Pb/^{206}Pb$) that shows the distribution of Pb isotope compositions in moss, soil horizons, tree rings and data reported in literature: black coal mined in Ostrava region and brown coal used in Ostrava from Mihaljevič et al. (2009).

The younger tree rings reflect a significant decrease in Pb deposition. According to Vejvoda et al. (1998) the overall decrease currently noticeable in Pb deposition in the territory of the Czech Republic occurred through the improvement of the emission limits for metallurgy, a decrease in the output of the economy and the transformation and completion of the installation of sulphur-removal equipment at the major energy sources in the Czech Republic, which occurred in 1996-1998. According to Klaminder et al. (2005) traffic-related Pb emissions lead to 70% of the surface Pb of anthropogenic origin found today in remote northern Scandinavian forests. Alkyl-Pb was used as an anti-knock additive in gasoline in significant amounts from 1950. Lead emissions from traffic in the Czech Republic peaked in 1985, and alkyl-Pb was completely phased out by law in 2000 (Novák et al., 2010). However, at least in the Czech Republic, no lasting impact from a European leaded gasoline signal is detectable in recent samples. None of the materials investigated provides any evidence for the importance of traffic related

Pb emissions on the distribution of the Pb concentrations or for the $^{206}Pb/^{207}Pb$ isotope ratios.

Suitability of selected samples

Mosses accumulate Pb over their lifetime, which can be between five to ten years. During this period, they integrate the metal input from various sources. This means that mosses can level out isotope differences between individual sources over the period of Pb deposition. This same behaviour was observed in lichen samples from the same area (Francová et al., 2017b). Nevertheless, because of the homogenisation of the signal over the years, mosses appear not to be well suited for detecting individual point sources over short and long distances. Still many studies confirm the reliability of suitably located and collected mosses as reflections of the atmospheric Pb isotope composition (Lee et al., 2005; Suchara et al., 2011; Sucharová et al., 2014).

The organic horizon of soil serves as the most important sink for contaminants, as well as for plant nutrients, as it accumulates elements over decades. The difference between soils and the isotope composition of the primary ore used in steelworks suggests that the Pb was integrated in the topsoils over the operating years of the factory, during which emissions and fallout fluxes must have greatly varied. The deepest soil horizons, e.g., C-horizon, are mainly influenced by the bedrock chemistry (Reimann et al., 2001). Soil, especially the upper horizons, can be successfully used as medium for fingerprinting the influence level of the main Pb sources (Morton-Bermea et al., 2011; Reimann et al., 2012; Galuskova et al., 2014), but, because of its long-term accumulation of elements, it is not useful for the tracing of recent pollution sources.

Tree cores obtained from sampled trees reflect the Pb isotope composition over fifty years. Tree rings do not precisely reflect the atmospheric pollution Pb signal as the ten-year averages used in this study may homogenize the signal same as the mosses. Ranges of $^{206}Pb/^{207}Pb$ ratios in moss and tree cores samples suggest this may be the case (see **Fig. 3.6**). Nevertheless, it is clear that the Pb isotope composition of tree rings is much closer to the values of the pollution Pb sources rather than the natural Pb isotope values of the mineral soils. The majority of Pb present in the trees is derived, directly or indirectly, from atmospheric pollution sources rather than from the uptake of natural Pb from the mineral soils (Novák et al., 2010). Trees are particularly useful for monitoring trace metal deposition in the immediate vicinity of metal processing works because several tree species are capable of surviving in soils with extremely high metal levels (Watmough, 1999). In addition, due to the buffering function of soils, tree rings

should be a suitable archive of past atmospheric pollution where most Pb enters the xylem directly from the atmosphere, with only a minor contribution of Pb uptake by roots. Tree cores seems to be a suitable archive of pollution for areas where other archive samples (e.g., peat or lake sediments) are not available. They can also be successfully used as a supplement to analyses of other types of environmental matrixes. The applicability of tree rings for tracing the deposition of historical metal(loid)s was confirmed by other studies (Mihaljevič et al., 2008; Novák et al., 2010; Zuna et al., 2011), where tree rings were successfully used to document trends in areas affected by Pb emissions.

Conclusions

Fingerprinting using Pb isotopes was proven as a reliable tool for the tracing of emissions derived from anthropogenic activities, even in heavily industrialised areas, where many polluting sources can be observed. Three types of environmental samples where studied, in which wide ratios of Pb isotope composition were observed. Most of the Pb was derived from anthropogenic sources, as indicated by the Pb isotope ratios of the samples. Two main sources of Pb in the Upper Silesia region were recognised: i) burning of fossil fuels in industry and households and ii) metallurgical activities. The use of coal, which has a long tradition in Czech Republic, remains a significant environmental issue. Although the vast majority of mining complexes in the Czech part of Upper Silesia were permanently closed, black coal is still the predominant type of fuel in the region. The decrease of coal mining led to the increased use of inferior coal types, mainly brown coal originating from NW Czech Republic. Household combustion is an especially important source of emissions, mainly in winter. Household combustion is hard to control as low quality fuels are often used and it is not easy to prove the combustion of banned materials. There should be an increased effort to control and improve the domestic heating situation. Signals in moss samples seems to be homogenised through years of its life, but the influence of the primary ore at the sampling site near steelworks was more visible in moss than in the lichen sample obtained at the same site. The isotope ratios of ^{206}Pb/^{207}Pb in soil samples varied greatly, the results of this study demonstrate that the A-horizon and C-horizon are decoupled. The upper soil layer is part of the biosphere and is greatly influenced by

anthropogenically Pb, while the C-horizon carries the geochemical signature of the lithosphere. The Pb isotope composition in tree cores was consistent with past atmospheric deposition of Pb and was also within the range of recent anthropogenic emission sources. Historic deposits of metal(loid)s in tree cores serve as clear evidence of the negative effects of the switch to brown coal use in households.

Chapter IV

Stable isotope tracing of Ni and Cu pollution in North-East Norway: Potentials and drawbacks

H. Šillerová, V. Chrastný, M. Vítková, A. Francová, J. Jehlička, M. R. Gutsch, J. Kocourková, P. E. Aspholm, L. O. Nilsson, T. F. Berglen, H. K. B. Jensen, M. Komárek

Content

Abstract

The use of Ni and Cu isotopes for tracing contamination sources in the environment remains a challenging task due to the limited information about the influence of various biogeochemical processes influencing stable isotope fractionation. This work focuses on a relatively simple system in north-east Norway with two possible endmembers (smelter-bedrock) and various environmental samples (snow, soil, lichens, moss, PM_{10}). In general, the whole area is enriched in heavy Ni and Cu isotopes highlighting the impact of the smelting activity. However, the environmental samples exhibit a large range of $\delta^{60}Ni$ (-0.01 ± 0.03‰ to 1.71 ± 0.02‰) and $\delta^{65}Cu$ (-0.06 ± 0.06‰ to -3.94 ± 0.3‰) values which exceeds the range of $\delta^{60}Ni$ and $\delta^{65}Cu$ values determined in the smelter, i.e. in feeding material and slag ($\delta^{60}Ni$ from 0.56 ± 0.06‰ to 1.00 ± 0.06‰ and $\delta^{65}Cu$ from -1.67 ± 0.04‰ to -1.68 ± 0.15‰). The shift toward heavier Ni and Cu δ values was the most significant in organic rich topsoil samples in the case of Ni ($\delta^{60}Ni$ up to 1.71 ± 0.02‰) and in lichens and snow in the case of Cu ($\delta^{65}Cu$ up to -0.06 ± 0.06‰ and -0.24 ± 0.04‰, respectively). These data suggest an important biological and biochemical fractionation (microorganisms and/or metal uptake by higher plants, organo-complexation etc.) of Ni and Cu isotopes, which should be quantified separately for each process and taken into account when using the stable isotopes for tracing contamination in the environment.

Introduction

Mining and smelting activities are important sources of metals and metalloids in the environment and soils near smelters are highly polluted by a wide range of elements such as Pb, Zn, Cd, Cr, Cu, Hg, Ni, As, Sb, etc. (Ettler, 2016). Concentration, chemical speciation, and/or mineralogical composition analysis are the standard methods to study fate of the metal(loid)s in the environment (Gregurek et al., 1999; Gunawardena et al., 2012). Since modern mass spectrometers are able to resolve slight variations in the stable isotope composition of elements, such as Cr, Ni, Cu, Zn, Se, Cd, Hg, isotope analysis has become a promising approach in the field of industrial contamination, especially in source tracing studies. In general, the identification of a source of metal contamination in the environment is based on comparison of the metal isotope composition in all potential sources (anthropogenic or natural) and in the environment (water, soil, air, or plants). Variation in stable isotope composition between the natural and anthropogenic sources is thus essential. Metals with relatively low boiling points such as Zn and Cd, were shown to evaporate during smelting, favouring escape of light isotopes in the exhaust (Cloquet et al., 2006; Chrastný et al., 2015). On the other hand, Ni and Cu are both known for high boiling temperatures (2913 °C and 2562 °C, respectively), therefore no isotope fractionation is expected during the smelting process and the products of Ni and Cu smelting as well as Ni and Cu emissions to the atmosphere have similar isotope signatures as the processed ores (Ratié et al. 2015b; Bigalke et al. 2010). Whether the anthropogenic input can be distinguished from the natural background in the specific environment depends on the range of $\delta^{60}Ni$ and $\delta^{65}Cu$ in both the natural and the anthropogenic source (Wiederhold, 2015). Nickel isotope composition in various terrestrial samples (Fe-Mn crust, ultramafic (UM) rocks and soils, fresh water and seawater, river sediments or methanogens cultures and plants) have been recently determined. Published data suggests that the range of $\delta^{60}Ni$ is between approximately -1.5 and 2.5‰ (Gall et al. 2013; Ratié et al. 2015b; Cameron and Vance 2014). Cameron et al. (2009) found that Ni assimilation during methanogenic growth produced substantial fractionation of Ni isotopes, up to $\Delta^{60}Ni_{cells-medium}$ -1.46‰. Accumulation of Ni by plants resulted in isotope fractionation, $\Delta^{60}Ni_{plant-solution}$ from -0.63 to -0.90‰ (Deng et al., 2014). Ratié et al. (2015a) reported Ni isotope fractionation between bedrock (ultramafic rocks) and the upper soil horizon up to -0.47‰ suggesting an overall trend of heavier isotope depletion in the solid phase during weathering. Finally, Ratié et al. (2015b) reported the mass-dependent

fractionation of Ni during Ni-laterite ore smelting and refining, δ^{60}Ni values from $0.01 \pm 0.05‰$ (fly ash) to $0.27 \pm 0.05‰$ (smelting slag). The dissolved Ni from the fly ash settling ponds appears to be enriched with heavy isotopes in comparison to pristine water. The authors thus highlighted the potential of Ni isotope analysis for distinguishing between anthropogenic Ni (heavier Ni isotope composition) and natural (lighter isotope composition) (Ratié et al. 2015b). In contrast to Ni, Cu isotope analysis have been applied in geochemical, biological, and environmental studies for over 15 years (Gale et al., 1999). The range of Cu stable isotope composition is much wider than in the case of Ni, with δ^{65}Cu of -16.5‰ to +10‰ in minerals and ores (Mathur et al., 2009). Large variations of δ^{65}Cu are found in sediments, biological material and secondary ore minerals, and mine tailings (Li et al., 2015; Rodríguez et al., 2013; Weinstein et al., 2011). Significant isotope fractionation was observed during interaction of Cu with Fe and Al oxy(hydr)oxides in solution, resulting in enrichment of heavy isotopes on the solid surface (Balistrieri et al., 2008; Pokrovsky et al., 2008). Cu adsorption from aqueous solutions onto bacteria and algae cause enrichment of the cell surface in the light isotope, especially at pH 1.8-3.5 (Pokrovsky et al., 2008).

In this study we evaluate the suitability of Ni and Cu isotope analyses for tracing their potential sources in the environment around a Ni-ore processing smelter. Our approach is based on concentration, mineralogical, and isotope analysis in various environmental samples (soil, snow, moss, lichens). The objective is to verify the suitability of each method and sample type on a convenient and relatively simple system of a pure environment with only one anthropogenic source of Ni and Cu. The key question of this study is whether analysis of these two isotope systems can significantly contribute to identify the smelting facility as the source of pollution in the area.

Materials and methods

Study area and sources of contamination

The sampling network covers approximately 2000 km^2 in North-Eastern (N/E) Norway, near the Norwegian-Russian border. The region is known for the largest remaining area of primeval pine forest in Norway, an offshoot of the Siberian taiga. The annual average temperature is -1 °C, annual precipitation 400-500 mm year^{-1}, and elevation between 80 and 280 m a.s.l. (Reimann, 1995). The population density in the area is low (2.4 inhabitants per km^2). The administrative centre is town Kirkenes with approximately 3500 inhabitants. Human activities are mostly limited to fishery, reindeer-herding and forestry. Exception is the iron ore mine and mill at Kirkenes (Tvrdý et al., 2004). Over the past 70 years the Russian non-ferrous metal processing industry at the western part of Kola Peninsula has led to the development of industrial deserts and the local ore-processing plants are considered the world's largest point source emitters of SO$_2$ and metals (Gregurek et al., 1998a; Khokhar et al., 2008). There are two important facilities, the smelter near the town of Nikel (5 km from the border) and the concentrating and roasting plant near the town of Zapolyarny (15 km from the border). The Zapolyarny plant process disseminated Ni-Cu sulphide ore mined at Kola Peninsula, to produce Ni-Cu concentrate and subsequently Ni-Cu pellets. Recently the roasting technology was replaced by briquetting technology that prevents SO$_2$ emissions. The facility in Nikel consists of a roasting station and a smelter; the Ni-Cu pellets from Zapolyarny are processed here (Bellona report, 2010). In the mid- 1990s the smelter processed Noril'sk ore, rich Pechanga ore, and lower-grade local ore (Boyd et al., 2009). The Pechanga district includes numerous massive and disseminated Ni-Cu sulphide ore deposits associated with mafic-ultramafic igneous rocks. These two plants combined with the farther complex in Monchegorsk, produced annually approximately 100 000 t of SO$_2$, 300 t of Ni and 180 t of Cu emissions (Reimann et al., 1997b), and a wide range of elements: Ag, Al, As, Cd, Co, Cr, Cu, Fe, Hg, Mn, Ni, Pb, Sb, Sr, Th, Tl, Zn and others (Kashulina et al., 2014; Reimann et al., 1996).

In total 17 sampling sites were chosen as a function of geography, geochemical background, prevailing wind direction, and distance from the smelters. The sampling sites are divided into 3 transects. Transects run approximately 50 km to the south-west (S/W; sites 1, 2, 3, 4, 5), 90 km to the north-west (N/W; sites 6, 7, 8, 9, 13) and 40 km to the north-east (N/E; sites 10, 11, 12, 14, 15, 16, 17) from the smelter. The prevailing

wind direction is north, north-east (N,N/E). Prevailing wind directions in the study area during summer and winter sea- son 2015 are shown in **Fig. S 4.2**. The study area, sampling sites, and the sources of Ni and Cu are shown in the **Fig. S 4.1**.

Sampling and sample treatment

Sampling was carried out in March 2015 (snow and lichens) and August 2015 (soil profiles, bedrock and moss). Snow, lichens, and mosses were collected at each site (1-17), and the soil profiles and bedrock only at selected sites of each transect (1, 4, 5, 6, 7, 8, 13, 15, 17). A PM_{10} fraction from two monitoring stations were provided by the Norwegian Institute for Air Research and represents a month of atmospheric deposition from January and March 2015. The PM_{10} samples come from the monitoring stations in Svanvik (near site 5, sampling 3 m above the ground) and in Karpdalen (near site 15, sampling 1.5 m above the ground). Finally, representative samples of the smelter slag (SS) and the feeding material (Ni-Cu concentrate from Zapolyarny) were obtained for analysis. Samples were homogenized and digested in a mixture of acids (HNO_3, HCl, HF) in order to obtain a liquid sample. Prior to digestion, the volume of the snow was reduced by evaporation on a hot plate to approximately 25 mL and the unfiltered samples were subsequently subjected to the acid digestion. Approximately 250 mg of lichen, moss and soil, and 100 mg of bedrock, smelter slag, and the feeding material was digested for each replicate. Particles of PM_{10} on Teflon filter bases were digested according to the USEPA 3050B method (USEPA, 1996a; Francová et al., 2017b). The samples were digested in duplicates (snow, PM_{10}) or triplicates (lichens, soil, bedrock, metallurgical samples and mosses), evaporated to dryness and taken up to 2% nitric acid for concentration analysis. All the samples and the pre-treatment methods are summarized in the Supporting material (**Table S 4.1**).

Analytical methods

Mineralogical and concentration analysis

A TESCAN VEGA3 XMU (TESCAN Ltd., Czech Republic) scanning electron microscope (SEM) equipped with a Bruker QUANTAX200 energy-dispersive X-ray spectrometer (EDS) was used for imaging and semi-quantitative chemical analyses of primary phases. Electron probe microanalyzer CAMECA SX-100 (CAMECA SAS, France) equipped with four crystal spectrometers was used for quantitative microanalyses. X-ray diffraction (XRD; PANalytical X'Pert Pro diffractometer with

X'Celerator detector and Cu-Ka radiation) analyses were used for basic mineralogical characterization of the bulk sample. Selected PM_{10}, lichen, and soil samples were fixed on a conductive tape, carbon-coated and investigated for metal-rich particles using SEM/EDS. Prior to analysis the lichens were carefully dry milled in agate mortar. Similar to sample pre-treatment steps described by Mattigod et al., (1986), the topsoil samples (i.e., the most contaminated layer at each site) were wet sieved through a 63 μm sieve using ethanol to avoid dissolution of target particles. Once sieved, dried (30 °C) samples were subjected to gravitational separation in heavy liquid (Na-metatungstate, density 2.82 g cm^{-3}) supported by ultrasound and subsequent centrifugation. Concentration of selected elements (Ni, Cu, Cd, As, Zn, Pb, Cr) was determined by mass spectrometer with inductively coupled plasma ionization (ICP MS, iCAP Q, Thermo Fisher Scientific, Germany). The certified reference materials BCR-482 Lichen (IRMM, Belgium), SRM 1640a Natural Water (NIST, USA), and SRM 2710a Montana I Soil (NIST, USA) were used to ensure the accuracy of the analytical method. The recovery of certified reference values was within the range of 89-111% for all of the elements.

Ion-exchange chromatography and isotope analysis

Selected samples were used for isotope analyses based on the concentration results and location. Specifically, lichen (*Hypogymnia physodes*), snow, and topsoil samples from sites 4, 5, 6, and 15 together with bedrock from sites 5, 6, 15 and smelting slag, feeding material, and PM_{10} fraction from January and March 2015 (near site 5 and 15) were analysed for both Ni and Cu isotope composition. The samples were digested, and Ni and Cu was separated from the matrix. The matrix separation prior to Ni isotope analysis was adapted from Gueguen et al., (2013). The first stage involves separation of Fe, Zn, and part of Co and Cu on the anionic resin in chloride form (BioRad, AG1-X8, 100-200 mesh, 2 mL bed volume). An aliquot of 1 mg of Ni in 6M HCl is loaded on the column. To ensure a complete elution of Ni, additional 10 mL of 6M HCl is passed through the column. The eluted sample is taken near dryness and dissolved in 0.24M HCl for the second stage, which involves Ni separation from the rest of the matrix on a Ni specific resin (TrisKem International, Ni-resin, 0.5 mL bed volume). A Ni double spike is added to the sample with a spike (^{61}Ni) to natural (^{58}Ni) isotope ratio of 1. The resin contains a dimethylglyoxime (DMG) molecule to form a Ni-DMG complex at pH 8-9. The samples from the first step are mixed with 0.3 mL of 1M ammonium citrate and pH is set again to 8-9 and loaded onto the activated Ni-resin, then the matrix is eluted with an additional volume of ammonium citrate and ultra-pure

H_2O. The Ni-DMG complex is then broken up by the addition of 3M HNO_3 to obtain a pure Ni fraction. The Ni fraction was evaporated to near dryness on a hot plate to final volume of 100 mL by distillation.

To separate Cu from a sample matrix, a modification of two anion exchange chromatography procedures described by Marechal et al. (1999) and Alliot et al., (2011) was used. An anion exchange resin (BioRad, AG1-X8, 200-400 mesh, 0.5 mL) was transferred to a polypropylene column (PolyPrep, BioRad, 90 mm height, 2 mL bed volume). The resin was rinsed with 20 mL of 2% HNO_3 and then transformed into Cl^- form with 20 mL of 6M HCl, split into two equal doses. A sample aliquot of 1 µg was completely dried and dissolved in 1 mL of HCl, then evaporated again and dissolved in 250 mL of 6M HCl +0.001% H_2O_2. The sample was loaded on the column carefully and the sample matrix was removed with the first 3 mL of 6M HCl +0.001% H_2O_2. The pure Cu fraction was then eluted with 10 mL of 6M HCl +0.001% H_2O_2 and the column was cleaned with 0.5M HNO_3. The Cu fraction was evaporated to almost dryness on a hot plate to remove Cl^- anions with HNO_3 (to a final volume of 100 mL) by distillation. For elimination of organic residues originating from the column resin bed, 100 mL of hydrogen peroxide was added and left overnight, then evaporated slowly on the hot plate. The separation methodology and the accuracy and precision of the Cu isotope analysis were verified by an addition of ERM-AE633 Cu isotope standard into a Cu-free matrix samples of soil, bedrock and lichen. The doped matrices were treated and purified in the same manner as the original samples. The average $\delta^{65}Cu$ values (-0.01 ± 0.03‰, -0.02 ± 0.03‰ and -0.02 ± 0.03‰ for lichen, soil and bedrock, respectively) are in agreement with the certified value of ERM-AE633 (-0.01± 0.05‰). Chemicals used for the ion-exchange chromatography were of the highest quality (ROTIPURAN Ultra, Carl Roth).

The isotope composition of Ni and Cu was measured using a multi-collector inductively coupled plasma mass spectrometer (MC ICP MS Neptune, Thermo Fisher Scientific, Germany). The Ni isotope analysis used a Ni double spike method for correcting instrumental mass bias. The isotopes used as the double-spike are ^{61}Ni and ^{62}Ni, obtained from IsoFlex, USA. Each isotope was weighed and digested separately in concentrated HNO_3 (ROTIPURAN Ultra, Carl Roth) in sealed PFA beakers. The solutions were then transferred to PFA bottles and diluted with ultra-pure water (milli-Q, MERCK Milli-pore) to 2% HNO_3. Finally, the double-spike was mixed together with respect to their purity. A mix of sample to spike was then calculated to achieve the conditions of 95% and more natural isotope coming from sample and 95% and more spiked isotope from the double spike. The precise isotopic composition of the spike was calibrated as described in Cameron et al. (2009). Samples analysed in this study include USGS geological reference materials, namely BHVO-2, a basalt from Hawaii

(USA). Several preparations and measurements of the reference material showed the values are in agreement with those published δ^{60}Ni= -0.02 ± 0.03‰ (SD, n = 7) (Deng et al., 2014; Gueguen et al., 2013). Ni isotope composition is expressed as delta notation (1), where R is ^{60}Ni/^{58}Ni ratio and indexes measured and standard refer to raw isotope data of unknown sample and NIST SRM 986 standard, respectively.

$$\delta^{60}Ni(‰) = \left(\frac{R_{measured}}{R_{standard}} - 1\right) \times 1000$$

(1)

Simultaneous measurement of ^{58}Ni, ^{60}Ni, ^{61}Ni, ^{62}Ni, as well as ^{56}Fe was performed using the high mass resolution mode of the instrument. The detector configuration was as follows: ^{56}Fe - L4, ^{58}Ni - L2, ^{60}Ni - C, ^{61}Ni - H1, ^{62}Ni - H2; due to potential interference of ^{64}Zn, ^{64}Ni was not monitored. The sample introduction was performed with desolvating nebulizer (Aridus II, Cetac). Isobaric overlap on ^{58}Ni from ^{58}Fe was addressed using online correction by measuring the ^{56}Fe ion beam. The interfering ^{58}Fe intensity is calculated for each measurement of sample or standard, from the 'reference' ^{58}Fe/^{56}Fe [0.003534]. The detector configuration layout was as follows: ^{60}Ni - L4, ^{62}Ni - L2, ^{63}Cu - L1, ^{65}Cu - H1. The isotope composition of Cu is presented in this study as a delta notation (2), where R is ^{65}Cu/^{63}Cu isotope ratio and indexes measured and standard refer to raw isotope data of unknown sample and ERM$^{(R)}$-AE633 standard, respectively.

$$\delta^{65}Cu(‰) = \left(\frac{R_{measured}}{R_{standard}} - 1\right) \times 1000$$

(2)

The mass bias on MC ICP MS was corrected by sample-standard bracketing with ERM$^{(R)}$-AE633 (Institute for Reference Materials and Measurements, IRMM, Belgium) due to the commonly used SRM NIST 976 (Cu) not being commercially available. The typical analytical sequence consisted of measuring the ERM$^{(R)}$-AE633 standard after each fifth unknown sample. A blank solution containing 2% HNO$_3$ was measured before each sample solution was measured three times. Typical precision for five replicates of ERM$^{(R)}$-AE633 and three sample replicates standard was better than 0.05 (2SD).

The traceability to commonly used SRM NIST 976 (Cu) was performed by cross-calibration of the standards of ERM$^{(R)}$-AE633, ERM$^{(R)}$-AE647 and SRM NIST 976 (Cu) (obtained with thanks to Dr. Richard Wanty of USGS laboratories). The ERM$^{(R)}$-AE633 yielded δ^{65}Cu 0.01 ± 0.05 to NIST 976 and 0.21 ± 0.05 to ERM$^{(R)}$-

AE647 and ERM$^{(R)}$-AE647 yielded 0.22 ± 0.05 to NIST 976. These values are in the closest accordance with the earlier published data by Moeller et al., (2012).

Results

Mineralogical investigation

The SEM observations together with EDS analyses of PM_{10} indicated the presence of smelter-derived material (**Fig. 4.1 A** and **B**). Many metallic particles and fragments were detected, mainly identified as Cu-Ni-Fe, Cu-Fe or Ni-Fe sulfides of various metal distributions. Generally, up to 31 wt% Cu and up to 35 wt% Ni was detected in the particles of PM_{10} at both sites. Angular metal-rich sulfates and globules or prisms of NaCl were determined, representing typical features for high-temperature combustion processes (Campos-Ramos et al., 2009; Vítková et al., 2010; Song et al., 2014). Therefore, both metallurgical slags and fly ash might be potential sources. Metallic fragments of several mm in size were observed within the lichen samples (**Fig. 4.1 C**). Target Ni-, Cu-rich particles were often observed in the form of Fe oxides or non-stoichiometric alloys with Fe and/or Cr. Up to 21 wt% of Ni was determined at site 9 within the samples of *Hypogymnia physodes* (**Fig. 4.1 C**).

Heavy mineral fraction of the studied topsoil samples showed the highest proportion of Ni-, Cu-rich particles at site 5 followed by sites 4 and 15. A host of (spinel-type) Fe oxides were identified, either pure or enriched with Ni (up to 5 wt%) or Cu (<1 wt%). Several metallic sulfides were detected, mainly represented by chalcopyrite ($CuFeS_2$; **Fig. 4.1 D**) and to a lesser extent by $NiFeS_2$ (**Fig. 4.1 E**). Numerous metal-bearing particles from Cu mining and smelting activities were detected in soils studied by Ettler et al., (2014a), in particular covellite (CuS) and chalcocite (Cu_2S) were determined in smelter-derived spherical particles and chalcopyrite ($CuFeS_2$) was identified in mining-derived angular particles. However, the most abundant species were represented by non-stoichiometric Ni-(Cu)-Fe-Cr alloys of various sizes from <1 mm to 20 mm, containing up to 65 wt% Ni and 3.5 wt% Cu.

Concentration analysis

Lichens, snow, moss and soil

Firstly, the data suggest that the concentration of Ni and Cu in all the samples was significantly higher than concentration of Zn, As, Cr, Pb and Cd, which is especially true for the most contaminated sites (see minimum-maximum range **Table S 4.2**). There were significant differences in Ni and Cu concentration between some sample types. The median concentration of Ni and Cu was the highest in lichens (93 mg kg^{-1} of Ni and 94 mg kg^{-1} of Cu). However, an extremely high concentration of Ni and Cu was determined in the topsoil in the vicinity of the smelter (up to 568 mg kg^{-1} of Ni and 380 mg kg^{-1} of Cu). The basic physicochemical characterization of studied soil samples is summarized in the **Table S 4.3**. Average Ni/Cu ratio was 0.99 in lichens, 1.86 in snow, and 1.46 in moss and topsoil, indicating that there is Ni enrichment relative to Cu mainly in snow samples but also in moss and topsoil samples. The highest levels of Ni and Cu were often determined at the N,N/E direction from the smelter (mainly site 15). The sampling sites in this direction are highlighted as black dots in **Fig. S 4.1**. The N/E transect together with sites 4 and 5 are the most contaminated reflecting the distance and prevailing wind direction from the sources. Additionally, the N/E transect is exposed to emissions from the ore processing plant in Zapolyarny the most. The N/W transect was the least contaminated with the lowest Ni and Cu levels at sites 6, 7, and 8.

Bedrock, smelter slag, feeding material and PM$_{10}$

The feeding material exhibits high Ni and Cu concentration (153 g/kg and 393 g kg^{-1}, respectively) with Ni/Cu ratio 1:2.5 and low Fe concentration (5.93 g kg^{-1}). Concentration (ng m^{-3}) of Ni and Cu in the PM$_{10}$ fraction from Svanvik (January and March 2015) and Karpdalen (March 2015) is in accordance with annual mean values from 2015 published by the Norwegian Environment Agency (Berglen, 2015). Elevated (approximately 10 times higher) Ni and Cu concentrations in the PM$_{10}$ fraction were observed in Karpdalen during March 2015. The chemical composition of bedrock from sites 4, 6 and 15, the smelting slag, and Ni-Cu concentrate and PM$_{10}$ from sites 5 and 15 are summarized in the **Table S 4.4**.
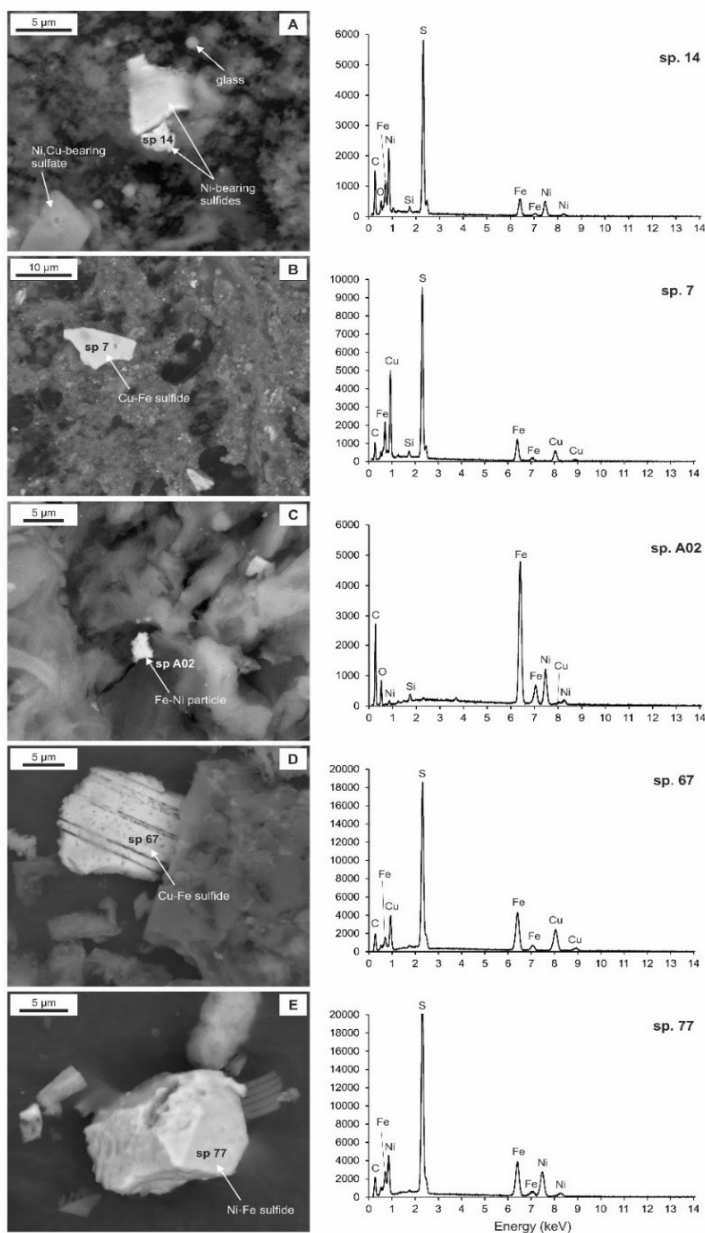
Figure 4.1 Image of metallic particles detected in different environmental samples in backscattered electrons (SEM). a) PM$_{10}$ collected at Svanhovd (site 5) in January 2015: fragmental Ni-Fe sulfide (35 wt% Ni), angular sulfate particle enriched with Ni and Cu, glassy silicate globules; b) PM$_{10}$ collected at Karpdalen (site 11) in January 2015: sharp fragment of Cu-Fe sulfide particle corresponding to chalcopyrite (CuFeS$_2$); c) *Hypogymnia physodes* collected at site 9: oxidized Fe-Ni particle containing 21 wt% Ni and 1.6 wt% Cu; d) topsoil heavy mineral fraction (site 5): altered Cu-Fe sulfide corresponding to CuFeS$_2$; e) topsoil heavy mineral fraction (site 15): altered Ni-Fe sulfide corresponding to NiFeS$_2$.

Isotope analysis

The measured δ^{60}Ni values for snow, lichen, soil, and bedrock range between -0.01 and 1.71‰. Metallurgical samples, i.e. feeding material and smelting slag, have average δ^{60}Ni value 1.00 ± 0.06‰ and 0.56 ± 0.06‰, respectively. The PM_{10} particles have δ^{60}Ni between -0.05 ± 0.06‰ and 0.79 ± 0.06‰ and represent the lighter Ni fraction. Selected δ^{60}Ni values as a function of Ni concentration in the studied samples are displayed in **Fig. 4.2 A**. In general, both Ni isotope composition and concentration vary; however, most of the environmental samples fall within a relatively narrow range of δ^{60}Ni values between 0.79 and 1.12‰ (highlighted in circle in **Fig. 4.2 A**). The isotope composition of smelter slag (1.00 ± 0.06‰) also falls within this range. Like the PM_{10}, the bedrock samples have a lighter Ni isotope signature (δ_{60}Ni between 0.22 ± 0.08‰ and 0.49 ± 0.09‰) indicating a different source of a heavier Ni fraction in the terrestrial samples. The Ni isotope composition in topsoils from site 4 and 5 is significantly heavier (δ^{60}Ni 1.71‰ and 1.65‰, respectively) than the composition of other samples. These two sampling sites are the most contaminated in terms of Ni and Cu concentration in topsoil. There has been a gradual accumulation of Ni and Cu in the soil for over 70 years. There is a high uniformity of δ^{60}Ni in snow, lichen, topsoil, and PM_{10} from site 15 and the Ni isotope composition (δ^{60}Ni between 0.53 ± 0.06‰ and 1.03 ± 0.11‰) matches the Ni isotope composition of the metallurgical samples (δ^{60}Ni value between 1.00 ± 0.06‰ and 0.56 ± 0.06‰). In contrast to sites 4 and 5, also the topsoil from site 15 matches the metallurgical samples, i.e. no shift towards heavier δ^{60}Ni values was observed.

The Cu isotope composition in this study ranges from -0.06 to -3.94‰ (**Table S 4.5**). The δ^{65}Cu values as a function of Cu concentration in the studied samples are displayed in **Fig. 4.2 B**. The lightest Cu isotope fraction was determined in bedrock (δ^{65}Cu between -3.52 ± 0.16‰ and -3.04 ± 0.32‰) and topsoil from site 6 (-3.94 ± 0.30‰). Smelter slag and feeding material have consistent δ^{65}Cu values (-1.68 ± 0.04‰ and -1.68 ± 0.15‰, respectively). The PM_{10} particles exhibit δ^{65}Cu values between -2.42 ± 0.02‰ and -3.05 ± 0.02‰ and represent the lighter Cu fraction with the isotope composition lying between the metallurgical samples and bedrock. The heaviest Cu fraction corresponds to lichens (δ^{65}Cu = -0.06 to -0.35‰) and snow (δ^{65}Cu = -0.24 to -1.07‰) samples. The δ^{65}Cu in most of the soil samples varied from -0.43 ± 0.08‰ to -2.40 ± 0.04‰. The topsoils from the contaminated sites 4, 5, and 15, which accumulate most of Cu, have similar δ^{65}Cu values (-1.23 ± 0.06‰, -1.02 ± 0.01‰ and -1.49 ± 0.22‰, respectively) and are the closest to the isotope signature of Cu in the

metallurgical samples. On the other hand, topsoil from the most remote site 6 is the closest to the bedrock in terms of Cu isotope composition (**Fig. 4.2 B**).
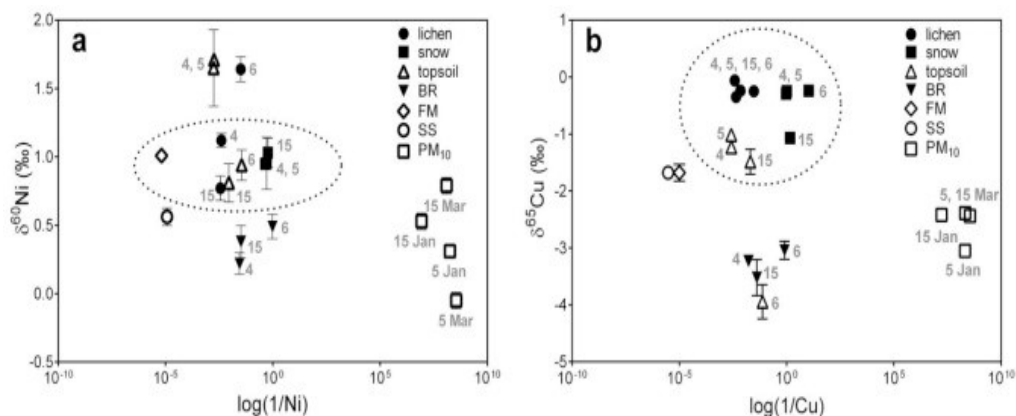
Figure 4.2 Ni and Cu isotope composition; a) Ni isotope composition vs. Ni concentration in the studied samples; b) Cu isotope composition vs. Cu concentration in the studied samples; the circles highlight the range of $\delta^{60}Ni$ and $\delta^{65}Cu$ values in majority of the environmental samples; The isotope signature ($\delta^{65}Cu$) of the vast majority of the environmental samples were between 0.06 ± 0.06 and -1.49 ± 0.22‰ and seems to be independent on the distance from the source, as the most remote and the less contaminated site (site 6) has similar $\delta^{65}Cu$ values in snow and lichen to the sites at the vicinity of the source. In contract, the points grouping according to the sample type (lichen, snow, topsoil) at Fig. 4.2b indicates that the isotope signature is likely affected by some specific fractionation processes.

Discussion

Different aspects of the concentration, mineralogical and isotope analyses

The concentration analysis confirmed that the distance from the source of emissions is the crucial parameter for Ni and Cu deposition. An area of approximately 4000 km^2 around the Severonikel complex (Nikel, Zapolyarny, Monchegorsk) was found to be contaminated by Ni and Cu with concentration 6-1500 times higher than European

background (Barcan, 2002; Reimann et al., 1996). It should be noted that the most remote and the least contaminated site 6 may still receive emissions from the smelter. The mineralogical investigation did not confirm the presence of smelter delivered particles in the topsoil samples from site 6. Conversely, common Fe oxides prevailed in topsoil at site 6, 7 and 8 within the north-west transect from the smelter pointing out the influence of the prevailing wind direction towards north, north-east (N,N/E) on Ni and Cu deposition. The isotope analysis, on the other hand, did not exclude the smelter as the source of Ni and Cu in site 6. The values of δ^{60}Ni and δ^{65}Cu in most of the environmental samples from this site fall within the same range as d values in samples from the most contaminated sites (**Fig. 4.2**). There was no clear effect of the distance from the smelter on Ni and Cu isotope composition.

In this study, Ni enrichment in snow relative to Cu was found as observed also by Gregurek et al. (1998a). The Ni/Cu ratio is attributed to composition of the primary ore, smelting technology, and processes used in Nikel and Zapolyarny. The Pachenga ore contain 0.5-3 wt% Ni and 0.5-1.8wt % Cu but according to some references the local ore used in Nikel smelter can be mixed in varying properties with Noril'sk ore (2- 4 wt% Ni and 3-5 wt% Cu) (Gregurek et al., 1998a, 1998b). The variability of Ni/Cu ratio in the feeding material is not so obvious in lichens, moss, and soil due to their ability to accumulate metal(loid)s over a long period of time for years (Darnajoux et al., 2015; Harmens et al., 2015). Snow samples provide different information, because its chemical composition reflects current or short time deposition. On the other hand, the excess Cu in the feeding material explains why more Cu-rich phases were found in PM_{10} samples from Karpdalen (site 15) than in PM_{10} from Svanvik (site 5); site 15 is located in the prevailing wind direction and not far from the facility producing the feeding material while site 5 is in the vicinity of the smelter. In general, the smelting slag was highly enriched in Cu and Ni in comparison with literature (Ratié et al., 2015a Ettler, 2016) and contained between 8.5 and 9.5 wt% of the metals with the Ni/Cu ratio of approximately 1:1.

Variability of the isotope data and its possible reasons

The Ni isotope data from this study are in accordance with the published δ^{60}Ni values for natural terrestrial samples, which range from -1.03‰ to 2.50‰ (Cameron and Vance, 2014; Estrade et al., 2015; Gall et al., 2013; Ratié et al., 2015a, 2015b; Gueguen et al., 2013). In general, smelting slag should present the heaviest δ values of all smelter samples however in the case of Ni, none or very little isotope fractionation is expected

during the smelting process (Bigalke et al., 2010; Ratié et al., 2015a; Sonke et al., 2008). Therefore we assume that the surprisingly lighter isotope composition of the smelting slag is not a result of isotope fractionation during the smelting process. This difference most probably reflects changing composition of the smelted ore. The smelting slag and feeding material, which we were able to obtain, may come from different periods of production and may represent ore from a different mining region and it is virtually impossible to obtain such information. This fact may, to some extent, contribute to the variability of the Ni and Cu isotope composition in the environmental samples. In case of PM_{10} samples the δ values vary significantly depending on the sampling site and sampling period. Each PM_{10} sample represents a period of one month; however, its composition depends strictly on the current wind direction and air mass flow and reflects the composition of particles that can travel long distances (Erel et al., 2006). In case of snow, lichen and mainly topsoil we assume that the wide range of $δ^{60}Ni$ and $δ^{65}Cu$ values is a result of various biogeochemical processes in the environment which can cause Ni and Cu isotope fractionation.

A significantly heavier Ni fraction was determined in the topsoil from site 4 and 5 ($δ^{60}Ni$ 1.71‰ and 1.65‰, respectively). We assume that the high content of organic carbon in this topsoil, associated with the presence of higher plants on these sites, promotes biological Ni isotope fractionation. The preferential uptake of lighter Ni isotopes by plants and lighter Ni isotopes assimilation by soil microorganisms was already described in other studies (Cameron et al., 2009; Deng et al., 2014). Additionally, microorganisms can migrate in soils (Abu-Ashour et al., 1994) resulting into Ni isotope redistribution/fractionation in soils. Varying Cd isotope composition according to land use (forest versus meadow soil) and soil horizons (organic versus mineral soil horizons) was already described by Chrastný et al. (2015). The authors found that Cd in fly ash and slag from the smelter was not isotopically fractionated and Cd found in topsoil near the smelter was heavier than in the deeper humus layer. According to Wasylenki et al. (2015), the adsorption of Ni onto ferrihydrite can cause Ni isotope fractionation with lighter Ni isotopes preferentially adsorbed giving an average $Δ^{60}Ni_{dissolved-sorbed} = 0.34 ± 0.05$‰. In other words, soil rich in Fe-(hydro)oxides could exhibit a lighter Ni isotope composition due to the preferential adsorption of lighter Ni isotopes. However, a heavier Ni isotope composition was determined in the topsoil from site 4 and 5. Comparing the basic physico-chemical characteristics of the topsoil from sites 4, 5, and 15 (**Table S 4.3**), sites 4 and 5 are enriched in TOC concentration as well as amorphous and poorly crystalline Fe-, Mn-, and Al-(hydro)oxides, highlighting again the role of biological fractionation.

The Ni and Cu isotope signatures determined in this study represents a wide range of values, considering that there is only one anthropogenic source of these metals in the

study area. The variation of Ni and Cu d values among the different sample types is displayed in **Fig. 4.3**. The most variable δ values were observed for both Ni and Cu in topsoils, followed by Ni δ values in lichens and Cu δ values in snow. The variation can to some extent reflect changes in composition of the smelted ore or in the smelting technology (Ettler, 2016); however, biological and/or biochemical processes are a significant source of isotope fractionation in the environment (Weiss et al., 2008).We assume that Cu fractionation in the studied samples can be caused mainly by adsorption onto mineral surfaces and organic matter (Li et al., 2015b), inorganic and organic complexation (Bigalke et al., 2010), fractionation during plant uptake, processes mediated by microorganisms (Weinstein et al., 2011), redox reactions or precipitation (Lanteigne et al., 2012; Ettler, 2016). Complexation of Cu with humic substances presented in soils results into a fractionation factor of 0.26 ± 0.11‰ (Bigalke et al., 2010). A fractionation factor of up to 0.94‰ between soils and plants was determined by Weinstein et al. (2011); plants were systematically enriched in lighter Cu in comparison to the soil. Relatively little is known about Ni isotopes fate in the environment but a few studies, including ours, indicate that biological processes play an important role in Ni fractionation process (Cameron et al., 2009; Deng et al., 2014; Estrade et al., 2015). According to our results, lichens serve mainly as a mechanical filter for metal particles from the emission source but isotope fractionation caused by lichen-metal interaction cannot be excluded. Some lichens are known to have several biochemical mechanisms for metal detoxification, mainly consisting in the complexation of Cu, Zn, Fe, Mn, Mg, etc. by low molecular weight organic acids (Carreras and Pignata, 2007).
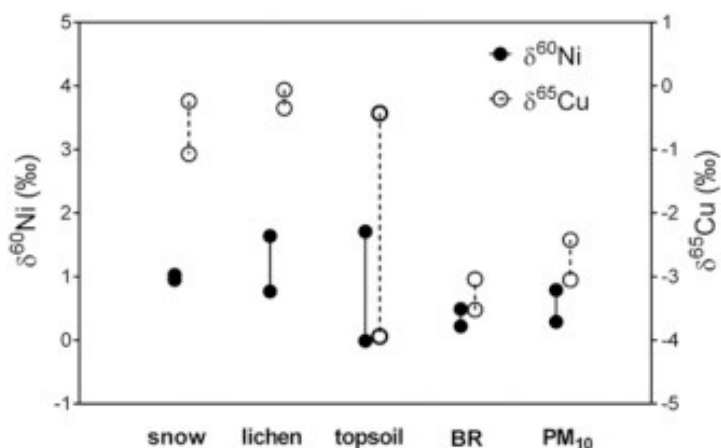

Figure 4.3 Range of $\delta^{60}Ni$ and $\delta^{65}Cu$ in relevant environmental samples.

Conclusion

Based on the obtained data we can conclude that:

- The mineralogical investigation of Cu and Ni confirmed the presence of smelter delivered particles in all types of samples, and both smelter slag and fly ash were identified as potential contaminating sources.
- The concentration analysis confirmed high levels of Cu and Ni contamination especially near the smelter and in the prevailing wind direction from the smelter and the ore-processing facility.
- The N,N/E transect receives the most emissions from both the smelter and the ore-processing plant.
- A significant difference in Cu and Ni concentration and variability of the Ni/Cu ratio between some sample types were observed indicating the different abilities of each sample to entrap and/or accumulate these metals.
- The isotope analysis of Cu and Ni results in a relatively wide range of $\delta^{60}Ni$ and $\delta^{65}Cu$ values in lichen, snow, and topsoil samples in comparison with literature.
- $\delta^{60}Ni$ in most of the snow, lichen, and topsoil samples have similar isotope composition to feeding material and/or smelter slag, while much lighter $\delta^{60}Ni$ values were determined in bedrock indicating the anthropogenic input of Ni.
- A significantly heavier $\delta^{60}Ni$ were determined in the topsoil from sites 4 and 5 and in lichen from site 6, which we suggest to be a result of additional isotope fractionation by soil microorganisms or plant uptake, or in the case of the lichen samples, specific entrapment of metal particles by the thallus.
- $\delta^{65}Cu$ in lichen, snow, and topsoil samples represents surprisingly the heavier Cu fraction in comparison with the industrial samples (SS, FM), bedrock, and PM_{10}, and this shift toward heavier Cu isotopes might be caused partially by heterogeneity in the processed ores. However, we suggest the main reason might be Cu isotope fractionation in the environment by biogeochemical processes explained above.
- A wide range of $\delta^{60}Ni$ and $\delta^{65}Cu$ values was determined mainly in the topsoil, while in snow $\delta^{60}Ni$ and $\delta^{65}Cu$ values were homogenous, highlighting again the role of soil biological systems in isotope fractionation.

According to our results, we are able to suggest that a complex analytical approach for tracing Ni and Cu in the environment and for identification of the sources is necessary. Mineralogical investigation and concentration analysis are reliable methods that can clarify the extent and partial origin of the Ni and Cu contamination. Ni and Cu isotope analysis as a tool for tracing potential sources is a challenging method even in relatively simple areas with only one potential anthropogenic source due to the complexity of the biogeochemical system. The isotope composition of Ni and Cu is not changed during the smelting process, but when the metals reach a biologically active natural environment, isotope fractionation by various processes is very probable. Quantification of the isotope fractionation by separate biogeochemical processes (mainly Ni interaction with microorganism and plants) in the environment is necessary and should be investigated in future studies.

Supplementary material

Figure S 4.1 The study area with marked sampling sites (1-17) and the two smelting facilities. The ore processing plant supply the smelter with the feeding material (Ni-Cu concentrate).
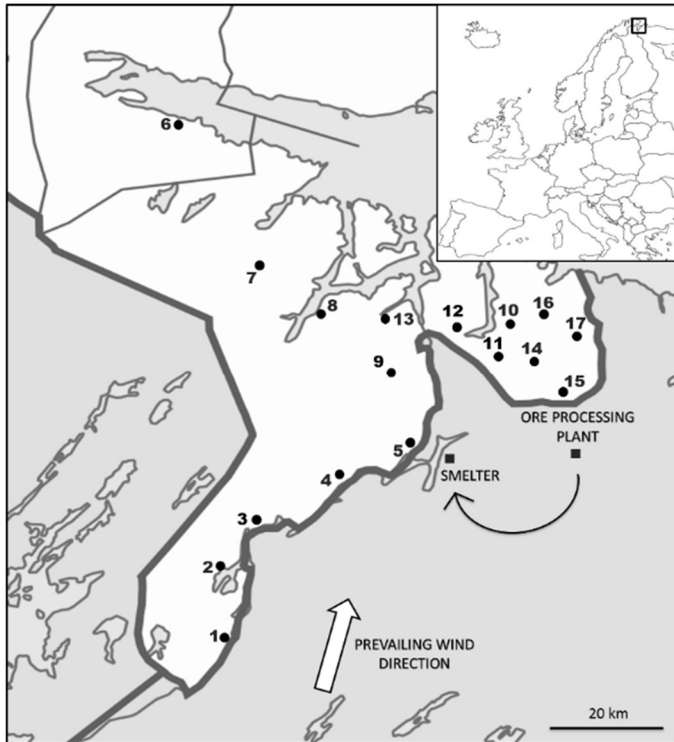
Figure S 4.2 Wind roses from Svanvik (site 5) for summer season April - September 2015 (a) and winter season October 2015 - March 2016 (b). These wind roses show frequency of wind from 12 different sectors, i.e. it shows how often the wind comes from these directions.
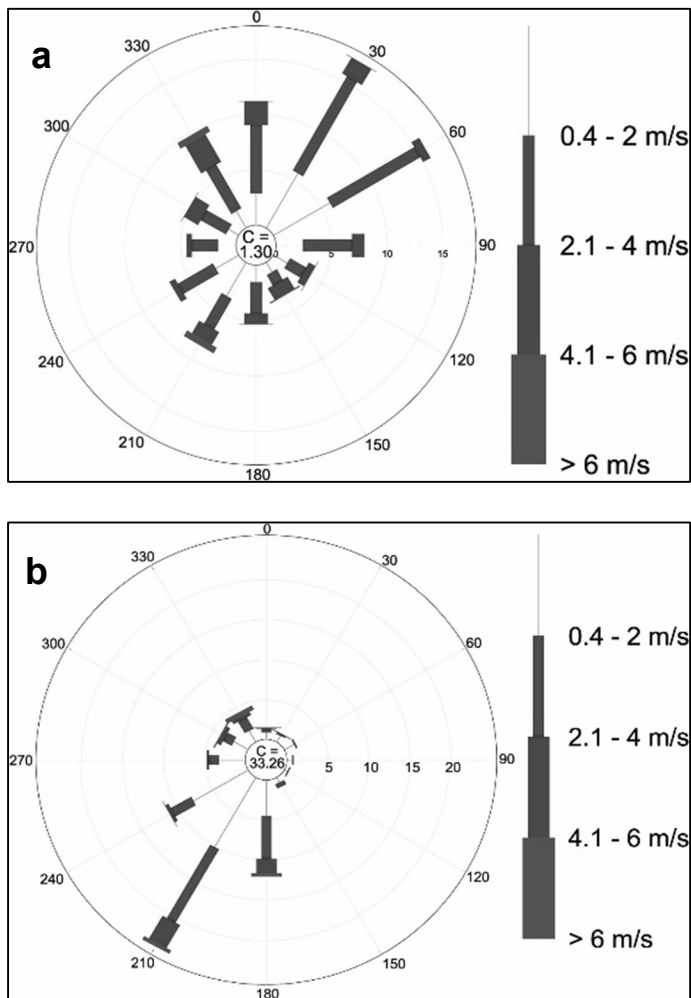
Figure S 4.3 illustrates Ni and Cu concentration in all sample types as a function of distance from the smelter. There was a distance-to-source trend of Ni and Cu in our study; the concentration increased from the most remote site (6) to the closest one (4). The three transects are highlighted as follows: O N/W transect; ● N/E transect; ⵔ S/W transect.
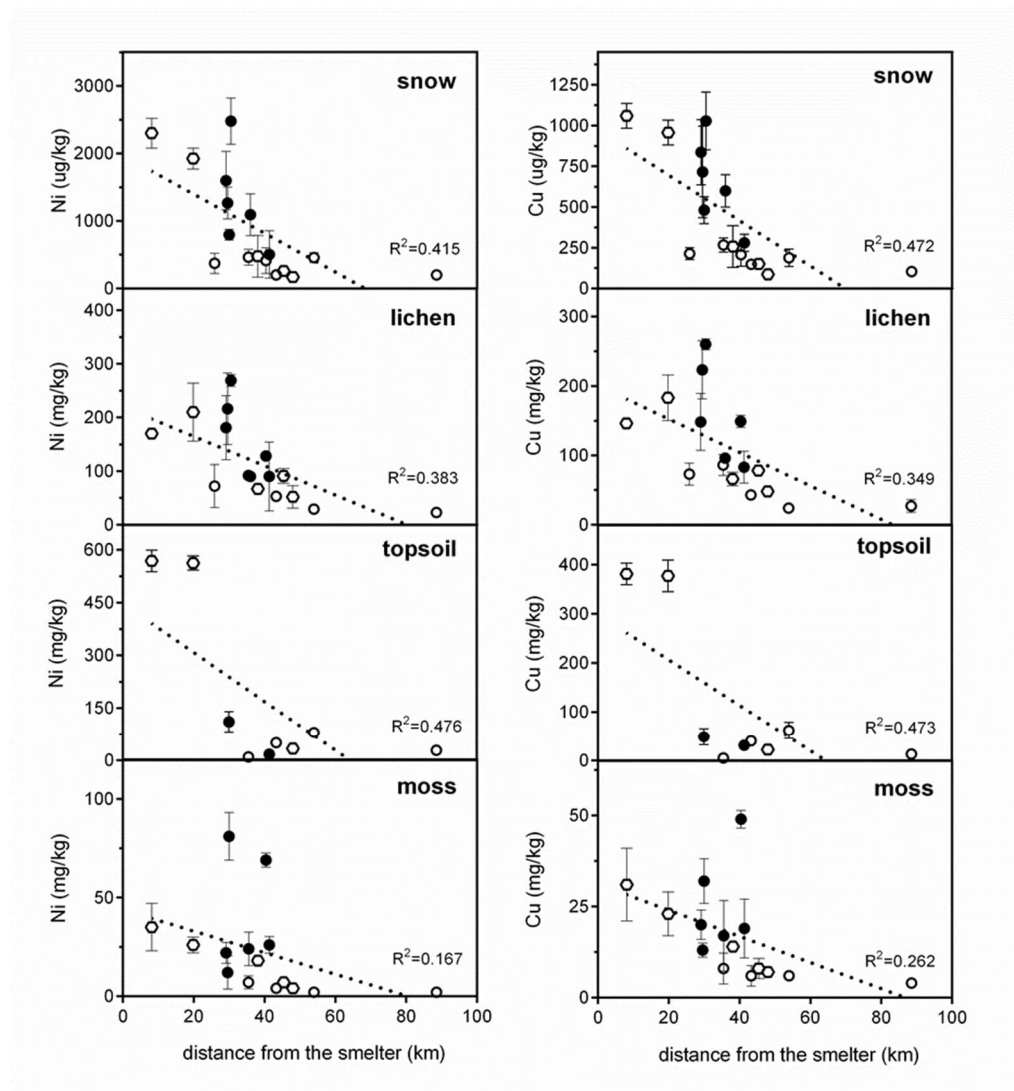
Table S 4.1 List of the samples, sampling sites, methods of pre-treatment and analyses.

Sample type	Sampling site	Pre-treatment methods	Analysis
Snow	1-17	acidification evaporation acid digestion	• ICP MS • MC ICP MS
Soil	1, 4, 5, 6, 7, 8, 13, 15, 17	drying, homogenization sieving (2 mm) acid digestion	• ICP MS • MC ICP MS • SEM/EDS
Moss	1-17	cleaning, drying milling homogenization acid digestion	• ICP MS
Lichen	1-17, except 14 where no lichens were found	cleaning, drying milling homogenization acid digestion	• ICP MS • MC ICP MS • SEM/EDS
PM$_{10}$	Monitoring station near site 5 and 14	acid digestion	• ICP MS • MC ICP MS • SEM/EDS
SS and FM	Nikel smelter	milling homogenization acid digestion	• ICP MS • MC ICP MS • EPMA • SEM/EDS • XRD

SS - smelting slag

FM - feeding material

Table S 4.2 Median and minimum-maximum range of element total concentration (mg kg^{-1}) in the environmental samples in the studied site in Norway. The median concentration of the selected elements in all types of the samples followed nearly consistent order: Ni (Cu) > Cu (Ni) >> Zn > As > Cr (Pb) > Pb (Cr) > Cd.

Sample	Ni (mg kg^{-1})	Cu (mg kg^{-1})	Cd (mg kg^{-1})	Pb (mg kg^{-1})	Zn (mg kg^{-1})	As (mg kg^{-1})
Lichen *Melanohalea o.*	78.9 14.7-247	75.6 16.9-217	0.32 0.07-5.60	4.50 0.80-42.9	49.2 18.8-101	11.6 1.30-30.3
Lichen *Hypogymnia p.*	93.4 14.1–277	94.0 20.8–207	0.35 0.07–2.11	5.91 1.51–55.5	56.9 24.9–206	9.58 0.75–21.1
Snow	0.56 0.47–3.26	0.30 0.07–1.36	0.002 0.001–0.04	0.007 0.004–0.01	0.28 0.12–0.14	0.01 0.003–0.07
Moss *Polytrichum c.*	17.1 1.11–89.2	11.7 2.90–27.1	0.10 0.02–0.18	0.52 0.30–1.48	10.5 3.14–18.3	6.54 2.65–17.2
Topsoil	33.1 8.50–568	22.4 3.4–380.9	0.16 0.05–0.43	25.6 6.12 – 65.7	56.3 15.9 - 101	4.31 2.44–15.8
Bedrock	5.10 0.98-36.2	6.56 1.25–76.4	0.11 0.05 0.16	– 7.03 3.91 – 10.0	58.1 28.9–126	21.7 13.6–24.0

Table S 4.3 Basic physico-chemical characteristics of the studied soil samples.

Site	Depth (cm)	pH	Fe_{ox} (g kg^{-1})	Mn_{ox} (mg kg^{-1})	Al_{ox} (g kg^{-1})	Ni_{TOT} (mg kg^{-1})	Ni_{HNO3} (mg kg^{-1})	Cu_{TOT} (mg kg^{-1})	Cu_{HNO3} (mg kg^{-1})
1	0-8	4.8	0.05	26.3	0.01	33.1	1.53	22.4	3.04
	8-18	5.2	0.20	2.61	0.09	28.6	0.82	20.7	2.15
	18-23	5.1	0.38	5.54	0.10	48.2	0.82	25.0	2.00
	23-x	5.4	0.09	50.3	0.01	70.9	2.39	60.1	4.42
4	0-2	4.0	0.29	30.7	0.15	562	87.7	376	38.6
	2-12	4.4	0.30	0.97	0.03	91.9	2.28	60.7	1.03
5	0-5	3.7	0.15	7.56	0.06	568	107	380	51.0
	5-15	4.5	0.17	0.30	0.09	27.3	1.81	6.5	0.76
	15-45	5.3	0.35	0.95	0.19	37.6	0.81	16.8	1.23
6	0-2	4.6	0.10	0.86	0.01	28.1	1.38	13.4	1.98
	2-20	5.8	0.08	14.1	0.00	77.1	3.09	52.9	5.65
	20-x	5.3	0.64	4.05	0.23	74.0	1.87	52.9	4.25
7	0-2	5.4	0.14	81.0	0.01	80.4	5.97	61.7	14.3
	2-23	5.3	0.35	3.15	0.26	58.6	1.13	47.2	3.39
	23-x	5.7	0.12	29.5	0.04	68.9	2.59	71.2	6.25
8	0-2	5.0	3.45	26.2	0.68	50.0	6.07	40.4	6.61
	2-x	5.3	1.37	44.4	1.36	20.8	1.10	9.60	1.19
13	0-5	4.1	0.02	0.84	0.02	9.06	0.94	4.55	0.74
	5-10	3.8	0.79	0.30	0.47	8.54	1.61	6.61	1.24
	10-x	4.4	0.15	0.77	0.11	11.4	0.21	3.40	0.12
15	0-10	4.7	0.08	2.31	0.02	111	26.6	48.7	7.54
	10-25	5.3	0.24	3.93	0.62	20.8	3.76	20.1	0.53
	25-x	4.8	0.29	1.53	0.03	24.7	0.97	8.72	0.66
17	0-15	4.7	0.57	0.23	0.64	17.0	3.41	31.4	5.35
	15-20	4.9	0.07	5.76	0.05	10.7	0.16	7.30	1.46
	20-35	5.0	0.53	0.05	0.53	20.6	0.48	21.6	4.01
	35-x	5.1	0.38	3.55	0.17	25.0	0.60	17.5	2.39

Table S 4.4 Total content of selected elements of bedrock (BR) and PM$_{10}$ from selected sampling sites, smelting slag (SS), feeding material (FM).

	Sampling site	Al (g kg^{-1})	Ca (g kg^{-1})	Mg (g kg^{-1})	Fe (g kg^{-1})	Mn (g kg^{-1})	Ni (g kg^{-1})	Cu (g kg^{-1})
BR	4	13.3	14.4	1.33	33.2	0.74	0.03	0.08
BR	6	13.6	16.5	0.11	11.9	0.35	0.001	0.001
BR	15	17.0	14.5	0.10	35.0	0.31	0.03	0.02
SS	-	143	3.48	1.96	36.9	0.18	84.8	95.4
FM	-	<LD	<LD	<LD	5.83	<LD	153	393
	Sampling site/Period	Al (ng m^{-3})	Ca (ng m^{-3})	Mg (ng m^{-3})	Fe (ng m^{-3})	Mn (ng m^{-3})	Ni (ng m^{-3})	Cu (ng m^{-3})
PM$_{10}$	5/Jan	134	0.57	20.1	698	2.28	5.57	7.56
PM$_{10}$	5/Mar	4.60	<LD	5.80	658	1.23	2.79	2.84
PM$_{10}$	15/Jan	<LD	<LD	20.6	7582	3.54	117	60.0
PM$_{10}$	15/Mar	23.0	<LD	12.8	858	53.7	7.90	4.75

Table S 4.5 Concentration of selected elements in the lichen, soil and bedrock sample before the separation process

	Na (mg L^{-1})	Mg (mg L^{-1})	Al (mg L^{-1})	Ca (mg L^{-1})	Fe (mg L^{-1})	Cu (mg L^{-1})	Zn (mg L^{-1})	Cr (mg L^{-1})
Lichen	23.6	0.49	1.6	8.85	5.50	0.85	1.03	0.02
Soil	45.2	13.9	102	56.1	69.1	2.90	0.58	0.27
Bedrock	171	30.7	8.31	200	670	1.11	1.48	1.78

Chapter V

Unleaded gasoline as a significant source of Pb emissions in the Subarctic

V. Chrastný, H. Šillerová, M. Vítková, A. Francová, J. Jehlička, J. Kocourková, P. E. Aspholm, L. O. Nilsson, T. F. Berglen, H. K. B. Jensen, M. Komárek

Content

Abstract

After the phasing out of leaded gasoline, Pb emissions to the atmosphere dramatically decreased, and other sources became more significant. The contribution of unleaded gasoline has not been sufficiently recognized; therefore, we evaluated the impact of Pb from unleaded gasoline in a relatively pristine area in Subarctic NE Norway. The influence of different endmembers (Ni slag and concentrate from the Nikel smelter in Russia, PM_{10} filters, and traffic) on the overall Pb emissions was determined using various environmental samples (snow, lichens, and topsoils) and Pb isotope tracing. We found a strong relationship between Pb in snow and the Ni smelter. However, lichen samples and most of the topsoils were contaminated by Pb originating from the current use of unleaded gasoline originating from Russia. Historical leaded and recent unleaded gasoline are fully distinguishable using Pb isotopes, as unleaded gasoline is characterized by a low radiogenic composition ($^{206}Pb/^{207}Pb$ = 1.098 and $^{208}Pb/^{206}Pb$ = 2.060) and remains an unneglectable source of Pb in the region.

Introduction

Air pollution by metals (i.e., Pb, Cd, Hg, and Zn) has been of great interest in the past two decades. Metals in the atmosphere are to a great extent associated with solid particles with diameters in the range of several tenths to 10 mm (Nriagu, 1980). The transportation of metal-bearing particles over long distances is feasible despite the highly variable residence time of the finer particles (Simonetti et al., 2003).

Many forms of Pb are highly toxic, and exposure to an organism can lead to severe physiological and neurological effects. One of the primary input pathways to the organisms is by respiration, and particles with relatively small diameters (less than 10 mm) are deposited in the lungs. Since the 1940s, tetraethyl lead (TEL) has been added into gasoline as an antiknock additive (Adriano, 2001). Leaded gasoline became a major source of Pb in the atmosphere with its maximum contribution in the 1970s (Nriagu, 1989), and the phasing out of leaded gasoline increased the relative proportion of other Pb sources in the atmosphere (mining and smelting activities, combustion of fossil fuels, etc.) (Veron et al., 1999). As expected, the phasing out of leaded gasoline decreased dramatically the concentration of Pb in Europe, Northern America and Asia (Annibaldi et al., 2009; Cimova et al., 2016; Li et al., 2009; Novák et al., 2003).

However, several authors have referred to unleaded gasoline as a new considerable anthropogenic source of lead emitting to the atmosphere (Shiel et al., 2012; Yao et al., 2015). For instance, Shiel et al.(2012) found that according to the Canadian Statistics report, unleaded gasoline consumption accounts for 8.4% of the total Pb emissions from fossil fuels (i.e., petroleum products and coal). Another source of Pb could be from the use of avgas (aviation gasoline) in spark-ignited internal combustion engines of small general aircrafts (personal aircrafts, seaplanes, crop dusters and bush planes) (Shiel et al., 2012). Similar to leaded gasoline, TEL is added to avgas, which is produced by only a few companies worldwide (Shiel et al., 2012).

Lead isotopes ^{204}Pb, ^{206}Pb, ^{207}Pb and ^{208}Pb are well known as a "fingerprint" tool for tracing the sources of Pb pollution (Komárek et al., 2008). Generally, European and U.S. leaded gasoline differed in Pb isotopes. While TEL added to European leaded gasoline originated from Australia (Broken Hill deposit) and was characterized by lower radiogenic values (^{206}Pb/^{207}Pb from 1.03 to 1.10), the U.S. leaded gasoline was more radiogenic (Mississippi Valley ore deposit, ^{206}Pb/^{207}Pb from 1.31 to 1.35) (Komárek et al., 2008).

Some authors have still observed low radiogenic Pb values in urban and traffic areas (Cloquet et al., 2006; Doucet and Carignan, 2001; Simonetti et al., 2003). Cloquet et al., (2006) attributed this fact to re-deposition of "older" Pb originating from leaded gasoline. Simonetti et al., (2003) observed lichen samples in NW North America and found an isotope range of $^{206}Pb/^{207}Pb$ from 1.15 to 1.17 of unclear origin. Similarly, Doucet and Carignan (2001) presented an average industrial Pb-signal around $^{206}Pb/^{207}Pb$ = 1.15 in France and attributed the source to a waste incinerator in Geneva, Switzerland.

Several authors provided another possible explanation for the source of low radiogenic Pb values after the phasing out of leaded gasoline (Shiel et al., 2012; Yao et al., 2015). Shiel et al., (2012) found a Pb composition in oysters from British Columbia similar to road dust and lichen samples described in the work by Simonetti et al., (2003). They reported that this composition is representative of the average modern Pb isotopic signature of unleaded gasoline and diesel fuel, however the authors did not provide direct analytical evidence for this statement. Another group of authors (Yao et al., 2015) measured Pb isotope composition in unleaded gasoline (octane numbers of 92, 95, 98) and diesel from local suppliers in Taipei, Taiwan. The average Pb isotope composition found in vehicle exhaust ($^{206}Pb/^{207}Pb$ = 1.148) overlapped with reported aerosol data, while the Pb isotope composition in unleaded gasoline and diesel fell within the ranges of 1.139-1.152 and 1.144-1.157, respectively (Yao et al., 2015).

Considering that direct evidences of Pb input from unleaded gasoline is missing and questionable, we decided to report Pb isotope data from various environmental samples (snow, lichen, moss, soil and aerosol - particulate matter, specifically PM_{10}) originating from NE Norway to show the impact of unleaded gasoline combustion in a relatively simple environment with only a few Pb endmembers. Snow, lichen and soil samples were further used to describe contamination pathways of Pb emissions from local dispersed and remote sources and we revised the idea of resuspension of the "old" gasoline lead in the environment.

Materials and methods

Study area and sources of contamination

The sampling network covers approximately 2000 square kilometres in north-eastern (NE) Norway, near the Norwegian-Russian border. The region is known for the largest remaining area of primeval pine forest in Norway, an offshoot of the Siberian taiga (**Fig. 5.1**). The study area is dominated by birch forests and low- productivity pine forests. The annual average temperature is -1 °C, the annual precipitation is 400-500 mm/year, and the elevation is between approximately 80 and 280 m a.s.l. (Räisänen et al., 1997). There are two important non-ferrous metal processing plants, the Nikel smelter (5 km from the border) and an ore enrichment plant in Zapolyarny (15 km from the border). The facilities emit SO_2 and risk elements, mainly Ni and Cu. Additionally, these types of industries remain a huge source of SO_2 and a wide range of elements: Ag, Al, As, Cd, Co, Cr, Cu, Fe, Hg, Mn, Ni, Pb, Sb, Sr, Th, Tl, Zn and others (Reimann et al., 1996).

In total, 17 sampling sites were chosen. The sampling sites can be divided into 3 transects. Transects go approximately 50 km south-west (transect 1; sites 1, 2, 3, 4, and 5), 90 km north-west (transect 2; sites 6, 7, 8, 9, and 13) and 40 km north-east (transect 3; sites 10, 11, 12, 14, 15, 16, and 17) from the Nikel smelter. The prevailing wind direction is north, north-east (N,NE) (**Fig. 5.1**).

Sampling and sample treatment

The sampling was performed in March 2015 (snow and lichens) and August 2015 (soil profiles and bedrock). Snow and lichens were collected at each site (1-17), soil profiles and bedrock were only collected at selected sites of each transect (1, 4, 5, 6, 7, 8, 13, 15, and 17). Moreover, PM_{10} fraction was provided by the Norwegian Institute for Air Research, from two monitoring stations, and included atmospheric deposition data from January and March 2015. The PM_{10} samples came from monitoring stations in Svanvik (3 m above the ground near site 5) and in Karpdalen (1.5 m above the ground near site 15). Finally, representative samples of the smelter slag and the feeding material (Ni-ore concentrate) were obtained for the analysis of Pb isotope composition.

Approximately 2 L of fresh snow was collected directly to a polypropylene bottle. Snow was collected in duplicate, and the sampling points were within 50-100 m from

each other. Only visually clean and fresh snow was collected to avoid collecting ground vegetation or ice layers. Only *Hypogymnia physodes* and *Melanohalea olivacea*, two foliose species, occurred within the study area. Approximately 30 thalli of each species were cut from several tree branches and trunks using a ceramic knife and stored in paper bags. The aboveground part of the moss *Polytrichum commune* was collected at each sampling site and stored in paper bags. Samples of soil profiles were collected from a 1 x 1-m-wide pit sectioned into 3 or 4 parts according to the natural development and visible changes within the profile down to the mineral horizon. The top surface composed of fresh litter or grass cover was removed. Bedrock samples were collected using a geological hammer. Each sample consisted of 5-7 rock fragments. All the samples were homogenized and decomposed in a mixture of acids (HNO_3, HCl, and HF) to obtain a liquid sample.
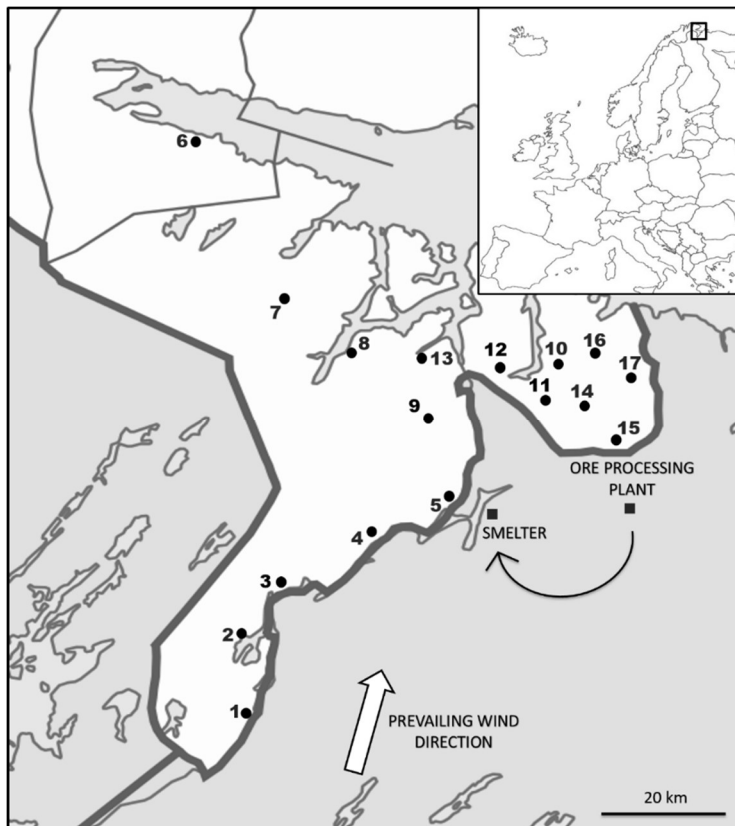

Figure 5.1 Study area and sampling sites.

Pb concentration and isotope analysis

Concentration of Pb was determined by an inductively coupled plasma-mass spectrometer (ICP MS, iCAP Q, Thermo Fisher Scientific, Germany) using an aqueous calibration standard Certi-PUR (Merck, Germany). The drift of an analytical signal was corrected using In as an internal standard.

Pb isotope ratios presented here were measured using ICP MS. Raw $^{206}Pb/^{207}Pb$ and $^{208}Pb/^{206}Pb$ were measured and the data were corrected according to instrumental mass bias. The correction was done on the basis of the standard-sample bracketing technique using SRM NIST 981 (common lead). Ten replicates were measured for each standard and sample measurement (120 sweeps for each measurement).

QA/QC procedures

The quality control procedures consisted of measurements of sample replicates and triplicates and certified reference materials. To ensure the accuracy of the analytical process, we used the certified reference materials as follow: BCR-482 Lichen (IRMM, Belgium), SRM 1640a Natural Water (NIST, USA) and SRM 2710a Montana I Soil (NIST, USA). The recovery of Pb certified reference values was within the range of 89-111% for all the materials used. Internal reproducibility for concentration and isotope measurements was better than 3 and 0.4% for all standards and sample analyses, respectively. The external reproducibility (between sample replicates and triplicates) was better than 15%. The method quantification limit (MQL) calculated based on all steps of analytical procedure was 13 ng L^{-1} and 6 µg kg^{-1}, for liquid (snow) and solid (soil, bedrock and lichen) samples, respectively.

Results and discussion

Pb concentrations in snow samples

Gregurek et al. (1998a) distinguish between snowmelt (dissolved metals defined by 0.45 µm filter porosity) and the filter residue (solid particles).We measured the total amount of metals in snow samples to avoid potential loss of analyte due to the fact that metal concentrations in snow is generally at ppb levels and snow melting can take place over 24 h. During that time, a certain amount of metals can adsorb on the PET wall. However, the slight acidification of snowmelt prevents sorption, and causes leaching of the particle surface and therefore, an overestimation of the snow melt metal fraction.

We summarize the snow and lichen concentrations in **Table 5.1**. The snow concentrations are relatively uniform and vary between 18 µg L^{-1} (# 1) and approximately 64 µg L^{-1} (# 17). The relatively higher Pb concentrations in snow samples were detected at sampling points very close to highly frequented roads. We found 48.5 µg L^{-1} at sampling points # 4 and # 9, both on the local road of 885 connecting the southern and northern parts of the area and at # 13, which is near to the city of Kirkenes. Additionally, higher Pb concentrations were detected at points #10, 11, 16 and 17 (the highest Pb concentration was 63.5 µg L^{-1}) (**Table 5.1**). This north-eastern area is a military border area frequented by military vehicles and snowmobiles or can be related to the emissions from the smelter and ore processing plant with a prevailing wind direction from the south.

Gregurek et al., (1998a) analysed snowpack samples from the vicinity of the Ni smelter in Monchegorsk (Russia), an area more than 200 km southeast from our sampling points. If we compare Pb concentrations in snow melt and filter residues with the study by Gregurek et al., (1998a), we can observe comparable results (several tens of µg L^{-1}) at those points of relatively low Pb concentrations (points 1-3, 5-8, 12, and 15). This fact means that the Russian Ni industry is not the main source of Pb contamination in this area. Reimann et al. (1996) characterized industrial emissions near the cities of Nikel and Zapoljarnyj (very close to our sampling points). They found that the Pb concentrations, even in the sub-ppb levels, were much lower than both the concentrations from Gregurek et al., (1998a) and the concentrations from this study. According to the Reimann et al., (1996) the Pb emissions came from the Ni smelter but the level of contamination was exceptionally low. The differences in our and earlier results by Reimann et al., (1996) could be due to different sampling strategies. We were

focused on sampling points near highly frequented roads, while Reimann et al., (1996) sampled more remote open areas.

Pb concentrations in lichen samples

The Pb concentration in both lichen species *Hypogymnia physodes* and *Melanohalea olivacea* are highly heterogeneous at some sampling points (# 4, 5, 8, 9, 11 and 13) (**Table 5.1**). Generally, at sampling points less exposed to emissions from highly frequented roads (# 1-3, 6 and 7), the sample replicates were more consistent (**Table 5.1**). We increased the amount of well-homogenized samples from the previous 250 mg - 500 mg, which is the maximum mass usable for the EPA 3051 method using microwave digestion, but without any substantial effect on Pb concentrations heterogenity. When considering, for instance, Pb concentration in *Melanohalea olivacea* at # 8 (22.1 mg kg^{-1}), the range was from 2.41 to 42 mg kg^{-1}, with a difference

Table 5.1 Pb concentrations in snow and lichen samples (mean ± 2SD).

| Site | Snow | Lichen (mg kg^{-1}) | |
		Melanohalea olivacea	*Hypogymnia physoides*
1	18.0 ± 5.66	3.04 ± 0.81	3.51 ± 0.32
2	22.0 ± 7.07	3.71 ± 1.20	0.23 ± 0.28
3	18.0 ± 2.83	3.55 ± 0.52	3.81 ± 0.75
4	48.5 ± 16.3	4.69 ± 0.36	24.9 ± 10.8
5	22.5 ± 2.12	6.53 ± 3.36	2.89 ± 1.23
6	28.1 ± 8.49	2.96 ± 0.19	1.80 ± 0.42
7	15.5 ± 9.90	2.08 ± 0.14	8.11 ± 0.04
8	30.5 ± 9.19	22.07 ± 27.8	5.54 ± 2.59
9	49.4 ± 10.9	8.69 ± 8.0	30.2 ± 35.8
10	43.1 ± 5.66	2.20 ± 0.20	5.59 ± 0.24
11	34.5 ± 4.95	3.28 ± 0.37	6.25 ± 4.22
12	27.5 ± 9.19	3.24 ± 0.07	8.16 ± 0.49
13	41.2 ± 5.66	6.77 ± 0.81	12.0 ± 3.39
14	32.8 ± 9.90	n.a.	n.a.
15	21.5 ± 4.95	5.11 ± 0.39	7.69 ± 0.12
16	55.5 ± 12.0	6.29 ± 0.49	5.91 ± 0.13
17	63.5 ± 16.3	4.60 ± 0,39	7.63 ± 1.27

of approximately 40 mg kg^{-1}. The Pb aliquot related to 0.5 g of the sample is 20 mg. In the case of PbO, it is 21.5 μg absolutely. From the density of PbO (9.53 g cm^{-3}), we can further calculate the diameter of a theoretical spherical particle, which is equal to 1.6 μm. In other words, only one spherical particle with the diameter of 1.6 μm can influence the above-mentioned range of Pb concentration in a lichen sample. Therefore, an efficient sample homogenization in such cases is almost impossible.

Our lichen data correspond well with the earlier work by Äyräs et al. (1997), which addressed the monitoring of terrestrial moss in northern Finland, Norway and Russia. Pb concentrations in their study varied between 0.8 and 29.4 mg kg^{-1}, and the authors attributed the sources of Pb to local mines, industry and traffic. They found higher Pb concentrations in the vicinities of cities, such as Nikel, Murmansk and Monchegorsk, and on the Norwegian side near local traffic centres, i.e., near the Norwegian-Finnish border (the main E6 road, close to our sampling points # 7 and 8, wherewe detected elevated Pb concentrations in snow and lichen samples, **Table 5.1**). Haack et al. (2004) analysed topsoils, mineral soil horizons, moss samples and melted snow. Using a coupled Pb concentration/stable isotope analyses they proved that Pb from Nikel and Zapolarnyi is probably not a major contributor.

We found elevated Pb concentrations in lichen samples near frequented roads, mainly at sampling point # 4, 8, 9 and 13. Point # 13 is near the city Kirkenes. At points # 8, 9, and 13 we measured higher Pb concentrations in snow samples (**Table 5.1**). Conversely, the highest Pb level in snow was at sampling point # 17 where only moderate Pb concentrations in lichen samples were found (**Table 5.1**). While snow reflects only current emissions, lichens integrate information of several years. We can therefore assume that traffic in the northeastern area (points # 11-17) is not so frequent compared to the westernmost region, and the surrounding points # 8, 9, and 13. However, during winter periods, military traffic is more likely responsible for Pb concentrations in the snow.

Pb concentrations in soil samples

We measured Pb concentrations in soils at sampling points where the soils had developed (points # 1, 4-8, 13, 15, and 17) (**Fig. 5.1 and Table 5.2**). Pb concentrations in topsoil layers varied by one order of magnitude from 15.4 (# 17) to 164 mgkg^{-1} (# 4).We found relatively higher Pb values at some sampling points (**Table 5.1**) compared to earlier works. For example, Räisänen et al. (1997) included in their study a sampling point at Skellbekken that corresponds to our sampling point # 4, while Räisänen et al., (1997) and Reimann et al. (1997a) found Pb concentrations of

approximately 15 mg kg[1],we observed a value more than 10 times higher (**Table 5.2**). Haack et al., (2004) had a sampling network with a larger grid and their sampling points did not overlap with ours but the highest value in their study was approximately 43 mg Pb kg^{-1} at the Russian site (almost 200 km south from our nearest sampling point # 1).

Our sampling strategy was adapted to prove the importance of traffic for the Pb emissions in this Subarctic area. Therefore, we designed the sampling points systematically near highly frequented roads (**Fig. 5.1**) contrary to other studies (Reimann et al. 1997a; Haack et al. 2004; Räisänen et al. 1997). Points # 1, 4 and 8 closer to higher traffic had higher Pb concentrations in the topsoil; the other sites, # 15 and 17, were influenced only by the Ni smelter and ore processing plant (**Fig. 5.1**), and the Pb concentrations were significantly lower (**Table 5.2**). Therefore, our findings are congruent with the findings by Äyräs et al. (1997) that the Russian metallurgical activities are of minor importance in terms of Pb emissions.

Pb isotope composition in snow, lichen and soil samples

The $^{206}Pb/^{207}Pb$ and $^{208}Pb/^{206}Pb$ isotope ratios were measured to determine the contributions of separate Pb sources (**Table S 5.1**). The $^{206}Pb/^{207}Pb$ ratio found in snow samples varied from 1.131 (# 16) to 1.209 (# 6) (**Fig. 5.2**). The continuous snow cover limits possible particle resuspension, as shown from the comparison of Pb isotope composition in topsoils and snow at sampling points # 1, 4, 6, 7, 13 and 15.We further hypothesize that mainly heavier particles from the nearest point sources can contaminate the surface of the snow cover and that the Pb isotope composition should reflect their contribution (Francová et al., 2017b). In our study area, there are only two potential main sources of Pb contamination: Russian metallurgy and traffic.

We were not able to obtain fly ash from the Nikel smelter, but we sampled the Ni concentrate from the Ni ore and Ni slag from the Ni ore processing plant. Instead of fly ash, we obtained the PM_{10} fraction (<10 μm) of particulate matter from the atmospheric aerosol from two sampling points near the Ni smelter (# 5) and near the ore processing plant (# 15). The Pb isotope composition of the potential endmembers is presented in **Table 5.3**. The $^{206}Pb/^{207}Pb$ ratios of the Ni concentrate and slag were homogenous with values of 1.150 and 1.146 for concentrate and slag, respectively. This Pb isotope signature can be observed in lichen samples at points # 1, 2, 12, and 15-17 and in snow samples from points # 11-17 (**Table 5.1, Fig. 5.2**.). Sampling points # 1 and 2 could not have been easily contaminated by either the smelter or the ore processing plant because of the long distance and prevailing wind directions (**Fig. 5.1**).

Table 5.2 Pb concentrations in snow and lichen samples (mean ± 2SD).

| Site	Depth	pH	Fe_{ox}	Mn_{ox}	Al_{ox}	Pb_{TOT}	Geological description
1	0–8	4.8	0.05	26.3	0.01	70.3 ± 10.6	peat (over 0.5 m)/glacifluvial and beach sediments/gneiss; granitic gneiss
	23-x	5.4	0.09	50.3	0.01	37.9 ± 10.1	
4	0–2	4.0	0.29	30.7	0.15	164 ± 10.5	moraine material (over 0.5 m)/ metamorphosed basalt and andesite
	2-x	4.4	0.30	0.97	0.03	65.3 ± 58.4	
5	0–5	3.7	0.15	7.56	0.06	100 ± 3.91	moraine material (over 0.5 m) / granitic gneiss
	45-x	5.3	0.35	0.95	0.19	24.9 ± 5.03	
6	0–2	4.6	0.10	0.86	0.01	25.0 ± 2.79	migmatitic, tonalitic and granodioritic gneiss
	20-x	5.3	0.64	4.05	0.23	29.0 ± 5.61	
7	0–2	5.4	0.14	81.0	0.01	64.1 ± 68.1	peat (over 0.5 m)/moraine material (up to 0.5 m)/gneiss; amphibolite
	23-x	5.7	0.12	29.5	0.04	42.1 ± 16.5	
8	0–2	5.0	3.45	26.2	0.68	114 ± 6.34	marine sediments (over 0.5 m) /tonalitic and granodioritic gneiss
	2-x	5.3	1.37	44.4	1.36	32.8 ± 7.56	
13	0–5	4.1	0.02	0.84	0.02	19.0 ± 5.29	marine sediments (over 0.5 m) /granitic gneiss
	10-x	4.4	0.15	0.77	0.11	22.3 ± 6.14	
15	0–10	4.7	0.08	2.31	0.02	17.1 ± 5.09	moraine material (over 0.5 m)/ granite („spotted granite")
	25-x	4.8	0.29	1.53	0.03	24.2 ± 9.46	
17	0–15	4.7	0.57	0.23	0.64	15.4 ± 3.42	moraine material (over 0.5 m)/ monzonite
	35-x	5.1	0.38	3.55	0.17	20.1 ± 5.07	
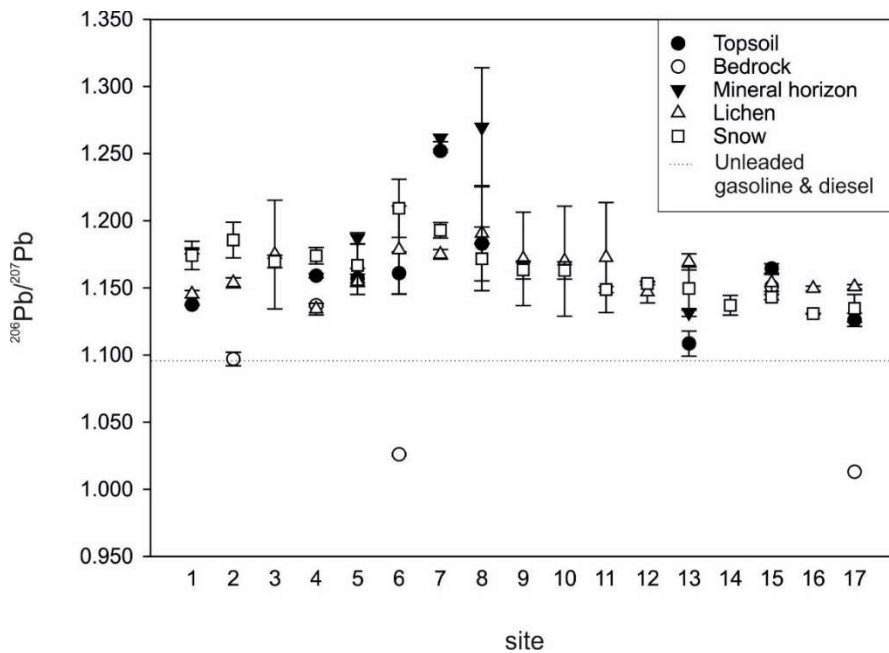
Figure 5.2 ^{206}Pb/^{207}Pb isotope composition in samples of topsoil, bedrock, mineral horizon, lichen and snow. The dotted line represents unleaded gasoline/diesel from the Russian gas station.

Therefore, the Pb isotope signal at the northeastern sampling points is more likely related to the metallurgical industry (**Fig. 5.1**).

This fact was further proven by the analyses of PM$_{10}$. Generally, Pb isotope signatures in PM$_{10}$ differ at both sampling points and different sampling times. PM$_{10}$ were sampled in January and March of 2015. While at some points we observed a homogenous (and the highest) Pb signature within both samples (# 5, ^{206}Pb/^{207}Pb = 1.189, **Table 5.3**), at other sites (e.g., # 15), we obtained different values for January and March (**Table 5.3**). The PM$_{10}$, contrary to snow samples, contain particles with very long residence times in the atmosphere, and can be transported over long distances (Francová et al., 2017b). Moreover, the credibility of PM$_{10}$ is related to the actual wind direction, thus the robustness of sampling replicas is limited.

Table 5.3 Pb concentration and isotope composition of endmembers. Results are given as mean ± 2SD.

Sampling campaign 2015		$^{206}Pb/^{207}Pb$	$^{208}Pb/^{206}Pb$	Pb (mg kg^{-1})
PM$_{10}$ (#5)	January	1.187 ± 0.003	2.061 ± 0.01	0.93 ± 0.07
	February	1.190 ± 0.005	2.064 ± 0.006	0.74 ± 0.04
PM$_{10}$ (#15)	January	1.156 ± 0.004	2.098 ± 0.007	1.57 ± 0.02
	February	1.177 ± 0.006	2.074 ± 0.01	1.75 ± 0.03
Ni slag		1.150 ± 0.003	2.101 ± 0.008	36 ± 0.09
Ni concentrate		1.146 ± 0.002	2.100 ± 0.009	n.d.
Unleaded gasoline - Russia		1.098 ± 0.003	2.060 ± 0.011	0.98[a]±0.1
Diesel - Russia		1.100 ± 0.002	2.062 ± 0.006	0.89[a]±0.1
Unleaded gasoline - Norway		1.148 ± 0.003	2.124 ± 0.008	0.38[a]±0.05
Diesel - Norway		1.153 ± 0.006	2.129 ± 0.009	0.50[a]±0.05

n.d. – not defined

[a] mg L^{-1}

The Pb isotope signatures of topsoils and environmental indicators are more or less congruent at most of the sites. For example, at point # 7, both snow and lichen samples differ from the topsoil, which is consistent with the mineral horizon. This fact can be explained either by the influence of the metallurgy or unleaded gasoline. The influence of the industry is unlikely due to the position of the sampling point and prevailing wind direction. Another explanation (and our hypothesis) can be related to the influence of unleaded gasoline to Pb emissions. We therefore analysed both gasoline and diesel from the local gasoline station in Kirkenes, Norway, and in Nikel, Russia (**Table 5.3**). The Pb in Russian unleaded gasoline, which is commonly used by the locals, is less radiogenic with $^{206}Pb/^{207}Pb$ at approximately 1.10 (**Table 5.3**). The difference in Pb isotope composition between topsoil and lichen samples at this locality excludes possible particle resuspension. The different bedrock or mineral Pb isotope composition is due to the complicated geological conditions characterized by deposition of secondary moraine material at most of the sampling points (**Table 5.1**).

Pb source apportionment in the Norway/Russian/Finland border area

For a better representation of Pb source apportionment, we constructed a three-isotope plot (**Fig. 5.3**) containing both $^{206}Pb/^{207}Pb$ and $^{208}Pb/^{206}Pb$ isotope ratios. The addition

of the ^{208}Pb isotope distributed our data into two main groups. The first group contains all of the snow samples, PM_{10}, Ni slag, concentrate and most of the bedrocks. The second contains most of the topsoils, lichens and data on unleaded gasoline (**Fig.5.3**). Continuous snow cover limits resuspension, hence, snow samples are distinguishable from lichen and topsoils, which have a large overlap in the Pb isotope composition (**Fig.5.3**). According to **Fig. 5.3**, snow samples contained Pb derived from the metallurgical industry; however, for the topsoil and lichen, the prevailing source was Russian unleaded gasoline. We suggest that snow contains mainly those particles traveling through the atmosphere at relatively higher altitudes, where the dry deposition can be created. This can explain the same Pb isotope composition found in PM_{10} samples, Ni products and waste materials, and snow samples. Topsoils and lichen samples from the vicinity of highly frequented roads contain particles from lower parts of the atmosphere coming primarily from vehicle exhausts. Some authors attribute low-value radiogenic Pb found in environmental samples (i.e., moss and lichen samples) to resuspension of previously used leaded gasoline (Cloquet et al., 2006; Doucet and Carignan, 2001; Haack et al., 2004); however, this does not discredit the possibility of Pb contribution from unleaded gasoline. Shiel et al. (2012) suggested that unleaded gasoline is a source of Pb contamination of bivalves collected from western Canada (British Columbia); however, the authors do not present clear evidence for this statement. They only suggest that the low radiogenic composition of Pb isotopes found in oyster samples are consistent with atmospheric aerosols reported by Simonetti et al. (2003) and in road dust analyzed along two highways in British Columbia collected by Preciado et al. (2007). The authors presented low-value radiogenic isotope ratios different from those related to leaded gasoline found deeper in roadside soils; however, the Pb isotope composition of unleaded gasoline was only taken from Erel et al. (1997) as an average value of ^{206}Pb/^{207}Pb approximately 1.11.

Additionally, Erel et al. (1997) did not present original data but referred to Monna et al. (1995) who characterized the automotive exhausts near a car parking. France completely phased out leaded gasoline by 2000 and their data represents thus effects from leaded gasoline. From our observations, we were able to distinguish between two main sources of Pb in the study area: Ni metallurgy (Ni concentrate -^{206}Pb/^{207}Pb = 1.146 and ^{208}Pb/^{206}Pb = 2.100, **Fig. 5.3**) and unleaded gasoline from Russia (Diesel -^{206}Pb/^{207}Pb = 1.100 and ^{208}Pb/^{206}Pb = 2.062 and gasoline ^{206}Pb/^{207}Pb = 1.098 and ^{208}Pb/^{206}Pb = 2.060, **Fig. 5.3**). Although, the possibility is unlikely, the resuspension of "old" Pb from leaded gasoline should still be considered by taking into account the lichen lifetime (less than 5 years, Simonetti et al., 2003) and time since the phasing out of leaded gasoline. When we compared the two Pb sources in the Subarctic area, the predominant source near the frequented roads was the combustion of unleaded gasoline
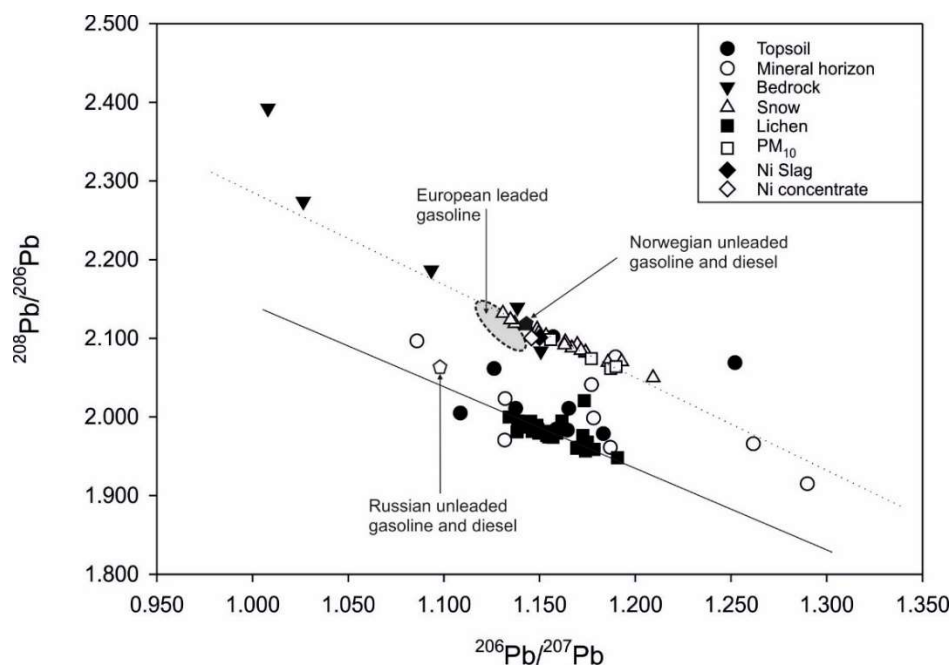
Figure 5.3 Three isotope plot of $^{208}Pb/^{206}Pb$ against $^{206}Pb/^{207}Pb$ of natural samples (topsoil, mineral horizon, bedrock, snow, lichen) and endmembers (PM_{10}, Ni slag, Ni concentrate). The isotope signature of leaded gasoline is from Komarek et al. (2008). Lines on graph represent the two possible sources: dotted line - Russian nickel industry ($y = -1.04x + 3.3$; $R^2 = 0.98$); straight line - Russian unleaded gasoline and diesel ($y = -1.28x + 3.48$; $R^2 = 0.47$).

originating from Russia; otherwise, a more diffusive pattern was observed from the lichen data, and as the lichen approached closer to the snow line (**Fig. 5.3**) the mixing of these two sources increased.

Many authors suggest that after the phasing out of leaded gasoline, Pb from this source has had a negligible impact on the whole Pb emission budget. Haack et al. (2004) concluded that in the Arctic area, Pb derived from gasoline additives is overlapped by Pb from other local sources. Russian gasoline/diesel is widely used in NE Norway, especially due to its lower price. The concentrations of Pb in gasoline/diesel samples from Norway were significantly lower compared to Russian ones with a different isotope signature (**Table 5.3**), indicating that the influence of the Norwegian gasoline/diesel is negligible.

Conclusions

The study focused on the identification of Pb sources in NE Norway. Our hypothesis was that Pb originating from current unleaded gasoline and diesel could be an important source in an environment with few anthropogenic Pb sources. We analysed locally used unleaded gasoline samples for Pb isotope composition, and because the ^{206}Pb/^{207}Pb isotope ratio in the Russian samples is similar to the Pb additives in European leaded gasoline, we suggest that conclusions based on resuspension of Pb from "old" gasoline determined from evidence of this isotope ratio, should be revised. Using suitable environmental indicators, we further traced Pb from the Ni metallurgy and combustion of unleaded gasoline. We describe the link between Pb isotope composition of unleaded gasoline and lichen within the majority of topsoil samples. The snow samples collected from the same localities were affected by metallurgy. Snow and lichen samples exhibited different contamination pathways and sources. Lichens integrated local dispersed sources, i.e., automotive; while snow integrated local point sources that emitted particles higher in the atmosphere.

Chapter VI

Health risk assessment of metal(loid)s in soil and particulate matter from industrialized regions: A multidisciplinary approach

A. Francová, V. Chrastný, M. Vítková, H Šillerová, M. Komárek

Content

Abstract

In this study, samples of soil and particulate matter obtained from the highly industrialized region of Ostrava, Czech Republic, are used for the toxicity evaluation of the selected metal(loid)s (Cd, Cr, Cu, Ni, Pb, Zn, As). We investigated the samples from sites supposedly affected the most by the local pollution sources using mineralogical techniques (XRD, SEM/EDS) to understand the solid speciation of the contaminants as the crucial factor affecting their release. Although the bulk composition was defined by common silicates and oxides that are rather resistant to leaching, the presence of tiny Ni, Pb, and/or Zn sulfate-like droplets indicated a potential increase of the solubility of these metals. In vitro tests simulating gastric and lung fluids were used to assess the exposure risk for humans, as well as metal(loid) bioaccessibility. Based on the results, the potential risk for the observed age group (3-year-old children) could be recognized, particularly in the cases of As, Pb and Cd for both oral and inhalation exposure. Arsenic exhibits high bioaccessibility (7.13 – 79.7 %, with the median values of 10.6 and 15.6 for SGL and SLF, respectively), high daily intake (1.4- to 8.5-fold higher than the tolerable daily intake) and high concentrations in atmospheric PM_{10} (2.5 times the tolerable concentration in air). In contrast, Ni exceeded tolerable concentrations in the atmosphere up to 20-fold, but its bioaccessibility remained relatively low (0.1 – 22 %), and Ni did not pose a major threat to human health. Cd, Pb and As originating from industrial activities and domestic heating have been suggested to be the most important pollutants (tolerable daily intake was exceeded by up to 74-, 34- and 8-fold for Cd, Pb and As, respectively).

Introduction

Atmospheric particulate matter (PM) is a complex mixture of particles of varying chemical composition and size, both of which depend on their source of emissions, environmental factors (e.g., temperature, relative humidity) and atmospheric processing. Important chemical components include organic carbon, elemental carbon, inorganic ions, and major and trace elements (Dewan et al., 2015). A considerable part of particulate matter comes from anthropogenic sources, such as production processes and the coal-based power generation and heat generation industries, coal coking processes, the iron and steel industries, traffic and urban surface resuspension processes (Zajusz-Zubek et al., 2015). In recent years, a general downward trend in aerosol emission from stationary sources has been observed in most developed countries (Wróbel et al., 2000). Less is known about emissions from small-scale combustion, for example, domestic boilers or resuspended dust particles. These sources are important, especially during winter, because different fuels are used, and the combustion processes are difficult to control. Ground sources with low chimneys potentially have a greater impact on air quality than industrial sources. Particulate matter emitted from domestic sources differs according to its chemical composition, especially with regard to trace elements and organic contaminants, and may be a threat to the human population, particularly in terms of its toxic impact (Zajusz-Zubek et al., 2015; Drahota et al., 2017; Francová et al., 2017a).

Urban soil contamination by metals and metalloids is of great concern due to widespread sources of metals, toxicity, non-biodegradable properties and accumulative behaviors. Urban soils are generally regarded as being a sink of trace metals and other pollutants from various industrial activities, coal and fuel combustion, vehicle emissions and municipal waste disposal (Qing et al., 2015). The rapid industrialization and urbanization pollution of urban soils and dust by trace elements have become major threats to human health. Analysis of metals concentrations in soils of old industrial regions is critical for the making of policies aimed at reducing pollution levels and improving the soil ecosystem (Qing et al., 2015). Despite the reduction of primary and secondary emissions from steel production in recent years, the steel industry is one of the most important sources of metal emissions (Feng et al., 2019). Steel production remains associated with a number of significant environmental problems, among them the emission of airborne particles into the atmosphere. PM emissions from steel plants are therefore a complex mix of stationary sources and diffuse emissions associated with major processes and general on-site operations (Almeida et al., 2015).

The Upper Silesia region, Czech Republic, where our study was conducted, has been polluted by human activities and to recent time, steel industry, mining, coal cake production and chemical industry has been active in this area, which has been extensively polluted and is among the highest in Europe (Blažek et al., 2013). The city of Ostrava is known for its long mining and smelting history. Among these activities, industry, mining and municipal coal burning are considered to be significant sources of metal contamination (Francová et al., 2017a). Black coal mines in the area originate from the 19th century; several stationary industrial sources of pollutants (e.g., metals, particulate matter, nitrogen oxides, sulfur dioxide, and benzo(a)pyrene) exist directly in the city or in its close vicinity (Francová et al., 2017b). With this situation in mind, tracing the sources of metals in the area is critical to understand metal pollution levels and their effects on inhabitants. To better constrain and distinguish sources and potential toxicity issues, multiple approaches had to be used, in addition to concentration analyses.

Although a significant decrease in the concentration of atmospheric aerosol was observed in Upper Silesia, e.g., in Polish Silesia, PM_{10} has been reduced at least three times, SO_2 almost six times and NO_x more than half of the initial concentrations (Brozek et al., 2010) in the last decade of the 20th century (Suchara and Sucharová, 2004) and this trend is well documented to the beginning of the 21th century (CHMI, 2014; OECD, 2018), there has been no decrease in respiratory incidents (including allergies) (Brozek et al., 2010). This phenomenon can be partially explained by a reduction in coarse dust particles usually being observed at the initial period of environmental quality improvement. Such action causes a significant reduction in total suspended particles, but the concentration of fine particles is reduced to a small extent (Grynkiewicz and Bylina et al., 2005). Not only aerosol concentration but also the aerodynamic diameter of particles is an important parameter from the health hazard point of view.

Inhalation and digestion of atmospheric PM present important contaminant pathways to human bodies. Particle diameter is an important factor influencing the deposition of PM in lungs (Kastury et al., 2017). Particles of diameter greater than 10 μm are not inhalable, so from the health point of view, concentrations of particles less than 10 μm is aerosol mode, which should be controlled (Kastury et al., 2017). The subsequent clearance of the dissolved fraction of PM may occur via blood (inhalation bioavailability), lymph nodes or through transport to gastrointestinal tract. On the other hand, oral bioavailability presents the fraction of pollutants in the blood system given by oral bioaccessibility of atmospheric PM in the gastrointestinal tract (Moreda–Piñeiro et al., 2019).

Despite efforts to improve air quality, mostly through the reductions of emissions from the power generation and industrial sectors, the study area continues to experience episodes of high pollutant concentrations, especially during fall and winter seasons. In addition to steel production and other industries, major sources of air pollutants in the region include coal-fired power plants providing power generation for domestic and industrial use, home heating by a variety of fuel types and transportation, which is primarily fueled by standard gasoline or diesel (Vossler et al., 2016).

The objective of this study is to: i) interpret results of the bioaccessibility testing for metal(loid)s in soil and airborne particulate matter (PM_{10}); and ii) assess the potential exposure and non-carcinogenic risk for children living in an industrial city.

Materials and methods

Sampling and sample preparation

Sampling sites were divided into two different places: the city of Ostrava and its surroundings. The sites were chosen according to the predominant wind direction and the position with respect to the main industries in the region. (**Fig. 6.1**). Sampling at each site was conducted during February/March 2016 (PM_{10}; n = 7) and June 2016 (soils; n = 7). The sampling points chosen in this study were according to our earlier work (Francová et al., 2017a, b) with respect to a relatively cleaner and more contaminated area (sampling point 2 versus points 6, 7, 8, 9, 10, 13). To keep coherence with our previous data, we did not renumber the sampling points. Duplicate soil samples were collected using a stainless-steel sampler. Each sample was divided according to the soil horizon. Only the upper horizon (approximately 2-10 cm) was used for further analysis. The uppermost part of the soil was removed because it contained a lot of organic material, e.g., leafs, branches which were not studied here. The soil samples were dried at 60°C, ground in a ceramic mortar and passed through a 200-µm sieve (Ruby et al., 1996). Particulate matter sampling from the atmosphere was performed by the Public Health Institute in Ostrava. Samples were collected on
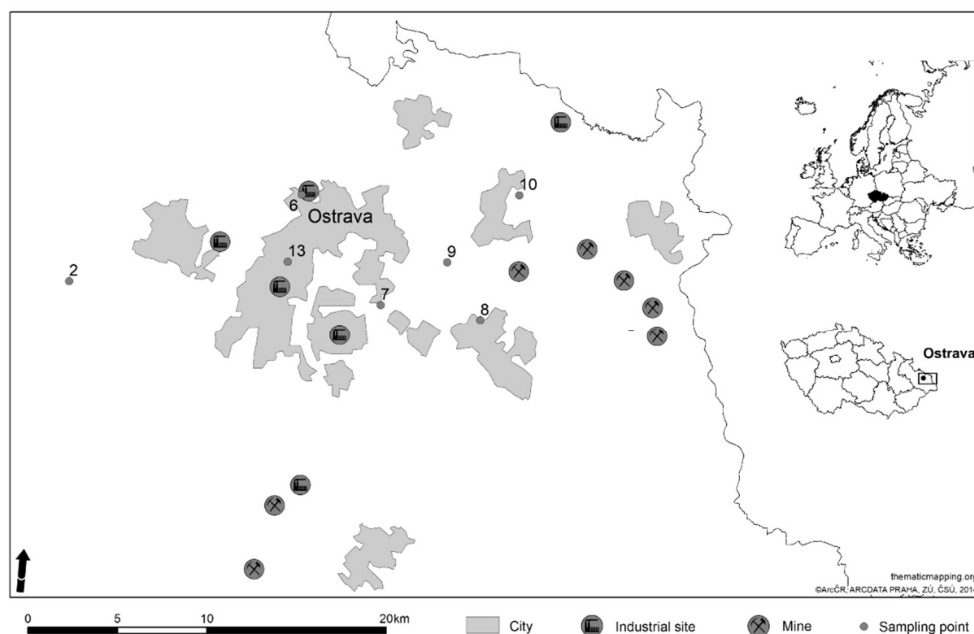
Figure 6.1 Simplified map of sampling points with industrial sites, mines and city outlines. Prevailing wind direction is expressed.

nitrocellulose filters using one mobile air sampler (High Volume Sampler DH-80, Digitel, Germany). The total sampling time was 24 h to obtain a sufficient air volume to determine the trace metal concentrations. The average air volume that was collected every 24 h was approximately 500 m^3.

Ultrapure chemicals (Rotipuran Ultra, Carl Roth, Germany) and ultrapure H_2O (Milli-Q System, $<1 \times 10^{-18}$ Ohm cm^{-1}) were used for sample treatment and all of the analyses. The concentrations of the trace elements were determined using inductively coupled plasma optical emission spectrometry (700 series ICP-OES, Agilent Technologies, USA).

Total mineralization

Total dissolution of soil samples was performed using a microwave unit (Anton-Paar, Austria). The dissolution method used was an EPA 3051A (USEPA, 2007): 9 mL of HNO_3, 3 mL of HCl and 1 mL of HF were added to a 0.250 g soil sample. Dissolved

samples were then transferred to a Savillex digestion vessel, completely evaporated and then diluted with 2 % HNO_3 to 25 mL. PM_{10} nitrocellulose filter bases were dissolved by using 10 mL of HCl in Savillex digestion vessels according to the USEPA protocol 3050B (USEPA, 1996). A volume of 9 mL of HNO_3, 3 mL HCl and 1 mL of HF were added to the vessels after the dissolution of the nitrocellulose digested in a microwave unit (Anton-Paar, Austria). The samples were then evaporated, acidified using 2 % HNO_3 and added to a final volume of 25 mL.

Bioaccessibility tests

Simulated gastric fluid (SGF) was used to investigate the amounts of harmful pollutants that could be extracted from the studied soils and PM_{10}. Prior to bioaccessibility tests, all of the soil samples were further sieved to ≤150 µm. The extraction fluid contained 0.4 M glycine, adjusted to a pH of 1.5 ± 0.05 by HCl. The solution was finalized by diluting to 1 L with deionized water and pH verification. An L/S ratio of 100 was used for the extraction (Ettler et al., 2014b). A mass of 0.1 g of soil and a matching mass of PM_{10} filter were placed in a 50-mL centrifuge tube along with 10 mL of extraction solution. The mixture was agitated at 200 rpm for 2 h at 37°C. The extractions were conducted in triplicate.

The extraction in simulated lung fluid (SLF) was performed according to Twining et al., (2005) and Ettler et al. (2014a). The exact composition of the SLF is reported in **Table S 6.1** in the Supplementary material. The pH of the used salt solution was adjusted to 7.4 ± 0.2, which roughly corresponds to Gamble's solution, simulating extracellular fluid of the skeletal muscle, more information is in Section 3.3.4. The samples were placed in PP centrifuge tubes and mixed with SLF to maintain an L/S ratio of 100 L/kg (0.1 g of soil/PM_{10} with 10 mL of extraction fluid). The samples were agitated at 200 rpm for 2 h and 24 h at 37°C. Caboche et al., (2011) observed that metal(loid)s dissolved rapidly at between 0.5 and 5 h and then asymptotically reached equilibria at between 24 and 48 h; 24 h were thus sufficient to achieve maximum metal(loid) dissolution. Both the 2-h and 24-h extractions were conducted in triplicate. After extractions, the samples were filtered through a 0.45-µm filter and diluted for analyses.

Exposure assessment

Oral exposure was calculated using bioaccessible concentrations and the ingestion rate for a child corresponding to 100 mg day^{-1}, as recommended by USEPA, (2008). The

obtained daily intakes of individual metal(loid)s were then compared with the tolerable daily intake (TDI) limits (Baars et al., 2001) and calculated for a 3-year-old child (USEPA, 2011). The hazard quotient for oral ingestion (HQ_{ing}) was subsequently calculated as the ratio of the contaminant daily intake and the level at which no adverse effects were expected as a result of exposure (TDI). A Hazard Quotient, HQ_{ing} or HQ_{inh} less than 1 indicates that there is no significant risk of noncarcinogenic effects, while a HQ_{ing} or HQ_{inh} higher than > 1 indicates that there is a possibility of noncarcinogenic effects, with increasing probability as the value of the quotients increases (USEPA, 2011).

The inhalation exposure is generally calculated using the bioaccessible concentrations of the individual contaminants in the aerosols or the total suspended particles in the air (Ettler et al., 2014b). The inhalation rate for the calculation of inhalation exposure of a 3-year-old child corresponds to 8.9 m^3 day. The contaminant concentrations for individual PM_{10} samples were calculated and compared with the limits for tolerable concentration in the air (TCA) taken from Baars et al. (2001) and calculated for a 3-year-old child. As a result, the HQ_{inh} was calculated as the ratio of the calculated contaminant concentration in the air and TCA to determine whether there was a risk of adverse health effects (Ettler et al., 2014b).

According to USEPA (2011), the potential exposure for many noncancer effects is expressed in the form of the average daily dose (ADD) according to the following equations (1) - (2):

$$ADDing = \frac{C \times IntR \times ED \times EF}{BodyWeight \times AT}$$

(1)

where C is the concentration of the contaminant (mg kg^{-1}); $IntR$ is the intake rate (mg day^{-1}); ED is the exposure duration (years); EF is the exposure frequency (days $year^{-1}$); and AT is the averaging time (days; AT = ED × 365).

Further,

$$ADDinh = \frac{C \times InhR \times ED \times EF}{BodyWeight \times AT}$$

(2)

where C is the concentration of the contaminant (mg kg^{-1}), *InhR* is the inhalation rate (m^3 day^{-1}); *EF* is the exposure frequency (days year^{-1}); *ED* is the exposure duration (years); and *AT* is the averaging time (days; AT = ED × 365)

The bioaccessible fraction (%$_{bio}$) was determined for each metal(loid), using the following equation:

$$\%_{bio} = \frac{C_{bio} \times V}{C_{total} \times m} \times 100$$

(3)

where C_{total} is the total concentration of an element in the sample (mg·kg^{-1}), m is the mass of the sample (g), C_{bio} is the concentration of an element in simulated fluid (mg·L^{-1}), and V is the volume of simulated fluid (mL) (Guney et al., 2017).

Scanning electron microscopy and X-ray diffraction analyses

Particles of PM$_{10}$ and heavy mineral fractions of selected soil samples were subjected to investigations by scanning electron microscopy (SEM). A circle approximately 1 cm in diameter was cut from selected PM$_{10}$ filters and placed on conductive tape. Similarly, particles of the heavy mineral fraction (obtained after separation in 1,1,2,2-tetrabromethane with a density of 2.96 g/cm^3) were fixed on conductive tape. All of the samples were carbon coated before analysis. A TESCAN VEGA3XMU (TESCAN Ltd., Czech Republic) scanning electron microscope equipped with a Bruker QUANTAX200 energy dispersive X-ray spectrometer (EDS) was used for imaging and semiquantitative chemical analyses of the particles (accelerating voltage 15 keV for PM$_{10}$ and 20 keV for soil heavy mineral particles). Specifically, the total number of spot EDS analyses was 73 for PM$_{10}$ and 92 for soil samples to comply with the representativeness. In addition, the separated soil heavy mineral fraction was subjected to X-ray diffraction (XRD) analysis using a Bruker D8 Discover diffractometer equipped with a silicon-strip linear LynxEye detector and a focusing germanium primary monochromator of the Johansson type providing Cu*Kα$_1$* radiation. Data

for mineral identification were collected in the 2Θ range of 3.5–80° with a step size of 0.020°, a counting time of 1 second at each step, and a detector angular opening of 1.507°. The phase identification (i.e., qualitative analysis) was performed with Diffrac.Eva software, version 4.2.2 (Bruker AXS GmbH, Karlsruhe, Germany; 2011–2016). The XRD method is suitable for bulk sample analysis of the major to minor crystalline phases composition, while the SEM observations show the mineral shapes and associations and the EDS spectra reflects the elemental composition of particles including trace phases. Based on the EDS quantification (performed by an experienced operator using QUANTAX EDS software) provided in wt.% of particular element and/or element in its oxide form and based on the specific ratio of particular elements, the mineral forms were indicated by comparison with the EDS data commonly available for the pure forms of the studied mineral phases. The results of XRD were used to support the interpretation determined by SEM/EDS.

Results and discussion

Elemental composition of soils and PM$_{10}$

The total concentrations of selected metal(loid)s in soil and airborne particulate matter PM$_{10}$ are presented in **Tables S 6.2** and **S 6.3**. **Table S 6.8** presents the statistical summary of metal(loid)s total concentrations in samples throughout all the sampling sites. The median concentrations followed the following order: Zn > Pb > Cr > Cu > Ni > As > Cd and Zn > Cr > Ni > Pb > Cu > As > Cd for soils and PM$_{10}$, respectively. On average, the highest concentrations of contaminants were observed at sites 6 and 13, which are located near large industrial sites (steelworks and a cooking plant; see **Fig. 6.1**). Soil samples exhibited the highest concentrations of Cr, Cu, Ni and Zn at site 6 (**Fig. 6.2**). Unexpectedly high concentrations of Cd were observed at site 13 representing the city center with repeatedly high metal concentration levels probably as a result of mixing of the majority of contamination sources as we found earlier (Francová et al., 2017a, b). Elevated concentrations of metal(loid)s in the PM$_{10}$ fraction from the winter season was observed at sites 13, 8 and 6 (**Fig. 6.3**). With respect to high

amounts of target contaminants, samples from these sites were further subjected to solid phase analysis.

Microscopic observations and mineralogical identification

The identification of the bulk soil heavy mineral fractions using XRD (**Fig. S 6.1**) showed that the samples yielded similar phase compositions with predominating Fe oxides (magnetite Fe_3O_4; hematite Fe_2O_3; or alternatively magnesioferrite $MgFe^{3+}_2O_4$), Ti oxides (anatase TiO_2, rutile TiO_2), and epidote ($Ca_2Al_2Fe^{3+}(Si_2O_7)(SiO_4)O(OH)$) and zircon ($Zr(SiO_4)$) to a lesser extent. Quartz was present in all the samples as ubiquitous abundant phase. The general composition thus corresponds to naturally occurring minerals. Moreover, several trace metal-bearing phases were determined by XRD, namely coronadite ($PbMn_8O_{16}$), Zn-bearing spinels (e.g., ($Zn_{0.54}Fe_{0.46}$)Fe_2O_4) or cerussite ($PbCO_3$).
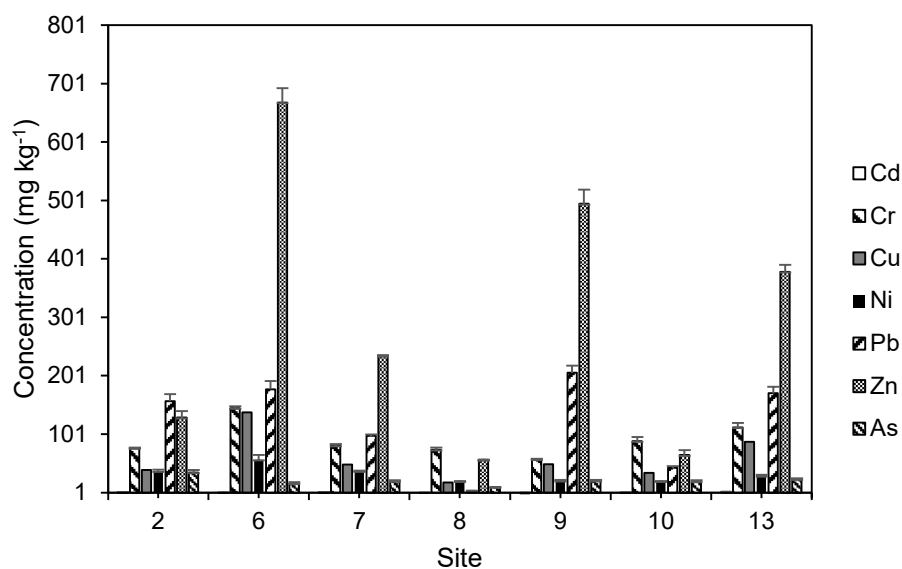

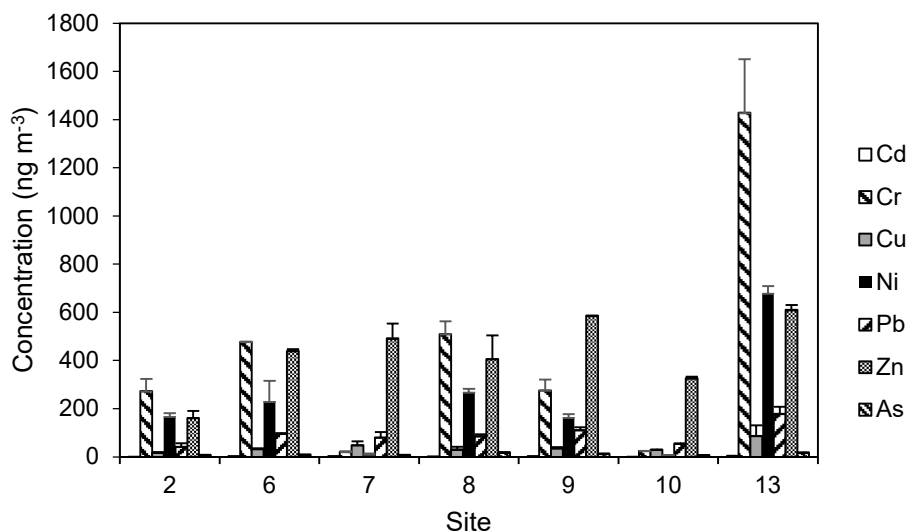**Figure 6.2** Selected metal(loid) concentrations in soil samples (median ± SD).

Figure 6.3 Selected metal(loid) concentrations in PM_{10} samples (median ± SD).

Figure 6.4 shows representative textures and identification based on EDS spot chemical analyses (SEM/EDS) subjected to quantification of each of the detected elements including deconvolution if elemental overlap occurred. Selected PM_{10} particles and corresponding soil heavy mineral fraction particles originating from identical sampling sites are depicted. The EDS spectra reflects all the elements detected in the analyzed spot, while values in wt.% (resulting from the mathematical integration of peaks from the spectrum) for particular elements are provided in the text. Nuances can be found in the presence of minor to trace Pb-, Zn-, Cu- or Ni-bearing phases of different origins (see details below). Generally, Zn was mainly detected in Fe oxides, indicating a potential substitution for Fe in the spinel structure as described in other studies (e.g., Colás et al., 2016). Copper was present in Fe oxides to a lesser extent. In contrast, tiny Pb-rich fragments were occasionally detected within both PM_{10} samples and the soil sample matrix, yielding the highest abundance at sites 6 and 9. The presence of Pb and Ni phases in PM_{10} and their instability upon interaction with electron beams indicated high susceptibility of such metallic particles to weathering, followed by release of Pb and Ni. In some cases, low abundances of metals and small particle sizes limited the detectability of the target risk metals during the spot EDS analyses.
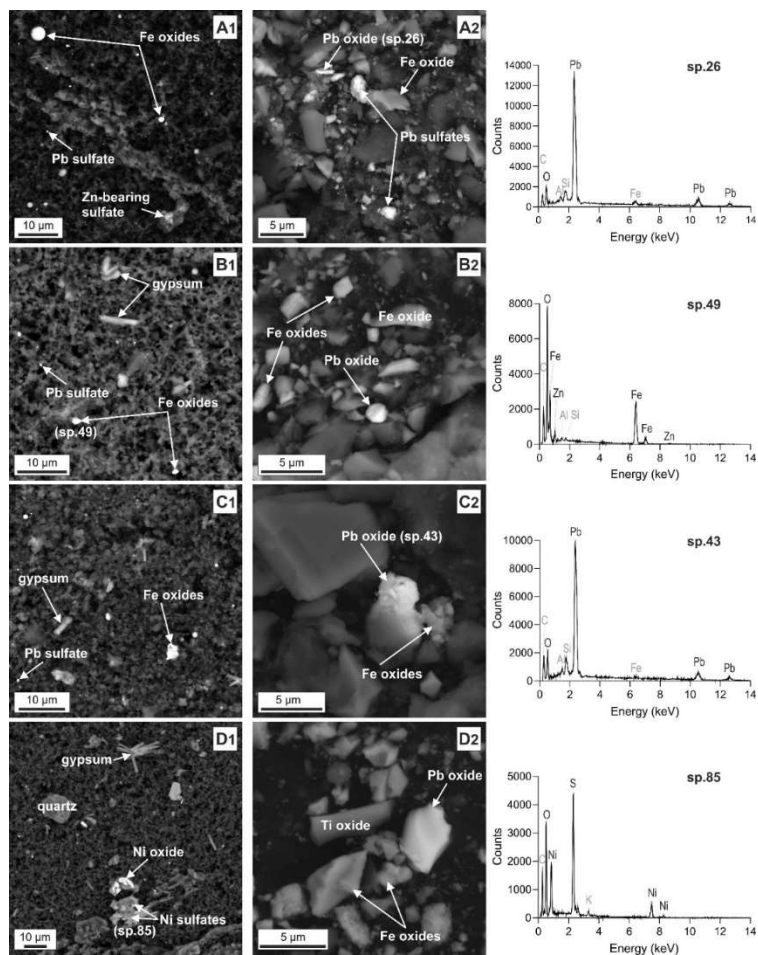
Figure 6.4 Images of PM_{10} (A1–D1) and soil-heavy mineral fractions (A2–D2) in backscattered electrons (SEM) with selected corresponding EDS spectra. (A1 - site 6) globules of Fe oxides containing <5 wt.% Zn and <1 wt.% Cu; tiny fragments of Pb sulfate-like particles, Zn-bearing Ca sulfates; (A2 - site 6) 2-μm fragments of Pb oxides, irregularly shaped Pb sulfates associated with common soil Fe oxides; (B1 - site 8) lath-like crystals of gypsum, Fe oxide droplets containing <3 wt.% Zn and 0.5 wt.% Cu, droplets of Pb sulfate; (B2 - site 8) globular particles of Pb oxide, various soil Fe oxides; (C1 - site 9) gypsum particles, agglomerate of Fe oxides containing up to 2.5 wt.% Cu, Pb sulfate droplets; (C2 - site 9) 3-μm fragment of Pb oxide associated with Fe oxides; (D1 - site 13) rod-shaped gypsum crystals, Ni oxide particles of irregular shapes containing up to 1.5 wt.% Cu and associated with Ni sulfates; (D2 - site 13) Pb oxide particles in the presence of common soil Ti and Fe oxides.

Droplets, rod-shaped or fragmental Fe oxides predominated in PM_{10} samples from site 6. Both pure Fe oxides and Zn-bearing (up to 5.4 wt.%) or Cu-bearing (up to 2.9 wt.%) ones were detected. Various sulfate-like particles were commonly observed, including gypsum ($CaSO_4 \cdot 2H_2O$) with typical crystal shapes but mainly S-rich dendritic formations (identified as sulphates or sulfur oxides based on the EDS elemental composition and elemental ratios) collapsing upon interaction with electron beams occurred in this sample. Furthermore, Pb sulfate-like droplets and Zn-bearing sulfates were determined (**Fig. 6.4 A1**). Fragments of Fe-Cr-Ni alloy were detected occasionally. Similarly, fragmental Pb-rich particles of sizes generally from <1 μm to 2 μm were observed within the soil heavy fraction (**Fig. 6.4 A2**). The EDS composition indicated the presence of Pb oxides and/or Pb sulfates. Nevertheless, the small size of some of the target particles did not allow for the precise analysis necessary for any phase composition calculation. Furthermore, we suppose that the observed anthropogenic particles were highly metastable and likely to be transformed in the soil environments (Tyszka et al., 2016).

Various Fe-oxide particles of different shapes (globules, angular or rod shaped), sizes and substituents or impurities were determined in PM_{10} at site 8 (up to 3 wt.% of Zn, 4 wt.% Cu, 1.3 wt.% Sn). Silicates, carbon-rich particles and gypsum ($CaSO_4 \cdot 2H_2O$) were determined. Moreover, tiny Pb sulfate-like particles, although unstable in contact with electron beams, were observed (**Fig. 6.4 B1**). Compared to PM_{10} fraction, no Pb sulfates were determined in the soil heavy mineral fraction, but ∼1-μm Pb oxide particles were detected occasionally (**Fig. 6.4 B2**).

Compared to other sites, PM_{10} filters from site 9 trapped fewer metallic particles, or the size of the particles was <1 μm (i.e., nondetectable). Nevertheless, tiny Fe-oxide globules containing up to 2.5 wt.% of Cu were determined. Additionally, gypsum ($CaSO_4 \cdot 2H_2O$) and Pb sulfates were detected (**Fig. 6.4 C1**). Various spinel oxides were detected in the soil heavy mineral fraction. Interestingly, Pb-rich particles 2−5 μm in size were often observed within the sample (**Fig. 6.4 C2**). The EDS analyses indicated that mainly Pb oxides were present (i.e., the Pb/O ratio was close that of common Pb oxides such as litharge PbO). Considering that no sulfates were detected compared to PM_{10}, we suppose that: i) high-density Pb oxides preferentially settle down in the soil, while small sulfate particles can be trapped by PM filters; or (ii) sulfate particles can be transformed immediately in soil environments.

Similar to site 6, S-rich dendritic formations (identified as sulphates or sulfur oxides) were often observed in PM_{10} at site 13. Rod-shaped particles of gypsum ($CaSO_4 \cdot 2H_2O$) were also identified (**Fig. 6.4 D1**). Various Fe oxides were determined, containing up

to 2 wt.% Zn and 2.9 wt.% Cu. Moreover, Ni oxides enriched with Cu were detected together with Ni sulfates (**Fig. 6.4 D1**). Occasionally, elevated concentrations of Zn (up to 8 wt.%) were determined in Fe oxides of the soil heavy mineral fraction, which, in accordance with the XRD result, suggested the presence of Zn-bearing spinels (**Fig. S 6.1**). Moreover, individual Pb-rich particles or fragments were infrequently observed (**Fig. 6.4 D2**).

Assessment of metal(loid)s potential toxicity

Extractability of metal(loid)s in simulated gastric fluids and exposure estimations

The range of bioaccessible contaminant concentrations in soil leached in SGF (**Table S 6.4**) varied among sites significantly: Cd (0.21 – 76.6 µg kg^{-1}), Cr (0.34 – 439 µg kg^{-1}), Cu (4.70 – 94.7 µg kg^{-1}), Ni (0.90 – 24.6 µg kg^{-1}), Pb (11.2 – 251 µg kg^{-1}), Zn (4.70 – 94.7 µg kg^{-1}), and As (1.00 – 6.66 µg kg^{-1}).

The bioaccessible fractions (in % of total concentrations) in soil samples were as follows: Cd (13.0 - 75.7 %), Cr (0.20 – 0.92 %), Cu (0.47 – 3.64 %), Ni (1.76 – 5.58 %), Pb (3.87 – 35.88 %), Zn (1.65 – 22.5 %) and As (1.91 – 8.91 %) (**Fig. 6.5**).

Cadmium proved to be the most bioaccessible, while Cr was the least bioaccessible. The calculated oral exposure of metal(loid)s via soil dust is reported in **Table S 6.9**. Calculated daily intakes of individual metal(loid)s were compared to tolerable daily intakes (TDIs), and HQ$_{ing}$ were obtained. Daily intake of As, Cd and Pb exceeded HQ$_{ing}$. Daily limits of As intake were exceeded at sites 6 (1.81×), 7 (1.34×), 10 (1.03×) and 13 (3.21×). Daily limits for Pb were exceeded at all of the sampling sites (1.50× - 33.7×). Sites exhibiting the largest amounts of Pb daily intake (site 6, 7 and 13) are located near industrial plants. Since anthropogenic particles are assumed to be highly metastable, rapid release of Pb is mainly related to the dissolution of Pb-bearing sulfates and tiny Pb fragments shown in **Fig. 6.4**. Complete dissolution of metallic sulphates, sulfides, and gypsum in gastric fluids was determined by Ettler et al. (2014b). Daily intake of Cd was exceeded at site 2 (1.15×) and at site 13 (73.8×). In contrast, Cr, Cu, Ni and Zn were not evaluated as hazardous for human health.

Concentrations of contaminants in PM$_{10}$ leached in SGF (**Table S 6.5**) are considerably lower than in cases of soils: Cd (0.01 – 0.55 µg kg^{-1}), Cr (0.12 – 0.90 µg kg^{-1}), Cu (0.68 – 4.55 µg kg^{-1}), Pb (1.64 – 106 µg kg^{-1}), Ni (0.43 – 1.42 µg kg^{-1}), Zn (10.5 – 47.2 µg kg^{-1}), and As (1.66 – 16.1 µg kg^{-1}). The percentages of bioaccessible metal(loid)s fractions in PM$_{10}$ were also lower than in case of soil: Cd (1.95 – 6.49 %), Cr (0.00 – 1.49 %), Cu (1.30 – 3.72 %), Ni (0.05 – 3.66 %), Pb (1.31 – 19.3 %),

Zn (2.16 – 4.56 %), and As (7.13 – 56.36 %) (**Fig. 6.6**). Arsenic seems to be the most bioaccessible metal(loid) in PM_{10} fraction. The lowest percentage of bioaccessible fractions was observed at site 2, which is considered to exhibit "background" values for whole study area (Francová et al., 2017b). The hazard quotient for As intake was exceeded at all sites (1.42× - 8.45×) except for site 2. The same observation was made with Pb: sites 2 and 8 were the only ones that did not exceed daily intake limits. Apart from the presence of readily soluble Pb sulfates in PM_{10} (**Fig. 6.4**), the small size (generally <1 μm or 1−2 μm) of Pb phases could contribute to the excessive leaching of Pb. Conversely, elevated concentrations of Zn detected even in tiny globules by SEM/EDS seemed to be more "preserved" due to the association with Fe oxides.

Extractability of metal(loid)s in simulated lung fluids and exposure estimations

Cumulative bioaccessible concentrations of selected metal(loid)s in SLF after 24 h (**Table S 6.6**) varied among sites significantly: Cd (0.04 – 0.13 μg kg-1), Cr (0.02 – 0.38 μg kg-1), Cu (1.47 – 3.95 μg kg-1), Ni (0.26 – 2.36 μg kg-1), Pb (0.39 – 0.92 μg kg-1), Zn (0.68 – 3.90 μg kg-1), and As (1.52 – 3.09 μg kg-1). The range of bioaccessible contaminant concentrations in PM_{10} leached in SLF after 24 h were as follows (**Table S 6.7**): Cd (0.05 – 0.13 μg kg^{-1}), Cr (0.37 – 0.88 μg kg^{-1}), Cu (0.64 – 1.10 μg kg^{-1}), Ni (0.35 – 1.65 μg kg^{-1}), Pb (0.26 – 1.26 μg kg^{-1}), Zn (0.03 – 1.39 μg kg^{-1}), and As (0.77 – 4.17 μg kg^{-1}). The bioaccessible fractions (in % of total concentrations) were as follows: Cd (1.45 - 22.6 %), Cr (0.02 – 1.09 %), Cu (1.10 – 4.43 %), Ni (0.08 – 21.9 %), Pb (0.18 – 1.84 %), Zn (0.01 – 1.08 %) and As (7.60 – 79.7 %) (see **Fig. 6.8**). Arsenic seemed to be very bioaccessible at site 10, where the bioaccessible fractions were observed to be very elevated (up to 80 %). Tolerable concentrations of metal(loid)s in air were exceeded by Ni (1.71× – 8.13×), while the highest hazard HQ_{inh} was observed at industrial site 7 (**Table S 6.12**). Tolerable concentrations of Pb were exceeded at site 8 (1.24×), and concentrations of As were exceeded at suburban site 10 (2.47×). Although As was not as abundant in mass terms, it is of concern given its toxicity and potential to elicit negative health responses in exposed individuals (Wiseman and Zereini, 2014).

Figure 6.5 Bioaccessible fractions of soil metal(loid)s in simulated gastric fluids.
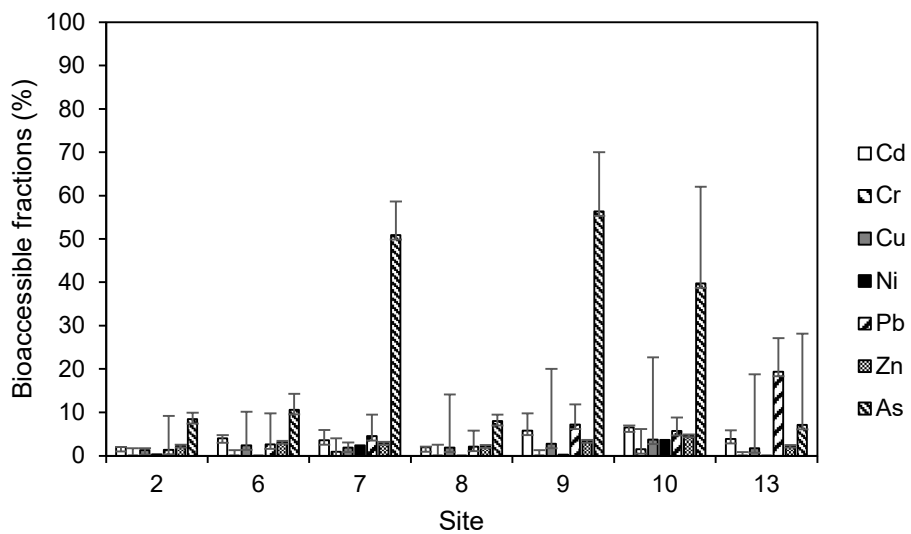
Figure 6.6 Bioaccessible fractions of PM$_{10}$ metal(loid)s in simulated gastric fluids.

Evaluating of exposure to metal(loid)s

Daily intakes/concentrations in air and HQ_{ing}, HQ_{inh} were calculated for both inhalation and ingestion pathways. The presented exposure risk calculations were performed to demonstrate the exposure to toddlers, who can ingest soil and dust through deliberate hand-to-mouth or object-to-mouth movements or unintentionally by eating food that has dropped on the floor (USEPA, 2008). In order to obtain more information from our results, we showed the contributions of both inhalation and ingestion to total exposure (sum of SLF 2h and SGL) in a balanced representation. In **Table S 6.13**, inhalation to total exposure is expressed. Relatively high doses of Cr, Ni were associated with inhalation (up to 78% of Cr at locality 13), contrary to Zn, Pb and As where ingestion prevails (**Table S 6.13**). A higher ingestion to inhalation ratio was found for Cd with the exception of sites 2 and 8, for Cu with the exception of site 2. This fact could be related to different physico-chemical characteristics of PM at studied sites.
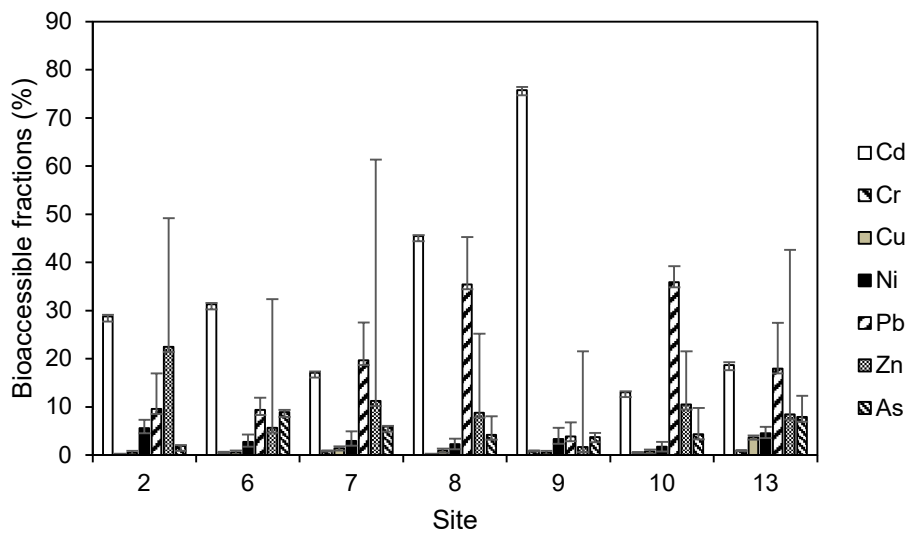

Figure 6.7 Bioaccessible fractions of soil metal(loid)s in simulated lung fluids.

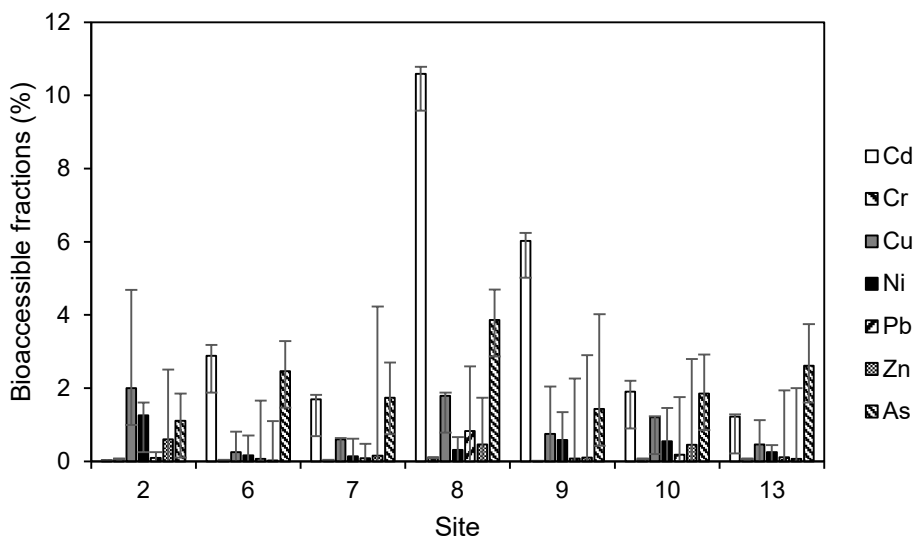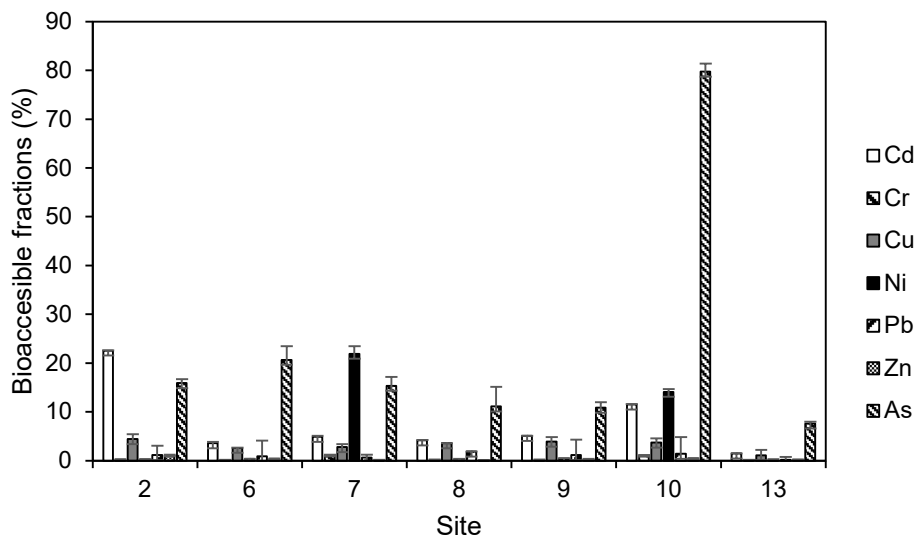**Figure 6.8** Bioaccessible fractions of PM_{10} metal(loid)s in simulated lung fluids.

Intake of contaminated soil frequently happens through dermal and oral routes (i.e., ingestion), and although it is negligible for adults, it could be significant for toddlers (particularly for small particles that adhere to the skin and are later ingested) (USEPA, 2008). Tolerable daily intakes via soil ingestion were exceeded by As, Cd and Pb. Daily intake of all three metal(loid)s was the highest at site 13, which is located close to the steel plant. Cadmium and Pb were also the most bioaccessible of all the metal(loid)s.

Daily intake of metal(loid)s via PM_{10} ingestion were again exceeded by As and Pb at most of the sampling sites, while both metal(loid)s extracted from PM_{10} proved to be highly bioaccessible; however, we used a very conservative protocol. Moreda-Pineiro (2019) assessed the bioavailability based on dialyses, and although the author found much lower metal(loid) concentrations in PM_{10} (Cu was comparable) at industrial sites, a much higher bioaccessible fraction was observed. For instance, the author detected total concentrations of up to 7.3, 98.1 and 19.4 ng m^{-3} for Ni, Cu and Pb, respectively, but found bioaccessible fractions of up to 45.7, 39.7 and 41.7 for the same elements, respectively.

Tolerable concentration of metal(loid)s in air were exceeded by As, Cu, Pb and Ni. Hazard quotients for Ni in particulate matter were the highest in samples obtained at sites 6, 10 and 7, which are close to industrial areas. This result might correspond to

the observed Ni sulfates (**Fig. 6.4**), which are supposed to be readily soluble. In contrast, emissions of Ni were lowest at site 2. However, completely reversed values were observed in airborne soil dusts. The HQ_{ing} was the highest at site 2, while the lowest was observed at site 7. Depending on the underlying geology and soil chemistry parameters, nickel in nonindustrial soils (site 2) can occur in a range of mineral forms, including oxides (together with Fe, Mn, Al, and other constituents) and silicates (McGrath, 1995 in Haber et al., 2017). Moreover, the availability of Ni in soils strongly depends on the weathering stage of Ni-bearing minerals. For example, to be able to specify the role of Fe oxides in Ni retention, the distribution of Fe and Ni in amorphous and crystallized phases must be determined (Massoura et al., 2006). Based on our results, however, we can assume that, even in industrial areas, Ni can be efficiently bound to soil Fe oxides, which are commonly found in the studied samples (**Fig. 6.4**).

Since the daily intake of As, Cd and Pb for children living in the industrial area surpasses the guidelines by up to 73-fold, this work highlights the importance of preventing children's exposure to metal(loid)s in the study area. Considering inhalation, particles generated from soil and PM_{10} can be suspended by wind and human activities and therefore have great potential to add to human exposure. However, all airborne particles are susceptible to inhalation (while 75% may be exhaled); hence, it is possible for any sorbed substances to be subsequently desorbed in vivo (Guney et al., 2017). Tolerable concentrations of Ni in air were exceeded at every sampling location. When compared to our data from studies at roadsides (Embiale et al., 2019), in which the authors found much lower HQ for inhalation and ingestion exposure, the dominant influence of heavy industry on health risks despite the preventive measures undertaken in the past is obvious.

According to SEM/EDS analyses (**Fig. 6.4**) at localities 6, 8, and 9, many Fe oxide phases were detected. Arsenic in soils is expected to be coprecipitated with/sorbed to Fe (hydr)oxides and thus relatively immobilized. However, Fe arsenates dominate in mine waste (Drahota et al., 2017) and fly ash samples from coal burning (Huggins et al., 2007). Similar results were found by Low and Zhang (2013) during controlled coal combustion in lab-scale drop-tube furnaces. From our results, the bioaccessibility testing showed that, for PM_{10} collected in 24 h, As occurs in very bioaccessible forms (up to 56.3 % for SGF leaching and up to 79.7 % for SLF leaching). In this context, many studies have shown that even a low concentration of major anions (such as PO_4^{3-} present in the SLF) can mobilize As from Fe (hydr)oxides by competitive desorption (Wenzel et al., 2001; Goh and Lim, 2005). While total As concentrations in samples remain relatively low, both high daily intake and the concentration in air suggest that As is a potentially dangerous element for human exposure. High bioaccessibility and

high concentrations in the air at sites across Ostrava city correspond to elevated content of As in brown coal, which is mainly used for household heating during winter (Francová et al., 2017a). The high solubility of As is of concern given the toxicity of this metal(loid), which is recognized as a human carcinogen (IARC, 2012). The bioaccessibility in soil samples leached in SGF was high (up to 75.7 %), but the total concentration of metal remained at low levels. In contrast, Ni, the concentration of which in air was greater than the tolerable limits at essentially every sampling site, was present mainly in non-bioaccessible forms, although Ni-bearing particles showed a high predisposition to weathering, followed by a release of Ni to environment.

The major exposure risk is likely related to As and Pb. According to Reis et al. (2014), Pb can occur in dust mineral phases that are very soluble in human gastric and lungs fluids. Metallic sulfates are readily soluble in the acidic environment of gastric fluids (Ettler et al., 2014b), which implies the low stability of the Pb sulfates observed in our samples. This phenomenon suggests that sources of Pb are probably anthropogenic since geogenic sources normally show low bioaccessible concentrations. Sites exhibiting the largest amounts of Pb daily intake (site 6, 7 and 13) are located near industrial plants. Steel production close to the sites in question supports presence of anthropogenically originated Pb. Moreover, according to the work of Moreda-Pineiro et al. (2019) the bioaccessibility of metals is influenced by other PM_{10} characteristics, such as black carbon and NH_4^+ concentrations and is site specific. According to analyses of the historic deposition of metal(loid)s in tree rings (Francová et al., 2017a), As occurring in Ostrava city originates overwhelmingly from the household usage of brown coal. The decrease of black coal mining in the Ostrava mines led to the increased use of inferior coal types, mainly brown coal originating from Bílina (northwestern part of Czech Republic), which is rich in As. Household combustion is an especially important source of emissions, mainly in winter. Household combustion is difficult to control since low-quality fuels are often used, and it is not easy to prove the combustion of banned materials.

The limitations of the bioaccessibility test

For the inhalation pathway, a validated method based on *in vitro in vivo* correlations is still not available. The main reason is that *in vivo* conditions, which would best represent the natural environment in human lungs cannot be easily repeated. Some attempts can be found in literature, e.g., Mirowsky et al. (2015) tested PM particles from urban and rural localities and correlated the bioaccessible fraction of metals with

reactive oxygen species (ROS) detected in the human pulmonary microvascular endothelial cell line (ST1.6R). Mice line (FVB/N) was exposed in another experiment to oropharyngeal aspiration of 50 µg of PM from the same localities and inflammatory responses were followed. Both factors were strongly correlated with the bioaccessible amount of trace metals and the coarse fraction of PM (between 2.5 and 10 µm) correlated more strongly compared to the finest particles (lower than 2.5 µm) (Mirowsky et al., 2015).

For the gastrointestinal route, standardized methods are available, but for solubility of elements in human lungs the *in vitro* protocol to simulate the bioaccessible elemental content of ambient atmospheric particles is still being intensively investigated (Wiseman, 2015). Therefore, hazard quotient calculations based on SLF *in vitro* bioaccessibility data is limited to a certain extent. Numerous protocols have been suggested for the simulation of lung bioaccessibility based on many extraction solutions, e.g., Gamble's solution with variable compositions found in literature (Wiseman, 2015).

The most important factors for a valuable extraction involve: (i) avoiding the use of only water as the extraction agent (risk of overestimation of the results), (ii) appropriate extraction conditions, e.g., pH around the physiological value, human body temperature being a very important factor and time of extraction and solid to liquid ratio (Wiseman, 2015).

In our protocol, we followed the experimental fluid proposed by Twining et al. (2005) as a method respecting the above-mentioned parameters with optimal values. The pH of the fluid was 7.4, which roughly corresponds to Gamble's solution. The solid to liquid ratio is another important parameter as showed by Sysalová et al. (2014) who confirmed earlier findings that higher solid to liquid ratio increases the extraction efficiency. The authors used the Hatch's solution with a solid to liquid ratio of 1000 and 16 h of extraction time (Sysalová et al., 2014). Ettler et al. (2014b) performed a simple kinetic test of the extraction procedure and found the optimum time of 24 h. Originally, Twining et al. (2005) recommended the factor of 20. Caboche et al. (2011) showed that solid to liquid ratios of 30 are not efficient enough to simulate the bioaccessible fraction of metals. Solid to liquid ratios over 50 should be, according to Caboche et al. (2011) and Ettler et al. (2014b), suitable for bioaccessibility testing. We used the factor of 100 for our samples and used an extended time of 24 h (Sysalová et al., 2014).

Conclusions

The soil and PM_{10} samples obtained in the vicinity of the Czech industrial city of Ostrava were subjected to chemical and mineralogical characterizations followed by extraction using simulated gastric fluids (SGF) and simulated lung fluids (SLF) to describe the bioaccessibility of selected metal(loid)s. In the next step, the potential risk was calculated for a 3-year-old child. Bioaccessible fractions for extractions in SGF varied between 0.2 % and 75% for soils and between 1.3 % and 56% for PM_{10}. Relatively low bioaccessible fractions were observed for 24-h SLF extractions in soil (1.1 – 10 %) but were remarkably higher for PM_{10} (0.1 – 79 %). Such a difference can be explained by different solid speciation of metal(loid)s and the response to simulated biological solutions chemistry and pH, i.e., by the presence of various metal(loid)-bearing phases and their transformations under acidic or near-neutral conditions. In particular, Pb-, Zn-, and Ni-sulfates and tiny metallic fragments were often observed in PM_{10}, indicating susceptibility to rapid dissolution and, thus, were assumed to be responsible for increased leaching of the target metals. Tolerable daily intakes were exceeded by Cd, Pb and As (up to 74-, 34- and 8-fold, respectively). Tolerable concentrations in air were exceeded by Ni, Cu, As and Pb (up to 28-, 2-, 2- and 1-fold, respectively). Lead and As originating in industrial activities and domestic heating were suggested to be the most important pollutants. It seems that, despite the overall improvement of air quality due to a reduction of dust emissions from industrial sources in Europe and in Upper Silesia, the real exposure to PM_{10} remains a threat to human health. Thus, it is important to control air quality not only through the existing monitoring system but also in the vicinity of frequented streets. However, ingestion presents for some metals a more important exposure pathway.

Supplementary material

Figure S 6.1 Diffractograms of soil heavy mineral fractions with corresponding results of qualitative XRD analysis (A – site 6; B – site 8; C – site 9; D – site 13). Dominant mineral phases are given in bold, trace mineral phases are given in italics, corresponding PDF card number from the PDF-2 database is provided for each phase identified in the individual samples.
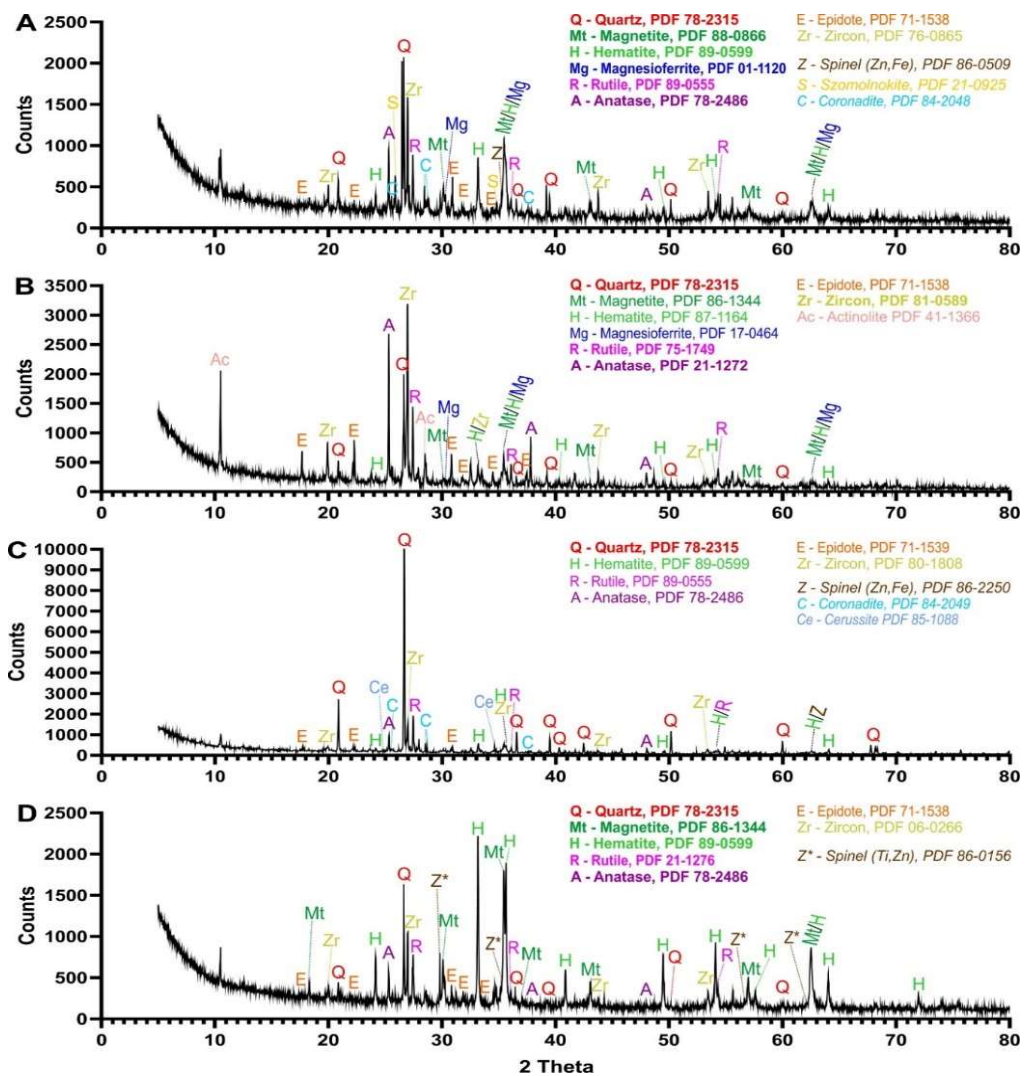
Table S 6.1 The chemical composition of the simulated lung fluid (SLF) (Twining et al., 2005.

Salt	Concentration (mM)	Mass (g L^{-1})
Sodium chloride, NaCl	110	6.43
Sodium bicarbonate, NaHCO$_3$	31	2.60
Calcium acetate, Ca(C$_2$H$_3$O$_2$)$_2$	2.5	0.40
Calcium chloride, CaCl$_2$·2H$_2$O	2.5	0.37
Magnesium acetate, Mg(C$_2$H$_3$O$_2$)$_2$·4H$_2$O	1	0.21
Magnesium chloride, MgCl$_2$·6H$_2$O	1	0.20
Potassium dihydrogen phosphate, KH$_2$PO$_4$	2	0.27
Dipotassium sulphate, K$_2$SO$_4$	1	0.17
Citric acid, C$_6$H$_8$O$_7$	1	0.07

Table S 6.2 Total concentrations of metal(loid)s in soil samples (mg kg^{-1}) (median ± SD).

Sampling site	Cd	Cr	Cu	Ni	Pb	Zn	As
2	1.82	76.9	39.6	37.7	158	129	35.5
	± 0.11	± 1.25	± 1.84	± 2.57	± 12.4	± 11.2	± 4.15
6	0.81	145	138	57.1	178	668	16.9
	± 0.24	± 3.48	± 4.58	± 8.34	± 14.2	± 25.2	± 2.04
7	1.51	81.5	48.8	37.7	98.1	235	20.7
	± 0.18	± 2.64	± 3.57	± 1.20	± 2.53	± 1.74	± 1.79
8	0.21	74.1	18.3	20.6	13.9	57.0	10.4
	± 0.35	± 4.21	± 1.73	± 0.24	± 0.14	± 0.25	± 0.25
9	0.20	57.8	49.3	21.2	206	495	21.3
	± 0.54	± 1.02	± 2.07	± 1.47	± 12.5	± 24.5	± 1.58
10	0.83	89.1	34.5	20.5	43.4	65.2	19.9
	± 0.14	± 7.24	± 1.49	± 0.17	± 3.07	± 8.67	± 2.62
13	2.19	113	87.6	29.2	171	379	23.7
	± 0.17	± 8.01	± 3.98	± 2.30	± 11.2	± 12.4	± 2.09

Table S 6.3 Total concentrations of metal(loid)s in PM$_{10}$ samples (ng m^{-3}) (median ± SD).

Sampling site	Cd	Cr	Cu	Ni	Pb	Zn	As
2	0.59 ± 0.11	272 ± 51.8	18.0 ± 1.86	166 ± 15.2	41.9 ± 14.5	161 ± 29.9	6.71 ± 2.38
6	2.95 ± 0.18	477 ± 0.75	32.9 ± 2.72	229 ± 85.7	96.5 ± 1.38	439 ± 8.31	8.88 ± 0.17
7	2.93 ± 1.44	20.5 ± 2.18	47.8 ± 17.3	9.44 ± 4.93	80.4 ± 23.1	491 ± 61.7	6.24 ± 3.08
8	1.64 ± 0.23	510 ± 53.2	30.3 ± 11.7	267 ± 14.6	85.3 ± 8.72	405 ± 99.0	17.9 ± 1.52
9	3.22 ± 0.18	275 ± 45.5	35.4 ± 4.59	163 ± 14.7	110 ± 13.0	586 ± 0.11	11.8 ± 2.54
10	1.19 ± 0.15	24.1 ±0.32	29.9 ± 0.70	6.83 ± 0.67	54.2 ± 0.71	326 ± 7.80	6.53 ± 0.35
13	4.68 ± 1.75	1 420 ± 223	86.4 ± 45.2	678 ± 31.4	178 ± 30.0	610 ± 21.2	16.9 ± 1.56

Table S 6.4 Bioaccessible concentrations of metal(loid)s in soil leached in simulated gastric fluids (µg kg^{-1}) (median ± SD).

Sampling site	Cd	Cr	Cu	Ni	Pb	Zn	As
2	1.19 ± 0.16	0.36 ± 0.12	4.62 ± 0.12	4.78 ± 0.26	34.2 ± 1.11	66.0 ± 4.02	1.55 ± 0.13
6	0.63 ±0.15	2.07 ± 0.11	17.8 ± 0.19	3.91 ± 0.23	41.5 ± 0.38	94.7 ± 4.50	3.76 ± 0.17
7	0.59 ± 0.50	1.59 ± 0.22	16.9 ± 2.17	2.54 ± 0.30	44.0 ± 7.20	59.8 ± 7.54	2.78 ± 0.13
8	0.21 ±0.14	0.34 ± 0.36	4.27 ± 0.36	1.05 ± 0.18	11.2 ± 1.48	11.3 ± 2.48	1.00 ± 0.58
9	0.37 ± 0.11	1.19 ± 1.14	6.04 ± 1.14	1.71 ± 0.35	19.0 ± 3.60	19.5 ± 2.99	1.89 ± 0.13
10	0.27 ± 0.13	1.17 ± 0.18	6.40 ± 0.88	0.90 ± 0.15	38.9 ± 3.51	17.1 ± 1.66	2.15 ± 0.83
13	76.6 ± 0.10	439 ± 0.20	79.8 ± 1.87	24.6 ± 0.20	251 ± 20.9	4.70 ± 5.14	6.66 ± 0.66

Table S 6.5 Bioaccessible concentrations of metal(loid)s in PM$_{10}$ leached in simulated gastric fluids (µg kg^{-1}) (median ± SD).

Sampling site	Cd	Cr	Cu	Ni	Pb	Zn	As
2	0.01	0.18	0.68	1.42	1.61	10.5	1.66
	± 0.11	± 0.25	± 0.06	± 0.84	± 1.19	± 2.23	± 0.22
6	0.12	0.43	2.27	0.46	7.12	38.8	2.69
	± 0.17	± 0.27	± 1.64	± 0.64	± 2.91	± 2.25	± 0.80
7	0.31	0.52	2.55	0.66	10.6	41.3	9.28
	± 0.35	± 0.47	± 3.19	± 0.93	± 1.77	± 5.84	± 0.65
8	0.02	0.27	1.83	0.43	5.71	28.0	4.61
	± 0.03	± 0.38	± 1.85	± 0.11	± 1.07	± 7.89	± 0.22
9	0.43	0.22	2.35	0.81	19.1	47.2	16.1
	± 0.61	± 0.19	± 2.60	± 0.17	± 1.16	± 2.84	± 1.10
10	0.19	0.90	0.79	0.63	7.77	37.2	6.51
	± 0.07	± 0.70	± 1.85	± 0.10	± 1.49	± 0.15	± 1.37
13	0.56	0.12	4.55	1.14	106	40.8	3.70
	± 0.31	± 0.12	± 1.57	± 0.32	± 13.9	± 4.17	± 0.16

Table S 6.6 Bioaccessible concentrations of metal(loid)s in soil samples leached for 24 hours in simulated lung fluids (µg kg^{-1}) (median ± SD).

Sampling site	Cd	Cr	Cu	Ni	Pb	Zn	As
2	0.04	0.25	3.95	2.36	0.70	3.90	1.97
	± 0.11	± 0.55	± 1.55	± 0.60	± 0.27	± 1.26	± 1.25
6	0.12	0.24	1.74	0.46	0.57	0.68	2.08
	± 0.51	± 0.91	± 0.95	± 0.92	± 0.69	± 1.83	± 1.39
7	0.13	0.13	1.47	0.26	0.40	1.80	1.80
	± 0.22	± 0.85	± 0.17	± 0.82	± 0.68	± 1.97	± 1.63
8	0.11	0.38	1.64	0.32	0.58	1.31	2.02
	± 0.34	± 0.14	± 0.17	± 0.61	± 1.98	± 1.26	± 1.41
9	0.16	0.02	1.84	0.62	0.78	2.58	1.52
	± 0.38	± 0.10	± 1.19	± 0.29	± 1.70	± 1.18	± 1.38
10	0.18	0.29	2.07	0.56	0.39	1.46	1.85
	± 0.50	± 0.80	± 0.16	± 0.55	± 0.67	± 1.98	± 1.81
13	0.13	0.37	2.00	0.36	0.92	1.23	3.09
	± 0.10	± 0.36	± 1.13	± 0.33	± 0.10	± 1.35	± 1.93

Table S 6.7 Bioaccessible concentrations of metal(loid)s in PM$_{10}$ leached for 24 hours in simulated lung fluids (µg kg^{-1}) (median ± SD).

Sampling site	Cd	Cr	Cu	Ni	Pb	Zn	As
2	0.11	0.83	0.64	0.35	0.38	1.39	0.85
	± 0.11	± 1.34	± 1.67	± 0.18	± 0.16	± 3.30	± 0.45
6	0.08	0.37	0.69	0.68	0.68	1.22	1.47
	± 0.46	± 1.25	± 0.11	± 0.18	± 1.37	± 1.50	± 1.73
7	0.11	0.44	1.05	1.65	0.39	0.25	0.77
	± 0.42	± 0.69	± 1.07	± 1.66	± 1.79	± 0.11	± 0.19
8	0.05	0.88	0.86	0.52	1.26	0.03	1.59
	± 0.17	± 0.77	± 0.16	± 0.30	± 0.55	± 0.14	± 0.68
9	0.13	0.41	1.10	0.55	1.00	1.19	1.02
	± 0.12	± 0.66	± 1.66	± 0.21	± 0.39	± 0.37	± 0.14
10	0.11	0.49	0.88	0.77	0.61	1.04	4.17
	± 0.18	± 1.66	± 1.56	± 1.05	± 0.91	± 0.87	± 1.89
13	0.05	0.65	0.76	0.41	0.26	0.72	1.03
	± 0.10	± 0.89	± 1.89	± 0.40	± 0.79	± 0.99	± 0.67

Table S 6.8 Total concentrations of metal(loid)s in PM$_{10}$ (ng m^{-3}) and soil (mg kg^{-1}) samples throughout all sampling sites.

Sample	Cd	Cr	Cu	Ni	Pb	Zn	As
PM$_{10}$							
Median	2.93	275	35.3	162	85.3	491	11.8
Min	0.59	20.4	18.0	6.83	41.9	161	6.24
Max	4.68	1 428	86.4	678	178	610	17.9
Soil (A-horizon)							
Median	0.83	81.5	48.8	29.2	158	235	20.7
Min	0.20	57.8	18.3	20.5	3.91	57.0	10.4
Max	2.19	145	138	57.1	206	668	35.5

Table S 6.9 Daily intake of metal(loid)s and hazard quotients for oral ingestion exposure of soil calculated for a child. Values exceeding TDI limits are indicated in bold (median ± SD).

Sampling site		2	6	7	8	9	10	13	TDI[a] (µg day⁻¹)
As	Intake (µg day⁻¹)	12.0 ± 1.49	**19.5 ± 3.75**	**67.2 ± 7.82**	**33.3 ± 1.49**	**116 ± 13.7**	**47.1 ± 22.3**	**26.7 ± 2.02**	13.8
	HQ_{ing}	0.87	**1.42**	**4.87**	**2.42**	**8.45**	**3.42**	**1.94**	
Cd	Intake (µg day⁻¹)	0.03 ± 0.04	0.89 ± 0.12	2.23 ± 0.34	0.14 ± 0.03	3.11 ± 0.27	1.41 ± 0.04	4.03 ± 1.04	6.9
	HQ_{ing}	0.00	0.13	0.32	0.02	0.45	0.20	0.58	
Cr	Intake (µg day⁻¹)	11.6 ± 1.68	27.9 ± 1.37	34.2 ± 3.14	17.5 ± 2.53	14.5 ± 1.27	58.9 ± 4.66	7.97 ± 0.83	69 000
	HQ_{ing}	0.00	0.00	0.00	0.00	0.00	0.00	0.00	
Cu	Intake (µg day⁻¹)	4.96 ± 0.43	16.4 ± 7.73	18.4 ± 1.23	13.2 ± 2.28	17.0 ± 7.28	20.2 ± 8.97	32.9 ± 7.09	1 935
	HQ_{ing}	0.00	0.01	0.01	0.01	0.01	0.01	0.02	
Pb	Intake (µg day⁻¹)	11.6 ± 1.88	**51.6 ± 7.21**	**77.4 ± 4.95**	41.3 ± 3.70	**138 ± 40.7**	**56.3 ± 3.11**	**768 ± 57.8**	49.6
	HQ_{ing}	0.23	**1.04**	**1.56**	0.83	**2.79**	**1.13**	**15.4**	
Ni	Intake (µg day⁻¹)	10.2 ± 5.58	3.30 ± 1.03	4.75 ± 2.16	3.10 ± 0.06	5.84 ± 1.10	4.55 ± 0.69	8.28 ± 2.15	690
	HQ_{in}	0.01	0.00	0.01	0.00	0.01	0.01	0.01	
Zn	Intake (µg day⁻¹)	76.7 ± 14.8	281 ± 98.7	299 ± 14.8	203 ± 85.5	342 ± 51.4	269 ± 66.3	296 ± 93.7	6 900
	HQ_{ing}	0.01	0.04	0.04	0.03	0.05	0.04	0.04	

[a] tolerable daily intake (TDI) values taken from Baars et al. (2001) and calculated for body weight

Table S 6.10 Daily intake of metal(loid)s and hazard quotients for oral ingestion exposure of PM_{10} calculated for a 3-year-old child. Values exceeding TDI limits are indicated in bold (median ± SD).

Sampling site		2	6	7	8	9	10	13	TDI[a] (µg day⁻¹)
As	Intake (µg day⁻¹)	12.0 ± 1.49	**19.5 ± 3.75**	**67.2 ± 7.82**	**33.3 ± 1.49**	**116 ± 13.7**	**47.1 ± 22.3**	**26.7 ± 2.02**	13.8
	HQ_{ing}	0.87	**1.42**	**4.87**	**2.42**	**8.45**	**3.42**	**1.94**	
Cd	Intake (µg day⁻¹)	0.03 ± 0.04	0.89 ± 0.12	2.23 ± 0.34	0.14 ± 0.03	3.11 ± 0.27	1.41 ± 0.04	4.03 ± 1.04	6.9
	HQ_{ing}	0.00	0.13	0.32	0.02	0.45	0.20	0.58	
Cr	Intake (µg day⁻¹)	11.6 ± 1.68	27.9 ± 1.37	34.2 ± 3.14	17.5 ± 2.53	14.5 ± 1.27	58.9 ± 4.66	7.97 ± 0.83	69 000
	HQ_{ing}	0.00	0.00	0.00	0.00	0.00	0.00	0.00	
Cu	Intake (µg day⁻¹)	4.96 ± 0.43	16.4 ± 7.73	18.4 ± 1.23	13.2 ± 2.28	17.0 ± 7.28	20.2 ± 8.97	32.9 ± 7.09	1 935
	HQ_{ing}	0.00	0.01	0.01	0.01	0.01	0.01	0.02	
Pb	Intake (µg day⁻¹)	11.6 ± 1.88	**51.6 ± 7.21**	**77.4 ± 4.95**	41.3 ± 3.70	**138 ± 40.7**	**56.3 ± 3.11**	**768 ± 57.8**	49.6
	HQ_{ing}	0.23	**1.04**	**1.56**	0.83	**2.79**	**1.13**	**15.4**	
Ni	Intake (µg day⁻¹)	10.2 ± 5.58	3.30 ± 1.03	4.75 ± 2.16	3.10 ± 0.06	5.84 ± 1.10	4.55 ± 0.69	8.28 ± 2.15	690
	HQ_{in}	0.01	0.00	0.01	0.00	0.01	0.01	0.01	
Zn	Intake (µg day⁻¹)	76.7 ± 14.8	281 ± 98.7	299 ± 14.8	203 ± 85.5	342 ± 51.4	269 ± 66.3	296 ± 93.7	6 900
	HQ_{ing}	0.01	0.04	0.04	0.03	0.05	0.04	0.04	

[a] tolerable daily intake (TDI) values taken from Baars et al. (2001) and calculated for body weight

Table S 6.11 Metal(loid) concentrations in air and hazard quotients for inhalation of soil calculated for a 3-year-old child. Values exceeding TCA limits are indicated in bold (median ± SD).

	Sampling site	2	6	7	8	9	10	13	TCA[a] ($\mu g\ m^{-3}$)
As	Conc. ($\mu g\ m^{-3}$)	**1.17** ± 0.74	**1.23** ± 0.82	**1.07** ± 0.96	**1.19** ± 0.83	0.90 ± 0.59	**1.10** ± 0.17	**1.83** ± 1.04	1.00
	HQ_{inh}	**1.17**	**1.23**	**1.07**	**1.19**	0.90	**1.10**	**1.83**	
Cd	Conc. ($\mu g\ m^{-3}$)	0.02 ± 0.01	0.07 ± 0.03	0.08 ± 0.30	0.07 ± 0.02	0.04 ± 0.30	0.05 ± 0.02	0.08 ± 0.06	nd
	HQ_{inh}	nd	nd	nd	nd	nd	nd	nd	
Cr	Conc. ($\mu g\ m^{-3}$)	0.15 ± 0.13	0.14 ± 0.24	0.07 ± 0.05	0.23 ± 0.03	0.01 ± 0.06	0.17 ± 0.07	0.22 ± 0.01	60.0
	HQ_{inh}	0.00	0.00	0.00	0.00	0.00	0.00	0.00	
Cu	Conc. ($\mu g\ m^{-3}$)	**2.34** ± 1.69	**1.03** ± 0.56	0.87 ± 0.04	0.97 ± 0.10	**1.09** ± 0.30	**1.23** ± 0.03	**1.18** ± 0.67	1.00
	HQ_{inh}	**2.34**	**1.03**	0.87	0.97	**1.09**	**1.23**	**1.18**	
Pb	Conc. ($\mu g\ m^{-3}$)	0.42 ± 0.16	0.34 ± 0.19	0.24 ± 0.10	0.34 ± 0.27	0.46 ± 0.19	0.23 ± 0.18	0.55 ± 0.13	0.60
	HQ_{inh}	0.69	0.56	0.40	0.57	0.77	0.38	0.91	
Ni	Conc. ($\mu g\ m^{-3}$)	**1.40** ± 0.36	**0.27** ± 0.04	**0.15** ± 0.09	**0.19** ± 0.06	**0.36** ± 0.27	**0.33** ± 0.12	**0.22** ± 0.19	0.05
	HQ_{inh}	**27.9**	**5.45**	**3.04**	**3.75**	**7.28**	**6.66**	**4.30**	
Zn	Conc. ($\mu g\ m^{-3}$)	2.31 ± 0.91	0.40 ± 0.22	1.07 ± 0.46	0.78 ± 0.28	1.53 ± 0.80	0.86 ± 0.35	0.73 ± 0.14	nd
	HQ_{inh}	nd	nd	nd	nd	nd	nd	nd	

[a] tolerable concentrations in air (TCA) values taken from Baars et al. (2001)

nd – not defined for TCA, not determined for HQ_{inh}

Table S 6.12 Metal(loid)s concentration in air and hazard quotients for inhalation of PM$_{10}$ calculated for a 3-year-old child. Values exceeding TCA limits are indicated in bold (median ± SD).

Sampling site		2	6	7	8	9	10	13	TCA[a] (µg m^{-3})
As	Conc. (µg m^{-3})	0.50 ± 0.44	0.87 ± 0.12	0.45 ± 0.26	0.94 ± 0.83	0.61 ± 0.59	**2.47** ± 1.07	0.61 ± 0.14	1
	HQ$_{inh}$	0.50	0.87	0.45	0.94	0.61	**2.47**	0.61	
Cd	Conc. (µg m^{-3})	0.06 ± 0.06	0.05 ± 0.03	0.07 ± 0.03	0.03 ± 0.02	0.08 ± 0.03	0.06 ± 0.03	0.03 ± 0.06	nd
	HQ$_{inh}$	nd	nd	nd	nd	nd	nd	nd	
Cr	Conc. (µg m^{-3})	0.49 ± 0.33	0.22 ± 0.14	0.26 ± 0.10	0.52 ± 0.30	0.24 ± 0.06	0.29 ± 0.07	0.39 ± 0.21	60.0
	HQ$_{inh}$	0.01	0.00	0.00	0.01	0.00	0.00	0.01	
Cu	Conc. (µg m^{-3})	0.38 ± 0.19	0.41 ± 0.26	0.62 ± 0.04	0.51 ± 0.10	0.65 ± 0.30	0.52 ± 0.03	0.45 ± 0.17	1.00
	HQ$_{inh}$	0.38	0.41	0.62	0.51	0.65	0.52	0.45	
Pb	Conc. (µg m^{-3})	0.23 ± 0.16	0.40 ± 0.29	0.23 ± 0.10	0.74 ± 0.37	0.59 ± 0.19	0.36 ± 0.28	0.16 ± 0.13	0.60
	HQ$_{inh}$	0.38	0.67	0.39	**1.24**	0.99	0.60	0.26	
Ni	Conc. (µg m^{-3})	**0.21** ± 0.26	**0.40** ± 0.14	**0.98** ± 0.49	**0.31** ± 0.26	**0.33** ± 0.27	**0.46 ±** 0.12	**0.24** ± 0.19	0.05
	HQ$_{inh}$	**4.12**	**8.08**	**19.5**	**6.13**	**6.55**	**9.12**	**4.84**	
Zn	Conc. (µg m^{-3})	0.82 ± 0.11	0.72 ± 0.08	0.15 ± 0.08	0.02 ± 0.18	0.71 ± 0.10	0.62 ± 0.25	0.42 ± 0.24	nd
	HQ$_{inh}$	nd	nd	nd	nd	nd	nd	nd	

[a] tolerable concentrations in air (TCA) values taken from Baars et al. (2001)

nd – not defined for TCA, not determined for HQ$_{inh}$

Table S 6.13 Relative contribution of inhalation (SLF 2h) to total exposure in % calculated for PM_{10}.

Sampling site	Cd	Cr	Cu	Ni	Pb	Zn	As
2	90.4	58.2	50.6	16.7	29.0	2.63	35.0
6	31.9	50.3	24.4	47.3	2.85	0.37	28.0
7	20.7	62.3	21.7	52.4	4.77	2.58	9.7
8	75.8	65.3	26.7	57.2	7.02	1.43	21.9
9	14.1	66.2	27.9	45.1	2.01	0.70	8.2
10	17.5	37.5	18.2	50.1	5.44	2.76	21.4
13	2.89	78.3	14.2	39.5	0.59	0.22	27.4

Chapter VII

Summary

The thesis evaluated the use of selected environmental samples for the monitoring of the pollution sources in two industrial areas, Upper Silesia in Czech Republic and North-Eastern Norway). We dealt with six types of specimen, three biotic and three abiotic, to cover a wide range of polluting scenarios. It was proven that different sample types are suitable for different conditions of pollution monitoring (long-term vs. short-term pollution, local vs. remote pollution sources).

In general, the experimental work can be divided into main five sections: i) sample mineralization and concentration analyses of selected metal(loid)s, ii) analyses of Pb, Ni and Cu isotope composition, iii) scanning electron microscopy analyses of PM_{10} and heavy mineral fraction of soil samples, iv) X-ray diffraction analyses of the separated soil heavy mineral fraction, v) extraction of pollutants using simulated gastric and lung fluids. The aim was thus to provide a complex view on chosen samples regarding not just their potential as a matrix for trace metal pollution tracking, but also to evaluate the applicability of samples as industrial pollution tracers and to validate traditional (Pb) and non-traditional isotope systems (Ni and Cu) as pollution tracers.

The following strong sources of selected metal(loid)s were observed: i) metallurgical activities, ii) the combustion of fossil fuels in industry and households, and iii) traffic as possible source of less radiogenic Pb. As expected, the most contaminated transects were those in upwind direction of the smelters (both in Czech Republic and Norway), while the distance of the source is crucial parameter for the metal(loid)s deposition in terms of metal(loid)s concentration. There is a high uniformity of Ni isotope composition in snow, lichen, topsoil, and PM_{10} from sites close to smelter, and also matches the Ni isotope composition of the metallurgical samples. Ni in most of the snow, lichen, and topsoil samples have similar isotope composition to feeding material and/or smelter slag, while a significantly heavier Ni were determined in the samples of topsoil and lichen from remote sampling sites, which we suggest to be a result of additional isotope fractionation in environment. Copper in lichen, snow, and topsoil samples represents the heavier Cu isotopes fraction in comparison with the industrial samples, bedrock, and PM_{10}, and this shift toward heavier Cu isotopes might be also caused by isotope fractionation. The isotope composition of Pb that is emitted into the atmosphere during metallurgical processes closely reflects the isotope composition of the processed material, such as Pb ore or secondary processed materials that contain Pb.

Snow is considered to be an ideal medium to monitor the deposition of pollutants from the atmosphere. During snowfall (or precipitation in general), larger particles tend to be deposited closer to the pollution source than finer particles. The snow samples showed a wide variability of isotope compositions, as it represents complex spectre of

heavy particles currently occurring in the atmosphere. Snow thus reflexes the actual amount of pollutants emitted from the source and contribution of particular source can be easily estimated. High concentrations of the selected elements in the snow samples are clear evidence of recent contamination originating from local sources. It is also very convenient to combine snow analyses with PM_{10} as PM_{10} represents the lighter part of atmospheric aerosols sedimenting further from the source. Fresh snow seems to be the most reliable and useful environmental sample for tracing recent industrial sources of metal contamination in complex industrial areas because continuous snow cover stops the re-suspension of particles that are deposited on surfaces covered by permanent snow cover.

The PM_{10} fraction consists of particles with a mean aerodynamic diameter of 10 µm or less, which can travel long distances. Assuming that, PM_{10} samples can reflect remote sources because of the mixing of air but can be easily homogenised. Thus, the composition of PM_{10} samples depends on the current wind direction and air mass flow. Significant variations were observed between the samples obtained in winter and summer, as these samples reflect changes in atmosphere during seasons. The samples of the summer PM_{10} showed contrasting results and were less isotopically variable than the samples from the winter campaign. Winter samples include metals from the combustion of local coal, while summer samples do not contain particles from those sources. The reason for this phenomenon could have been the unstable wind direction during the sampling period, which mixed sources from different directions. Strong effects from the meteorological conditions during sampling must be taken in consideration in evaluation of results. Our results thus suggest that PM_{10} samples are not very useful for tracing long-term activities of local sources of contamination because they reflect sources in relation to the actual wind direction. On the other hand, the combination of PM_{10} and snow can become a powerful tool for evaluation of current pollution sources as PM_{10} provides information on pollution for a particular single day. Short term sampling reflects the influence of local point sources.

Daily intakes/concentrations in air and hazard quotients (HQ_{ing}, HQ_{inh}) were calculated for both inhalation and ingestion pathways. The presented exposure risk calculations were performed to demonstrate the exposure to toddlers. Relatively high doses of Cr, Ni were associated with inhalation, contrary to Zn, Pb and As where ingestion prevails. Tolerable daily intakes via soil ingestion were exceeded by As, Cd and Pb. Daily intake of three previously mentioned metal(loid)s was the highest at site which is located close to the steel plant. Cadmium and Pb were also the most bioaccessible of all the metal(loid)s. Daily intake of metal(loid)s via PM_{10} ingestion were again exceeded by As and Pb at most of the sampling sites, while both metal(loid)s extracted from PM_{10} proved to be highly bioaccessible. The bioaccessibility testing showed that, for PM_{10}

collected in 24 h, As occurs in very bioaccessible forms. While total As concentrations in samples remain relatively low, both high daily intake and the concentration in air suggest that As is a potentially dangerous element for human exposure. High bioaccessibility and high concentrations in the air at sites across Ostrava city correspond to elevated content of As in brown coal, which is mainly used for household heating during winter. According to analyses of the historic deposition of metal(loid)s in tree rings As occurring in Ostrava city originates overwhelmingly from the household usage of brown coal. The decrease of black coal mining in the Ostrava mines led to the increased use of inferior coal types, mainly brown coal originating from Bílina (northwestern part of Czech Republic), which is rich in As. Household combustion is difficult to control since low-quality fuels are often used, and it is not easy to prove the combustion of banned materials.

Epiphytic lichens used for pollution tracing in this thesis are *Physcia tenella* (Scop.) DC., *Hypogymnia physodes* (L.) Nyl. and *Melanohalea olivacea* (L.) O. Blanco, A. Crespo, Divakar, Essl., D. Hawksw. & Lumbsch. Lichens present suitable monitoring matrix for the metals atmospheric deposition because they have no roots or well-developed cuticles, which allows them to absorb moisture and nutrients exclusively from the atmosphere. Lichens can also accumulate pollutants by re-suspension of dust particles. Lichens can thus accumulate and integrate pollution from many different sources, including local and even distant sources, and accumulate contaminants for several years or even over their entire lifetime, which corresponds with lower Pb isotope variations observed in lichen samples as opposed to abiotic samples. For this reason, the concentration of atmospheric Pb and Pb isotope ratios tend to be homogenised through time. We suggest lichens to be used as tracers of the long-term activity of local and remote sources of contamination.

Mosses are bryophytes that have no roots or cuticle layer and thus obtain most of their nutrients from atmospheric deposition than from the mineral components of the soil. Bryophyte used for pollution tracing in this thesis is *Hypnum cupressiforme* (Hedw.). Mosses accumulate Pb over their lifetime, which can be between five to ten years. During this period, they integrate the metal input from various sources. Similarly to the lichens samples, mosses homogenise the Pb isotopic signal over the years. Mosses thus appear not to be well suited for detecting individual point sources over short and long distances. On the other hand, mosses seem to be more abundant than lichens, thus making them more suitable for air pollution monitoring than lichens.

Lichens and mosses are widely used biotic tracers of environmental pollution, although unlike tree rings, they cannot be used as archives of historical pollution. Due to the buffering function of soils, tree rings should be a suitable archive of past atmospheric

pollution where most Pb enters the xylem directly from the atmosphere, with only a minor contribution of Pb uptake by roots. In this thesis, tree rings samples were extracted from coniferous trees *Larix decidua* (Mill.), *Picea abies* (L.) H. Karst. and *Pinus sylvestris* (L.). Tree cores obtained from sampled trees reflect the Pb concentration and isotope composition over fifty years. Tree rings do not precisely reflect the atmospheric pollution Pb signal as the ten-year averages used in presented experiment may homogenize the signal same as the moss or lichen sample. Nonetheless, tree cores from all the examined trees in the Upper Silesia area exhibit highest Pb concentrations in the 1980's, which correspond to Pb emissions from coal combustion and industry in the area. The samples further indicate a recent reduction of the concentration of airborne Pb and an increase in the $^{206}Pb/^{207}Pb$ ratio values. This observation is in agreement with the introduction of Pb-free gasoline in Czech Republic and further reductions in industrial emissions. Tree cores seems to be a suitable archive of pollution for areas where other archive samples (e.g., peat or lake sediments) are not available. They can also be successfully used as a supplement to analyses of other types of environmental matrixes.

The organic horizon of soils serves as the most important sink for contaminants, as well as for plant nutrients, as it accumulates elements over decades. The results presented in this PhD thesis indicate that Pb is strongly enriched in topsoil (A-horizon) compared to the values observed in mineral soils (C-horizon). Soils reflect the accumulated Pb contamination of tens of years. They integrate the metal input from various sources and, thus, level out isotope differences of individual sources that might have existed at the time of Pb deposition. Soil, especially the upper horizons, can be successfully used as medium for fingerprinting the influence level of the main Pb sources but, because of its long-term accumulation of elements, it is not useful for the tracing of recent pollution sources

The use of environmental samples generally represents viable solution for pollution fingerprinting. Particular fingerprinting method has to be selected with respect to contaminating metal(loid)s, site specifications, source distance and exposure time (including historic deposition). Combination of different samples and analyses methods provide an overall view on urban pollution in the area. Fr3om the six samples studied in this PhD thesis, the combination of snow and PM_{10} sample analyses proved to be most accurate in terms of actual local industrial pollution. On the other hand, snow may be unavailable during winter due to global warming, which we already experienced during snow sampling in Czech Republic, and PM_{10} deposition is heavily dependent on the current wind direction. Results of this PhD thesis thus highlight the need for a complex approach starting with thorough site investigation, historical metal(loid)s

deposition survey, up to choosing the suitable environmental sample or combination of samples.

References

Abouchami, W., Zabel, M., 2003. Climate forcing of the Pb isotope record of terrigenous input into the Equatorial Atlantic. Earth Planet. Sci. Lett. 213, 221–234. https://doi.org/10.1016/S0012-821X(03)00304-2

Abu-Ashour, J., Joy, D.M., Lee, H., Whiteley, H.R., Zelin, S., 1994. Transport of microorganisms through soil. Water Air Soil Pollut. 141–158.

Adamo, P., Dudka, S., Wilson, M.J., McHardy, W.J., 1996. Chemical and mineralogical forms of Cu and Ni in contaminated soils from the Sudbury mining and smelting region, Canada. Environ. Pollut. 91, 11–19. https://doi.org/10.1016/0269-7491(95)00035-P

Adriano, D.C., 2001. Bioavailability of Trace Metals, in: Trace Elements in Terrestrial Environments.

Agnan, Y., Séjalon-Delmas, N., Probst, A., 2013. Comparing early twentieth century and present-day atmospheric pollution in SW France: A story of lichens. Environ. Pollut. 172, 139–148. https://doi.org/10.1016/j.envpol.2012.09.008

Aleksandropoulou, V., Lazaridis, M., 2013. Development and application of model (ExDoM) for calculating the respiratory tract dose and retention of particles under variable exposure conditions. AIR QUAL ATMOS HLTH. 6, 13-26. https://doi.org/10.1007/s11869-010-0126-z

Alliot, C., Michel, N., Bonraisin, A.-C., Bossé, V., Laizé, J., Bourdeau, C., Mokili, B.M., Haddad, F., 2011. One step purification process for no-carrier-added 64Cu produced using enriched nickel target. Radiochim. Acta 99. https://doi.org/https://doi.org/10.1524/ract.2011.1821

Alloway, B.J., 2013. Sources of Heavy Metals and Metalloids in Soils. pp. 11–50. https://doi.org/10.1007/978-94-007-4470-7_2

Almeida, S.M., Lage, J., Fernández, B., Garcia, S., Reis, M.A., Chaves, P.C., 2015. Chemical characterization of atmospheric particles and source apportionment in the vicinity of a steelmaking industry. Sci. Total Environ. 521–522, 411–420. https://doi.org/10.1016/j.scitotenv.2015.03.112

Annibaldi, A., Truzzi, C., Illuminati, S., Scarponi, G., 2009. Recent sudden decrease of lead in Adriatic coastal seawater during the years 2000-2004 in parallel with the phasing out of leaded gasoline in Italy. Mar. Chem. 113, 238–249. https://doi.org/10.1016/j.marchem.2009.02.005

Ares, A., Varela, Z., Aboal, J.R., Carballeira, A., Fernández, J.A., 2015. Active biomonitoring with the moss Pseudoscleropodium purum: Comparison between different types of transplants and bulk deposition. Ecotoxicol. Environ. Saf. 120, 74–79. https://doi.org/10.1016/j.ecoenv.2015.05.033

Aubert, D., Le Roux, G., Krachler, M., Cheburkin, A., Kober, B., Shotyk, W., Stille, P., 2006. Origin and fluxes of atmospheric REE entering an ombrotrophic peat bog in Black Forest (SW Germany): Evidence from snow, lichens and mosses. Geochim. Cosmochim. Acta 70, 2815–2826. https://doi.org/10.1016/j.gca.2006.02.020

Äyräs, M., Niskavaara, H., Bogatyrev, I., Chekushin, V., Pavlov, V., De Caritat, P., Halleraker, J.H., Finne, T.E., Kashulina, G., Reimann, C., 1997. Regional patterns of heavy metals (Co, Cr, Cu, Fe, Ni, Pb, V and Zn) and sulphur in terrestrial moss samples as indication

of airborne pollution in a 188,000 km2 area in northern Finland, Norway and Russia. J. Geochemical Explor. 58, 269–281. https://doi.org/10.1016/S0375-6742(96)00077-5

Aznar, J.C., Richer-Laflèche, M., Cluis, D., 2008. Metal contamination in the lichen Alectoria sarmentosa near the copper smelter of Murdochville, Québec. Environ. Pollut. 156, 76–81. https://doi.org/10.1016/j.envpol.2007.12.037

Baars, A.J., Theelen, R.M.C., Janssen, P.J.C.M., Hesse, J.M., van Apeldoorn, M.E., Meijerink, M.C.M., Verdam, L., Zeilmaker, M.J., 2001. Re-evaluation of human-toxicological maximum permissible risk levels, RIVM report 711701 025. https://doi.org/10.1051/vetres:2008046

Bacon, J.R., Dinev, N.S., 2005. Isotopic characterisation of lead in contaminated soils from the vicinity of a non-ferrous metal smelter near Plovdiv, Bulgaria. Environ. Pollut. 134, 247–255. https://doi.org/10.1016/j.envpol.2004.07.030

Balistrieri, L.S., Borrok, D.M., Wanty, R.B., Ridley, W.I., 2008. Fractionation of Cu and Zn isotopes during adsorption onto amorphous Fe(III) oxyhydroxide: Experimental mixing of acid rock drainage and ambient river water. Geochim. Cosmochim. Acta 72, 311–328. https://doi.org/10.1016/j.gca.2007.11.013

Banat, K.M., Howari, F.M., Al-Hamad, A.A., 2005. Heavy metals in urban soils of central Jordan: Should we worry about their environmental risks? Environ. Res. 97, 258–273. https://doi.org/10.1016/j.envres.2004.07.002

Barcan, V., 2002. Nature and origin of multicomponent aerial emissions of the copper-nickel smelter complex. Environ. Int. https://doi.org/10.1016/S0160-4120(02)00064-8

Bargagli, R., Monaci, F.F., Borghini, F., Bravi, F.F., Agnorelli, C., 2002. Mosses and lichens as biomonitors of trace metals. A comparison study on Hypnum cupressiforme and Parmelia caperata in a former mining district in Italy. Environ. Pollut. 116, 279–287. https://doi.org/10.1016/S0269-7491(01)00125-7

Battipaglia, G., Marzaioli, F., Lubritto, C., Altieri, S., Strumia, S., Cherubini, P., Cotrufo, M.F., 2010. Traffic pollution affects tree-ring width and isotopic composition of Pinus pinea. Sci. Total Environ. 408, 586–593. https://doi.org/10.1016/j.scitotenv.2009.09.036

Bellis, D.J., Satake, K., Noda, M., Nishimura, N., McLeod, C.W., 2002. Evaluation of the historical records of lead pollution in the annual growth rings and bark pockets of a 250-year-old Quercus crispula in Nikko, Japan. Sci. Total Environ. 295, 91–100. https://doi.org/10.1016/S0048-9697(02)00054-2

Berg, T., Steinnes, E., 1997. Use of mosses (Hylocomium splendens and Pleurozium schreberi) as biomonitors of heavy metal deposition: From relative to absolute deposition values. Environ. Pollut. 98, 61–71. https://doi.org/10.1016/S0269-7491(97)00103-6

Bergamaschi, L., Rizzio, E., Valcuvia, M.G., Verza, G., Profumo, A., Gallorini, M., 2002. Determination of trace elements and evaluation of their enrichment factors in Himalayan lichens. Environ. Pollut. 120, 137–144. https://doi.org/10.1016/S0269-7491(02)00138-0

Berglen, B.F., 2015. Russian-Norwegian ambient air monitoring in the border areas.

Bigalke, M., Weyer, S., Kobza, J., Wilcke, W., 2010. Stable Cu and Zn isotope ratios as tracers of sources and transport of Cu and Zn in contaminated soil. Geochim. Cosmochim. Acta 74, 6801–6813. https://doi.org/10.1016/j.gca.2010.08.044

Bindler, R., Renberg, I., Klaminder, J., Emteryd, O., 2004. Tree rings as Pb pollution archives? A comparison of 206Pb/ 207Pb isotope ratios in pine and other environmental media. Sci. Total Environ. 319, 173–183. https://doi.org/10.1016/S0048-9697(03)00397-8

Blažek, Z., Černikovský, L., Krejčí, B., Volná, V., 2013. Vliv Meteorologických Podmínek Na Kvalitu Ovzduší V Přeshraniční Oblasti Slezska a Moravy. Český hydrometeorologický ústav. Praha.

Bohdalkova, L., Novak, M., Voldrichova, P., Prechova, E., Veselovsky, F., Erbanova, L., Krachler, M., Komarek, A., Mikova, J., 2012. Atmospheric deposition of beryllium in Central Europe: Comparison of soluble and insoluble fractions in rime and snow across a pollution gradient. Sci. Total Environ. 439, 26–34. https://doi.org/10.1016/j.scitotenv.2012.08.089

Bollhöfer, A., Chisholm, W., Rosman, K.J.R., 1999. Sampling aerosols for lead isotopes on a global scale. Anal. Chim. Acta 390, 227–235. https://doi.org/10.1016/S0003-2670(99)00182-8

Bollhöfer, A., Rosman, K.J.R., 2001. Isotopic source signatures for atmospheric lead: The Northern Hemisphere. Geochim. Cosmochim. Acta 65, 1727–1740. https://doi.org/10.1016/S0016-7037(00)00630-X

Bourennane, H., Douay, F., Sterckeman, T., Villanneau, E., Ciesielski, H., King, D., Baize, D., 2010. Mapping of anthropogenic trace elements inputs in agricultural topsoil from Northern France using enrichment factors. Geoderma 157, 165–174. https://doi.org/10.1016/j.geoderma.2010.04.009

Boyd, R., Barnes, S.J., De Caritat, P., Chekushin, V.A., Melezhik, V.A., Reimann, C., Zientek, M.L., 2009. Emissions from the copper-nickel industry on the Kola Peninsula and at Noril'sk, Russia. Atmos. Environ. 43, 1474–1480. https://doi.org/10.1016/j.atmosenv.2008.12.003

Brozek, G.M., Zejda, J.E., Kowalska, M., Gębuś, M., Kępa, K., Igielski, M., 2010. Opposite trends of allergic disorders and respiratory symptoms in children over a period of large-scale ambient air pollution decline. Polish J. Environ. Stud. 19, 1133–1138.

Brunekreef, B., Holgate, S.T., 2002. Air pollution and health. Lancet 360, 1233–1242. https://doi.org/10.1016/S0140-6736(02)11274-8

Bussotti, F., Ferretti, M., 1998. Air pollution, forest condition and forest decline in Southern Europe: An overview. Environ. Pollut. 101, 49–65. https://doi.org/10.1016/S0269-7491(98)00039-6

Caboche, J., Perdrix, E., Malet, B., Laurent, A.Y., 2011. Development of an in vitro method to estimate lung bioaccessibility of metals from atmospheric particles. J. Environ. Monit. 13, 621–630. https://doi.org/10.1039/c0em00439a

Cameron, V., Vance, D., 2014. Heavy nickel isotope compositions in rivers and the oceans. Geochim. Cosmochim. Acta 128, 195–211. https://doi.org/10.1016/j.gca.2013.12.007

Cameron, V., Vance, D., Archer, C., House, C.H., 2009. A biomarker based on the stable isotopes of nickel. Proc. Natl. Acad. Sci. 106, 10944–10948. https://doi.org/10.1073/pnas.0900726106

Campos-Ramos, A., Aragon-Pina, A., Galindo-Estrada, I., Querol, X., Alastuey, A., 2009.

Characterization of atmospheric aerosols by SEM in a rural area in the western part of Mexico and its relation with different pollution sources. Atmos. Environ. 43, 6159–6167. https://doi.org/10.1016/j.atmosenv.2009.09.004

Candelone, J.-P., Hong, S., Boutron, C.F., 1994. An improved method for decontaminating polar snow or ice cores for heavy metal analysis. Anal. Chim. Acta 299, 9–16.

Cao, T., An, L., Wang, M., Lou, Y., Yu, Y., Wu, J., Zhu, Z., Qing, Y., Glime, J., 2008. Spatial and temporal changes of heavy metal concentrations in mosses and its indication to the environments in the past 40 years in the city of Shanghai, China. Atmos. Environ. 42, 5390–5402. https://doi.org/10.1016/j.atmosenv.2008.02.052

Carreras, H., Pingnata, M.L., 2007. Effects of the heavy metals Cu^{2+}, Ni^{2+}, Pb^{2+}, and Zn^{2+} on some physiological parameters of lichen Usnea amblyoclada. Ecotox. Environ. Safe. 67, 1, 59-66. https://doi.org/10.1016/j.ecoenv.2006.05.005

Ceburnis, U.D., Valiulis, D., 1999. Investigation of absolute metal uptake efficiency from precipitation in moss. Sci. Total Environ. 226, 247253.

Cereceda-Balic, F., Palomo-Marín, M.R., Bernalte, E., Vidal, V., Christie, J., Fadic, X., Guevara, J.L., Miro, C., Pinilla Gil, E., 2012. Impact of Santiago de Chile urban atmospheric pollution on anthropogenic trace elements enrichment in snow precipitation at Cerro Colorado, Central Andes. Atmos. Environ. 47, 51–57. https://doi.org/10.1016/j.atmosenv.2011.11.045

Chatelin, R., Anne-Archard, D., Murris-Espin, M., Thiriet, M., Poncet, P., 2017. Numerical and experimental investigation of mucociliary clearance breakdown in cystic fibrosis. J. Biomech. 53, 56–63. https://doi.org/10.1016/j.jbiomech.2016.12.026

Chen, M., Boyle, E.A., Switzer, A.D., Gouramanis, C., 2016. A century long sedimentary record of anthropogenic lead (Pb), Pb isotopes and other trace metals in Singapore. Environ. Pollut. 213, 446–459. https://doi.org/10.1016/j.envpol.2016.02.040

CHMI, 2014. VÝROČNÍ ZPRÁVA ČESKÉHO HYDROMETEOROLOGICKÉHO ÚSTAVU / ANNUAL REPORT OF THE CZECH HYDROMETEOROLOGICAL INSTITUTE.

Chrastný, V., Čadková, E., Vaněk, A., Teper, L., Cabala, J., Komárek, M., 2015. Cadmium isotope fractionation within the soil profile complicates source identification in relation to Pb-Zn mining and smelting processes. Chem. Geol. 405, 1–9. https://doi.org/10.1016/j.chemgeo.2015.04.002

Cimova, N., Novak, M., Chrastny, V., Curik, J., Veselovsky, F., Blaha, V., Prechova, E., Pasava, J., Houskova, M., Bohdalkova, L., Stepanova, M., Mikova, J., Krachler, M., Komarek, A., 2016. Lead fluxes and 206Pb/207Pb isotope ratios in rime and snow collected at remote mountain-top locations (Czech Republic, Central Europe): Patterns and sources. Atmos. Environ. 143, 51–59. https://doi.org/10.1016/j.atmosenv.2016.07.057

Cloquet, Christophe, Carignan, J., Libourel, G., 2006. Atmospheric pollutant dispersion around an urban area using trace metal concentrations and Pb isotopic compositions in epiphytic lichens. Atmos. Environ. 40, 574–587. https://doi.org/10.1016/j.atmosenv.2005.09.073

Cloquet, C., Estrade, N., Carignan, J., 2015. Ten years of elemental atmospheric metal fallout and Pb isotopic composition monitoring using lichens in northeastern France. Comptes Rendus - Geosci. 347, 257–266. https://doi.org/10.1016/j.crte.2015.04.003

Cocozza, C., Ravera, S., Cherubini, P., Lombardi, F., Marchetti, M., Tognetti, R., 2016. Integrated biomonitoring of airborne pollutants over space and time using tree rings, bark, leaves and epiphytic lichens. Urban For. Urban Green. 17, 177–191. https://doi.org/10.1016/j.ufug.2016.04.008

Colás, V., Padrón-Navarta, J.A., González-Jiménez, J.M., Griffin, W.L., Fanlo, I., O'reilly, S.Y., Gervilla, F., Proenza, J.A., Pearson, N.J., Escayola, M., 2016. Compositional effects on the solubility of minor and trace elements in oxide spinel minerals: Insights from crystal-crystal partition coefficients in chromite exsolution. Am. Mineral. 101, 1360–1372. https://doi.org/https://doi.org/10.2138/am-2016-5611

Conti, M.E., Cecchetii, G., 2001. Biological monitoring; lichens as bioindicators of air pollution assessment - a review. Environ. Pollut. 1114, 471–492.

Darnajoux, R., Lutzoni, F., Miadlikowska, J., Bellenger, J.P., 2015. Determination of elemental baseline using peltigeralean lichens from Northeastern Canada (Québec): Initial data collection for long term monitoring of the impact of global climate change on boreal and subarctic area in Canada. Sci. Total Environ. 533, 1–7. https://doi.org/10.1016/j.scitotenv.2015.06.030

Das, R., Khezri, B., Srivastava, B., Datta, S., Sikdar, P.K., Webster, R.D., Wang, X., 2015. Trace element composition of PM2.5 and PM10 from Kolkata – a heavily polluted Indian metropolis. Atmos. Pollut. Res. 6, 742–750. https://doi.org/10.5094/APR.2015.083

De Caritat, P., Danilova, S., Jaeger, O., Reimann, C., Storro, G., 1998. Groundwater composition near the nickel-copper smelting industry on the Kola Peninsula, central Barents Region (NW Russia and NE Norway). J. Hydrol. 208, 92–107. https://doi.org/10.1016/S0022-1694(98)00147-4

Dean, J.R., Elom, N.I., Entwistle, J.A., 2017. Use of simulated epithelial lung fluid in assessing the human health risk of Pb in urban street dust. Sci. Total Environ. 579, 387–395. https://doi.org/10.1016/j.scitotenv.2016.11.085

Deboudt, K., Flament, P., Weis, D., Mennessier, J.P., Maquinghen, P., 1999. Assessment of pollution aerosols sources above the Straits of Dover using lead isotope geochemistry. Sci. Total Environ. 236, 57–74. https://doi.org/10.1016/S0048-9697(99)00286-7

Del Rio-Salas, R., Ruiz, J., De la O-Villanueva, M., Valencia-Moreno, M., Moreno-Rodriguez, V., Gomez-Alvarez, A., Grijalva, T., Mendivil, H., Paz-Moreno, F., Meza-Figueroa, D., 2012. Tracing geogenic and anthropogenic sources in urban dusts: Insights from lead isotopes. Atmos. Environ. 60, 202–210. https://doi.org/10.1016/j.atmosenv.2012.06.061

Deng, T.H.B., Cloquet, C., Tang, Y.T., Sterckeman, T., Echevarria, G., Estrade, N., Morel, J.L., Qiu, R.L., 2014. Nickel and zinc isotope fractionation in hyperaccumulating and nonaccumulating plants. Environ. Sci. Technol. 48, 11926–11933. https://doi.org/10.1021/es5020955

Dewan, N., Majestic, B.J., Ketterer, M.E., Miller-Schulze, J.P., Shafer, M.M., Schauer, J.J., Solomon, P.A., Artamonova, M., Chen, B.B., Imashev, S.A., Carmichael, G.R., 2015. Stable isotopes of lead and strontium as tracers of sources of airborne particulate matter in Kyrgyzstan. Atmos. Environ. 120, 438–446. https://doi.org/10.1016/j.atmosenv.2015.09.017

Dmuchowski, W., Gozdowski, D., Baczewska, A.H., 2011. Comparison of four bioindication

methods for assessing the degree of environmental lead and cadmium pollution. J. Hazard. Mater. 197, 109–118. https://doi.org/10.1016/j.jhazmat.2011.09.062

Doğrul Demiray, A., Yolcubal, I., Akyol, N.H., Çobanoğlu, G., 2012. Biomonitoring of airborne metals using the Lichen Xanthoria parietina in Kocaeli Province, Turkey. Ecol. Indic. 18, 632–643. https://doi.org/10.1016/j.ecolind.2012.01.024

Doležalová Weissmannová, H., Pavlovský, J., Chovanec, P., 2015. Heavy metal Contaminations of Urban soils in Ostrava, Czech Republic: Assessment of Metal Pollution and using Principal Component Analysis. Int. J. Environ. Res. 9, 683–696.

Doucet, F.J., Carignan, J., 2001. Atmospheric Pb isotopic composition and trace metal concentration as revealed by epiphytic lichens: An investigation related to two altitudinal sections in Eastern France. Atmos. Environ. 35, 3681–3690. https://doi.org/10.1016/S1352-2310(00)00510-0

Drahota, P., Raus, K., Rychlíková, E., Rohovec, J., 2017. Bioaccessibility of As, Cu, Pb, and Zn in mine waste, urban soil, and road dust in the historical mining village of Kaňk, Czech Republic. Environ. Geochem. Health 40, 1495–1512. https://doi.org/10.1007/s10653-017-9999-1

Dudka, S., Ponce-Hernandez, R., Tate, G., Hutchinson, T.C., 1996. Forms of Cu, Ni, and Zn in soils of Sudbury, Ontario and the metal concentrations in plants. Water. Air. Soil Pollut. 90, 531–542. https://doi.org/10.1007/BF00282667

Embiale, A., Zewge, F., Chandravanshi, B.S., Sahle-Demessie, E., 2019. Levels of trace elements in PM10 collected at roadsides of Addis Ababa, Ethiopia, and exposure risk assessment. Environ. Monit. Assess. 191. https://doi.org/10.1007/s10661-019-7503-3

Epelde, L., Martín-Sánchez, I., González-Oreja, J.A., Anza, M., Gómez-Sagasti, M.T., Garbisu, C., 2012. Impact of sources of environmental degradation on microbial community dynamics in non-polluted and metal-polluted soils. Sci. Total Environ. 433, 264–272. https://doi.org/10.1016/j.scitotenv.2012.06.049

Erel, Y., Dayan, U., Rabi, R., Rudich, Y., Stein, M., 2006. Transboundary transport of pollutants by atmospheric mineral dust. Environ. Sci. Technol. 40, 2996–3005. https://doi.org/10.1021/es051502l

Erel, Y., Veron, A., Halicz, L., 1997. Tracing the transport of anthropogenic lead in the atmosphere and in soils using isotopic ratios. Geochim. Cosmochim. Acta 61, 4495–4505. https://doi.org/10.1016/S0016-7037(97)00353-0

Estrade, N., Cloquet, C., Echevarria, G., Sterckeman, T., Deng, T., Tang, Y.T., Morel, J.L., 2015. Weathering and vegetation controls on nickel isotope fractionation in surface ultramafic environments (Albania). Earth Planet. Sci. Lett. 423, 24–35. https://doi.org/10.1016/j.epsl.2015.04.018

Ettler, V., 2016. Soil contamination near non-ferrous metal smelters: A review. Appl. Geochemistry 64, 56–74. https://doi.org/10.1016/j.apgeochem.2015.09.020

Ettler, V., Konečný, L., Kovářová, L., Mihaljevič, M., Šebek, O., Kříbek, B., Majer, V., Veselovský, F., Penížek, V., Vaněk, A., Nyambe, I., 2014a. Surprisingly contrasting metal distribution and fractionation patterns in copper smelter-affected tropical soils in forested and grassland areas (Mufulira, Zambian Copperbelt). Sci. Total Environ. 473–474, 117–

124. https://doi.org/10.1016/j.scitotenv.2013.11.146

Ettler, V., Mihaljevič, M., Komárek, M., 2004. ICP-MS measurements of lead isotopic ratios in soils heavily contaminated by lead smelting: Tracing the sources of pollution. Anal. Bioanal. Chem. 378, 311–317. https://doi.org/10.1007/s00216-003-2229-y

Ettler, V., Mihaljevič, M., Šebek, O., Molek, M., Grygar, T., Zeman, J., 2006. Geochemical and Pb isotopic evidence for sources and dispersal of metal contamination in stream sediments from the mining and smelting district of Příbram, Czech Republic. Environ. Pollut. 142, 409–417. https://doi.org/10.1016/j.envpol.2005.10.024

Ettler, V., Vítková, M., Mihaljevič, M., Šebek, O., Klementová, M., Veselovský, F., Vybíral, P., Kříbek, B., 2014b. Dust from Zambian smelters: mineralogy and contaminant bioaccessibility. Environ. Geochem. Health 36, 919–933. https://doi.org/10.1007/s10653-014-9609-4

European Environment Agency, 2015. Air quality in Europe -2015 report. Copenhagen. https://doi.org/10.2800/62459

Facchinelli, A., Sacchi, E., Mallen, L., 2001. Multivariate statistical and GIS-based approach to identify heavy metal sources in soils.

Feng, Ch., Huang, J., Wang, M., 2019. The sustainability of China's metal industries: features, challenges and future focuses. Resour. Policy. 60, 215-224. https://doi.org/10.1016/j.resourpol.2018.006

Fernandez-Olmo, I., Andecochea, C., Ruiz, S., Fernandez-Ferreras, J.A., Irabien, A., 2016. Local source identification of trace metals in urban/industrial mixed land-use areas with daily PM10 limit value exceedances. Atmos. Res. 171, 92–106. https://doi.org/10.1016/j.atmosres.2015.12.010

Figueira, R., Sérgio, C., Sousa, A.J., 2002. Distribution of trace metals in moss biomonitors and assessment of contamination sources in Portugal. Environ. Pollut. 118, 153–163. https://doi.org/10.1016/S0269-7491(01)00203-2

Francová, A., Chrastný, V., Šillerová, H., Kocourková, J., Komárek, M., 2017a. Suitability of selected bioindicators of atmospheric pollution in the industrialised region of Ostrava, Upper Silesia, Czech Republic. Environ. Monit. Assess. 189, 478. https://doi.org/10.1007/s10661-017-6199-5

Francová, A., Chrastný, V., Šillerová, H., Vítková, M., Kocourková, J., Komárek, M., 2017b. Evaluating the suitability of different environmental samples for tracing atmospheric pollution in industrial areas. Environ. Pollut. 220, 286–297. https://doi.org/10.1016/j.envpol.2016.09.062

Gale, N.H., Woodhead, A.P., Stos-Gale, Z.A., Walder, A., Bowen, I., 1999. Natural variations detected in the isotopic composition of copper: Possible applications to archaeology and geochemistry. Int. J. Mass Spectrom. 184, 1–9. https://doi.org/10.1016/S1387-3806(98)14294-X

Gall, L., Williams, H.M., Siebert, C., Halliday, A.N., Herrington, R.J., Hein, J.R., 2013. Nickel isotopic compositions of ferromanganese crusts and the constancy of deep ocean inputs and continental weathering effects over the Cenozoic. Earth Planet. Sci. Lett. 375, 148–155. https://doi.org/10.1016/j.epsl.2013.05.019

Galuskova, I., Mihaljevic, M., Boruvka, L., Drabek, O., Fruhauf, M., Nemecek, K., 2014. Lead isotope composition and risk elements distribution in urban soils of historically different cities Ostrava and Prague, the Czech Republic. J. Geochemical Explor. 147, 215–221. https://doi.org/10.1016/j.gexplo.2014.02.022

Gao, P., Guo, H., Zhang, Z., Ou, C., Hang, J., Fan, Q., He, C., Wu, B., Feng, Y., Xing, B., 2018. Bioaccessibility and exposure assessment of trace metals from urban airborne particulate matter (PM10 and PM2.5) in simulated digestive fluid. Environ. Pollut. 242, 1669–1677. https://doi.org/10.1016/j.envpol.2018.07.109

Garty, J., Garty-Spitz, R.L., 2011. Neutralization and neoformation: Analogous processes in the atmosphere and in lichen thalli-A review. Environ. Exp. Bot. 70, 67–79. https://doi.org/10.1016/j.envexpbot.2010.08.002

Gerdol, R., Marchesini, R., Iacumin, P., Brancaleoni, L., 2014. Monitoring temporal trends of air pollution in an urban area using mosses and lichens as biomonitors. Chemosphere 108, 388–395. https://doi.org/10.1016/j.chemosphere.2014.02.035

Gioia, S.M.C.L., Babinski, M., Weiss, D.J., Kerr, A.A.F.S., 2010. Insights into the dynamics and sources of atmospheric lead and particulate matter in São Paulo, Brazil, from high temporal resolution sampling. Atmos. Res. 98, 478–485. https://doi.org/10.1016/j.atmosres.2010.08.016

Godinho, R.M., Verburg, T.G., Freitas, M.C., Wolterbeek, H.T., 2009. Accumulation of trace elements in the peripheral and central parts of two species of epiphytic lichens transplanted to a polluted site in Portugal. Environ. Pollut. 157, 102–109. https://doi.org/10.1016/j.envpol.2008.07.021

Goh, K.H., Lim, T.T., 2005. Arsenic fractionation in a fine soil fraction and influence of various anions on its mobility in the subsurface environment. Appl. Geochemistry 20, 229–239. https://doi.org/10.1016/j.apgeochem.2004.08.004

Gregurek, D., Melcher, F., Niskavaara, H., Pavlov, V.A., Reimann, C., Stumpfl, E.F., 1999. Platinum-group elements (Rh, Pt, Pd) and Au distribution in snow samples from the Kola Peninsula, NW Russia. Atmos. Environ. 33, 3281–3290. https://doi.org/10.1016/S1352-2310(98)00434-8

Gregurek, D, Reimann, C., Stumpfl, E.., 1998a. Trace elements and precious metals in snow samples from the immediate vicinity of nickel processing plants, Kola Peninsula, northwest Russia. Environ. Pollut. 102, 221–232. https://doi.org/10.1016/S0269-7491(98)00090-6

Gregurek, D., Reimann, C., Stumpfl, E.F., 1998b. Mineralogical fingerprints of industrial emissions - An example from Ni mining and smelting on the Kola Peninsula, NW Russia. Sci. Total Environ. 221, 189–200. https://doi.org/10.1016/S0048-9697(98)00293-9

Grodzińska, K., Szarek-Łukaszewska, G., 2001. Response of mosses to the heavy metal deposition in Poland — an overview. Environ. Pollut. 114, 443–451. https://doi.org/10.1016/S0269-7491(00)00227-X

Grodzińska, K., Szarek-Lukaszewska, G., Godzik, B., 1999. Survey of heavy metal deposition in Poland using mosses as indicators. Sci. Total Environ. 229, 41–51. https://doi.org/10.1016/S0048-9697(99)00071-6

Grynkiewicz Bylina, B., Rakwic, B., Pastuszka, J.S., 2005. Assessment of exposure to traffic-related aerosol and to particle-associated PAHs in Gliwice, Poland. Polish J. Environ. Stud. 14, 117–123.

Gueguen, B., Rouxel, O., Ponzevera, E., Bekker, A., Fouquet, Y., 2013. Nickel isotope variations in terrestrial silicate rocks and geological reference materials measured by MC-ICP-MS. Geostand. Geoanalytical Res. 37, 297–317. https://doi.org/10.1111/j.1751-908X.2013.00209.x

Gunawardena, J., Egodawatta, P., Ayoko, G.A., Goonetilleke, A., 2012. Role of traffic in atmospheric accumulation of heavy metals and polycyclic aromatic hydrocarbons. Atmos. Environ. 54, 502–510. https://doi.org/10.1016/j.atmosenv.2012.02.058

Guney, M., Bourges, C.M.J., Chapuis, R.P., Zagury, G.J., 2017. Lung bioaccessibility of As, Cu, Fe, Mn, Ni, Pb, and Zn in fine fraction (< 20 μm) from contaminated soils and mine tailings. Sci. Total Environ. 579, 378–386. https://doi.org/10.1016/j.scitotenv.2016.11.086

Haack, U., Kienholz, B., Reimann, C., Schneider, J., Stumpfl, E.F., 2004. Isotopic composition of lead in moss and soil of the European Arctic. Geochim. Cosmochim. Acta 68, 2613–2622. https://doi.org/10.1016/j.gca.2003.12.019

Haber, L.T., Bates, H.K., Allen, B.C., Vincent, M.J., Oller, A.R., 2017. Derivation of an oral toxicity reference value for nickel. Regul. Toxicol. Pharmacol. 87, S1–S18. https://doi.org/10.1016/j.yrtph.2017.03.011

Hansmann, W., Koppeï, V., 2000. Lead-isotopes as tracers of pollutants in soils. Chem. Geol. 171, 123–144.

Harmens, H., Norris, D.A., Sharps, K., Mills, G., Alber, R., Aleksiayenak, Y., Blum, O., Cucu-Man, S.M., Dam, M., De Temmerman, L., Ene, A., Fernández, J.A., Martinez-Abaigar, J., Frontasyeva, M., Godzik, B., Jeran, Z., Lazo, P., Leblond, S., Liiv, S., Magnússon, S.H., Maňkovská, B., Karlsson, G.P., Piispanen, J., Poikolainen, J., Santamaria, J.M., Skudnik, M., Spiric, Z., Stafilov, T., Steinnes, E., Stihi, C., Suchara, I., Thöni, L., Todoran, R., Yurukova, L., Zechmeister, H.G., 2015. Heavy metal and nitrogen concentrations in mosses are declining across Europe whilst some "hotspots" remain in 2010. Environ. Pollut. 200, 93–104. https://doi.org/10.1016/j.envpol.2015.01.036

Hassanvand, M.S., Naddafi, K., Faridi, S., Nabizadeh, R., Sowlat, M.H., Momeniha, F., Gholampour, A., Arhami, M., Kashani, H., Zare, A., Niazi, S., Rastkari, N., Nazmara, S., Ghani, M., Yunesian, M., 2015. Characterization of PAHs and metals in indoor/outdoor PM10/PM2.5/PM1 in a retirement home and a school dormitory. Sci. Total Environ. 527–528, 100–110. https://doi.org/10.1016/j.scitotenv.2015.05.001

Hernandez, L., Probst, A., Probst, J.L., Ulrich, E., 2003. Heavy metal distribution in some French forest soils: Evidence for atmospheric contamination. Sci. Total Environ. 312, 195–219. https://doi.org/10.1016/S0048-9697(03)00223-7

Hoatson, D.M., Jaireth, S., Jaques, A.L., 2006. Nickel sulfide deposits in Australia: Characteristics, resources, and potential. Ore Geol. Rev. 29, 177–241. https://doi.org/10.1016/j.oregeorev.2006.05.002

Horalek, J., Denby, B., Smet, P. De, Leeuw, F. De, Swart, R., Noije, T. Van, 2007. Spatial mapping of air quality for European scale assessment.

Huang, J., Kang, S., Zhang, Q., Guo, J., Chen, P., Zhang, G., Tripathee, L., 2013. Atmospheric deposition of trace elements recorded in snow from the mt. nyainqntanglha region, southern tibetan plateau. Chemosphere 92, 871–881. https://doi.org/10.1016/j.chemosphere.2013.02.038

Huggins, F.E., Senior, C.L., Chu, P., Ladwig, K., Huffman, G.P., 2007. Selenium and Arsenic Speciation in Fly Ash from Full-Scale Coal-Burning Utility Plants. Environ. Sci. Technol. 41, 32843289. https://doi.org/DOI: 10.1021/es062069y

IARC, 2012. Monographs on arsenic, metals, fibres and dusts: a review of human carcinogens.

Jeran, Z., Jaimovi, R., Batič, F., Mavsar, R., 2002. Lichens as integrating air pollution monitors. Environ. Pollut. 120, 107–113. https://doi.org/10.1016/S0269-7491(02)00133-1

Kalinovic, T.S., Serbula, S.M., Radojevic, A.A., Kalinovic, J. V., Steharnik, M.M., Petrovic, J. V., 2016. Elder, linden and pine biomonitoring ability of pollution emitted from the copper smelter and the tailings ponds. Geoderma 262, 266–275. https://doi.org/10.1016/j.geoderma.2015.08.027

Kampa, M., Castanas, E., 2008. Human health effects of air pollution. Environ. Pollut. 151, 362–367. https://doi.org/10.1016/j.envpol.2007.06.012

Kashulina, G., De Caritat, P., Reimann, C., 2014. Snow and rain chemistry around the "Severonikel" industrial complex, NW Russia: Current status and retrospective analysis. Atmos. Environ. 89, 672–682. https://doi.org/10.1016/j.atmosenv.2014.03.008

Kastury, F., Smith, E., Juhasz, A.L., 2017. A critical review of approaches and limitations of inhalation bioavailability and bioaccessibility of metal(loid)s from ambient particulate matter or dust. Sci. Total Environ. 574, 1054–1074. https://doi.org/10.1016/j.scitotenv.2016.09.056

Kelepertzis, E., Komárek, M., Argyraki, A., Šillerová, H., 2016. Metal(loid) distribution and Pb isotopic signatures in the urban environment of Athens, Greece. Environ. Pollut. 213, 420–431. https://doi.org/10.1016/j.envpol.2016.02.049

Khokhar, M.F., Platt, U., Wagner, T., 2008. Temporal trends of anthropogenic SO2 emitted by non-ferrous metal smelters in Peru and Russia estimated from Satellite observations. Atmos. Chem. Phys. Discuss. 8, 17393–17422. https://doi.org/10.5194/acpd-8-17393-2008

Klaminder, J., Bindler, R., Emteryd, O., Renberg, I., 2005. Uptake and recycling of lead by boreal forest plants: Quantitative estimates from a site in northern Sweden. Geochim. Cosmochim. Acta 69, 2485–2496. https://doi.org/10.1016/j.gca.2004.11.013

Klaminder, J., Farmer, J.G., Mackenzie, A.B., 2011. The origin of lead in the organic horizon of tundra soils: Atmospheric deposition, plant translocation from the mineral soil or soil mineral mixing? Sci. Total Environ. 409, 4344–4350. https://doi.org/10.1016/j.scitotenv.2011.07.005

Klaminder, J., Renberg, I., Bindler, R., Emteryd, O., 2003. Isotopic trends and background fluxes of atmospheric lead in northern Europe: Analyses of three ombrotrophic bogs from south Sweden. Global Biogeochem. Cycles 17, 1–10. https://doi.org/10.1029/2002gb001921

Knight, B.P., Chaudri, A.M., McGrath, S.P., Giller, K.E., 1998. Determination of chemical

availability of cadmium and zinc in soils using inert soil moisture samplers. Environ. Pollut. 99, 293–298. https://doi.org/10.1016/S0269-7491(98)00021-9

Komárek, M., Chrastný, V., Štíchová, J., 2007. Metal/metalloid contamination and isotopic composition of lead in edible mushrooms and forest soils originating from a smelting area. Environ. Int. 33, 677–684. https://doi.org/10.1016/j.envint.2007.02.001

Komárek, M., Ettler, V., Chrastný, V., Mihaljevič, M., 2008. Lead isotopes in environmental sciences: A review. Environ. Int. 34, 562–577. https://doi.org/10.1016/j.envint.2007.10.005

Konieczyński, J., Zajusz-Zubek, E., Jabłońska, M., 2012. The Release of Trace Elements in the Process of Coal Coking. Sci. World J. 2012, 1–8. https://doi.org/10.1100/2012/294927

Kunstmann, F.H., Bodenstein, L.B., 1961. THE ARSENIC CONTENT OF SOUTH AFRICAN COALS. J. South African Inst. Min. Metall. 234–244.

Kunzli, N., Kaiser, R., Medina, S., Studnicka, M., Chanel, O., Filliger, P., Herry, M., Horak, F., Puybonnieux-Texier, V., Quenel, P., Schneider, J., Seethaler, R., Vergnaud, J.C., Sommer, H., 2000. Public-health impact of outdoor and traffic-related air pollution: A European assessment. Lancet 356, 795–801. https://doi.org/10.1016/S0140-6736(00)02653-2

Kuoppamäki, K., Setälä, H., Rantalainen, A.-L., Kotze, D.J., 2014. Urban snow indicates pollution originating from road traffic. Environ. Pollut. 195, 56–63. https://doi.org/10.1016/j.envpol.2014.08.019

Lanteigne, S., Schindler, M., McDonald, A.M., Skeries, K., Abdu, Y., Mantha, N.M., Murayama, M., Hawthorne, F.C., Hochella, M.F., 2012. Mineralogy and weathering of smelter-derived spherical particles in soils: Implications for the mobility of Ni and Cu in the surficial environment. Water. Air. Soil Pollut. 223, 3619–3641. https://doi.org/10.1007/s11270-012-1135-3

Le Roux, G., Aubert, D., Stille, P., Krachler, M., Kober, B., Cheburkin, A., Bonani, G., Shotyk, W., 2005. Recent atmospheric Pb deposition at a rural site in southern Germany assessed using a peat core and snowpack, and comparison with other archives. Atmos. Environ. 39, 6790–6801. https://doi.org/10.1016/j.atmosenv.2005.07.026

Le Roux, J.P., Gómez, C., Fenner, J., Middleton, H., 2004. Sedimentological processes in a scarp-controlled rocky shoreline to upper continental slope environment, as revealed by unusual sedimentary features in the Neogene Coquimbo Formation, north-central Chile. Sediment. Geol. 165, 67–92. https://doi.org/10.1016/j.sedgeo.2003.11.006

Lee, C.S.L., Li, X., Zhang, G., Peng, X., Zhang, L., 2005. Biomonitoring of trace metals in the atmosphere using moss (Hypnum plumaeforme) in the Nanling Mountains and the Pearl River Delta, Southern China. Atmos. Environ. 39, 397–407. https://doi.org/10.1016/j.atmosenv.2004.09.067

LeGalley, E., Widom, E., Krekeler, M.P.S., Kuentz, D.C., 2013. Chemical and lead isotope constraints on sources of metal pollution in street sediment and lichens in southwest Ohio. Appl. Geochemistry 32, 195–203. https://doi.org/10.1016/j.apgeochem.2012.10.020

Leonelli, G., Battipaglia, G., Siegwolf, R.T.W., Saurer, M., Morra di Cella, U., Cherubini, P., Pelfini, M., 2012. Climatic isotope signals in tree rings masked by air pollution: A case

study conducted along the Mont Blanc Tunnel access road (Western Alps, Italy). Atmos. Environ. 61, 169–179. https://doi.org/10.1016/j.atmosenv.2012.07.023

Li, D., Liu, S.A., Li, S., 2015. Copper isotope fractionation during adsorption onto kaolinite: Experimental approach and applications. Chem. Geol. 396, 74–82. https://doi.org/10.1016/j.chemgeo.2014.12.020

Li, X., Zhang, Y., Tan, M., Liu, J., Bao, L., Zhang, G., Li, Y., Iida, A., 2009. Atmospheric lead pollution in fine particulate matter in Shanghai, China. J. Environ. Sci. 21, 1118–1124. https://doi.org/10.1016/S1001-0742(08)62390-6

Loppi, S., Bonini, I., 2000. Lichens and mosses as biomonitors of trace elements in areas with thermal springs and fumarole activity (Mt. Amiata, central Italy). Chemosphere 41, 1333–1336. https://doi.org/10.1016/S0045-6535(00)00026-6

Low, F., Zhang, L., 2013. Arsenic emissions and speciation in the oxy-fuel fly ash collected from lab-scale drop-tube furnace. P. Combust. Inst. 34, 2, 2877-2884. https://doi.org/10.1016/j.proci.2012.05.026

Luo, X.-S., Xue, Y., Wang, Y.-L., Cang, L., Xu, B., Ding, J., 2015. Source identification and apportionment of heavy metals in urban soil profiles. Chemosphere 127, 152–7. https://doi.org/10.1016/j.chemosphere.2015.01.048

Magiera, T., Kapička, A., Petrovský, E., Strzyszcz, Z., Fialová, H., Rachwał, M., 2008. Magnetic anomalies of forest soils in the Upper Silesia-Northern Moravia region. Environ. Pollut. 156, 618–627. https://doi.org/10.1016/j.envpol.2008.06.030

Maher, B.A., Moore, C., Matzka, J., 2008. Spatial variation in vehicle-derived metal pollution identified by magnetic and elemental analysis of roadside tree leaves. Atmos. Environ. 42, 364–373. https://doi.org/10.1016/j.atmosenv.2007.09.013

Marx, S.K., McGowan, H.A., Kamber, B.S., 2009. Long-range dust transport from eastern Australia: A proxy for Holocene aridity and ENSO-type climate variability. Earth Planet. Sci. Lett. 282, 167–177. https://doi.org/10.1016/j.epsl.2009.03.013

Massoura, S.T., Echevarria, G., Becquer, T., Ghanbaja, J., Leclerc-Cessac, E., Morel, J.L., 2006. Control of nickel availability by nickel bearing minerals in natural and anthropogenic soils. Geoderma 136, 28–37. https://doi.org/10.1016/j.geoderma.2006.01.008

Mathur, R., Titley, S., Hart, G., Wilson, M., Davignon, M., Zlatos, C., 2009. The history of the United States cent revealed through copper isotope fractionation. J. Archaeol. Sci. 36, 430–433. https://doi.org/10.1016/j.jas.2008.09.029

Mattielli, N., Petit, J.C.J., Deboudt, K., Flament, P., Perdrix, E., Taillez, A., Rimetz-Planchon, J., Weis, D., 2009. Zn isotope study of atmospheric emissions and dry depositions within a 5 km radius of a Pb-Zn refinery. Atmos. Environ. 43, 1265–1272. https://doi.org/10.1016/j.atmosenv.2008.11.030

Mattielli, N., Rimetz, J., Petit, J., Perdrix, E., Deboudt, K., Flament, P., Weis, D., 2006. Zn–Cu isotopic study and speciation of airborne metal particles within a 5-km zone of a lead/zinc smelter. Geochim. Cosmochim. Acta 70, A401. https://doi.org/10.1016/j.gca.2006.06.808

Mattigod, S. V., Page, A.L., Thornton, I., 1986. Identification of Some Trace Metal Minerals in a Mine-waste Contaminated Soil. Soil Sci. Soc. Am. J. https://doi.org/https://doi.org/10.2136/sssaj1986.03615995005000010050x

Mielke, H.W., Gonzales, C.R., Smith, M.K., Mielke{, P.W., 1999. The Urban Environment and Children's Health: Soils as an Integrator of Lead, Zinc, and Cadmium in New Orleans, Louisiana, U.S.A.

Mihaljevič, M., Ettler, V., Šebek, O., Strnad, L., Chrastný, V., 2006. Lead isotopic signatures of wine and vineyard soils - Tracers of lead origin. J. Geochemical Explor. 88, 130–133. https://doi.org/10.1016/j.gexplo.2005.08.025

Mihaljevič, M., Ettler, V., Strnad, L., Šebek, O., Vonásek, F., Drahota, P., Rohovec, J., 2009. Isotopic composition of lead in Czech coals. Int. J. Coal Geol. 78, 38–46. https://doi.org/10.1016/j.coal.2008.09.018

Mihaljevič, M., Zuna, M., Ettler, V., Chrastný, V., Šebek, O., Strnad, L., Kyncl, T., 2008. A comparison of tree rings and peat deposit geochemical archives in the vicinity of a lead smelter. Water. Air. Soil Pollut. 188, 311–321. https://doi.org/10.1007/s11270-007-9546-2

Mikuška, P., Křůmal, K., Večeřa, Z., 2015. Characterization of organic compounds in the PM2.5 aerosols in winter in an industrial urban area. Atmos. Environ. 105, 97–108. https://doi.org/10.1016/j.atmosenv.2015.01.028

Mirowsky, J.E., Jin, L., Thurston, G., Lighthall, D., Tyner, T., Horton, L., Galdanes, K., Chillrud, S., Ross, J., Pinkerton, K.E., Chen, L.C., Lippmann, M., Gordon, T., 2015. In vitro and in vivo toxicity of urban and rural particulate matter from California. Atmos. Environ. 103, 256–262. https://doi.org/10.1016/j.atmosenv.2014.12.051

Moeller, K., Schoenberg, R., Pedersen, R.B., Weiss, D., Dong, S., 2012. Calibration of the New Certified Reference Materials ERM-AE633 and ERM-AE647 for Copper and IRMM-3702 for Zinc Isotope Amount Ratio Determinations. Geostand. Geoanalytical Res. 36, 177–199. https://doi.org/10.1111/j.1751-908X.2011.00153.x

Monna, F., Ben Othman, D., Luck, J.M., 1995. Pb isotopes and Pb, Zn and Cd concentrations in the rivers feeding a coastal pond (Thau, southern France): constraints on the origin(s) and flux(es) of metals. Sci. Total Environ. 166, 19–34. https://doi.org/10.1016/0048-9697(95)04514-2

Monna, F., Lancelot, J., Croudace, I.W., Cundy, A.B., Lewis, J.T., 1997. Pb Isotopic Composition of Airborne Particulate Material from France and the Southern United Kingdom: Implications for Pb Pollution Sources in Urban Areas. Environ. Sci. Technol. 31, 2277–2286.

Monna, F., Poujol, M., Losno, R., Dominik, J., Annegarn, H., Coetzee, H., 2006. Origin of atmospheric lead in Johannesburg, South Africa. Atmos. Environ. 40, 6554–6566. https://doi.org/10.1016/j.atmosenv.2006.05.064

Moreda-Piñeiro, J., Moreda-Piñeiro, A., Romarís-Hortas, V., Moscoso-Pérez, C., López-Mahía, P., Muniategui-Lorenzo, S., Bermejo-Barrera, P., Prada-Rodríguez, D., 2011. In-vivo and in-vitro testing to assess the bioaccessibility and the bioavailability of arsenic, selenium and mercury species in food samples. TrAC - Trends Anal. Chem. 30, 324–345. https://doi.org/10.1016/j.trac.2010.09.008

Moreda–Piñeiro, J., Dans-Sánchez, L., Sánchez-Piñero, J., Turnes-Carou, I., Muniategui-Lorenzo, S., López-Mahía, P., 2019. Oral bioavailability estimation of toxic and essential trace elements in PM10. Atmos. Environ. 213, 104–115.

https://doi.org/10.1016/j.atmosenv.2019.06.001

Morton-Bermea, O., Rodriguez-Salazar, M.T., Hernandez-Alvarez, E., Garcia-Arreola, M.E., Lozano-Santacruz, R., 2011. Lead isotopes as tracers of anthropogenic pollution in urban topsoils of Mexico City. Chemie der Erde - Geochemistry 71, 189–195. https://doi.org/10.1016/j.chemer.2011.03.003

Moskalyk, R.R., Alfantazi, A.M., 2002. Nickel laterite processing and electrowinning practice. Miner. Eng. 15, 593–605. https://doi.org/10.1016/S0892-6875(02)00083-3

Mukai, H., Machida, T., Tanaka, A., Vera, P., Uematsu, M., 2001. Lead isotope ratios in the urban air of eastern and central Russia. Atmos. Environ. 35, 2783–2793.

Muránszky, G., Ovari, M., Virág, I., Csiba, P., Dobai, R., Záray, G., 2011. Chemical characterization of PM10 fractions of urban aerosol. Microchem. J. 98, 1–10. https://doi.org/10.1016/j.microc.2010.10.002

Mutlu, E.A., Comba, I.Y., Cho, T., Engen, P.A., Yazıcı, C., Soberanes, S., Hamanaka, R.B., Niğdelioğlu, R., Meliton, A.Y., Ghio, A.J., Budinger, G.R.S., Mutlu, G.M., 2018. Inhalational exposure to particulate matter air pollution alters the composition of the gut microbiome. Environ. Pollut. 240, 817–830. https://doi.org/10.1016/j.envpol.2018.04.130

Nabais, C., Freitas, H., Hagemeyer, J., 1999. Dendroanalysis: a tool for biomonitoring environmental pollution? Sci. Total Environ. 232, 3337.

Novák, M., Emmanuel, S., Vile, M.A., Erel, Y., Véron, A., Pačes, T., Wieder, R.K., Vaněček, M., Štěpánová, M., Břízová, E., Hovorka, J., 2003. Origin of lead in eight central European peat bogs determined from isotope ratios, strengths, and operation times of regional pollution sources. Environ. Sci. Technol. 37, 437–445. https://doi.org/10.1021/es0200387

Novak, M., Erel, Y., Zemanova, L., Bottrell, S.H., Adamova, M., 2008. A comparison of lead pollution record in Sphagnum peat with known historical Pb emission rates in the British Isles and the Czech Republic. Atmos. Environ. 42, 8997–9006. https://doi.org/10.1016/j.atmosenv.2008.09.031

Novák, M., Mikova, J., Krachler, M., Kosler, J., Erbanova, L., Prechova, E., Jackova, I., Fottova, D., 2010. Radial distribution of lead and lead isotopes in stem wood of Norway spruce: A reliable archive of pollution trends in Central Europe. Geochim. Cosmochim. Acta 74, 4207–4218. https://doi.org/10.1016/j.gca.2010.04.059

Nriagu, J.O., 1989. A global assessment of natural sources of atmospheric trace metals. Nature 388, 47–49.

Nriagu, J.O., 1988. A Silent Epidemic of Environmental Metal Poisoning? Environ. Pollut. 50, 139–161.

Nriagu, J.O., 1980. Cadmium in the atmosphere and in precipitation, in: Cadmium in the Environment. pp. 71–114.

OECD, 2018. ENVIRONMENTAL PERFORMANCE: TRENDS AND RECENT DEVELOPMENTS, Environmental performance: Trends and recent developments. https://doi.org/10.1787/888933722903

Pacyna, E.G., Pacyna, J.M., Fudala, J., Strzelecka-Jastrzab, E., Hlawiczka, S., Panasiuk, D.,

Nitter, S., Pregger, T., Pfeiffer, H., Friedrich, R., 2007. Current and future emissions of selected heavy metals to the atmosphere from anthropogenic sources in Europe. Atmos. Environ. 41, 8557–8566. https://doi.org/10.1016/j.atmosenv.2007.07.040

Pacyna, J.M., Pacyna, E.G., Aas, W., 2009. Changes of emissions and atmospheric deposition of mercury, lead, and cadmium. Atmos. Environ. 43, 117–127. https://doi.org/10.1016/j.atmosenv.2008.09.066

Padoan, E., Malandrino, M., Giacomino, A., Grosa, M.M., Lollobrigida, F., Martini, S., Abollino, O., 2016. Spatial distribution and potential sources of trace elements in PM10 monitored in urban and rural sites of Piedmont Region. Chemosphere 145, 495–507. https://doi.org/10.1016/j.chemosphere.2015.11.094

Patrick, G.J., Farmer, J.G., 2006. A stable lead isotopic investigation of the use of sycamore tree rings as a historical biomonitor of environmental lead contamination. Sci. Total Environ. 362, 278–291. https://doi.org/10.1016/j.scitotenv.2005.12.004

Pérez Rodríguez, N., Engström, E., Rodushkin, I., Nason, P., Alakangas, L., Öhlander, B., 2013. Copper and iron isotope fractionation in mine tailings at the Laver and Kristineberg mines, northern Sweden. Appl. Geochemistry 32, 204–215. https://doi.org/10.1016/j.apgeochem.2012.10.012

Pešek, J., Sivek, M., 2012. Uhlonosné pánve a ložiska černého a hnědého uhlí České republiky, Česká geologická služba.

Pichat, S., Douchet, C., Albarède, F., 2003. Zinc isotope variations in deep-sea carbonates from the eastern equatorial Pacific over the last 175 ka. Earth Planet. Sci. Lett. 210, 167–178. https://doi.org/10.1016/S0012-821X(03)00106-7

Pokrovsky, O.S., Viers, J., Emnova, E.E., Kompantseva, E.I., Freydier, R., 2008. Copper isotope fractionation during its interaction with soil and aquatic microorganisms and metal oxy(hydr)oxides: Possible structural control. Geochim. Cosmochim. Acta 72, 1742–1757. https://doi.org/10.1016/j.gca.2008.01.018

Preciado, H.F., Li, L.Y., Weis, D., 2007. Investigation of past and present multi-metal input along two highways of British Columbia, Canada, using lead isotopic signatures. Water. Air. Soil Pollut. 184, 127–139. https://doi.org/10.1007/s11270-007-9402-4

Qi, L., Zhang, Y., Ma, Yinghui, Chen, M., Ge, X., Ma, Yan, Zheng, J., Wang, Z., Li, S., 2016. Source identification of trace elements in the atmosphere during the second Asian Youth Games in Nanjing, China: Influence of control measures on air quality. Atmos. Pollut. Res. 7, 1–10. https://doi.org/10.1016/j.apr.2016.01.003

Qing, X., Yutong, Z., Shenggao, L., 2015. Assessment of heavy metal pollution and human health risk in urban soils of steel industrial city (Anshan), Liaoning, Northeast China. Ecotoxicol. Environ. Saf. 120, 377–385. https://doi.org/10.1016/j.ecoenv.2015.06.019

Rai, P.K., 2016. Impacts of particulate matter pollution on plants: Implications for environmental biomonitoring. Ecotoxicol. Environ. Saf. 129, 120–136. https://doi.org/10.1016/j.ecoenv.2016.03.012

Räisänen, M.L., Kashulina, G., Bogatyrev, I., 1997. Mobility and retention of heavy metals, arsenic and sulphur in podzols at eight locations in northern Finland and Norway and the western half of the Russian Kola Peninsula. J. Geochemical Explor. 59, 175–195.

https://doi.org/10.1016/S0375-6742(97)00014-9

Ratié, G., Jouvin, D., Garnier, J., Rouxel, O., Miska, S., Guimarães, E., Cruz Vieira, L., Sivry, Y., Zelano, I., Montarges-Pelletier, E., Thil, F., Quantin, C., 2015a. Nickel isotope fractionation during tropical weathering of ultramafic rocks. Chem. Geol. 402, 68–76. https://doi.org/10.1016/j.chemgeo.2015.02.039

Ratié, G., Quantin, C., Jouvin, D., Calmels, D., Ettler, V., Sivry, Y., Vieira, L.C., Ponzevera, E., Garnier, J., 2015b. Nickel isotope fractionation during laterite Ni ore smelting and refining: Implications for tracing the sources of Ni in smelter-affected soils. Appl. Geochemistry 64, 136–145. https://doi.org/10.1016/j.apgeochem.2015.09.005

Reimann, C., 1995. National report, Kola Project. Catchment study 1994.

Reimann, C., Boyd, R., Halleraker, J.H., Kashulina, G., Niskavaara, H., Bogatyrev, I., 1997a. Topsoil (0-5 cm) composition in eight arctic catchments in Northern Europe. Environ. Pollut. 95, 45–56.

Reimann, C., De Caritat, P., Halleraker, J.H., Volden, T., Äyräs, M., Niskavaara, H., Chekushin, V.A., Pavlov, V.A., 1997b. Rainwater composition in eight arctic catchments in northern Europe (Finland, Norway and Russia). Atmos. Environ. 31, 159–170. https://doi.org/10.1016/1352-2310(96)00197-5

Reimann, C., Fabian, K., Flem, B., Schilling, J., Roberts, D., Englmaier, P., 2016. Pb concentrations and isotope ratios of soil O and C horizons in Nord-Trøndelag, central Norway: Anthropogenic or natural sources? Appl. Geochemistry 74, 56–66. https://doi.org/10.1016/j.apgeochem.2016.09.002

Reimann, C., Flem, B., Fabian, K., Birke, M., Ladenberger, A., Négrel, P., Demetriades, A., Hoogewerff, J., The GEMAS Project Team, 2012. Lead and lead isotopes in agricultural soils of Europe - The continental perspective. Appl. Geochemistry 27, 532–542. https://doi.org/10.1016/j.apgeochem.2011.12.012

Reimann, C., Halleraker, J.H., Kashulina, G., Bogatyrev, I., 1999. Comparison of plant and precipitation chemistry in catchments with different levels of pollution on the Kola Peninsula, Russia. Sci. Total Environ. 243–244, 169–191. https://doi.org/10.1016/S0048-9697(99)00390-3

Reimann, C., Koller, F., Kashulina, G., Niskavaara, H., Englmaier, P., 2001. Influence of extreme pollution on the inorganic chemical composition of some plants. Environ. Pollut. 115, 239–252. https://doi.org/10.1016/S0269-7491(01)00106-3

Reimann, C., Niskavaara, H., De Caritat, P., Finne, T.E., Äyräs, M., Chekushin, V., 1996. Regional variation of snowpack chemistry in the vicinity of Nikel and Zapoljarnij, Russia, northern Finland and Norway. Sci. Total Environ. 182, 147–158. https://doi.org/10.1016/0048-9697(95)05061-2

Reimann, C., Siewers, U., Tarvainen, T., Bityukova, L., Eriksson, J., Gilucis, A., Gregorauskiene, V., Lukashev, V., Matinian, N.N., Pasieczna, A., 2000. Baltic soil survey: Total concentrations of major and selected trace elements in arable soils from 10 countries around the Baltic Sea. Sci. Total Environ. 257, 155–170. https://doi.org/10.1016/S0048-9697(00)00515-5

Reis, A.P., Patinha, C., Noack, Y., Robert, S., Dias, A.C., Ferreira Da Silva, E., 2014. Assessing

the human health risk for aluminium, zinc and lead in outdoor dusts collected in recreational sites used by children at an industrial area in the western part of the Bassin Minier de Provence, France. J. African Earth Sci. 99, 724–734. https://doi.org/10.1016/j.jafrearsci.2013.08.001

Renberg, I., Brannvall, M.-L., Bindler, R., Emteryd, O., 2002. Stable lead isotopes and lake sediments-a useful combination for the study of atmospheric lead pollution history. Sci. Total Environ. 292, 45–54.

Report Bellona, 2010. Environmental Challenges in the Arctic. Norilsk Nickel: the Soviet Legacy of Industrial Pollution.

Riga-Karandinos, A.N., Karandinos, M.G., 1998. Assessment of air pollution from a lignite power plant in the plain of Megalopolis (Greece) using as biomonitors three species of lichens; impacts on some biochemical parameters of lichens. Sci. Total Environ. 215, 167–183. https://doi.org/10.1016/S0048-9697(98)00119-3

Rosman, K.J.R., Ly, C., Van De Velde, K., Boutron, C.F., 2000. A two century record of lead isotopes in high altitude Alpine snow and ice. Earth Planet. Sci. Lett. 176, 413–424. https://doi.org/10.1016/S0012-821X(00)00013-3

Ruby, M. V., Davis, a, Schoof, R., Eberle, S., Sellstone, C.M., 1996. Esitimation of Lead and Arsenic Bioavailabilty Using a Physiologically Based Exration Test. 1Environmental Sci. Technol. 30, 422–433. https://doi.org/10.1021/es950057z

Rühling, Å., Tyler, G., 2004. Changes in the atmospheric deposition of minor and rare elements between 1975 and 2000 in south Sweden, as measured by moss analysis. Environ. Pollut. 131, 417–423. https://doi.org/10.1016/j.envpol.2004.03.005

Sakalys, J., Kvietkus, K., Sucharova, J., Suchara, I., Valiulis, D., 2009. Changes in total concentrations and assessed background concentrations of heavy metals in moss in Lithuania and the Czech Republic between 1995 and 2005. Chemosphere 76, 91–97. https://doi.org/10.1016/j.chemosphere.2009.02.009

Salo, H., Bućko, M.S., Vaahtovuo, E., Limo, J., Mäkinen, J., Pesonen, L.J., 2012. Biomonitoring of air pollution in SW Finland by magnetic and chemical measurements of moss bags and lichens. J. Geochemical Explor. 115, 69–81. https://doi.org/10.1016/j.gexplo.2012.02.009

Sapkota, B., Cioppa, M.T., 2012. Using magnetic and chemical measurements to detect atmospherically-derived metal pollution in artificial soils and metal uptake in plants. Environ. Pollut. 170, 131–144. https://doi.org/10.1016/j.envpol.2012.06.010

Saunier, J.B., Losfeld, G., Freydier, R., Grison, C., 2013. Trace elements biomonitoring in a historical mining district (les Malines, France). Chemosphere 93, 2016–2023. https://doi.org/10.1016/j.chemosphere.2013.07.024

Savard, M.M., 2010. Tree-ring stable isotopes and historical perspectives on pollution - An overview. Environ. Pollut. 158, 2007–2013. https://doi.org/10.1016/j.envpol.2009.11.031

Scerbo, R., Ristori, T., Possenti, L., Lampugnani, L., Barale, R., Barghigiani, C., 2002. Lichen (Xanthoria parietina) biomonitoring of trace element contamination and air quality assessment in Pisa Province (Tuscany, Italy). Sci. Total Environ. 286, 27–40. https://doi.org/10.1016/S0048-9697(01)00959-7

Seaward, M.R.D., 1993. Lichen Sensitivity and Air Pollution--A Review of Literature Data.

Environ. Pollut. 81, 193–195.

Sen, I.S., Bizimis, M., Tripathi, S.N., Paul, D., 2016. Lead isotopic fingerprinting of aerosols to characterize the sources of atmospheric lead in an industrial city of India. Atmos. Environ. 129, 27–33. https://doi.org/10.1016/j.atmosenv.2016.01.005

Sharma, S.K., Mandal, T.K., Saxena, M., Rashmi, Sharma, A., Datta, A., Saud, T., 2014. Variation of OC, EC, WSIC and trace metals of PM10 in Delhi, India. J. Atmos. Solar-Terrestrial Phys. 113, 10–22. https://doi.org/10.1016/j.jastp.2014.02.008

Shen, X.-M., Rosenb, J.F., Guoa, D., Wua, S.-M., 1996. Childhood lead poisoning in China. Sci. Total Environ. 181, 101–109.

Shiel, A.E., Weis, D., Cossa, D., Orians, K.J., 2013. Determining provenance of marine metal pollution in French bivalves using Cd, Zn and Pb isotopes. Geochim. Cosmochim. Acta 121, 155–167. https://doi.org/10.1016/j.gca.2013.07.005

Shiel, A.E., Weis, D., Orians, K.J., 2012. Tracing cadmium, zinc and lead sources in bivalves from the coasts of western Canada and the USA using isotopes. Geochim. Cosmochim. Acta 76, 175–190. https://doi.org/10.1016/j.gca.2011.10.005

Shotyk, W., Goodsite, M.E., Roos-Barraclough, F., Givelet, N., Le Roux, G., Weiss, D., Cheburkin, A.K., Knudsen, K., Heinemeier, J., van Der Knaap, W.O., Norton, S.A., Lohse, C., 2005. Accumulation rates and predominant atmospheric sources of natural and anthropogenic Hg and Pb on the Faroe Islands. Geochim. Cosmochim. Acta 69, 1–17. https://doi.org/10.1016/j.gca.2004.06.011

Shotyk, W., Kempter, H., Krachler, M., Zaccone, C., 2015. Stable (206Pb, 207Pb, 208Pb) and radioactive (210Pb) lead isotopes in 1year of growth of Sphagnum moss from four ombrotrophic bogs in southern Germany: Geochemical significance and environmental implications. Geochim. Cosmochim. Acta 163, 101–125. https://doi.org/10.1016/j.gca.2015.04.026

Simonetti, A., Gariépy, C., Carignan, J., 2003. Tracing sources of atmospheric pollution in Western Canada using the Pb isotopic composition and heavy metal abundances of epiphytic lichens. Atmos. Environ. 37, 2853–2865. https://doi.org/10.1016/S1352-2310(03)00210-3

Song, X., Shao, L., Zheng, Q., Yang, S., 2014. Mineralogical and geochemical composition of particulate matter (PM10) in coal and non-coal industrial cities of Henan Province, North China. Atmos. Res. 143, 462–472. https://doi.org/10.1016/j.atmosres.2014.03.015

Sonke, J.E., Sivry, Y., Viers, J., Freydier, R., Dejonghe, L., André, L., Aggarwal, J.K., Fontan, F., Dupré, B., 2008. Historical variations in the isotopic composition of atmospheric zinc deposition from a zinc smelter. Chem. Geol. 252, 145–157. https://doi.org/10.1016/j.chemgeo.2008.02.006

Steffen, A., Schroeder, W., Bottenheim, J., Narayan, J., Fuentes, J.D., 2002. Atmospheric mercury concentrations: Measurements and profiles near snow and ice surfaces in the Canadian Arctic during Alert 2000. Atmos. Environ. 36, 2653–2661. https://doi.org/10.1016/S1352-2310(02)00112-7

Sterckeman, T., Douay, F., Baize, D., Fourrier, H., Proix, N., Schvartz, C., Carignan, J., 2006. Trace element distributions in soils developed in loess deposits from northern France. Eur.

J. Soil Sci. 57, 392–410. https://doi.org/10.1111/j.1365-2389.2005.00750.x

Stille, P., Schmitt, A.D., Labolle, F., Pierret, M.C., Gangloff, S., Cobert, F., Lucot, E., Gu??guen, F., Brioschi, L., Steinmann, M., Chabaux, F., 2012. The suitability of annual tree growth rings as environmental archives: Evidence from Sr, Nd, Pb and Ca isotopes in spruce growth rings from the Strengbach watershed. Comptes Rendus - Geosci. 344, 297–311. https://doi.org/10.1016/j.crte.2012.04.001

Sturm, R., 2010. Theoretische modelle der dynamischen formfaktoren und lungendeposition von kleinen, aus verbrennungsprozessen stammenden partikelaggregaten. Z. Med. Phys. 20, 226–234. https://doi.org/10.1016/j.zemedi.2010.04.001

Suchara, I., Sucharová, J., 2004. Current Atmospheric Deposition Loads and Their Trends in the Czech Republic Determined by Mapping the Distribution of Moss Element Contents. J. Atmos. Chem. 49, 503–519.

Suchara, I., Sucharova, J., Hola, M., Reimann, C., Boyd, R., Filzmoser, P., Englmaier, P., 2011. The performance of moss, grass, and 1- and 2-year old spruce needles as bioindicators of contamination: A comparative study at the scale of the Czech Republic. Sci. Total Environ. 409, 2281–2297. https://doi.org/10.1016/j.scitotenv.2011.02.003

Sucharová, J., Suchara, I., 1998. Atmospheric deposition levels of chosen elements in the Czech Republic determined in the framework of the International Bryomonitoring Program 1995. Sci. Total Environ. 223, 37–52. https://doi.org/10.1016/S0048-9697(98)00306-4

Sucharová, J., Suchara, I., Holá, M., Reimann, C., 2014. Contemporary lead concentration and stable lead isotope ratio distribution in forest moss across the Czech Republic. Appl. Geochemistry 40, 51–60. https://doi.org/10.1016/j.apgeochem.2013.10.012

Sucharová, J., Suchara, I., Reimann, C., Boyd, R., Filzmoser, P., Englmaier, P., 2011. Spatial distribution of lead and lead isotopes in soil B-horizon, forest-floor humus, grass (Avenella flexuosa) and spruce (Picea abies) needles across the Czech Republic. Appl. Geochemistry 26, 1205–1214. https://doi.org/10.1016/j.apgeochem.2011.04.009

Sysalová, J., Száková, J., Tremlová, J., Kašparovská, K., Kotlík, B., Tlustoš, P., Svoboda, P., 2014. Methodological Aspects of In Vitro Assessment of Bio-accessible Risk Element Pool in Urban Particulate Matter. Biol. Trace Elem. Res. 161, 216–222. https://doi.org/10.1007/s12011-014-0101-x

Szczepaniak, K., Biziuk, M., 2003. Aspects of the biomonitoring studies using mosses and lichens as indicators of metal pollution. Environ. Res. 93, 221–230. https://doi.org/10.1016/S0013-9351(03)00141-5

Telmer, K., Bonham-Carter, G.F., Kliza, D.A., Hall, G.E.M., 2004. The atmospheric transport and deposition of smelter emissions: Evidence from the multi-element geochemistry of snow, Quebec, Canada. Geochim. Cosmochim. Acta 68, 2961–2980. https://doi.org/10.1016/j.gca.2003.12.022

Tippayawong, N., Pengchai, P., Lee, A., 2006. Characterization of ambient aerosols in Northern Thailand and their probable sources. Int. J. Environ. Sci. Technol. 3, 359–369. https://doi.org/10.1007/BF03325945

Tommasini, S., Davies, G.R., Elliott, T., 2000. Lead isotope composition of tree rings as bio-geochemical tracers of heavy metal pollution: A reconnaissance study from Firenze, Italy.

Appl. Geochemistry 15, 891–900. https://doi.org/10.1016/S0883-2927(99)00106-7

Tvrdý, L., Lev, Ms., Aspholm, P.E., 2004. Regional development in the arctic regions.

Twining, J., McGlinn, P., Loi, E., Smith, K., Gieré, R., 2005. Risk ranking of bioaccessible metals from fly ash dissolved in simulated lung and gut fluids. Environ. Sci. Technol. 39, 7749–7756. https://doi.org/10.1021/es0502369

Tyszka, R., Pietranik, A., Kierczak, J., Ettler, V., Mihaljevič, M., Medyńska-Juraszek, A., 2016. Lead isotopes and heavy minerals analyzed as tools to understand the distribution of lead and other potentially toxic elements in soils contaminated by Cu smelting (Legnica, Poland). Environ. Sci. Pollut. Res. 23, 24350–24363. https://doi.org/10.1007/s11356-016-7655-4

USEPA, 2011. Exposure Factors Handbook: 2011 Edition, U.S. EPA. https://doi.org/EPA/600/R-090/052F

USEPA, 2008. Child-Specific Exposure Factors Handbook. https://doi.org/EPA/600/R-06/096F.

USEPA, 2007. Method 3051A: Microwave assisted acid digestion of sediments, sludges, soils, and iols. Cambridge University Press.

USEPA, 1996a. Method 3050B - Acid digestion of sediments, sludges, and soils., 1996. https://doi.org/10.1117/12.528651

USEPA, 1996b. Method 3052: Microwave assisted acid digestion of siliceous and organically based matrices.

Vejvoda, J., Buryan, P., Svrček, P., 1998. Desulphurisation of waste gases in Czech republic. Acta Montan. Slovaca 3, 262–266.

Veron, A., Flament, P., Bertho, M.L., Alleman, L., Flegal, R., Hamelin, B., 1999. Isotopic evidence of pollutant lead sources in northwestern France. Atmos. Environ. 33, 3377–3388. https://doi.org/10.1016/S1352-2310(98)00376-8

Vítková, M., Ettler, V., Johan, Z., Kříbek, B., Šebek, O., Mihaljevič, M., 2010. Primary and secondary phases in copper-cobalt smelting slags from the Copperbelt Province, Zambia. Mineral. Mag. 74, 581–600. https://doi.org/10.1180/minmag.2010.074.4.581

Voldrichova, P., Chrastny, V., Sipkova, A., Farkas, J., Novak, M., Stepanova, M., Krachler, M., Veselovsky, F., Blaha, V., Prechova, E., Komarek, A., Bohdalkova, L., Curik, J., Mikova, J., Erbanova, L., Pacherova, P., 2014. Zinc isotope systematics in snow and ice accretions in Central European mountains. Chem. Geol. 388, 130–141. https://doi.org/10.1016/j.chemgeo.2014.09.008

Vossler, T., Černikovský, L., Novák, J., Williams, R., 2016. Source apportionment with uncertainty estimates of fine particulate matter in Ostrava, Czech Republic using Positive Matrix Factorization. Atmos. Pollut. Res. 7, 503–512. https://doi.org/10.1016/j.apr.2015.12.004

Vuković, G., Urošević, M.A., Tomašević, M., Samson, R., Popović, A., 2015. Biomagnetic monitoring of urban air pollution using moss bags (Sphagnum girgensohnii). Ecol. Indic. 52, 40–47. https://doi.org/10.1016/j.ecolind.2014.11.018

Walker, T.R., Crittenden, P.D., Young, S.D., 2003a. Regional variation in the chemical

composition of winter snow pack and terricolous lichens in relation to sources of acid emissions in the Usa river basin, northeast European Russia. Environ. Pollut. 125, 401–412. https://doi.org/10.1016/S0269-7491(03)00080-0

Walker, T.R., Young, S.D., Crittenden, P.D., Zhang, H., 2003b. Anthropogenic metal enrichment of snow and soil in north-eastern European Russia. Environ. Pollut. 121, 11–21. https://doi.org/10.1016/S0269-7491(02)00212-9

Wang, C.X., Zhu, W., Peng, A., Guichreit, R., 2001. Comparative studies on the concentration of rare earth elements and heavy metals in the atmospheric particulate matter in Beijing, China, and in Delft, the Netherlands.

Wang, X., Pu, W., Zhang, X., Ren, Y., Huang, J., 2015. Water-soluble ions and trace elements in surface snow and their potential source regions across northeastern China. Atmos. Environ. 114, 57–65. https://doi.org/10.1016/j.atmosenv.2015.05.012

Wasylenki, L.E., Howe, H.D., Spivak-Birndorf, L.J., Bish, D.L., 2015. Ni isotope fractionation during sorption to ferrihydrite: Implications for Ni in banded iron formations. Chem. Geol. 400, 56–64. https://doi.org/10.1016/j.chemgeo.2015.02.007

Waterlot, C., Bidar, G., Pruvot, C., Douay, F., 2012. Effects of grinding and shaking on Cd, Pb and Zn distribution in anthropogenically impacted soils. Talanta 98, 185–196. https://doi.org/10.1016/j.talanta.2012.06.068

Watmough, S.A., 1999. Monitoring historical changes in soil and atmospheric trace metal levels by dendrochemical analysis. Environ. Pollut. 106, 391–403. https://doi.org/10.1016/S0269-7491(99)00102-5

Watmough, S.A., Hutchinson, T.C., 2003. Uptake of 207Pb and 111Cd through bark of mature sugar maple, white ash and white pine: A field experiment. Environ. Pollut. 121, 39–48. https://doi.org/10.1016/S0269-7491(02)00208-7

Weinstein, C., Moynier, F., Wang, K., Paniello, R., Foriel, J., Catalano, J., Pichat, S., 2011. Isotopic fractionation of Cu in plants. Chem. Geol. 286, 266–271. https://doi.org/10.1016/j.chemgeo.2011.05.010

Weiss, D., Shotyk, W., Kramers, J.D., Gloor, M., 1999. Sphagnum mosses as archives of recent and past atmospheric lead deposition in Switzerland. Atmos. Environ. 33, 3751–3763.

Weiss, D.J., Rehkamper, M., Schoenberg, R., McLaughlin, M., Kirby, J., Campbell, P.G.C., Arnold, T., Chapman, J., Peel, K., Gioia, S., 2008. Application of nontraditional stable-isotope systems to the study of sources and fate of metals in the environment. Environ. Sci. Technol. 42, 655–664. https://doi.org/10.1021/es0870855

Wenzel, W.W., Kirchbaumer, N., Prohaska, T., Stingeder, G., Lombi, E., Adriano, D.C., 2001. Arsenic fractionation in soils using an improved sequential extraction procedure. Anal. Chim. Acta 436, 309–323.

Wiederhold, J.G., 2015. Metal stable isotope signatures as tracers in environmental geochemistry. Environ. Sci. Technol. 49, 2606–2624. https://doi.org/10.1021/es504683e

Wiseman, C.L.S., 2015. Analytical methods for assessing metal bioaccessibility in airborne particulate matter: A scoping review. Anal. Chim. Acta 877, 9–18. https://doi.org/10.1016/j.aca.2015.01.024

Wiseman, C.L.S., Zereini, F., 2014. Characterizing metal(loid) solubility in airborne PM10, PM2.5 and PM1 in Frankfurt, Germany using simulated lung fluids. Atmos. Environ. 89, 282–289. https://doi.org/10.1016/j.atmosenv.2014.02.055

Witt, M.L.I., Mather, T.A., Baker, A.R., De Hoog, J.C.M., Pyle, D.M., 2010. Atmospheric trace metals over the south-west Indian Ocean: Total gaseous mercury, aerosol trace metal concentrations and lead isotope ratios. Mar. Chem. 121, 2–16. https://doi.org/10.1016/j.marchem.2010.02.005

Wolterbeek, B., 2002. Biomonitoring of trace element air pollution: Principles, possibilities and perspectives. Environ. Pollut. 120, 11–21. https://doi.org/10.1016/S0269-7491(02)00124-0

Wong, C.S.C., Li, X., Thornton, I., 2006. Urban environmental geochemistry of trace metals. Environ. Pollut. 142, 1–16. https://doi.org/10.1016/j.envpol.2005.09.004

Wragg, J., Cave, M.R., Environment Agency., 2003. In-vitro methods for the measurement of the oral bioaccessibility of selected metals and metalloids in soils : a review of guidance and selected industry practices. Environment Agency.

Wróbel, A., Rokita, E., Maenhaut, W., 2000. Transport of traffic-related aerosols in urban areas. Sci. Total Environ. 257, 199–211. https://doi.org/10.1016/S0048-9697(00)00519-2

Wu, L., Taylor, M.P., Handley, H.K., Wu, M., 2016. Australian atmospheric lead deposition reconstructed using lead concentrations and isotopic compositions of archival lichen and fungi. Environ. Pollut. 208, 678–687. https://doi.org/10.1016/j.envpol.2015.10.046

Yao, P.H., Shyu, G.S., Chang, Y.F., Chou, Y.C., Shen, C.C., Chou, C.S., Chang, T.K., 2015. Lead isotope characterization of petroleum fuels in Taipei, Taiwan. Int. J. Environ. Res. Public Health 12, 4602–4616. https://doi.org/10.3390/ijerph120504602

Yu, G., Xu, J., Kang, S., Zhang, Q., Huang, J., Ren, Q., Ren, J., Qin, D., 2013. Lead isotopic composition of insoluble particles from widespread mountain glaciers in western China: Natural vs. anthropogenic sources. Atmos. Environ. 75, 224–232. https://doi.org/10.1016/j.atmosenv.2013.04.018

Zajusz-Zubek, E., Mainka, A., Korban, Z., Pastuszka, J.S., 2015. Evaluation of highly mobile fraction of trace elements in PM10 collected in Upper Silesia (Poland): Preliminary results. Atmos. Pollut. Res. 6, 961–968. https://doi.org/10.1016/j.apr.2015.05.001

Zhang, J., Liu, C.-Q., 2004. Major and rare earth elements in rainwaters from Japan and East China Sea: Natural and anthropogenic sources. Chem. Geol. 209, 315–326. https://doi.org/10.1016/j.chemgeo.2004.06.014

Zuna, M., Mihaljevič, M., Šebek, O., Ettler, V., Handley, M., Navrátil, T., Goliáš, V., 2011. Recent lead deposition trends in the Czech Republic as recorded by peat bogs and tree rings. Atmos. Environ. 45, 4950–4958. https://doi.org/10.1016/j.atmosenv.2011.06.007

Curriculum vitae

&

List of publications

Anna Francová

Born: 12[th]March, 1990, Uherské Hradiště (Czech Republic)

Address: Na Vinici 566, 27401, Slaný, Czech Republic

E-mail: kuncikova@fzp.czu.cz

Education

2014 – present: Ph.D. studies

Applied and landscape ecology, Faculty of Environmental Sciences

Czech University of Life Sciences, Prague, Czech Republic

Thesis: *The isotope tracing methods for industrial contamination of the atmosphere*

2012 – 2014:   Master programme

Agroecology, Faculty of AgriSciences

Mendel University in Brno, Brno, Czech Republic

Thesis: *Study of revitalization pond on Hlinka water flow*

Rector's Award for Excellent Study Results, The honorable acknowledgment of the Dean for an excellent diploma thesis

2009 – 2012:   Bachelor programme

Agroecology, Faculty of AgriSciences

Mendel University in Brno, Brno, Czech Republic

Thesis: *Possible sources of pollution in the selected section of river basin study*

Publications

Francová A., Chrastný V., Vítková M., Šillerová H., Komárek M. (2020) Health risk assessment of metal(loid)s in soil and particulate matter from industrialized regions: A multidisciplinary approach. Environmental Pollution 260: 114057

Chrastný V., Šillerová H., Vítková M., **Francová A**., Jehlička J, Kocourková J., Aspholm P.E., Nilsson L.O., Berglen T.F., Jensen H.K.B., Komárek M. (2018) Unleaded gasoline as a significant source of Pb emissions in the Subarctic. Chemosphere 193: 230-236

Francová A., Chrastný V., Šillerová H., Kocourková J., Komárek M. (2017) Suitability of selected bioindicators of atmospheric pollution in the industrialized region of Ostrava, Upper Silesia, Czech Republic. Environmental Monitoring and Assessment (2017) 189:478

Šillerová H., Chrastný V., Vítková M., **Francová A.,** Jehlička J., Gutsch M.R., Kocourková J., Aspholm P.E., Nilsson L.O., Berglen T.F., Jensen H.K.B., Komárek M. (2017) Stable isotope tracing of Ni and Cu pollution in North-East Norway: Potentials and drawbacks. Environmental Pollution 228: 149-157

Chrastný V., Komárek M., **Francová A**., Šillerová H. (2017) Identifikace zdrojů znečistění atmosféry v průmyslových oblastech za využití stabilních izotopů olova, Identification of sources of atmospheric pollution in industrial areas using stable lead isotopes, isotopes; pollution; atmosphere; industry; tracing, 2017, XX - Nepřiřazeno, A - Certifikovaná metodika (NmetC), M037/M/2017, Certifikovaná metodika byla publikována v rámci projektu ISOFIN 7F14330, Česko-norský výzkumný program CZ09, Certifikovaná metodika prezentuje účinný nástroj pro identifikaci zdrojů atmosférického znečištění, konkrétně v průmyslové oblasti Ostravska., C - Výsledek je využíván bez omezení okruhu uživatelů, Česká společnost pro jakost, z.s., 18. 04. 2017

Francová A., Chrastný V., Šillerová H., Vítková M., Kocourková J., Komárek M. (2017) Evaluating the suitability of different environmental samples for tracing atmospheric pollution in industrial areas. Environmental Pollution 220: 286-297

Vítková M., Šillerová H., **Francová A.,** Komárek M., Nilsson L. (2016) Identification of metal distribution in smelter-affected area of Finnmark using various environmental indicators. In Energy and clean technologies conference proceedings, SGEM 2016, Vol. II 30.06.2016, Albena. Bulgaria: STEF92 TECHNOLOGY LTD, 2016. s. 397-402

Grants and projects

- Co-woker on grant: A new methodological approach for identification of industrial pollution: Isotope fingerprinting and bacterial community changes (ISOFIN).

  7F14330 (Norwegian Financial Mechanism 209-2014)

- Principal investigator on grant: Izotopové stopování průmyslového znečistění atmosféry v ČR a v Norsku. Podpora zapojení studentů do grantu Norských fondů

  IGA 4240013123161 (Internal Grant Agency of the Faculty of Environmental Sciences, CULS Prague)

- Co-investigator on grant: Izotopy niklu a kadmia jako důkaz původu znečištění atmosféry v industriálních oblastech

  CIGA 20164201 (Czech University of Life Sciences)

Teaching activities

- Environmental Soil Chemistry – laboratory course

- Practical and Computational Chemistry – laboratory course

- Field Practise for EGS – laboratory course

- Supervision of 10 bachelor theses